Chemistry and biosynthesis of highly complex marine alkaloids from Mediterranean biodiversity

Siguara Bastos de Lemos E Silva

université PARIS-SACLAY

NNT : 2017SACLS214

Thèse de doctorat

UNIVERSITÉ PARIS SUD
Comprendre le monde, construire l'avenir

Chimie et biosynthèse de substances naturelles hautement complexes de la biodiversité méditerranéenne

Thèse de doctorat de l'Université Paris-Saclay
préparée à l'Université Paris-Sud

École doctorale n°569 Innovation thérapeutique: du fondamental à l'appliqué
Spécialité de doctorat: Chimie de substances naturelles

Thèse présentée et soutenue à Châtenay-Malabry, le 29 septembre de 2017, par

Mme Siguara Bastos de Lemos e Silva

Composition du Jury :

M. Pierre Champy Professeur, Université Paris-Sud	Président et examinateur
Mme. Soizic Prado Professeur, Museum National d'Histoire Naturelle	Rapporteur
M. Grégory Genta-Jouve Maître de Conférences, Université Paris Descartes	Rapporteur
M. Michel Rohmer Professeur, Université de Strasbourg	Examinateur
M. Erwan Poupon Professeur, Université Paris-Sud	Directeur de thèse
M. Olivier P. Thomas Professeur, National University of Ireland Galway	Co-Directeur de thèse
M. Laurent Evanno Maître de Conférences, Université Paris-Sud	Co-encadrant de thèse

In memory of Prof. Dr. Luiz Fernando da Silva Jr (1971-2017), for transmitting his knowledge in Organic Chemistry in a clear and fascinating way and for always demanding the best of his collaborators

Acknowledgements

I acknowledge to Prof. Dr. Michel Rohmer, member of the *Académie des Sciences*, for the honour of accepting to participate of my PhD jury.

I acknowledge to Prof. Dr. Soizic Prado and Dr. Grégory Genta-Jouve for accepting the invitation to evaluate this work as *rapporteurs*.

I acknowledge to Prof. Dr. Pierre Champy for accepting the invitation to judge this thesis and for being the president of the PhD jury.

I kindly thank you all members of the jury for their valuable contribution to improve this work through the discussion.

I would like to acknowledge Prof. Dr. Erwan Poupon and Prof. Dr. Olivier Thomas for accepting me as their PhD student and for design this motivating and interdisciplinary project. It was a big pleasure to discover that I would be in collaboration with professors that were long term friends. I specially thank professor Erwan for all his help with the administration service, for his patience during the hard parts of the project, for his enthusiasm with the promising results, and for always be concerned with me on the personal level. I really thank professor Olivier for directly guiding me in the practical work, for collecting samples, for warmly receiving me in his laboratory in Nice and for all the opportunities and efforts that he continuously did to improve the quality of this work and my professional skills; like the big chance to be intern in IAEA-Monaco. It was a great experience to work with these two high level professors that have such an integrated view about science and that are so motivated.

I want to acknowledge Dr. Laurent Evanno for the guidance on the laboratory, for all the great Chemistry suggestions (on the practical and theoretical fields), and for the pleasant quotidian relationship. I am indebted with Dr. Laurent for the patience that he had to always speak in French with me, improving my language skills. It was a wonderful opportunity to work with such a clever chemist and a generous person.

I acknowledge all the staff of IAEA for the support to the biosynthesis project, specially to my supervisors Jean-Louis Teyssié and François Oberhänsli. I thank them for the training with radiolabelled compounds, for the innumerable results discussions, for all the kindness and, mainly from the part of Jean-Louis, for the concernment with my professional future. These three months in IAEA were an intensive experience. I want to specifically acknowledge Mr. Juan Carlos Miquel

for accepting me as intern in his team.

I am grateful to all the professors, colleagues, technicians and the administration staff from Chemistry Institute of University of Nice and University Paris-Sud (BIOCIS). I specially acknowledge: Daniel Rodrigues, Marie-Aude Tribalat, Dr. Aurelie Barats, Eva Ternon, Jean-Pierre Goudour, Anna Maria Orani, Blandine Seon-Meniel, Nathalie Lemière, Agnés Rasneur, Laurent Ferrié, Natacha Bonneau, Asmaa Boufridi, Kevin Cotet, David Lackar, Adam Skiredj, Xinming Zhang, Linh Nguyen, Sara Vallerotto, Thi Hong Long Nguyen, Hazrina Hazni, Pedro Vasquez-Ocmin, Elvis Otogo, Charlotte Alcover, Alexander Enrique Fox Ramos, Alexandre Farag, and Serai Ural, some of them for supporting the project in different levels and some for the good moments spent inside and outside the university. I specially acknowledge my friend Kevin Calabro, not only for being a wonderful person, but also for had helped me many times in the laboratory and with the administration service. Thank you very much to: Dr. Mehdi Beniddir, for the motivation and help concerning the isolation project; to Karine Leblanc, for the support with the mass analysis service and HPLC purifications; to Marc Gaysinski, Jean-Christophe Jullian, and Camille Dejean, for the NMR analyses. I acknowledge director Prof. Dr. Bruno Figadère for admitting me in BIOCIS group.

Thank you to my good friends: Maria Isabel Acosta, Ramona Galantonu, Christina Werner, Erika Garcia, Lucrezia Martino, Gabriela Ramos Chagas, Mauro Safir Filho, Maysa Puccinelli, Mathiew Bannwarth, Rui Costa, Maëlle Kelner, and Sabine Bossard. I am glad to had shared this adventure of living abroad with you.

I acknowledge with all my heart to my family: Francisco de Assis da Silva Filho, Maria das Graças Bastos de Lemos, Estela Gomes Aoto, and Elaine Cristina Patriota, for supporting my project of studying abroad since it was just a dream.

Thank you very much to my husband: Yuri Alexandre Aoto. This journey was delightful with you. Thank you for the mutual respect, for the continuous motivation, and for always accompanying my steps.

Finally, I would like to acknowledge the funding agency Capes (process: 99999.010184/2013-09) for conceding me a scholarship to develop this project.

Abbreviations

ACN : acetonitrile

BINAP: (2,2'-*bis*-(diphenylphosphino)-1,1'-binaphthyl)

Boc: *tert*-butyloxycarbonyl

CBZ: carboxybenzyl

CDI: carbonyldiimidazole

COSY: correlation spectroscopy

DCC: *N*, *N*'-dicyclohexylcarbodiimide

DCM: dichloromethane

DHPM: 3,4-dihydropyrimidin-2(1*H*)-one

DIBAL-H: diisobutylaluminium hydride

DIPEA: *N*, *N*-diisopropylethylamine

DMAP: 4-methylaminopyridine

DMF: dimethylformamide

DMSO: dimethyl sulfoxide

EDC: 1-ethyl-3-(3-dimethylaminopropyl)carbodiimide

ELSD: evaporative light scattering detector

FDA: US Food and Drug Administration

HMBC: heteronuclear multiple-bond correlation spectroscopy

HPLC: high pressure liquid chromatography

HRMS: high resolution mass spectrometry

HSQC: heteronuclear single-quantum correlation spectroscopy

IR: infrared spectroscopy

IUPAC: International Union of Pure and Applied Chemistry

LC-MS: liquid chromatography mass spectrometry

LSC: liquid scintillation counting

MS-TOF: time-of-flight mass spectrometry

NMR: nuclear magnetic resonance

NOESY: nuclear overhauser effect spectroscopy

OXONE: potassium peroxymonosulfate

PGA: polycyclic guanidine alkaloids

pH: potential of hydrogen

PLP: pyridoxal phosphate

radio-TLC: radioactivity thin layer chromatography

RP: reverse phase

SCUBA: self-contained underwater breathing apparatus

SPE: solid phase extraction

TBDMS: *tert*-butyldimethylsilyl

TBDMSO: *O*-*tert*-butyldimethylsilyl

TCCA: trichloroisocyanuric acid

TEA: triethylamine

TFA: trifluoroacetic acid

TFE: 2, 2, 2-trifluoroethanol

THF: tetrahydrofuran

TLC: thin layer chromatography

TPP: triamine diphosphate

UPLC: ultra performance liquid chromatography

DAD: diode array detector

VLC: vacuum liquid chromatography

Note

For convenience, each chapter has its own numeration of chemical structures

Table of Contents

Acknowledgements i

Abbreviations iii

Table of Contents v

Chapter 1. Isolation and Structure Elucidation of Specialized Metabolites from Poecilosclerida Mediterranean Sponges 1

1. 1 Introduction 3

1. 1. 1 Natural products chemistry, alkaloids and the importance of Porifera on discovery of original structures 3

1. 1. 2 *Phorbas tenacior* sponge - an incursion into the family of anchinopeptolides 6

1. 1. 3 Crambeidae sponges and the guanidine polycyclic alkaloids crambescins, crambescidins and derivatives 10

1. 2 Objectives of this Project 12

1. 3 Results and Discussion 13

1. 3. 1 Identification of specialized metabolites produced by *P. tenacior* 13

1. 3. 2 Isolation of specialized metabolites produced by *C. tailliezi* 18

1. 3. 3 Purification of *C. crambe* sponge 23

1. 4 Conclusions and perspectives 24

Chapter 2. ^{14}C-Feeding Experiments with *C. crambe*: First Insights into the Biosynthesis of Crambescin C1 25

2. 1 Introduction 27

2. 1. 1 Marine sponges and biosynthetic studies 27

2. 1. 2 Difficulties associated to sponge feeding experiments 28

2. 1. 3 Detection Techniques 30

2. 1. 4 Biosynthesis hypothesis for crambescins and derivatives 31

2. 2 Objectives of this project 35

2. 3 Results and Discussion 36

2. 4 Conclusions 45

Chapter 3. Biomimetic Synthesis of Crambescin A2 and Derivatives 47

3. 1 Introduction 49

3. 1. 1 "Nature knows best": biomimetic synthesis of natural products 49

3. 1. 2 The guanidine bicyclic alkaloid crambescin A2 448 and analogues 52

3. 1. 3 Biomimetic synthesis of crambescins 53

3. 2 Objectives of this project 55

3. 3 Results and Discussion 56

3. 3. 1 Synthesis of aliphatic fragment 21 56

3. 3. 2 Synthesis of fragment 17 58
3. 3. 2. 1 Preparation of alcohols 20a and 20c 58
3. 3. 2. 2 Attempts to the formation of fragment 17 by transesterification 61
3. 3. 2. 3 Formation of fragment 17 promoted by coupling reagents 63
3. 3. 3 Synthesis of guanidinated pyrrolidinium 18 65
3. 3. 3. 1 Preparation of 18 by sequential reductions of L-arginine 65
3. 3. 3. 2 Preparation of 18 by oxidative decarboxylation of L-arginine 68
3. 3. 4 Key-step: formation of the bicyclic guanidine core 70
3. 3. 4. 1 Formation of structures 45a and 45b 70
3. 3. 4. 2 Formation of crambescin A2 448 (5a) and *iso*-crambescin A2 448 (5k) 75
3. 4 Conclusions and perspectives 81
Conclusions and Perspectives 83
Résumé en Français 87
Introduction 88
1. Étude chimique d'éponges marines de l'ordre des Poeciloscerida 88
1. 1 Étude chimique de *Phorbas tenacior* 88
1. 2 Étude chimique de *Crambe tailliezi* 90
1. 3* Étude chimique de *Crambe crambe 91
2. Élucidation de la biosynthèse de la crambescine C1 par des études d'incorporation *in vivo* de précurseurs marqués au ^{14}C 92
3. Synthèse biomimétique de la crambescine A2 448 et molécules apparentées 95
3. 1. Synthèse des fragments pour la synthèse biomimétique de la crambescine A2 448 96
3. 2. Étape-clé: assemblage biomimétique du cœur des cambescines 98
3. 3. Assemblage biomimétique de la crambescine A2 448 et de son isomère 99
Experimental Section 103
1. General Information 105
2. Isolation and Structure Elucidation of Specialized Metabolites from Poecilosclerida Mediterranean Sponges 106
2. 1 Isolation of metabolites from *P. tenacior* sponge 106
2. 2 Isolation of metabolites from *C. taillezi* sponge 115
2. 3 Isolation of metabolites from *C. crambe* sponge 117
3. ^{14}C-Feeding Experiments with *C. crambe* Sponge: Initial Insights into the Biosynthesis of Crambescin C1 117
3. 1. Sponges Collection and *in vivo* feeding experiments with ^{14}C-labelled precursors 117
3. 2. Radioactivity TLC and autoradiography beta-imager analyses 118
3. 3. Control Experiments 119
4. Biomimetic Synthesis of Crambescin A2 and Derivatives 119

4. 1. Preparation of benzyl 3-oxotetradecanoate (25a) 119
4. 2. Preparation of ethyl 3-oxotetradecanoate (25b) 120
4. 3. Preparation of 3-oxotetradecanoic acid (21) 121
4. 4. Preparation of 4-guanidinobutanoic acid (31) 122
4. 5. Preparation of 1-(4-hydroxybutyl)guanidine (20a) 123
4. 6. Preparation of 4-(*N*,*N*'-di-*t*-butoxycarbonylguanidino)-butan-1-ol (20c) 123
4. 7. Synthesis of 4-(2,3-*bis*(*tert*-butoxycarbonyl)guanidino)butyl 3-oxotetradecanoate (17b) 124
4. 8. Preparation of 1-carbamimidoyl-3,4-dihydro-2H-pyrrol-1-ium (18) 125
4. 9. Synthesis of crambescin A2 448 (5a) and *iso*-crambescin A2 (5k) 126
4. 10. Molecular complexity calculation 128
NMR Spectra 129
References 185
Abstract 189

Chapter 1. Isolation and Structure Elucidation of Specialized Metabolites from Poecilosclerida Mediterranean Sponges

1. 1 Introduction

1. 1. 1 Natural products chemistry, alkaloids and the importance of Porifera on discovery of original structures

Natural products, also referred as "secondary metabolites" or better "specialized metabolites", are the result of years of adaptation and evolution of terrestrial and marine organisms to diverse biotic and abiotic stressing conditions. As a result, these compounds usually exhibit interesting bioactivity properties for pharmaceutical applications.[1]

Traditional medicine has been empirically employing extracts of plants and animals in the treatment of diseases, with hunting purposes or as pesticides. Apothecaries and the seminal pharmaceutical companies were for years producing partially crude therapeutic formulations.[1, 2] In the early 19th century the isolation of morphine by Friedrich Sertürner started a new era to the drug formulations, were the active principle became based on pure natural products. This represented a great advance in the drug discovery and development processes, that led to a continuous improvement on isolation and characterization techniques.

In the early medicine, alkaloids were the major class of natural products present in drug formulations. Well known examples include: morphine, quinine, atropine, and ephedrine. Nowadays, they are underrepresented in medicine market, in part because the lack of an unique definition concerning what exactly constitutes an alkaloid.[2] Indeed, alkaloids have been described as nitrogen containing natural products, typically as primary, secondary or tertiary amines, a feature that usually confers basicity on the alkaloid. The name itself comes from the word "alkali". The basicity of the nitrogen atom varies a lot, depending on the other functional groups of the molecule and on the location of the nitrogen functionalities. If the nitrogen is an amide function, for example, the alkaloid will be non basic. Alkaloids containing positive charges (quaternary ammonium species) can also be found in nature.[3]

Alkaloids can be subdivided according to the nature of the nitrogen-containing structure: pyrrolidine, piperidine, quinoline, isoquinoline, indole, etc. As the nitrogen is usually derived from an amino acid, and the carbon skeleton is often retained, they can be subdivided according to the

[1] B. David, J.-L. Wolfender, D. A. Dias, *Phytochem. Rev.* **2015**, *14*, 299-315.
[2] V. Amirkia, M. Heinrich, *Phytochem. Lett.* **2014**, *10*, xlviii-liii.
[3] P. M. Dewick, in *Medicinal Natural Products*, John Wiley & Sons, Ltd, **2009**, pp. 311-420.

amino acid precursor.[3] A popular division (but somehow old fashioned) based on the amino acid, creates three categories of alkaloids: 1) true alkaloids (derived from amino acids and containing a heterocyclic ring with nitrogen); 2) protoalkaloids (derived from amino acid but without a heterocycle containing nitrogen); 3) pseudoalkaloids (compounds where the carbon skeleton is not derived from amino acids).[2]

Frequently and historically the alkaloid structures are associated mainly to plants, but they can also be found in microorganisms and animals, such as sponges. The advent of SCUBA (Self-Contained Underwater Breathing Apparatus) diving technique after the Second World War (1950 - 1960) made the access to deeper marine habitats and their biodiversity possible. This led the discovery of a plethora of interesting molecular structures, usually different from those found in the terrestrial environment. During the last 50 years, Porifera (sponges) became the most popular studied phylum, although its popularity has been decreasing since 1990 (Figure 1).[4]

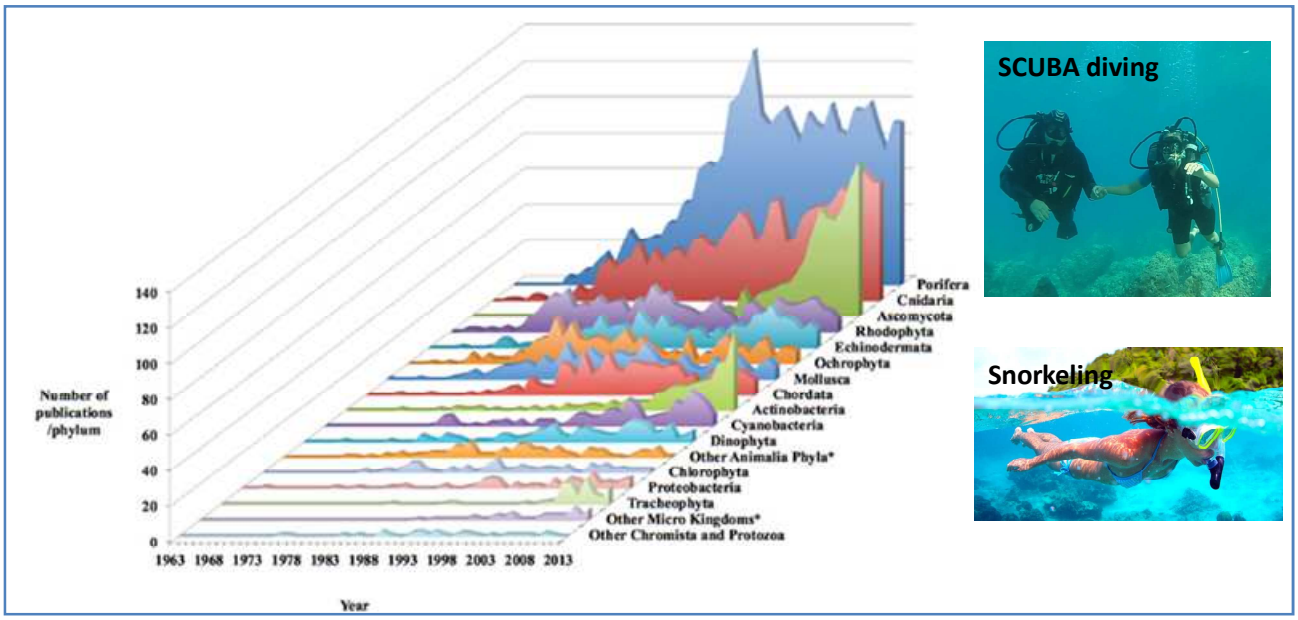

Figure 1. The phylum-preferences of the marine natural product research community across a 50-year period from 1963[4]

Sponges are the first metazoan animals, with more than 8,500 species distributed along a variety of habitats: rivers, seas, abyssal regions (up to 8,000 m deep), and Antarctic environments. Although they are simple animals that lack tissues differentiation and organs, sponges diversity is

[4] J. W. Blunt, B. R. Copp, R. A. Keyzers, M. H. G. Munro, M. R. Prinsep, *Nat. Prod. Rep.* **2015**, *32*, 116-211.

still surprising scientists. In the last 20 years, for example, carnivorous species were discovered.[5] Currently the phylum Porifera is sub-divided in four classes: 1) Hexactinellida ("glass sponges", sponges with a skeleton made of six-pointed siliceous spicules, called hexactines); 2) Calcarea (sponges with a skeleton of calcium carbonate spicules), 3) Demospongiae (sponges with a siliceous and/or spongin skeleton), and 4) Homoscleromorpha (the skeleton, if present, is composed by small siliceous spicules with caltrops shapes).[6, 7, 8] The Demospongiae comprises about 81% of all living sponges,[9] including the sponges that will be studied in this thesis.

The "toxicity" of sponges has been documented since the Antiquity. As sessile animals, they need to produce specific metabolites for chemical communication and to defense against: predation, overgrowth by fouling organisms or to competition for space. Between the metabolites isolated from sponges, recent outstanding examples with application as pharmaceuticals are halichondrin B (**1**) and eribulin (**2**) (Figure 2). Eribulin is a synthetic compound partially biomimicry of the halichondrin B, isolated almost 30 years ago from the marine sponge *Halichondria okadai*. Halichondrin B exhibited potent anti-tumoral activity but was present in very low concentrations (a ton-scale isolation allowed the isolation of just 300 mg of the compound). Meanwhile, Prof. Yoshito Kishi from Harvard University developed a total synthesis of halichondrin B in his laboratory and years later his methodology was applied to the development of the analogue eribulin mesylate. Eribulin takes 62 steps to be synthesized but is more potent than halichondrin B and is smaller and easier to synthesize than the natural compound. In 2010 the US Food and Drug Administration (FDA) approved the use of this compound for the treatment of metastatic breast cancer.[10]

[5] J. Vacelet, N. Boury-Esnault, *Nature* **1995**, *373*, 333-335.
[6] A. M. P. Almeida, R. G. S. Berlinck, E. Hajdu, *Quim. Nova* **1997**, *20*, 170-185.
[7] R. W. M. Van Soest, N. Boury-Esnault, J. N. A. Hooper, K. Rützler, N. J. de Voogd, B. Alvarez de Glasby, E. Hajdu, A. B. Pisera, R. Manconi, C. Schoenberg, M. Klautau, B. Picton, M. Kelly, J. Vacelet, M. Dohrmann, M.-C. Díaz, P. Cárdenas, J. L. Carballo, P. Rios Lopez, in *World Porifera Database*, Acessed at http://www.marinespecies.org/porifera on 2017-09-15, **2017**.
[8] E. Gazave, P. Lapébie, A. Ereskovsky, J. Vacelet, E. Renard, P. Cárdenas, C. Borchiellini, *Hydrobiologia* **2012**, *687*, 3-10.
[9] C. Morrow, P. Cárdenas, *Front. Zool.* **2015**, *12*, 7.
[10] T. K. Huyck, W. Gradishar, F. Manuguid, P. Kirkpatrick, *Nat. Rev. Drug Discov.* **2011**, *10*, 173-174.

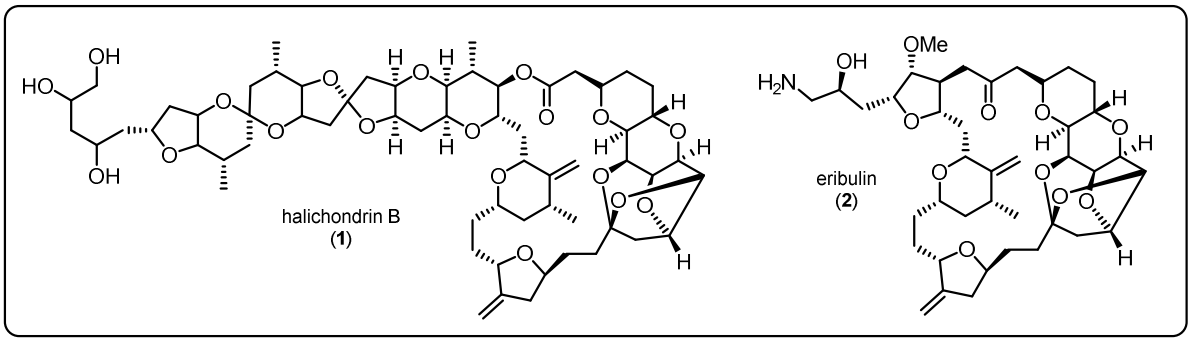

Figure 2. Halichondrin B and eribulin structures

1. 1. 2 *Phorbas tenacior* sponge - an incursion into the family of anchinopeptolides

Phorbas tenacior, previously known as *Anchinoe tenacior* (Topsent, 1925), is a deeply blue marine sponge found in the Mediterranean Sea and in the Atlantic Macaronesia (Figure 3).[7]

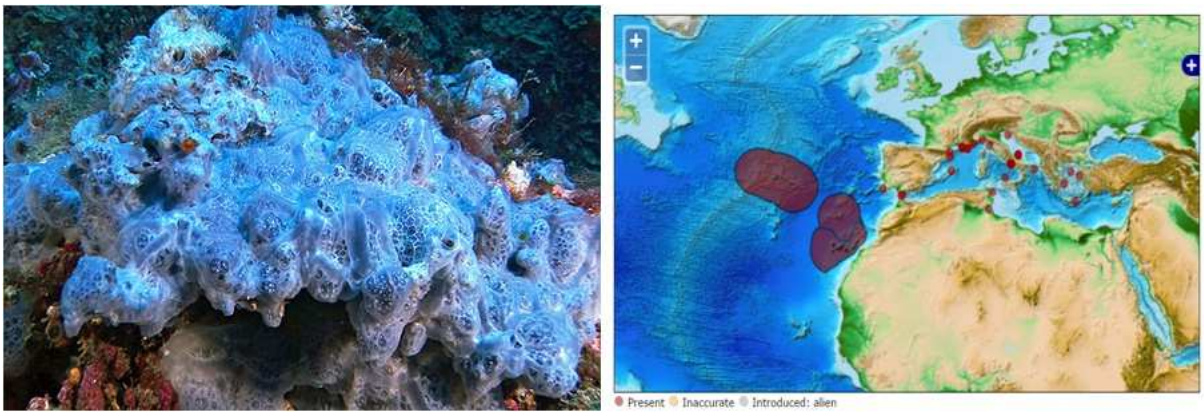

Figure 3. *P. tenacior* sponge (left) and itsgeographic distribution (right)

In the 90s Minale and collaborators performed the first natural product studies on *P. tenacior* discovering a family of cyclic peptide alkaloids: the anchinopeptolides A-D (**3a**-**3d**) and the interesting cycloanchinoptolide C (**4c**), clearly a cycloaddition derivative formed by a head-to-head [2 + 2] cycloaddition of the hydroxystyrylamido groups of anchinopeptolide C (Scheme 1). Moreover, two minor compounds distinct of anchinopeptolides were identified: **5** and **6**.[11,12,13] Minale's group also reported that anchinopeptolides B-D displace specific ligands from the

[11] A. Casapullo, E. Finamore, L. Minale, F. Zollo, *Tetrahedron Lett.* **1993**, *34*, 6297-6300.
[12] A. Casapullo, L. Minale, F. Zollo, *Tetrahedron Lett* **1994**, *35*, 2421-2422.
[13] A. Casapullo, L. Minale, F. Zollo, J. Lavayre, *J. Nat. Prod.* **1994**, *57*, 1227-1233.

receptors of somatostatin, human B2 bradykinin and neuropeptide Y. Anchinopeptolide A exhibited weaker activities on these biological essays.[13]

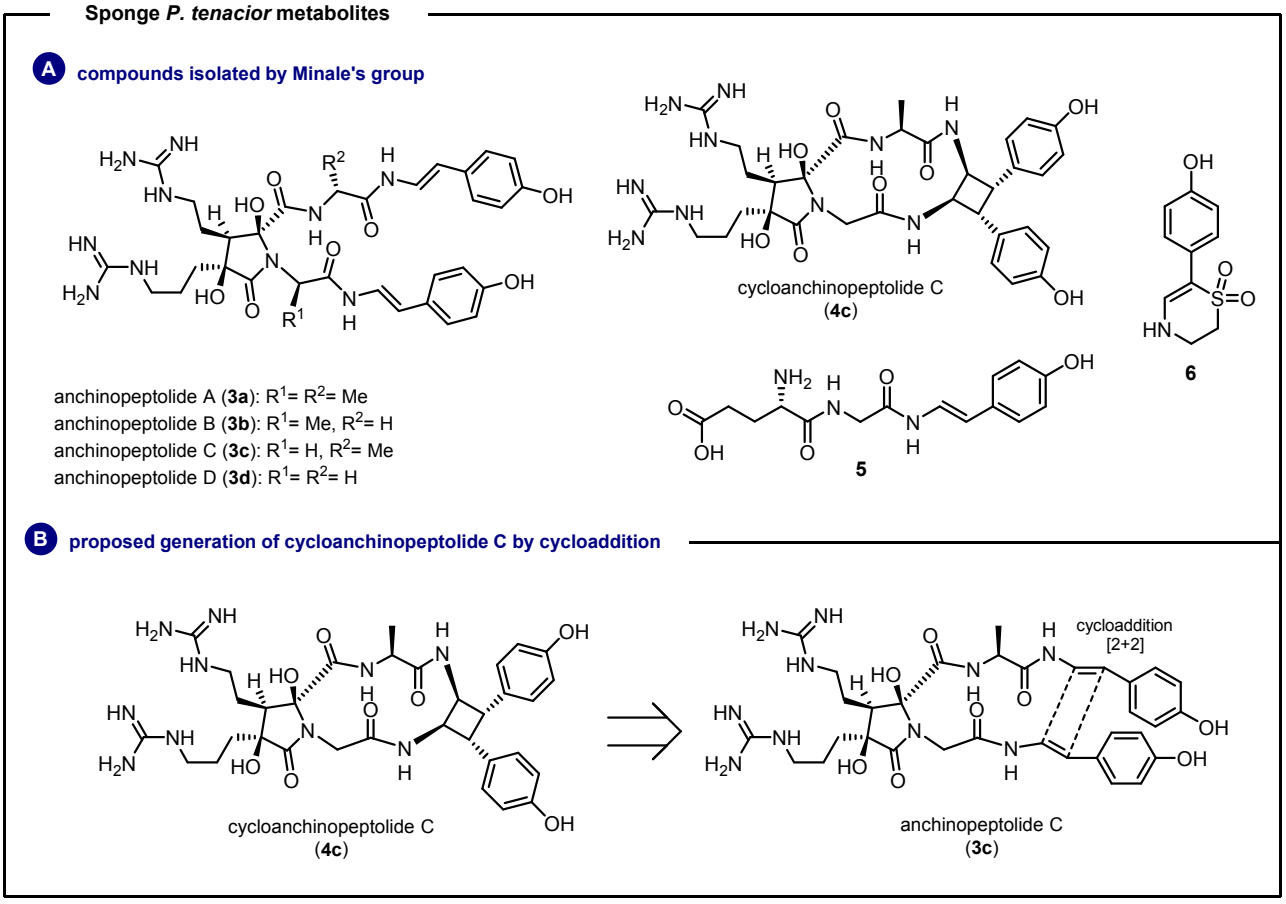

Scheme 1

A biogenic hypothesis to the formation of anchinopeptolides is based on dimerization between two halves of a tripeptide holding residues of L-arginine, L-alanine or glycine, and hydroxystyrylamide, that might come from tyrosine (Scheme 2). The core hydroxy-pyrrolidinone is formed by an aldolization and a subsequent addition of the amide of one half of the tripeptide to the carbonyl group of the second unit.[11, 13]

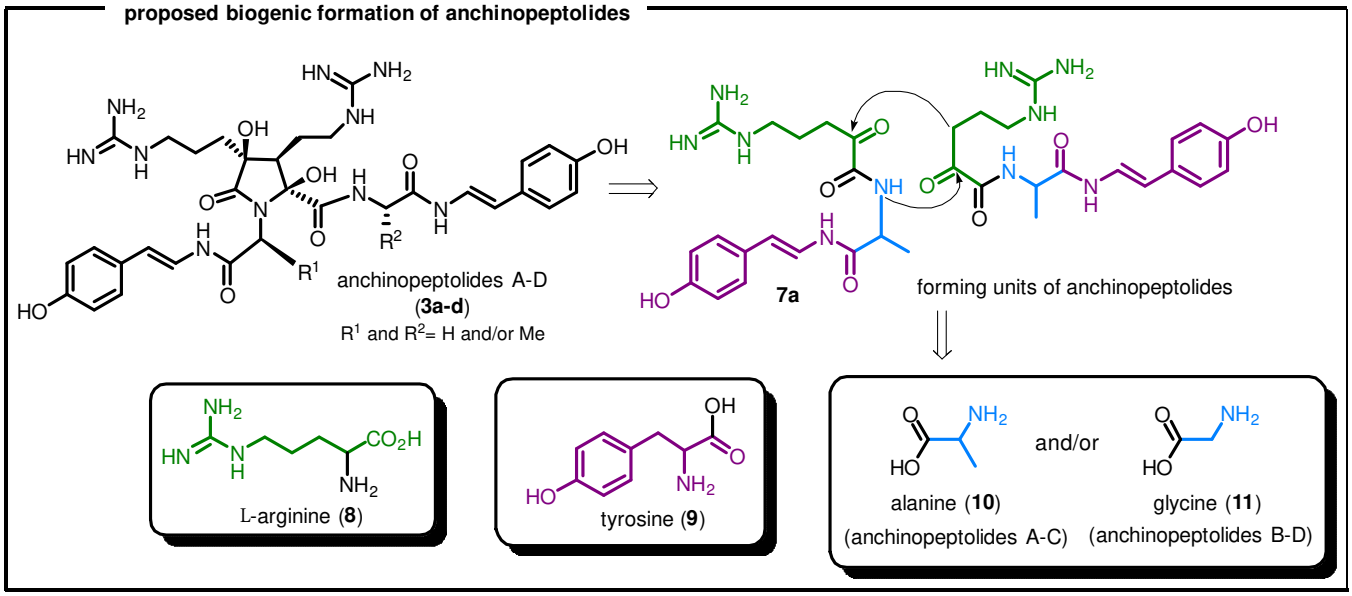

Scheme 2

Based on these works, Snider's group proposed a biomimetic synthesis of anchinopeptolide D in which the key-step is the aldol dimerization of **7b**, a modified structure of tripeptide **7a** (Scheme 3). The preparation of the **unnatural** cycloanchinopeptolide D (**4d**) was achieved by a [2 + 2] photocycloaddition of anchinopeptolide D under mild conditions, giving thereby strong evidence concerning the biosynthesis of natural cycloanchinopeptolide C.[14]

[14] B. B. Snider, F. Song, B. M. Foxman, *J. Org. Chem.* **2000**, *65*, 793-800.

biomimetic synthesis of anchinopeptolide D and cycloanchinopeptolide D (Snider's group)

A **Preparation of fragment 14a**

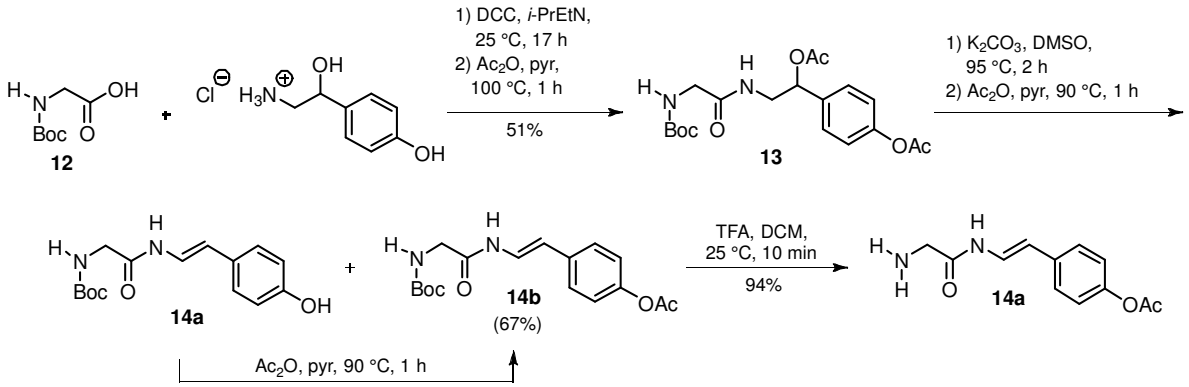

B **formation of anchinopeptolide D**

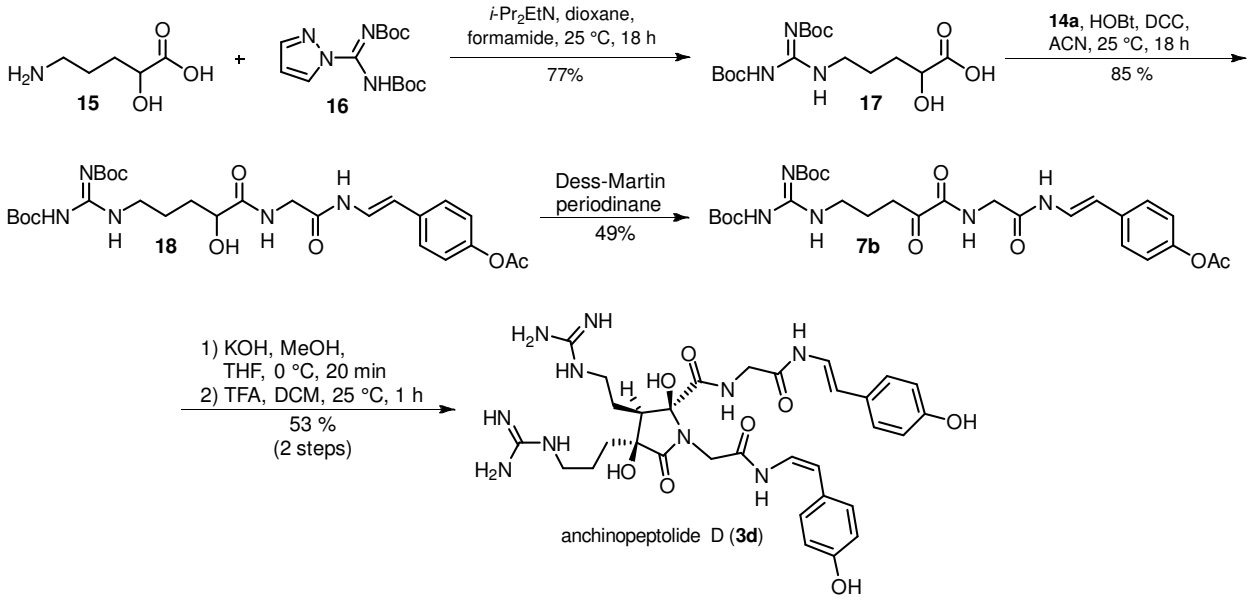

C **cycloaddition of anchinopeptolide D**

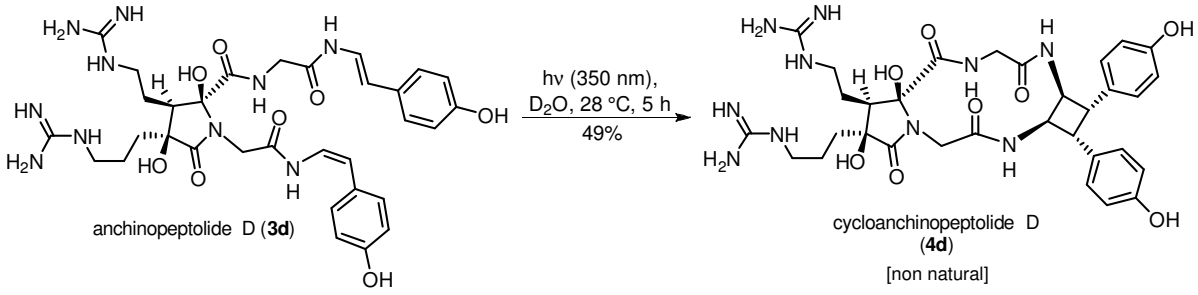

Scheme 3

1. 1. 3 Crambeidae sponges and the guanidine polycyclic alkaloids crambescins, crambescidins and derivatives

Crambeidae is a family of sponges from the Poecilosclerida order. Among the four genera of this family, sponges from the genera *Crambe* and *Monanchora* have been widely studied for their production of a range of polycyclic guanidine alkaloids (PGAs), for instance: crambescins, crambescidins, urupocidins, and monanchocidins. These compounds are chemotaxonomic markers of the Crambeidae family used naturally as animals defense.[15] Therefore, they possess a plethora of biological activities[16,17,18], including *in vitro* HIV inhibition[19]. Representative PGAs structures produced by Crambeidae and related compounds produced by other natural sources are depicted on Scheme 4.[20, 21]

Crambe crambe (Schmidt, 1862) is a marine red incrusting sponge mainly found all across the Mediterranean Sea and now in Macaronesia (Figure 4). This sponge is already known to produce specialized metabolites from two families of alkaloids: crambescins and crambescidins. The crambescidins are pentacyclic PGAs named according to their molecular masses. They display a broad range of biological activities, such as antifungal[22], antimalaria[23], and cytotoxicity against diverse human tumor cell lines[24]. The crambescins are mono- and bicyclic guanidine alkaloids classified into three sub-families: A, B, and C, which differs from the presence of a pyrrolidine ring (A), a spiro-aminal (B), and a 3-hydroxypropyl chain (C). Crambescins presented a more specific activity on ion channels.[25]

[15] R. W. M. Van Soest, in *Systema Porifera: A Guide to the Classification of Sponges* (Eds.: J. N. A. Hooper, R. W. M. Van Soest, P. Willenz), Springer US, Boston, MA, **2002**, pp. 547-555.
[16] Z. D. Aron, H. Pietraszkiewicz, L. E. Overman, F. Valeriote, C. Cuevas, *Bioorg. Med. Chem. Lett.* **2004**, *14*, 3445-3449.
[17] M. Roel, J. A. Rubiolo, J. Guerra-Varela, S. B. Silva, O. P. Thomas, P. Cabezas-Sainz, L. Sanchez, R. Lopez, L. M. Botana, *Oncotarget* **2016**, *7*, 83071-83087.
[18] S. A. Dyshlovoy, K. M. Tabakmakher, J. Hauschild, R. K. Shchekaleva, K. Otte, A. G. Guzii, T. N. Makarieva, E. K. Kudryashova, S. N. Fedorov, L. K. Shubina, C. Bokemeyer, F. Honecker, V. A. Stonik, G. von Amsberg, *Mar. Drugs* **2016**, *14*.
[19] A. Olszewski, K. Sato, Z. D. Aron, F. Cohen, A. Harris, B. R. McDougall, W. E. Robinson, L. E. Overman, G. A. Weiss, *Proc. Natl. Acad. Sci. USA* **2004**, *101*, 14079-14084.
[20] H. Nagarajaiah, A. Mukhopadhyay, J. N. Moorthy, *Tetrahedron Lett.* **2016**, *57*, 5135-5149.
[21] T. N. Makarieva, E. K. Ogurtsova, V. A. Denisenko, P. S. Dmitrenok, K. M. Tabakmakher, A. G. Guzii, E. A. Pislyagin, A. A. Es'kov, V. B. Kozhemyako, D. L. Aminin, Y.-M. Wang, V. A. Stonik, *Org. Lett.* **2014**, *16*, 4292-4295.
[22] J. A. Rubiolo, E. Ternon, H. López-Alonso, O. P. Thomas, F. V. Vega, M. R. Vieytes, L. M. Botana, *Mar. Drugs* **2013**, *11*, 4419-4434.
[23] J. E. H. Lazaro, J. Nitcheu, N. Mahmoudi, J. A. Ibana, G. C. Mangalindan, G. P. Black, A. G. Howard-Jones, C. G. Moore, D. A. Thomas, D. Mazier, C. M. Ireland, G. P. Concepcion, P. J. Murphy, B. Diquet, *J. Antibiot.* **2006**, *59*, 583-590.
[24] J. A. Rubiolo, H. López-Alonso, M. Roel, M. R. Vieytes, O. Thomas, E. Ternon, F. V. Vega, L. M. Botana, *Br. J. Pharmacol.* **2014**, *171*, 1655-1667.
[25] V. Martin, C. Vale, S. Bondu, O. P. Thomas, M. R. Vieytes, L. M. Botana, *Chem. Res. Toxicol.* **2013**, *26*, 169-178.

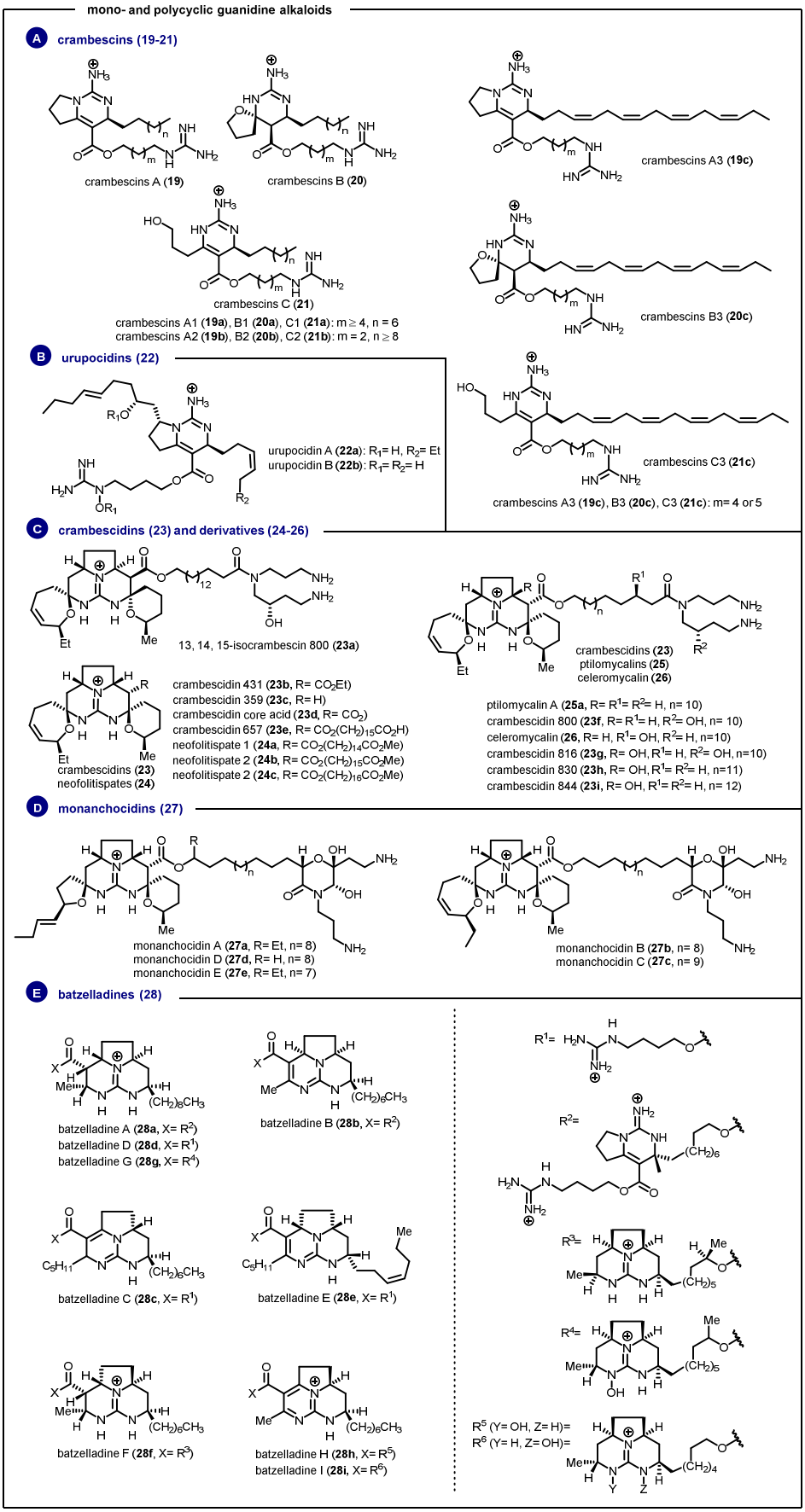
mono- and polycyclic guanidine alkaloids
A crambescins (19-21)
crambescins A (19)
crambescins B (20)
crambescins A3 (19c)
crambescins C (21)
crambescins B3 (20c)
crambescins A1 (19a), B1 (20a), C1 (21a): m ≥ 4, n = 6
crambescins A2 (19b), B2 (20b), C2 (21b): m = 2, n ≥ 8
B urupocidins (22)
urupocidin A (22a): R1= H, R2= Et
urupocidin B (22b): R1= R2= H
crambescins C3 (21c)
crambescins A3 (19c), B3 (20c), C3 (21c): m= 4 or 5
C crambescidins (23) and derivatives (24-26)
13, 14, 15-isocrambescin 800 (23a)
crambescidin 431 (23b, R= CO2Et)
crambescidin 359 (23c, R= H)
crambescidin core acid (23d, R= CO2)
crambescidin 657 (23e, R= CO2(CH2)15CO2H)
neofolitispate 1 (24a, R= CO2(CH2)14CO2Me)
neofolitispate 2 (24b, R= CO2(CH2)15CO2Me)
neofolitispate 2 (24c, R= CO2(CH2)16CO2Me)
crambescidins (23)
neofolitispates (24)
crambescidins (23)
ptilomycalins (25)
celeromycalin (26)
ptilomycalin A (25a, R= R1= R2= H, n= 10)
crambescidin 800 (23f, R= R1= H, R2= OH, n= 10)
celeromycalin (26, R= H, R1= OH, R2= H, n=10)
crambescidin 816 (23g, R= OH, R1= H, R2= OH, n=10)
crambescidin 830 (23h, R= OH, R1= R2= H, n=11)
crambescidin 844 (23i, R= OH, R1= R2= H, n= 12)
D monanchocidins (27)
monanchocidin A (27a, R= Et, n= 8)
monanchocidin D (27d, R= H, n= 8)
monanchocidin E (27e, R= Et, n= 7)
monanchocidin B (27b, n= 8)
monanchocidin C (27c, n= 9)
E batzelladines (28)
batzelladine A (28a, X= R2)
batzelladine D (28d, X= R1)
batzelladine G (28g, X= R4)
batzelladine B (28b, X= R2)
batzelladine C (28c, X= R1)
batzelladine E (28e, X= R1)
batzelladine F (28f, X= R3)
batzelladine H (28h, X= R5)
batzelladine I (28i, X= R6)
R1=
R2=
R3=
R4=
R5 (Y= OH, Z= H)=
R6 (Y= H, Z= OH)=

Scheme 4

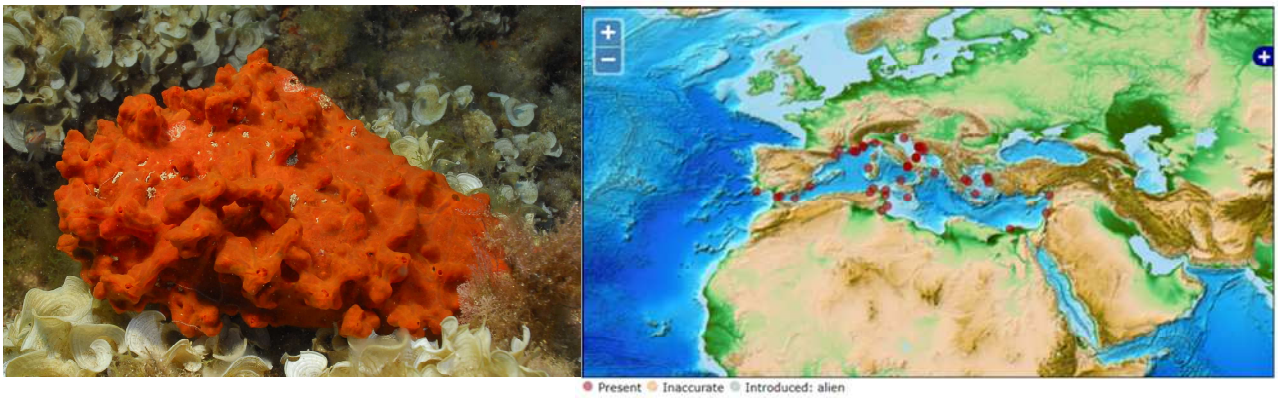

Figure 4. *Crambe crambe* (left) and its natural distribution (right)

Crambe tailliezi (Vacelet and Boury-Esnault, 1982) is an incrusting creamy sponge found in the Mediterranean and Macaronesian areas (Figure 5), where its abundance seems to increase along the French Riviera (between 15 and 40 m)[26]. Even if the sister species *C. crambe* has been largely chemically studied leading to bioactive guanidine alkaloids, there is no report concerning the isolation and identification of metabolites from *C. tailliezi*.

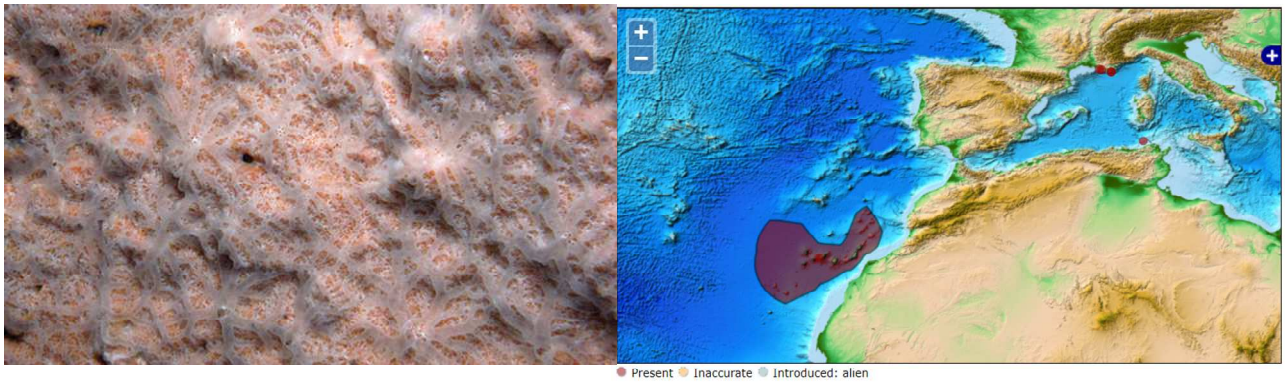

Figure 5. Sponge *C. tailliezi* (left) and its geographic distribution (right)

1. 2 Objectives of this Project

This project aimed at the description of complex guanidine alkaloids produced by Poecilosclerida Mediterranean sponges in order to discovery new structures and fully characterize the already described compounds. We also performed a big scale purification of *C. crambe* sponge in order to provide crambescidins and crambescins for biological studies in collaboration with

[26] J. Vacelet, N. Boury-Esnault, *Trav. Sci. Parc Natl. Port-Cros* **1982**, *8*, 107-113.

pharmacologists.

The general isolation procedure used in this project is depicted on Figure 6. The freeze-dried sponges were initially fractionated by Vacuum Liquid Chromatography (VLC) for desalting and the separation of hydrophilic compounds from lipophilic ones. All the fractions obtained from VLC were submitted to ^{1}H-NMR and to analytical Ultra Pressure Liquid Chromatography (UPLC)-DAD-ELSD to identify the class of compounds present in each sample. As our goal was to isolate alkaloids, only fractions with these compounds were purified by HPLC.

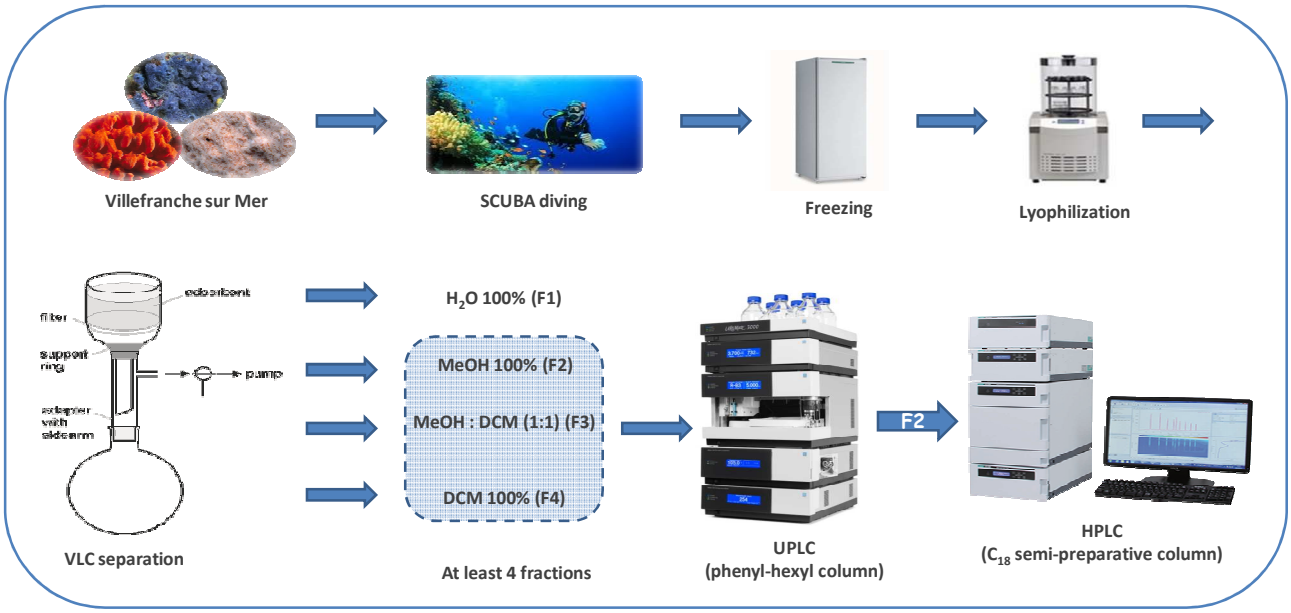

Figure 6. General methodology used for the isolation of alkaloids from Poecilosclerida sponges

1. 3 Results and Discussion

1. 3. 1 Identification of specialized metabolites produced by *P. tenacior*

We decided to first perform the complete chemical study of the sponge *Phorbas tenacior*. In addition to the compounds previously described (anchinopeptolides A-D, **3a-d**) and **5**, we found a new compound named ***epi*-anchinopeptolide C** (Figure 7, **3e**). Curiously, we did not find cycloanchinopeptolide C (**4c**) during the purification process.

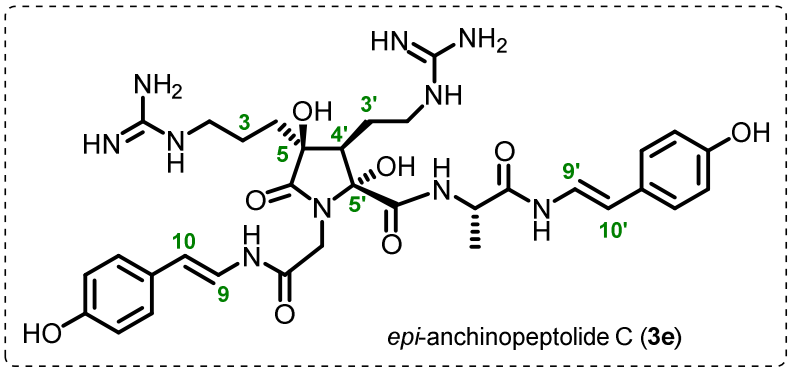

Figure 7. Structure of the new compound *epi*-anchinopeptolide C isolated from *P. tenacior*

The ^{1}H-NMR spectrum of this compound is similar to the one of anchinopeptolide C, with the main difference being in the signal of H-4' (dd at 2.72 ppm in spectrum of **3c** and a dd at 2.37 ppm in **3e**, Figure 8). The NOESY spectrum of **3e** in DMSO-d_6 did not show the cross peaks between 5-OH and 5'-OH protons, neither the correlations between the 3'-methylene protons and both the OH protons that were described to anchipeptolides[11, 12], suggesting that **3e** has a different relative configuration. In the NOESY spectrum of **3e** (Figure 9) cross-peaks between H-4' and H-3, H-4' and H-2, as well as H-4' and 5'-OH were observed, confirming that H-4' is in *cis* relative configuration with the side chain at C-5 and with the OH at C-5'. Trying to epimerize **3c** in acidic medium failed to give **3e** then suggesting that this compound is not formed during the purification process.

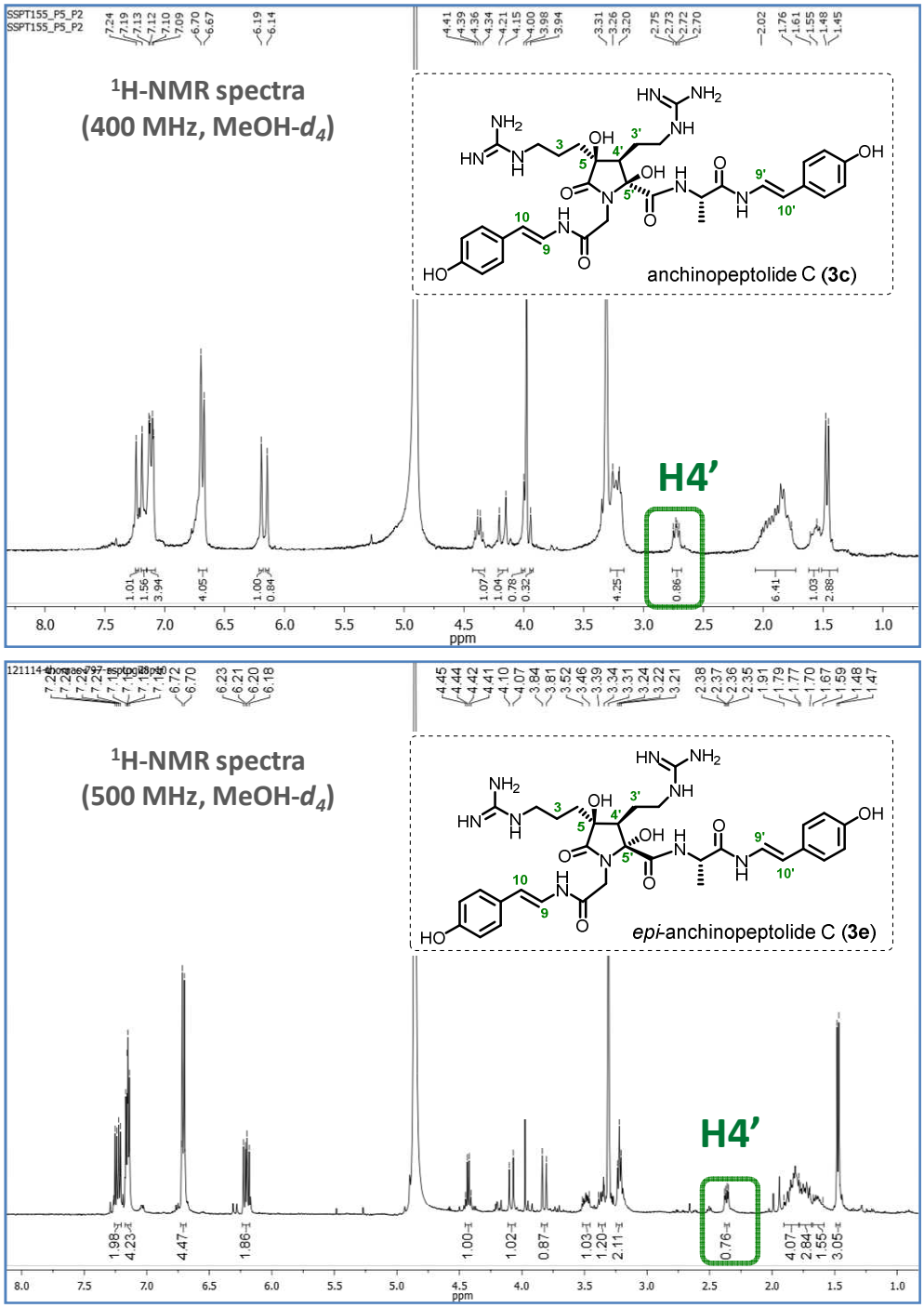

Figure 8. Comparison between the ^{1}H-NMR spectra of anchinopeptolide C and *epi*-anchinopeptolide C

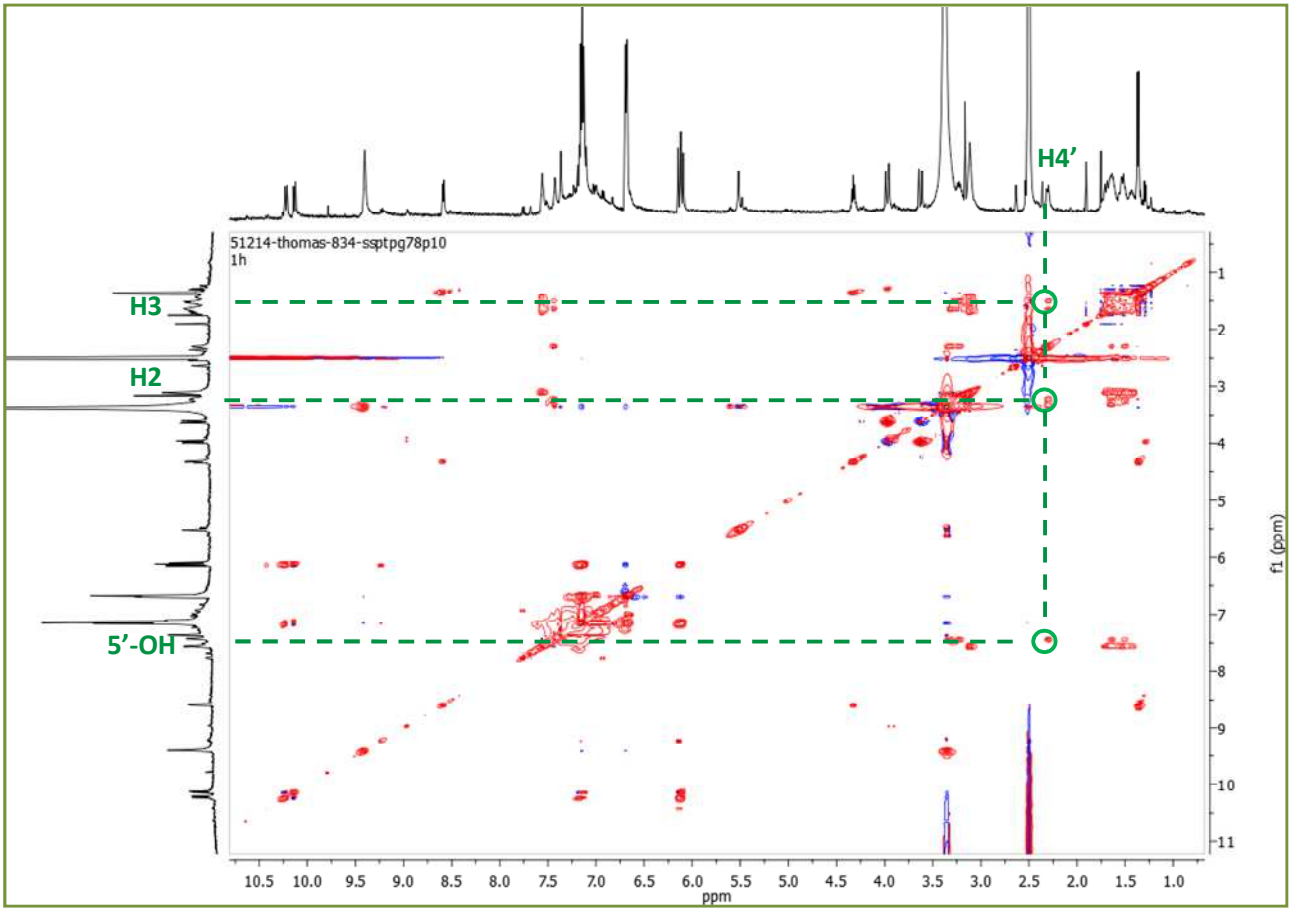

Figure 9. NOESY (DMSO-d_6, 500 MHz) spectra of *epi*-anchinopeptolide C (**3e**)

As the absolute configuration of anchinopeptolides is not described, we performed the circular dichroism analysis of anchinopeptolides A and C-D. The data analyses as well as the computational calculations of these molecules have been performed by our collaborator Dr. Grégory Genta-Jouve (Université Paris Descartes). The results are currently being processed.

To finalize the structure and the absolute configuration of cycloanchinopeptolide C, we attempted the cycloaddition of anchinopeptolide C (**3c**) in similar conditions that Snider's group used to prepare cycloanchinopeptolide D. After irradiation of **3c** with a UV-B enriched lamp that mimics sunlight (lamps ReptiSun 10.0 ZOOMED® UV-B (10%) 26W) for 23 h the ^{1}H-NMR signals correspondent to H-9, H-9', H-10 and H-10' (signals at 6.2 and 7.2 ppm) decreased and new signals on the region of 4 ppm appeared, what indicated the formation of the cycloaddition product (Figure 10). This product was purified by preparative HPLC, furnishing the desired cycloanchinopeptolide C (**4c**) as a white solid, in 17% of yield (2.3 mg).

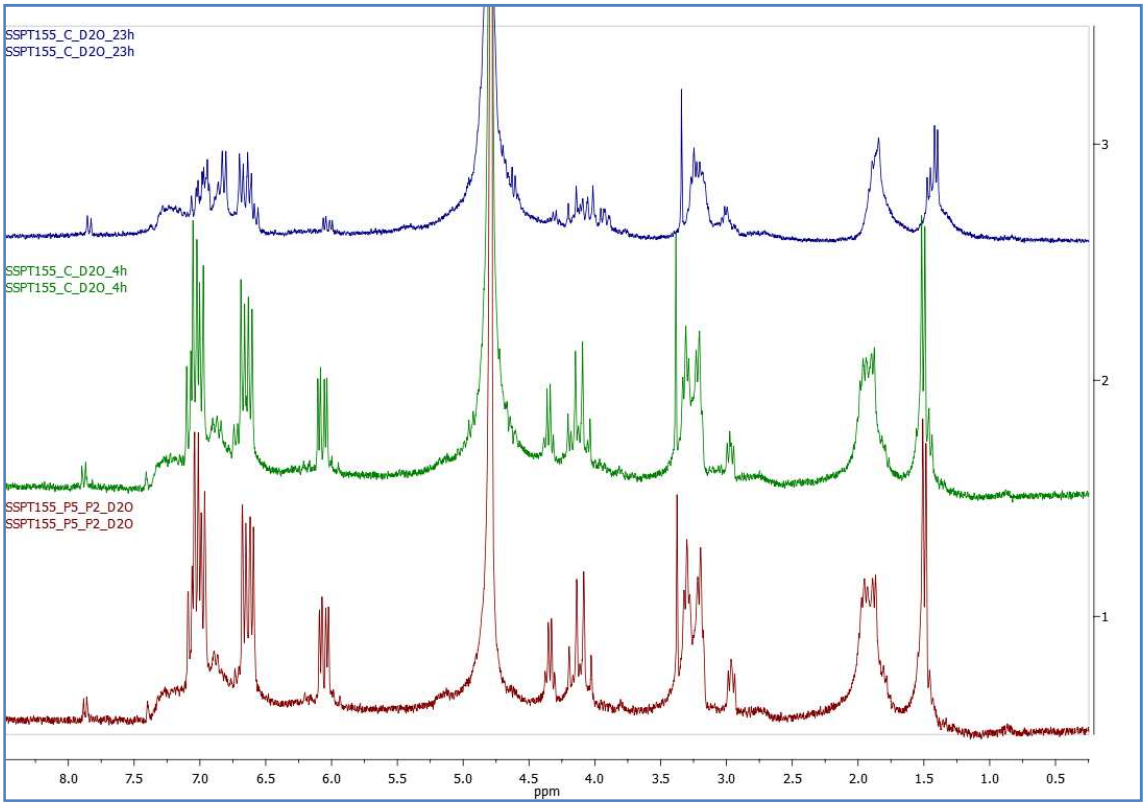

Figure 10. Comparison of ^{1}H-NMR spectra of anchinopeptolide C (**3c**) after 23 h and 4 h of artificial sunlight irradiation (top and middle, in D_2O) and before the irradiation (bottom, in D_2O)

The attributions of the compound **4c** obtained by hemisynthesis are in complete agreement with the literature data[13] available for the compound isolated from the natural source (Figure 11). The signals corresponding to the carbons of the cyclobutane appear in the region of 50 ppm and in the ^{1}H-NMR spectrum the hydrogens of this cycle has signals between 4 and 4.8 ppm. The easy generation of cycloanchinopeptolide C by photocyclization of anchinopeptolide C indicates that this compound can be an artefact produced by, for example, drying the samples under the sunlight during the purification process. The determination of the absolute configuration of the cyclobutane moiety by circular dichroism is an ongoing work.

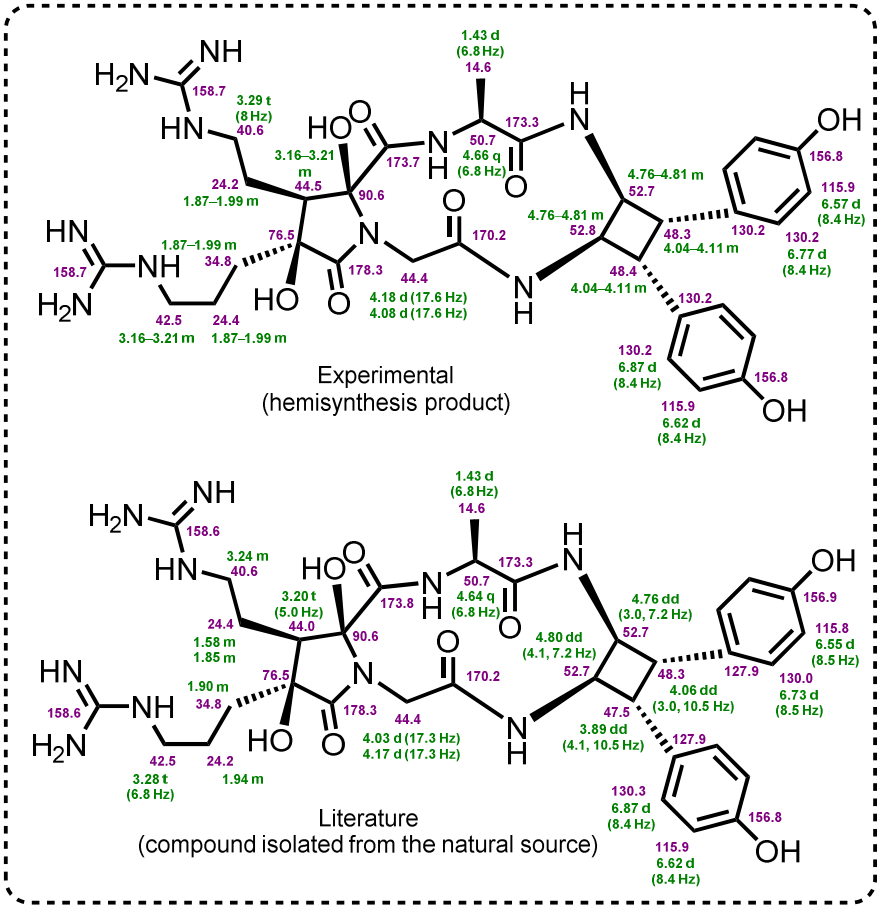

Figure 11. Comparison between the attributions of cycloanchinopeptolide C obtained by hemisynthesis with the data from the literature

1. 3. 2 Isolation of specialized metabolites produced by *C. tailliezi*

The crude extract (DCM : MeOH, 1 : 1) of *C. tailliezi* was eluted by VLC furnishing 7 fractions, namely: F1 (100% H_2O), F2 (H_2O : MeOH, 1 : 1), F3 (H_2O : MeOH, 1 : 2), F4 (H_2O : MeOH, 1 : 3), F5 (100% MeOH), F6 (MeOH : DCM, 1 : 1), and F7 (100% DCM). The UPLC analyses of F2-F6 resulted in similar profiles for F2 and F3. Applying the method previously described (Figure 6), we observed peaks in the region where alkaloids usually come out (R_t: 6.5-8 min, Figure 13). The ^{1}H-NMR spectra of these fractions (Figure 12) confirmed the presence of guanidine alkaloids with caracteristic signals at the region of 3.2 and 4.0 ppm (typical of hydrogens alpha to amines and guanidines). The signals at 5.5 ppm are very similar to the ones generated by the hydrogens of the double bond present on the seven membered ring of crambescidins and analogues (**23**-**26**, Scheme 4). The fractions F4-F6 were composed mainly by nonpolar compounds (R_t: 9-12 min), probably fatty acids and steroids.

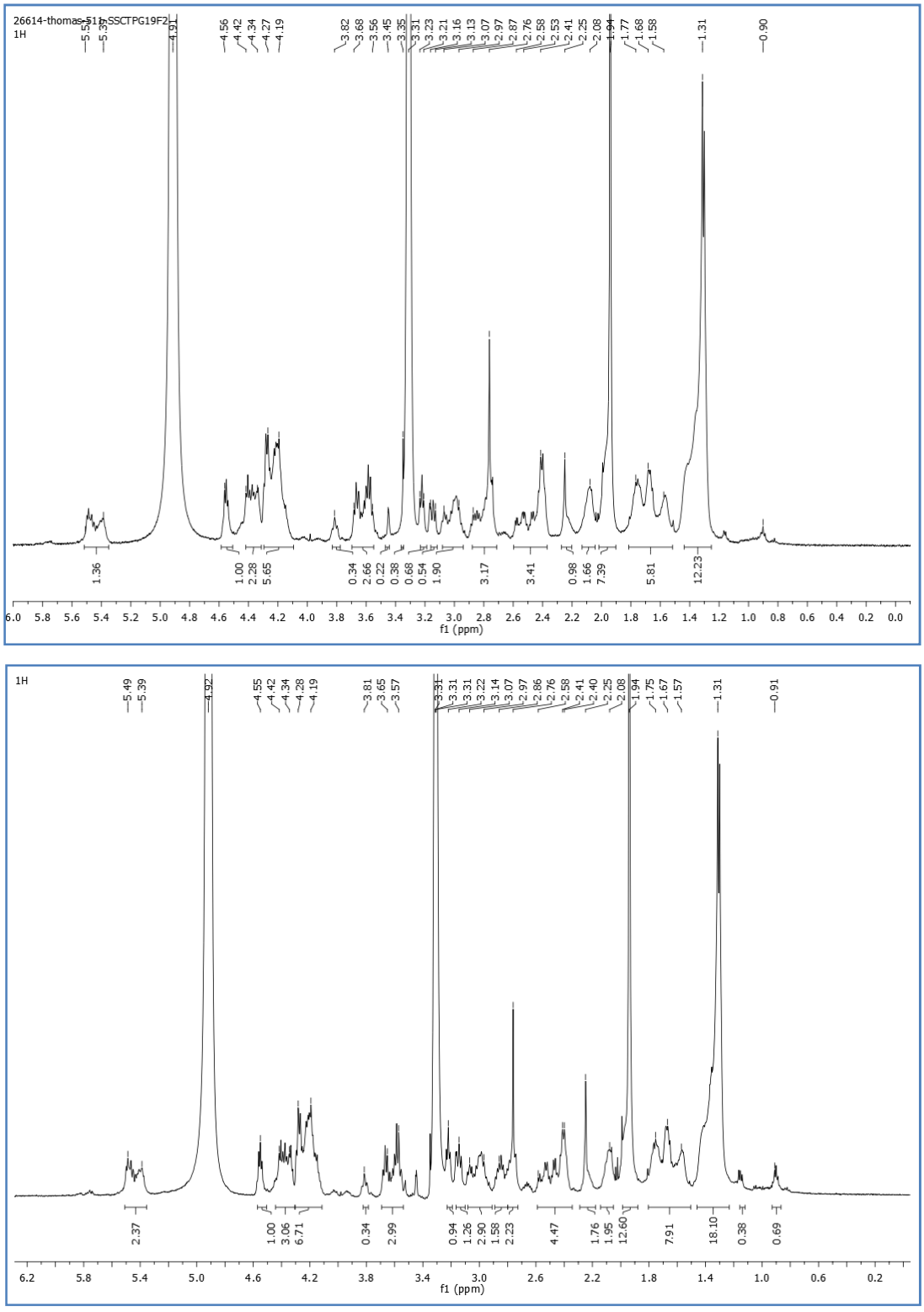

Figure 12. ^{1}H-NMR of fractions F2 (top) and F3 (bottom) of *C. tailliezi* in MeOD-d_4

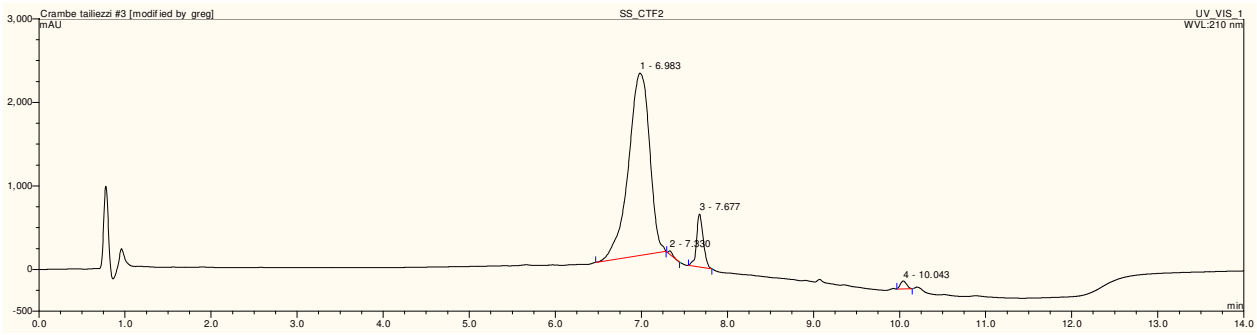

Figure 13. UPLC chromatogram profile of F2 (210 nm)
Conditions: UPLC Ultimate 3000 Dionex, column Phenomenex Kinetex 1.7 µm phenyl-hexyl (100 x 2.10 mm), mobile phase: H_2O : ACN : TFA. Elution: isocratic 0-2 min (90 : 10 : 0.1), gradient 2-8 min (from 90 : 10 : 0.1 to 0 : 100 : 0.1), isocratic 8-10 min (0 : 100 : 0.1) and gradient 10-14 min (from 0 : 100 : 0.1 to 90 : 10 : 0.1) (flow: 0.5 mL.min^{-1}, injection volume: 5 mL, concentration: 10 mg.mL^{-1}).

Considering the outstanding alkaloid diversity isolated from Crambeidae sponges, such as crambescins and crambescidins produced by *C. crambe*, we decided to purify the fractions F2 and F3. Some of the assayed conditions are showed on Table 1. The initial attempts were performed with standard methods and according to the preliminary results, column and elution were modified.

Table 1. Conditions tested on the purification of F2 and F3

Entry	Conditions*	Mobile phase
1	XSelect CSH Prep Phenyl-Hexyl 5 µm OBD	H_2O : ACN : TFA (0.1%)
2	XSelect CSH Prep Phenyl-Hexyl 5 µm OBD	H_2O : ACN : AcOH (0.05%)
3	XSelect CSH Prep Phenyl-Hexyl 5 µm OBD	H_2O : MeOH : AcOH (0.05%)
4	XSelect CSH Prep C18 5 µm	H_2O : ACN : TFA (0.1%)
5	Symmetry C18 Prep 7 µM	H_2O: MeOH : AcOH (0.05%)
6	Nucleodur C18 Htec 5 µM	H_2O : ACN
7	Nucleodur C18 Htec 5 µM	H_2O : ACN : TFA (0.01%)
8	Nucleodur C18 Htec 5 µM	H_2O : ACN: TFA (0.1%)
9	Nucleodur C18 Htec 5 µM	H_2O : MeOH : TFA (0.1%)
10	Nucleodur C18 Htec 5 µM	H_2O : ACN : Formic Acid (0.1%)
11	XSelect CSH Prep Fluoro-Phenyl 5 µM	H_2O : ACN : TFA (0.1%)

*Elution: Semi-preparative columns - isocratic 0-4 min (90 : 10), gradient 4-28 min (from 90 : 10 to 0 : 100), isocratic 28-30 min (0 : 100), gradient 30-32 min (from 0 : 100 to 90 : 10) and isocratic 32-34 min (90 : 10) (flow: 3-4 mL.min^{-1} , injection volume: 10 mL, concentration: 100 mg.mL^{-1}). Preparative columns - isocratic 0-2 min (90 : 10), gradient 2-15 min (from 90 : 10 to 0 : 100), isocratic 15-18 min (0 : 100), gradient 18-20 min (from 0 : 100 to 90 : 10) and isocratic 20-22 min (90 : 10) (flow: 10 mL.min^{-1}, injection volume: 20 mL, concentration: 100 mg.mL^{-1}). Equipment: Jasco LC-4000.

Although no condition has provided a satisfactory resolution between the peaks, the purification of F2 was performed as indicated in entry 4, using the following elution: isocratic 0-3 min (65 : 35 : 0.1), gradient 3-15 min (from 65 : 35 : 0.1 to 60 : 40 : 0.1), gradient 15-17 min (from 60 : 40 : 0.1 to 40 : 60 : 0.1), isocratic 17-20 min (40 : 60 : 0.1), gradient 20-22 min (from 40 : 60 : 0.1 to 65 : 35 : 0.1) and isocratic 22-25 min (65 : 35 : 0.1) (flow: 10 mL.min^{-1} , injection volume: 200 mL, concentration: 100 mg.mL^{-1}). Similar results were obtained with F3.

The chromatogram (Figure 14) was separated in 14 peaks. Peaks F2P3-P8 presented almost the same NMR spectra (Figure 15), with absence of the characteristic methyl groups present in crambescidins, crambescins and ptilomycalins identified by signals between 0.8 and 1.2 ppm. After comparing such spectra with literature, we concluded that *C. tailliezi* produces a distinct family of alkaloids.

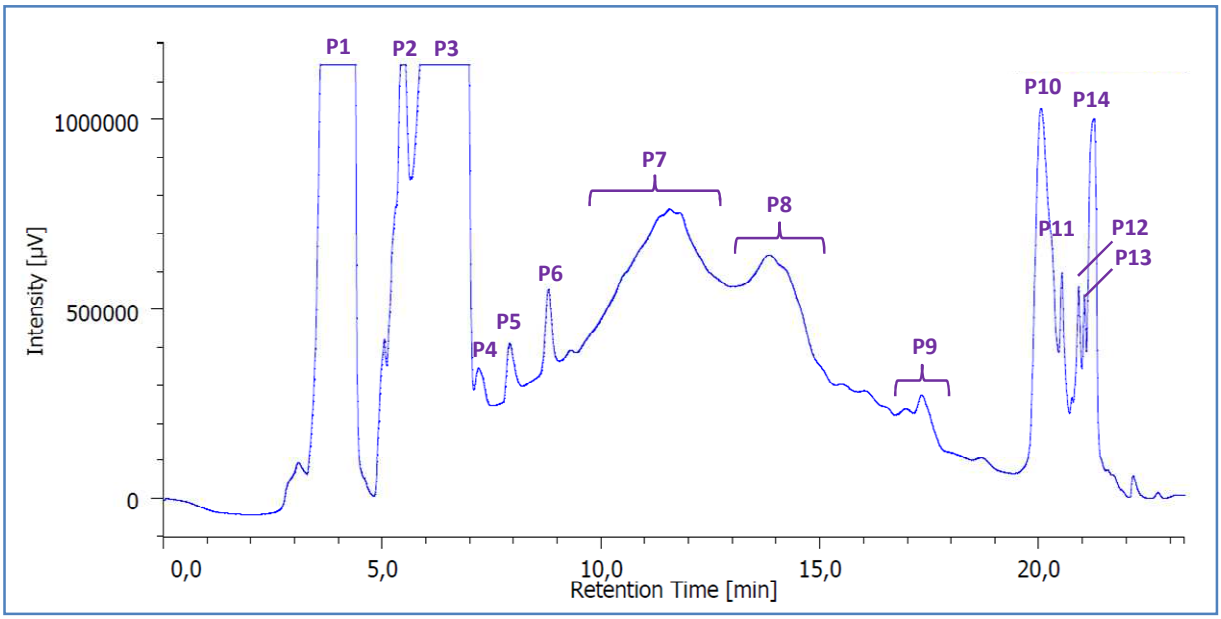

Figure 14. Chromatogram of F2 in preparative HPLC

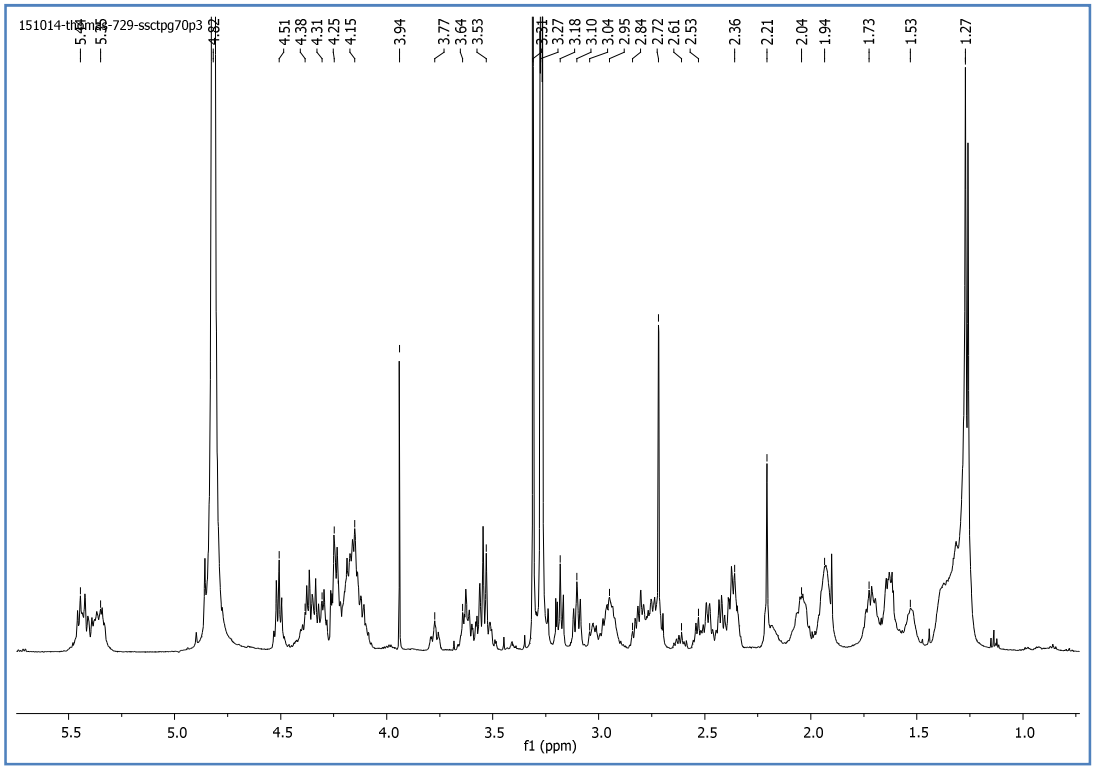

Figure 15. ^{1}H-NMR spectrum (500 MHz – MeOH-d_4) of F2P3

The peak F2P3 was submitted to a set of NMR experiments (1D: ^{1}H and ^{13}C, 2D: COSY, NOESY, TOCSY, HMBC and HSQC), leading us to recognize guanidine fragments similar to the ones present in batzelladines and especially the methyl doublet at 1.27 ppm[27] (Figure 16). This would be the first report of batzelladine derivatives in a Mediterranean sponge, as most of them are found in Caribbean species of the genus *Batzella* or *Monanchora*. Although the structure of this major compound seemed highly promising we could not go further due to the impossibility to obtain a pure compound from this mixture.

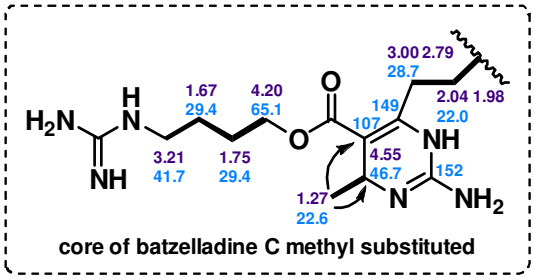

Figure 16. Fragment of batzelladine discovered in F2P3

[27] R. Laville, O. P. Thomas, F. Berrué, D. Marquez, J. Vacelet, P. Amade, *Journal of Natural Products* **2009**, *72*, 1589-1594.

The NMR and HRMS (Figure 17) analyses of F2P10-P14 allowed the identification of the already described compounds crambescidin 816 (**23g**) and crambescidin 800 (**23f**) (Scheme 4). It is worth noticing that *C. crambe* and *C. tailliezi* share common secondary metabolites.

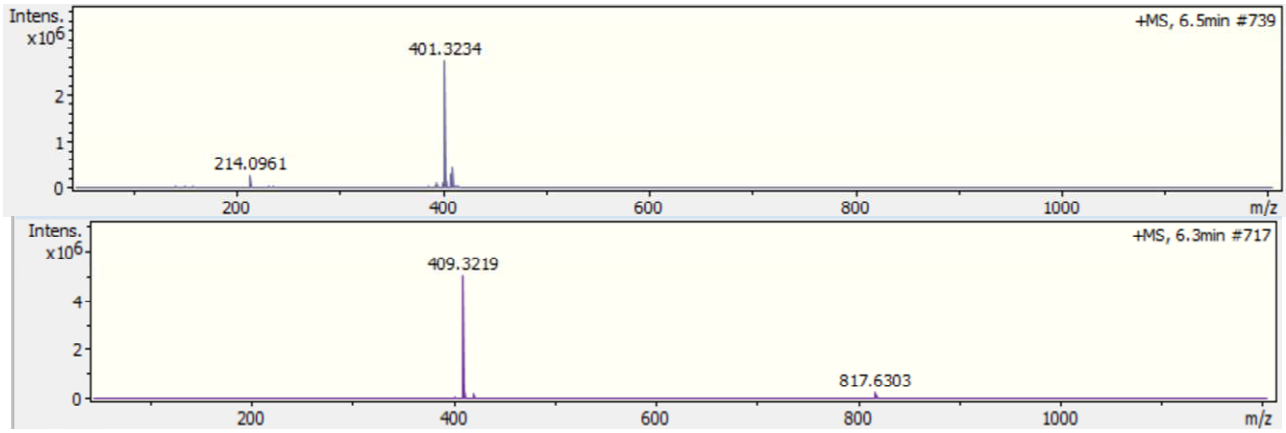

Figure 17.HRMS spectra of crambescidins 800 (**23f**, calcd for $[C_{45}H_{82}N_6O_6]^{2+}$= 401.3142) (above, F2P12) and 816 (**23g**, calcd for $[C_{45}H_{81}N_6O_7]^{+}$= 817.6161) (bellow, F2P14)

Conditions: UPLC Ultimate 3000 Dionex equipped with an autosampler and a Dionex Ultimate 3000 diode array dual absorbance wavelength detector (210 and 280 nm), linked to QT of mass spectrometer fitted with an electrospray ionization interface (Bruker Impact II). Mass spectra were recorded in the positive mode. UPLC conditions: column Nucleodur PolarTec column (100 x 2 mm, 1.8 µm, Macherey Nagel). Linear elution gradient of H_2O : ACN : formic acid to which was added 10 mM of ammonium formate from 80 : 20 : 0.1 (isocratic from 0 to 2 min) to 40 : 60 : 0.1 (isocratic from 8 to 10 min), flow rate: 0.45 mL.min^{-1} for a total of 14 min. Injected volume: 10 µL. Detection: 280 nm.

1. 3. 3 Purification of *C. crambe* sponge

The purification of 24 g of freeze-dried *C. crambe* sponge was performed by the procedure showed on Figure 6. Crambescins and crambescidins were sent to diverse biological assays[17, 28] in collaboration with professor Botana's group (University of Santiago de Compostela). In one of this studies, it was showed that crambescidins 800 (**23f**), 816 (**23g**), and 830 (**23h**) (Scheme 4) strongly inhibited colorectal tumor cell proliferation using *in vivo* zebrafish model.[17] Aside the biological application, crambescins C1 and A2 isolated by this project were used as standards for HPLC and NMR analyses required during our biosynthesis and biomimetic synthesis studies (chapters 2 and 3).

[28] A. G. Mendez, A. B. Juncal, S. B. L. Silva, O. P. Thomas, V. Martín Vázquez, A. Alfonso, M. R. Vieytes, C. Vale, L. M. Botana, *ACS. Chem. Neurosci.* **2017**, *8*, 1609-1617.

1. 4 Conclusions and perspectives

In this part, we described the identification of a new compound isolated from the Mediterranean sponge *Phorbas tenacior*. The compound (**3e**) is an epimer of the previously described anchinopeptolide C (**3c**). We also performed the cycloaddition of anchinopeptolide C (**3c**) to access cycloanchinopeptolide C (**4a**), that was absent during our purification. These compounds will have their absolute configuration determined by circular dichroism analyses.

The purification of *C. tailliezi* was a very challenging task and, unfortunately, we were not able to isolate and identify any new derivative. However, we identified crambescidin 816 (**23g**) and crambescidin 800 (**23f**), compounds previously isolated from *C. crambe*, as well as a mixture of new alkaloids containing similar guanidine fragments found in batzelladines. To the best of our knowledge, it is the first time that batzelladines analogs are observed in a Mediterranean sponge.

The purification of *C. crambe* sponge furnished a range of crambescins and crambescidins that valorized the potential biotechnological application of these compounds and furnished standards for the biosynthesis and biomimetic synthesis studies that will be discussed on next chapters. Crambescidins 800 (**23f**), 816 (**23g**), and 830 (**23h**) were discovered as potent carcinoma inhibitors on a *in vivo* animal model.[17]

Chapter 2. ^{14}C-Feeding Experiments with *C. crambe*: First Insights into the Biosynthesis of Crambescin C1

2. 1 Introduction

2. 1. 1 Marine sponges and biosynthetic studies

Physical-chemical peculiarities of seawater such as buffered pH (between 8.2 to 8.5), high saline concentration (up to 40%), and osmotic pressure of 15-25 atm create special conditions to an evolution of specialized marine metabolites.[29,30] As sponges are sessile animals, their specialized metabolites are supposed to also have the role of chemical cues, being responsible for ecological communications with the environment and ensuring the development and defense of the whole organism[31].

Despite the evident interest on the isolation, structural elucidation and application of sponge natural products, knowledge regarding their biosynthetic pathways is scarce. Conceptually a biosynthetic pathway is the sequence of chemical transformations that converts a substrate into a more complex product inside a living metabolism.[32]

Sponges are early metazoans with a long evolutionary history and produce an outstanding chemical diversity. Hence, the understanding of sponges metabolites biogenetic origin can help in the identification of the genes involved in their specialized metabolic pathways, furnishing some clues about their evolution.[33] On pathways where enzymatic control is not crucial, research on specialized metabolite biosynthesis may inspire the development of biomimetic or biomimicry synthetic approaches based on spontaneous reactions.[34] Moreover the identification and isolation of a specific gene will allow its expression within a heterologous organism[35,36], rendering feasible a commercial scale production of bioactive metabolites.

The starting point to a biosynthetic study is to imagine and to draw a sequence of reactions involved in the production of a target metabolite. This hypothesis can be based on previously described biosynthetic pathways and/or on comparisons with similar metabolites (produced by the same organism or different ones). Subsequently it is necessary to demonstrate that the suggested substrate is converted into the metabolite by the living organism or enzymes. A classical

[29] M. J. Garson, *Nat. Prod. Rep.* **1989**, *6*, 143-170.
[30] G. Genta-Jouve, O. P. Thomas, *Phytochem. Rev.* **2013**, *12*, 425-434.
[31] E. Ternon, L. Zarate, S. Chenesseau, J. Croué, R. Dumollard, M. T. Suzuki, O. P. Thomas, *Sci. Rep.* **2016**, *6*, 29474.
[32] P. M. Dewick, in *Medicinal Natural Products*, John Wiley & Sons, Ltd, **2009**, pp. 7-38.
[33] G. Genta-Jouve, O. P. Thomas, in *Advances in Marine Biology, Vol. 62* (Eds.: Mikel A. Becerro, Maria J. Uriz, Manuel Maldonado, Xavier Turon), Academic Press, **2012**, pp. 183-230.
[34] E. Gravel, E. Poupon, *Eur. J. Org. Chem.* **2008**, 27-42.
[35] M. Pozzolini, S. Scarfì, F. Mussino, S. Ferrando, L. Gallus, M. Giovine, *Mar. Biotechnol.* **2015**, *17*, 393-407.
[36] Y. Takeshige, Y. Egami, T. Wakimoto, I. Abe, *Mol. BioSyst.* **2015**, *11*, 1290-1294.

approach to achieve this goal is to feed, inject or grow the host organism with an isotopic labelled precursor. After the incorporation time, the metabolite of interest is isolated, purified and analyzed to detect the presence of the isotope. Identification of a product labelled in specific positions will provide experimental data to understand how the precursor is incorporated into the final product. To evaluate the origin of each fragment from a target molecule, consecutive incorporation experiments may be necessary[32], as well as genetic and enzymatic studies. As a consequence the complete elucidation of a biosynthetic pathway may demand long investigation and the involvement of researchers from diverse fields.[37]

2. 1. 2 Difficulties associated to sponge feeding experiments

Most of the available hypotheses on the biosynthesis of sponge metabolites arise from pathways already described on terrestrial organisms. Unfortunately, the peculiarities of marine environment and the difficulties to adapt and cultivate sponges in controlled aquaria conditions represent hurdles to experimental validation of biosynthetic hypotheses. The main challenges of the sponge biosynthetic studies are presented below[29, 30, 38]:

- ✓ Sponges often produce a complex chemical diversity in which the desired metabolites are usually present in small quantities.

- ✓ Environmental conditions can change animals metabolic profile and the concentration of a desired metabolite. *In situ* protocols are prone to weather and tide interferences, as well as seasonal modifications of seawater composition. Experiments in laboratory, even if more controlled, will subject the animals to stressing and artificial conditions during their collection, transport and confinement in aquaria.

- ✓ The metabolic turnover in sponges is apparently slow, although no clear kinetic study proved this conclusion.[30] Thus biosynthetic experiments would require long feeding periods for a detectable precursors incorporation. However not all sponge species survive in aquaria for many days.

[37] A. L. Lane, B. S. Moore, *Nat. Prod. Rep.* **2011**, *28*, 411-428.
[38] M. J. Garson, *Chem. Rev.* **1993**, *93*, 1699-1733.

- ✓ Incorporation rate of precursors is usually low and they need to be detected among a high concentration of non-labelled material. It is important to emphasize that some precursors like amino acids can be involved in both primary and specialized metabolism, reducing even more the incorporation.

- ✓ Precursors concentration should be maintained close to natural occurrence of aminoacids and sugars in oceans (around 0 - 25 mg.dm^{-3}) to avoid any modifications of metabolic pathways caused by an overload of substrate or an intoxication by an exogenous substance. Considering this precursors dilution requirement, the incorporation will take place against a concentration gradient.

- ✓ Precursors must be available in a form that allows them to be transported intact into the cells where the metabolites will be synthesized. Considering that the seawater is a polar environment and that cellular membranes are lipid bilayers, differences in hydrophilicity can pose difficulties to the precursors transportation to metabolization sites. An alternative could be the addition of surfactants to facilitate the incorporation.

- ✓ Sponges create symbiotic associations with micro-organisms and in many cases the specific metabolites arise, at least partially, from these associations. There are few descriptions of sponge specialized metabolites isolated from the cultured microbial symbiont[39] but several specialized metabolites share structural similarities with microbial fermentation products[40]. Sponges can also accumulate metabolites produced by algae, microalgae or even other invertebrates as a mechanism of auto-defense.[40] Whilst all of the influences of the microbial population to the metabolism of sponges are still unclear, microbial associations should be maintained as near as possible from natural conditions during the feeding experiments in order to ensure the host fitness and its natural metabolic profile.[30]

[39] K. J. Nicacio, L. P. Ióca, A. M. Fróes, L. Leomil, L. R. Appolinario, C. C. Thompson, F. L. Thompson, A. G. Ferreira, D. E. Williams, R. J. Andersen, A. S. Eustaquio, R. G. S. Berlinck, *J. Nat. Prod.* **2017**, *80*, 235-240.

[40] B. S. Moore, *Nat. Prod. Rep.* **2006**, *23*, 615-629.

The influence of so many factors makes difficult the repeatability of a biosynthetic experiment. Nevertheless, feeding experiments are still a direct way to obtain initial experimental evidences toward the elucidation of a metabolic biosynthetic pathway.

2. 1. 3 Detection Techniques

The first element to consider when planning a feeding experiment is to decide the precursors labelling positions. Another important question is related to the choice of stable or radioactive isotopes. On one hand, stable isotopes are easier to manipulate and can be detected by routine techniques, such as NMR and HRMS. On the other hand, the techniques associated with the detection of stable isotopes have low sensitivity, demanding the incorporation of high concentrations of precursors that can be toxic or modify the metabolic pathways, as previously mentioned. To give an idea, experiments using stable isotopes require a precursor concentration of $mg.L^{-1}$ whereas radiolabelled compounds are required on tracer amounts of $\mu g.L^{-1}$. For this reason, radioactive isotopes are a better choice for feeding experiments using sponges.[29,30]

Radionuclides often employed in biological studies, namely ^{14}C, ^{3}H, ^{32}P and ^{35}S, are weak β-emitters. A method broadly used to detect this kind of radiation is liquid scintillation counting (LSC). This method consists in dissolving the sample with a scintillation cocktail that undergoes an excitation by collision with β-particles and emits photons when returns to the ground state. LSC is highly automated, has low detection limits (ca. 370 Bq)[30] and allows the quick measurement of hundreds of samples, being possible also to count multiple isotopes on the same sample. Despite the advantages, the method has a low sensitivity due to quenching effects (interferences on the energy transfer between β-particles and the liquid scintillator), what in some cases can generate artifacts and a false results interpretation.[41]

Searching for a higher sensitivity, our group developed a sponge feeding experiment protocol[30, 42] that applies detection methods based on gas ionization. One of the techniques is the radio-TLC on which a silica TLC plate containing sample deposits is submitted to a chamber filled with methane : argon (1 : 9) where the β-radiation causes gas ionization.[41] This technique possess

[41] G. F. Knoll, *Radiation Detection and Measurement*, John Wiley & Sons, **2010**.
[42] G. Genta-Jouve, N. Cachet, S. Holderith, F. Oberhaensli, J.-L. Teyssie, R. Jeffree, A. Al Mourabit, O. P. Thomas, *Chem. Bio. Chem.* **2011**, *12*, 2298-2301.

a low detection limit (ca. 7.4 Bq)[30] and does not present the undesired quenching effects observed with liquid scintillation.

Another technique recently developed is the β-imager autoradiography. In comparison with the classical autoradiography, the β-imager possess the advantage of lower background and a higher sensitivity (ca. 37 mBq).[30,43] It is based on gas scintillation effect, therefore when β-particles deposited on TLC silica plate interact with the detection medium their energy is partially converted into photons. The light emitted by photons is recorded and intensified on a special camera, generating images on which the luminosity is related to the sample activity.

The combination of these two sensible techniques, radio-TLC and β-imager, offers the opportunity to work with precursors close to natural concentrations and constitutes on powerful tools to biosynthesis experiments with sponges.

2. 1. 4 Biosynthesis hypothesis for crambescins and derivatives

Crambe crambe, introduced in Chapter 1, is a red incrusting Mediterranean sponge that produces guanidine alkaloids from two groups: crambescins and crambescidins.

In the early 90's Snider and Shi reported a biomimetic synthesis of crambescins (Chapter 3) in which the guanidine cyclic core was achieved by a Michael addition of an *O*-methylisourea on an enone[44] (Scheme 5).

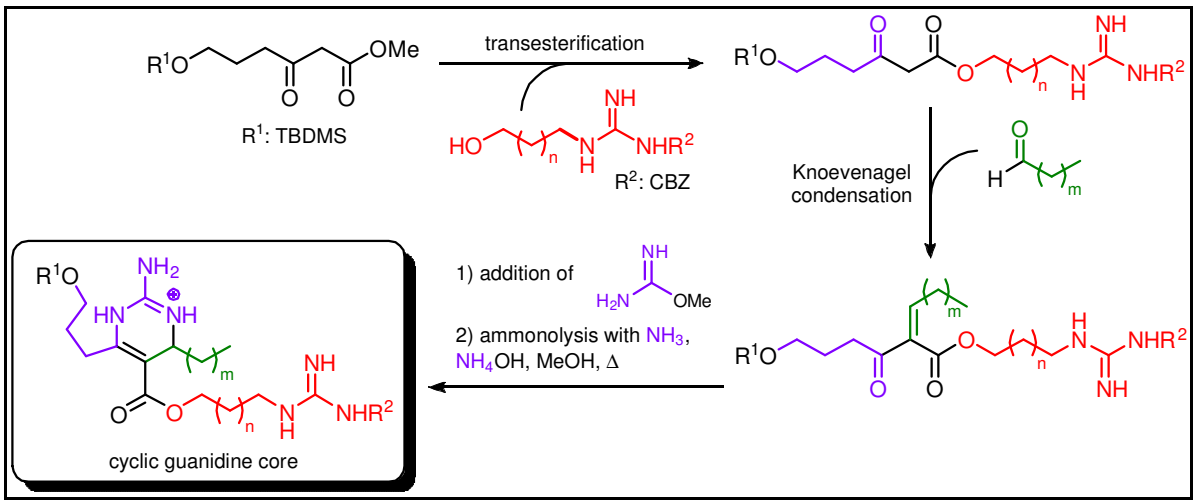

Scheme 5. Snider and Shi "biomimetic" synthesis of cyclic guanidine core of crambescins

[43] N. Barthe, K. Chatti, P. Coulon, S. Maîtrejean, B. Basse-Cathalinat, *Nucl. Instrum. Meth. A* **2004**, *527*, 41-45.
[44] B. B. Snider, Z. Shi, *J. Org. Chem.* **1993**, *58*, 3828-3839.

In the light of recently discovered guanidine alkaloids produced by Crambeidae sponges[45, 21] our groups elaborated a biosynthesis hypothesis[46] reconsidering the origin of the guanidine core through a Mannich-type reaction between a guanidinylated pyrrolidinium derived from agmatine and a long β-keto fatty acid (Scheme 6).

It is worth noting that in our proposition crambescins C are intermediates for conversion of crambescins A into B. Among crambescins C, we will focus our discussion on crambescin C1[47,48] (Figure 18), a compound that possess a mono-cyclic-*6*-membered ring guanidine core substituted by three side chains: 1) a linear 3-hydroxypropyl chain; 2) an aliphatic nonanyl chain; 3) a 6-guanidino-heptyl acetate chain (Figure 18). As many others *C. crambe* metabolites, crambescin C1 also exhibit biological activity[49].

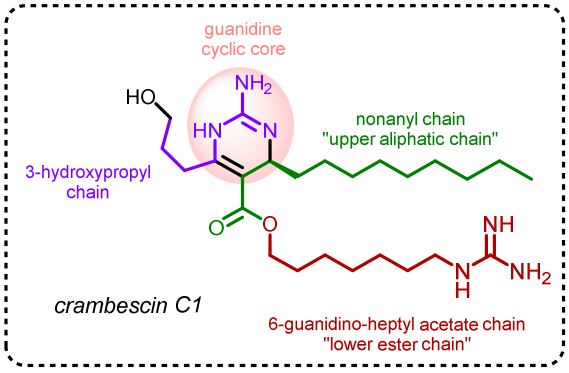

Figure 18. Detailed structure of crambescin C1

[45] S. Bondu, G. Genta-Jouve, M. Leiros, C. Vale, J.-M. Guigonis, L. M. Botana, O. P. Thomas, *RSC Adv.* **2012**, *2*, 2828-2835.
[46] G. Genta-Jouve, J. Croué, L. Weinberg, V. Cocandeau, S. Holderith, N. Bontemps, M. Suzuki, O. P. Thomas, *Phytochem. Lett.* **2014**, *10*, 318-323.
[47] R. G. S. Berlinck, J. C. Braekman, D. Daloze, I. Bruno, R. Riccio, D. Rogeau, P. Amade, *J. Nat. Prod.* **1992**, *55*, 528-532.
[48] E. A. Jares-Erijman, A. A. Ingrum, F. Sun, K. L. Rinehart, *J Nat Prod* **1993**, *56*, 2186-2188.
[49] M. Roel, J. A. Rubiolo, L. M. Botana, E. Ternon, O. P. Thomas, O. P. Thomas, M. R. Vieytes, *Mar Drugs* **2015**, *13*, 4633-4653.

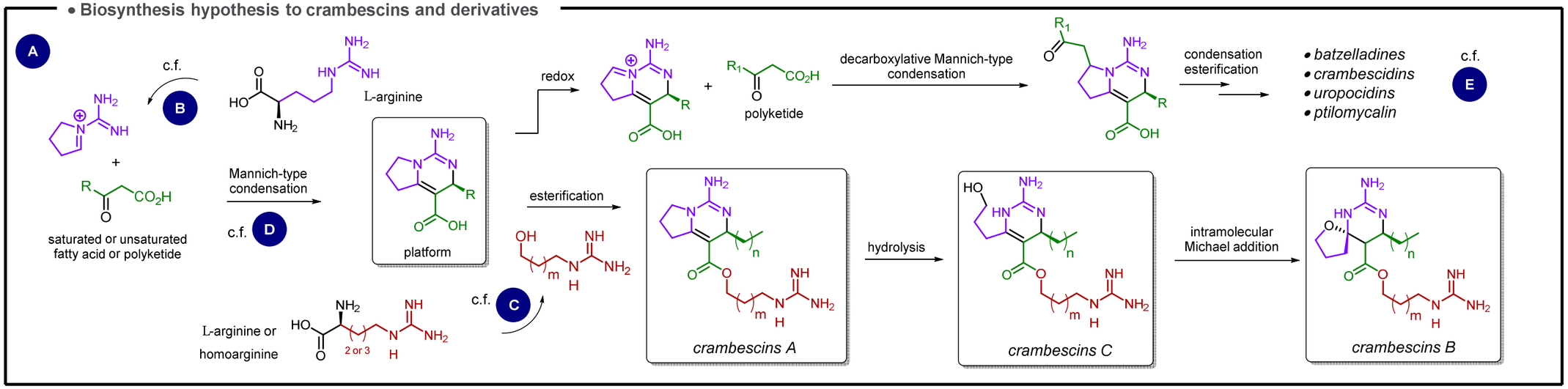
• Biosynthesis hypothesis to crambescins and derivatives
A
c.f.
B
L-arginine
saturated or unsaturated fatty acid or polyketide
Mannich-type condensation
c.f. D
platform
redox
polyketide
decarboxylative Mannich-type condensation
condensation esterification
• batzelladines
• crambescidins
• uropocidins
• ptilomycalin
c.f. E
esterification
c.f. C
L-arginine or homoarginine
2 or 3
crambescins A
hydrolysis
crambescins C
intramolecular Michael addition
crambescins B

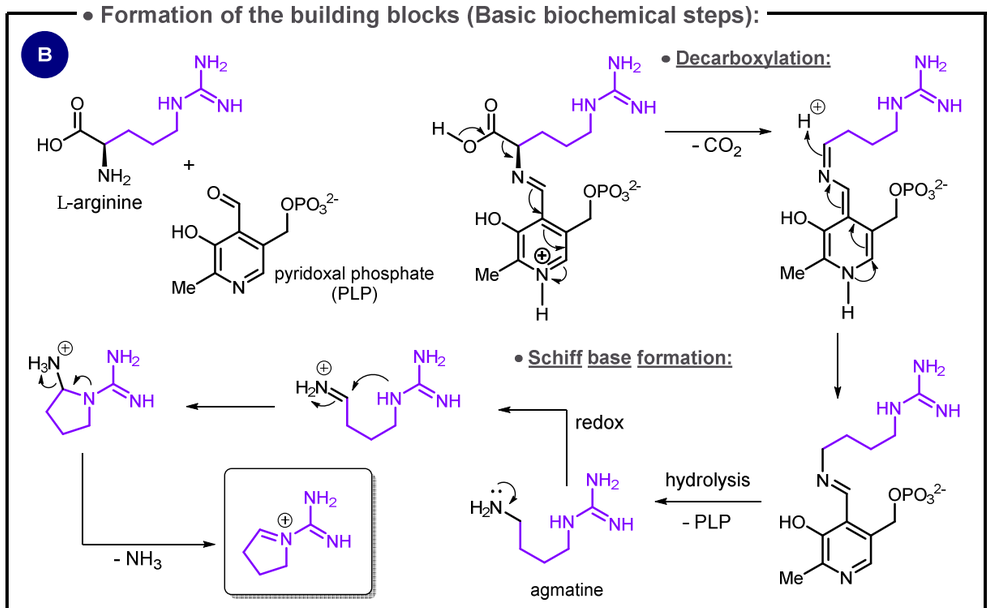
• Formation of the building blocks (Basic biochemical steps):
B
L-arginine
pyridoxal phosphate (PLP)
• Decarboxylation:
- CO2
• Schiff base formation:
redox
hydrolysis
- PLP
agmatine
- NH3

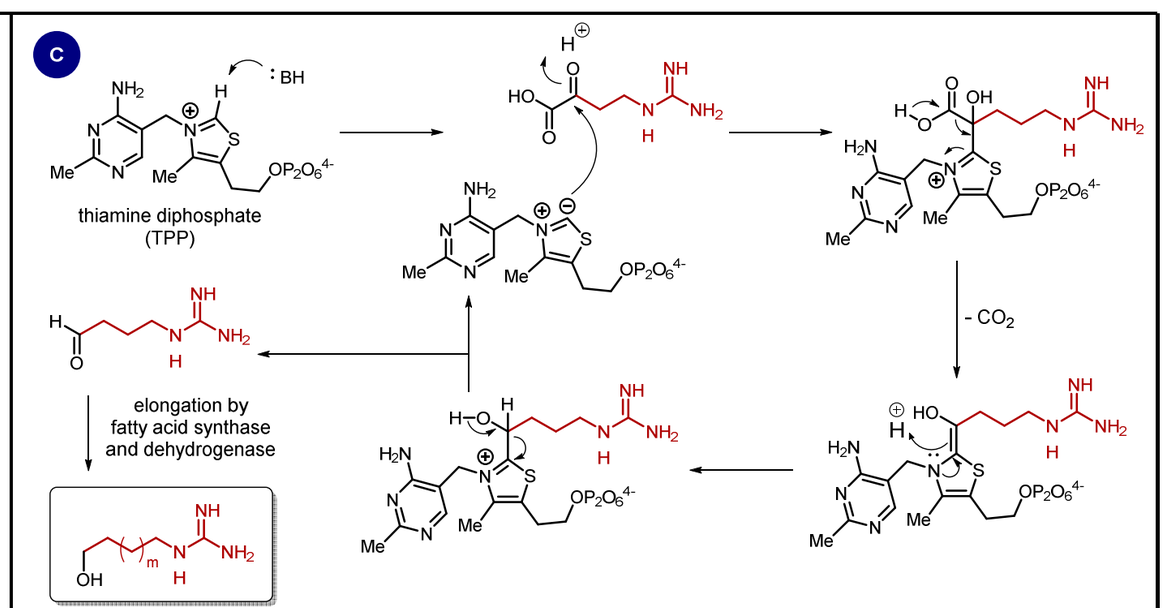
C
: BH
thiamine diphosphate (TPP)
elongation by fatty acid synthase and dehydrogenase
- CO2

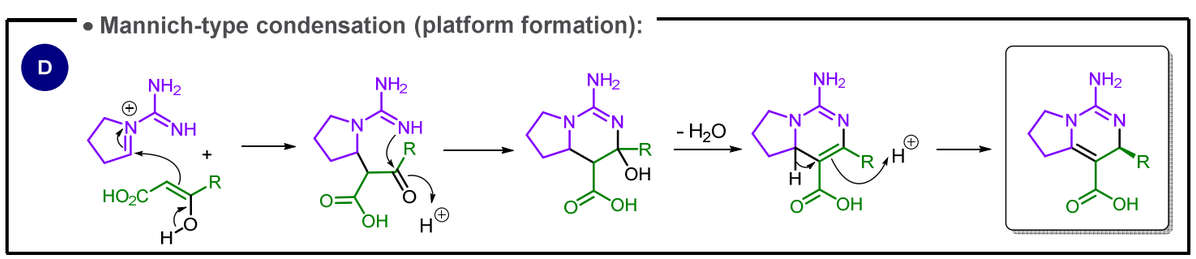
• Mannich-type condensation (platform formation):
D
- H2O

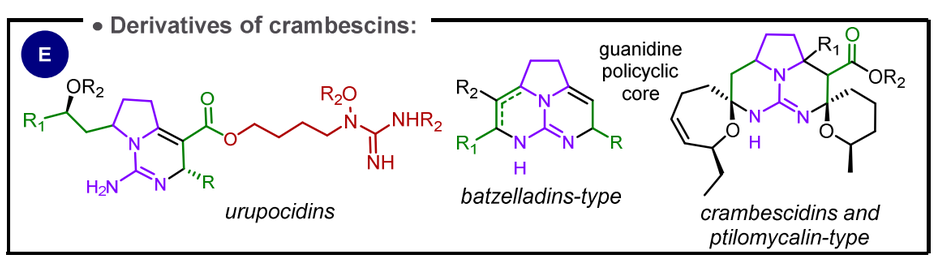
• Derivatives of crambescins:
E
urupocidins
batzelladins-type
guanidine policyclic core
crambescidins and ptilomycalin-type

Scheme 6

2. 2 Objectives of this project

Herein we present a biosynthetic study that aims to demonstrate and understand the production of the guanidine alkaloid crambescin C1 by the sponge *C. crambe* using *in vivo* ^{14}C-feeding experiments. In accordance with the biosynthetic hypothesis presented on Scheme 6, *C. crambe* specimens were fed with the following putative and commercially available precursors: L-[guanidino-^{14}C]arginine, [guanidino-^{14}C]agmatine, L-[U-^{14}C]-lysine, L-[5-^{14}C]-ornithine, [U-^{14}C]acetic acid, and [1-^{14}C]lauric acid.

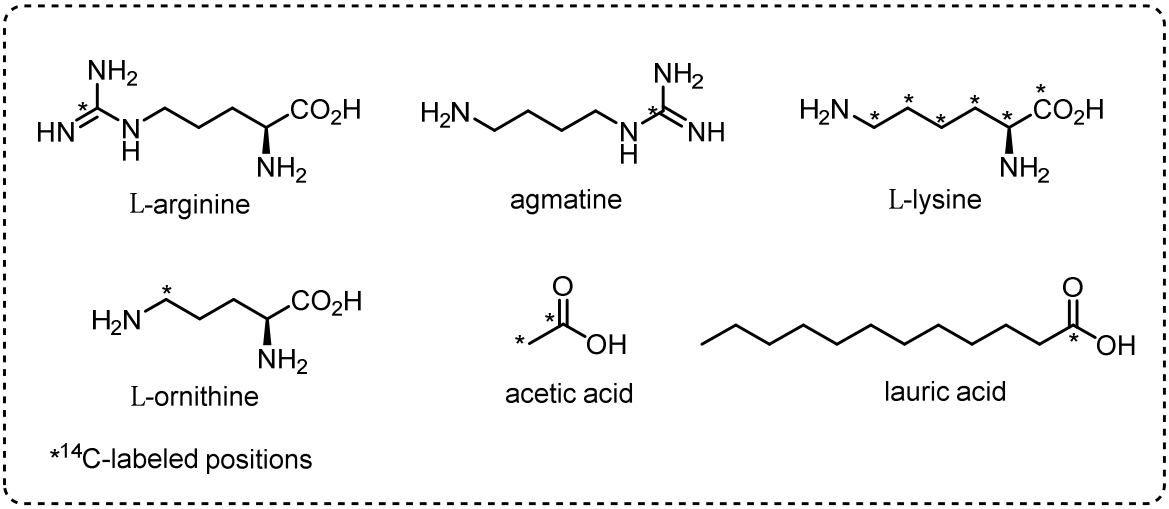

Figure 19. Precursors applied on ^{14}C-feeding experiments with *C. crambe* sponge

The protocol[30,42] used was adapted from the one developed for the biosynthetic study of oroidin in *Axinella damicornis* and was planned to circumvent as best as possible the main problems associated with sponge feeding experiments. A summary is depicted on Figure 20.

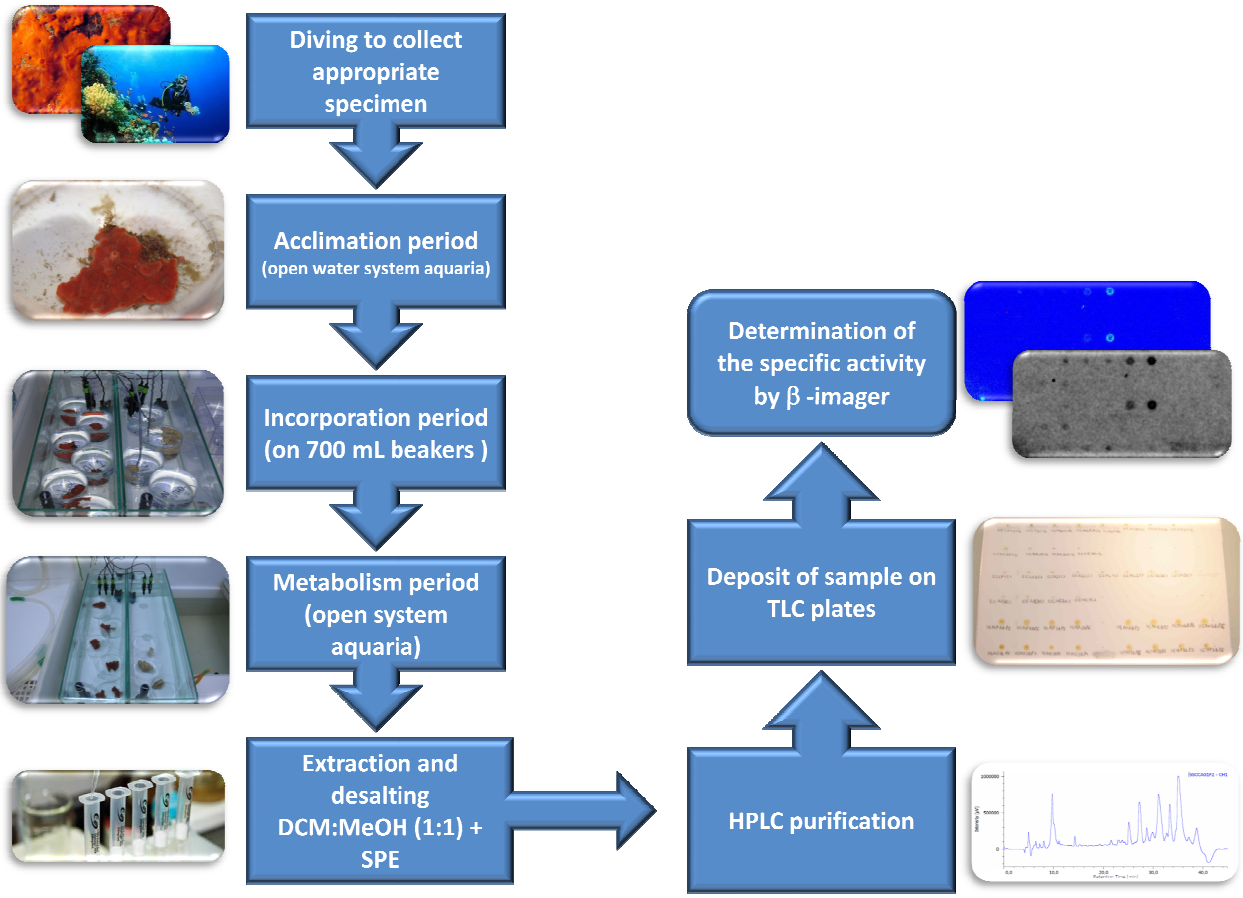

Figure 20. Workflow to *in vivo* sponge feeding experiments

2. 3 Results and Discussion

2. 3. 1 Feeding Experiments with *C. crambe*

The sponge specimens were collected and acclimated in aquaria to avoid stressful conditions that would interfere on their filtration activity and downturn the incorporation of labelled precursors during the feeding experiments. The following conditions described for cultivation of marine sponges[50,51] and specially for cultivation of *C. crambe* were applied[52,53]: the animals were daily fed with phytoplankton (*Isocrysis galbana*) and the temperature of the aquaria (two tanks of 20 L) filled with natural seawater supply was adjusted to 18 °C. After one up to three weeks of acclimation, the sponge morphology and especially opened oscules indicated that they were healthy and well adapted to the laboratory conditions.

[50] R. Osinga, J. Tramper, H. R. Wijffels, *Mar. Biotechnol.* **1999**, *1*, 509-532.
[51] R. Osinga, J. Tramper, R. H. Wijffels, *Trends Biotechnol.* **1998**, *16*, 130-134.
[52] X. Turon, J. Galera, M. J. Uriz, *J. Exp. Zool.* **1997**, *278*, 22-36.
[53] E. H. Belarbi, M. R. Dominguez, G. M. C. Ceron, G. A. Contreras, C. F. Garcia, G. E. Molina, *Biomol. Eng.* **2003**, *20*, 333-337.

Based on our biosynthetic hypothesis, L-[guanidino-^{14}C]arginine, [guanidino-^{14}C]agmatine, L-[U-^{14}C]lysine, and L-[5-^{14}C]ornithine were chosen as possible precursors of the guanidine core and [U-^{14}C]acetic acid and [1-^{14}C]lauric acid were used as possible precursors of the aliphatic chain formation (Scheme 7). Our proposition is that both guanidine moieties may be derived from L-arginine and the cyclic guanidine core formation can arise from two possible pathways: A) a transamination of L-arginine followed by decarboxylation and an intramolecular condensation, without the involvement of agmatine; B) a decarboxylation leading to agmatine, that by an intramolecular condensation generates the iminium. It is well known that L-ornithine is the precursor of L-arginine (way C) and together with its analogous L-lysine, these three aminoacids are usually involved in the biosynthesis of alkaloids[3, 32], what justifies our choice. Lauric acid was selected as it possesses the same number of carbons necessary to build the upper aliphatic chain of crambescin C1, our target metabolite. The use of acetic acid was intended to analyze if the aliphatic moieties were formed by a *de novo* process.

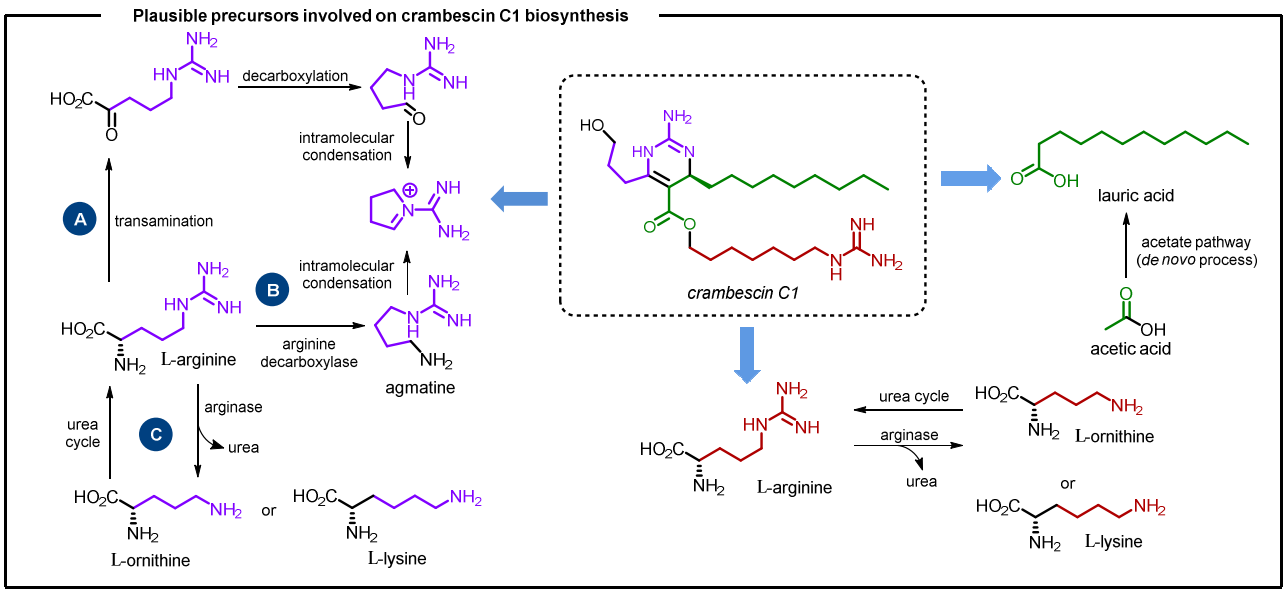

Scheme 7

During the ^{14}C-feeding experiments, the sponges were placed inside opened plastic boxes of 700 mL filled with seawater for incubation with the radiolabeled precursors during 18 h (Figure 21). The experiments were performed in triplicates, which means that for each precursor evaluated, three sponges were fed in the same conditions. To keep a low concentration of precursors, we performed eight to ten incubations, each one containing an activity of 37 kBq (1

μCi). To access the decrease of radioactivity in the seawater due to incorporation in the sponge tissues, the β-radioactivity of the water surrounding the specimens was monitored by liquid scintillation at the beginning of the incubation period and at the end. Surprisingly, we noticed a significant decrease of activity even for the controls (empty plastic boxes filled with seawater). Assuming this decrease was caused by microbial activity, we set an experiment with labelled lauric acid and agmatine to monitor controls during a long term. The aim was to compare the water column activity of controls containing sterile medium (distilled water, and sea water with sodium hypochlorite solution) against controls with pure seawater.

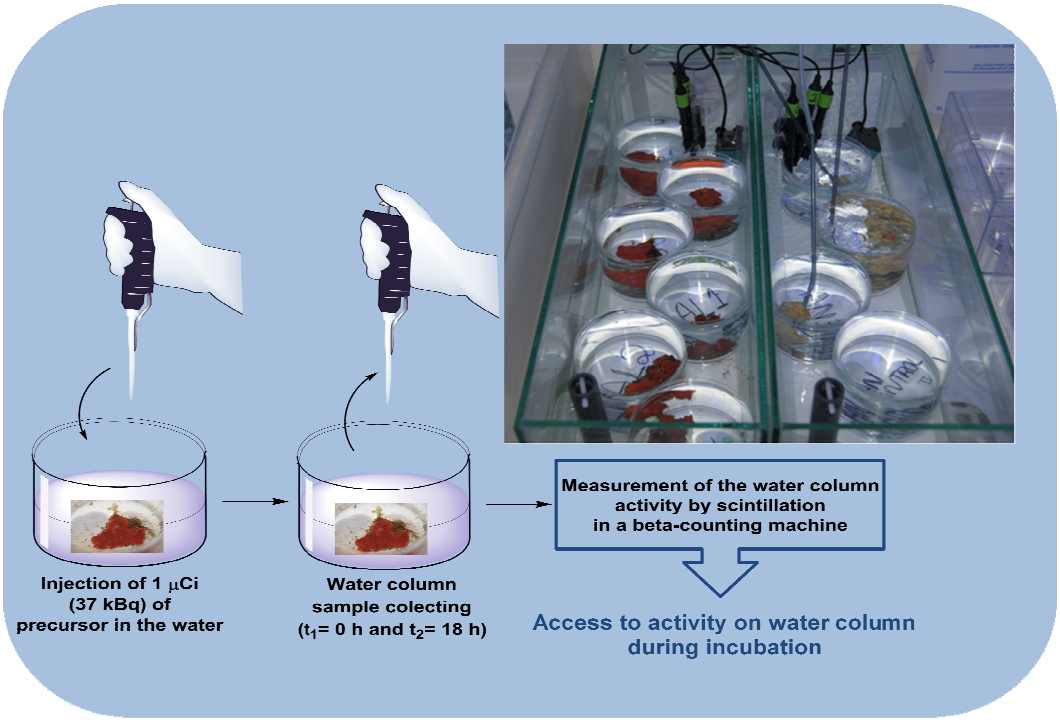

Figure 21. Picture of sponges during incubation period

Graphic 1 (Figure 22, controls with lauric acid) is in accordance with the hypothesis of a role of microbial activity on the precursor decrease from the medium. During the four first days, the counting related with the controls of distilled water and sea water containing disinfectant were stable (red and green lines, controls 2 and 3), having virtually the same amount of activity of t_0. In contrast, the sample containing only seawater (blue line, control 1) presented a visible decrease of the activity since the first days. To evaluate the role of the support, we prepared a control containing a sponge rock support (purple line, control 4). In this case, there was a small decrease in the activity of the water column after the first days, probably due to residual microorganisms

present on the rock. After the 5th day, there was a significant decrease of the radioactivity of the controls 2-4, probably due to a microbial proliferation, and after the 20th day the activity left was minimum.

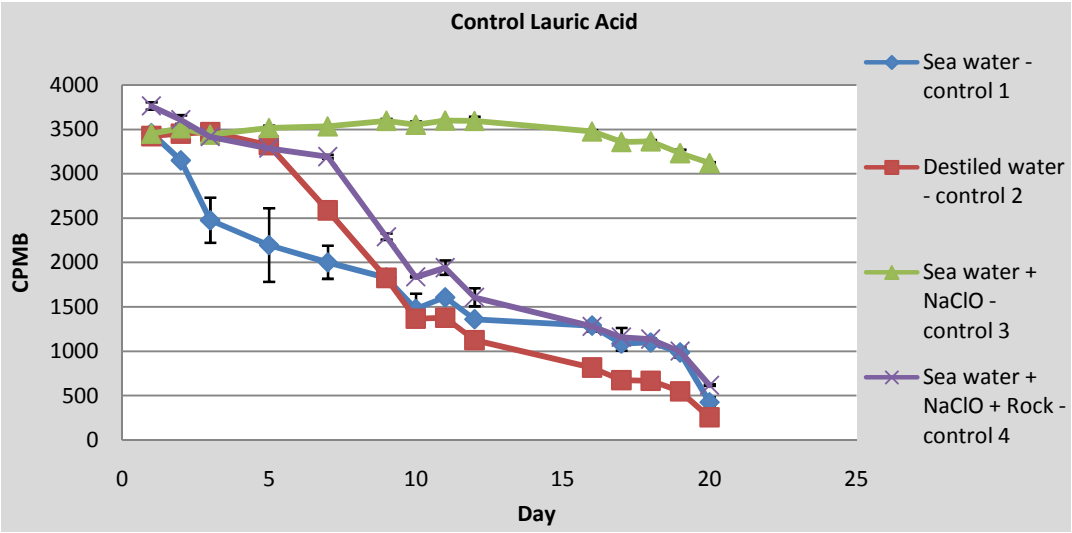

Graphic 1

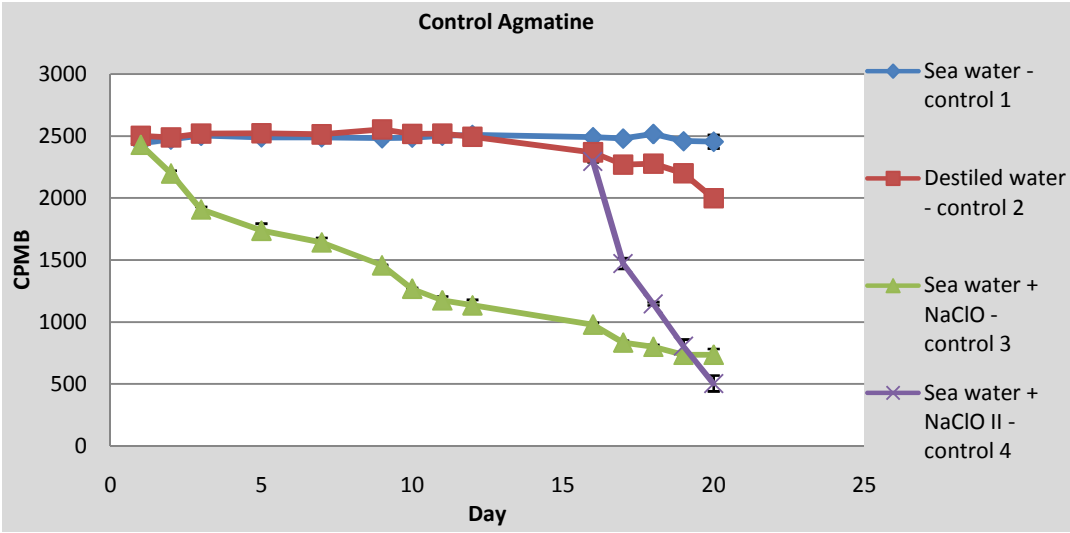

Graphic 2

Figure 22. Long term controls using labeled lauric acid (Graphic 1, top) and agmatine (Graphic 2, bottom)

(CPMB: beta counts per minute)

Controls of agmatine (Graphic 2, Figure 22) presented a depletion of the radioactivity related to the samples containing NaClO. The samples without hypoclorite (controls 1 and 2, blue and red lines) kept almost the same activity until the last day of experiment whereas control 3 (green line) presented a significant depletion since the beginning. In order to confirm such result, on the 17th day we created a new control that consisted on transferring half of the volume of

control 3 to another plastic box and adding 2 mL of 10% NaClO solution. The result was a higher depletion in the activity of agmatine (control 4, purple line), proving the influence of hypochlorite on the activity disappearance. This result can be explained by an oxidation of the guanidine moiety promoted by hypochloride, which would transform the labeled ^{14}C-guanidine into ^{14}C-labeled carbon dioxide gas (Scheme 8), in similarity with the transformation of agmatine into putrescine observed in living organisms.[3]

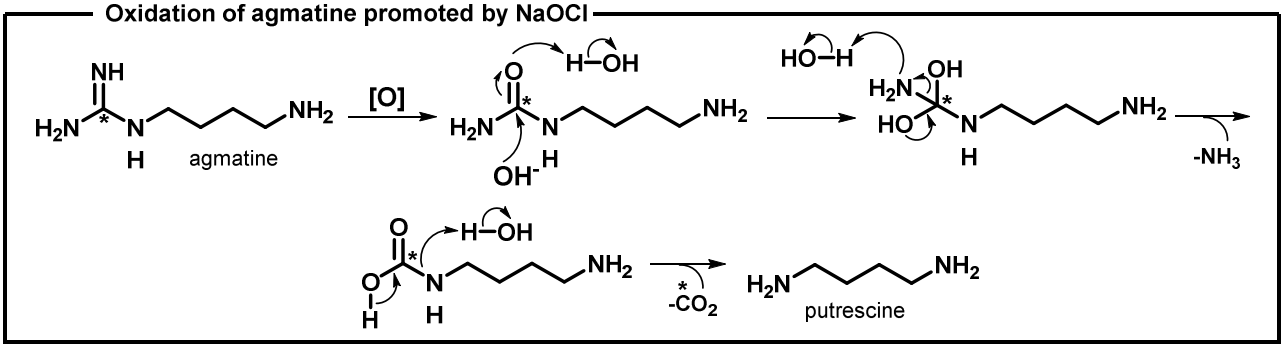

Scheme 8

Considering the control experiment results, the boxes used to store the sponges during the feeding were cleaned with sea water, dried with paper and let at air until the next usage. This simple procedure decreased the microbial proliferation and the depletion in activity observed with the controls during the feeding experiments. As NaClO can interfere with the activity of agmatine, we avoided the use of any antimicrobial substance to clean the boxes.

After the feeding and metabolism cycles, the animals were freeze-dried and extracted with MeOH. Extracts were submitted to desalting by C18 Solid Phase Extraction (SPE). Four fractions were generated, namely: F1 (100% H_2O), F2 (H_2O : MeOH, 1 : 1), F3 (H_2O : MeOH, 1 : 3) and F4 (100% MeOH). Methanolic fractions were evaluated on radio-TLC in order to provide a preliminary result concerning their radioactivity. We observed a significant radioactivity (1.0 Bq or more, Table 2 and Figure 23) associated to the fractions of samples fed with agmatine, lauric acid, ornithine and arginine. Among the sponges fed with lysine, the fractions of specimens 1 and 2 presented a high activity but the fractions of specimen 3 had low values, that could be explained by a filtering problem of this individual in relation with physiological state.

Table 2. Specific activity of SPE fractions from *C. crambe* sponges fed with ^{14}C-labeled precursors

Precursor	Specific Activity (MBq.mol^{-1})								
	Specimen 1			Specimen 2			Specimen 3		
	F2	F3	F4	F2	F3	F4	F2	F3	F4
L-[guanidino-^{14}C]Arginine	0.62	0.37	0.93	0.81	1.06	1.13	1.35	1.44	2.23
[guanidino-^{14}C]Agmatine	0.68	0.56	1.24	1.02	2.76	2.66	1.80	2.50	2.23
L-[U-^{14}C]-Lysine	1.22	0.63	1.70	2.57	2.11	3.02	0.36	0.25	0.25
L-[5-^{14}C]-Ornithine	0.50	0.87	1.89	0.65	0.50	1.78	0.49	0.44	1.71
[U-^{14}C]Acetic acid	0.00	0.00	2.77	0.00	0.00	0.53	0.15	0.00	1.40
[1-^{14}C]Lauric Acid	0.58	7.81	49.06	1.18	3.85	66.47	4.90	7.64	96.88

Regarding the sponges fed with acetate, only fractions F4 showed some radioactivity. From our previous experience on the isolation of crambescins and crambescidins by the protocol applied on this work, the higher content of such specific metabolites should be in fractions F2 and F3. Therefore, the acetate data suggest that the precursor might be metabolized into fatty acids, explaining why the most apolar fractions presented higher activities, being mainly metabolized into the primary metabolism.

To each set of three sponges fed with the same precursor, we selected fractions F2 of two animals to be purified on a phenyl-hexyl semi-preparative HPLC column. The peaks with retention time 24.5 min were identified by ^{1}H-NMR as being crambescin C1 (Figure 24). In order to avoid radioactive contaminants that could lead to a false positive result, the crambescin C1 samples were further purified by a final C18 analytical HPLC column. Both crambescins C1 obtained in the first and second HPLC purifications were deposited on a TLC plate and had their specific activities determined by the highly sensitive technique β-imager autoradiography (Table 3).

Table 3. Activities of pure crambescin C1 isolated from sponges fed with ^{14}C-precursors

Precursor	Measured Activity (x10^{-2}/ Bq)[a]		Specific Activity (x10^{-5}/ Bq.nmol^{-1})	
	1st HPLC purification	2nd HPLC purification	1st HPLC purification	2nd HPLC purification
L-[guanidino-^{14}C]arginine	3.15	4.07	7.56	9.78
	3.54	5.25	8.52	12.6
[guanidino-^{14}C]agmatine	3.15	0	7.57	0
	3.41	0	8.20	0
L-[U-^{14}C]-lysine	0	0	0	0
	4.46	0	10.7	0
L-[5-^{14}C]-ornithine	0	0	0	0
	0	0	0	0
[U-^{14}C]acetic acid	0	5.25	0	12.6
	0	0	0	0
[1-^{14}C]lauric Acid	10.6	9.71	25.6	23.3
	19.4	21.0	46.7	50.5

[a]Efficiency= 12.7% (standard: L-[U-^{14}C]proline)

Figure 25 and Table 3 evidence the incorporation of arginine and lauric acid. Activities associated with agmatine, lysine and acetic acid are presumably contamination, as they are clearly different between the first and second purifications and between the duplicates in case of lysine and acetic acid.

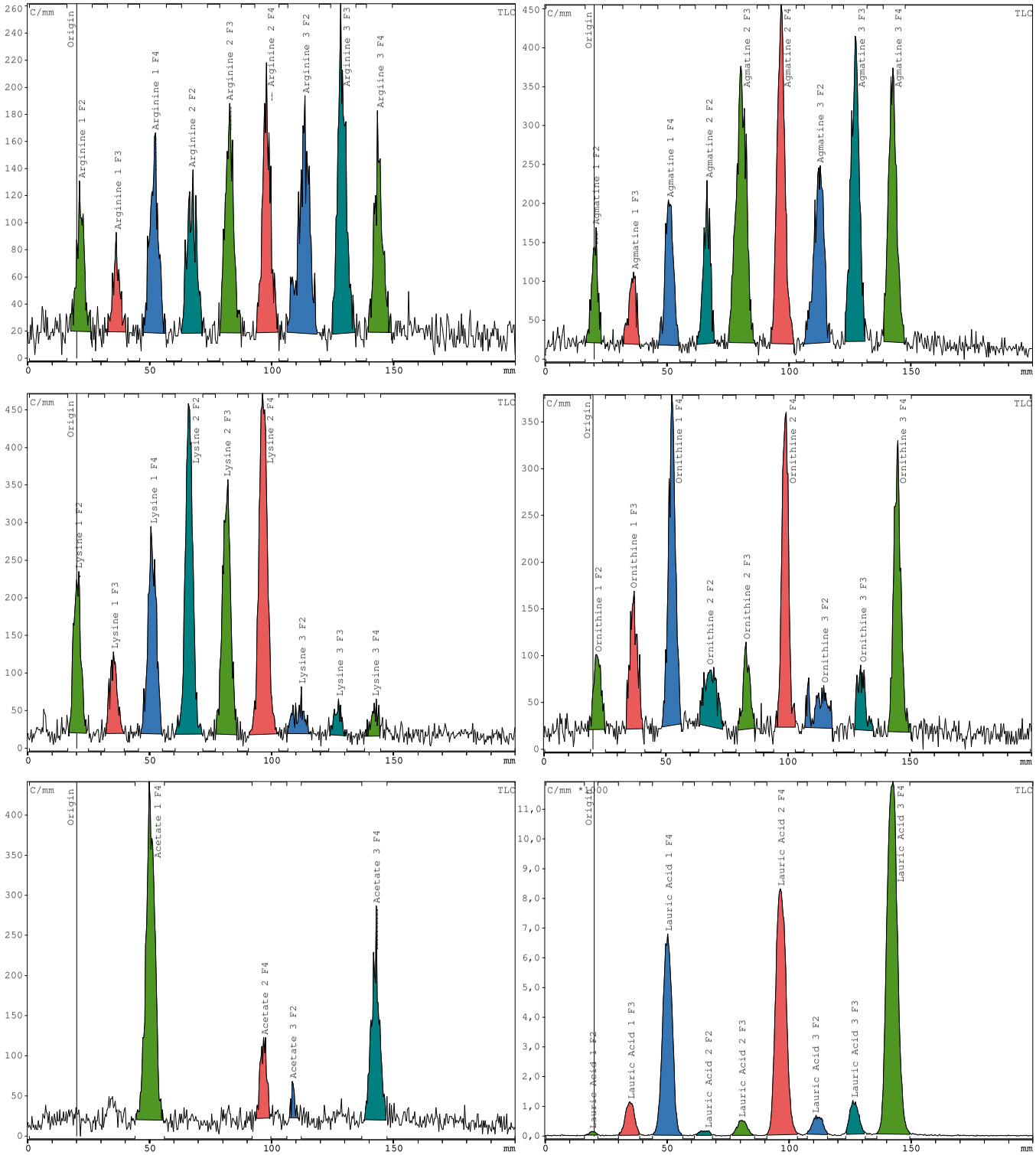

Figure 23. Radio-TLC counting of SPE fractions from sponges fed with ^{14}C-labeled precursors

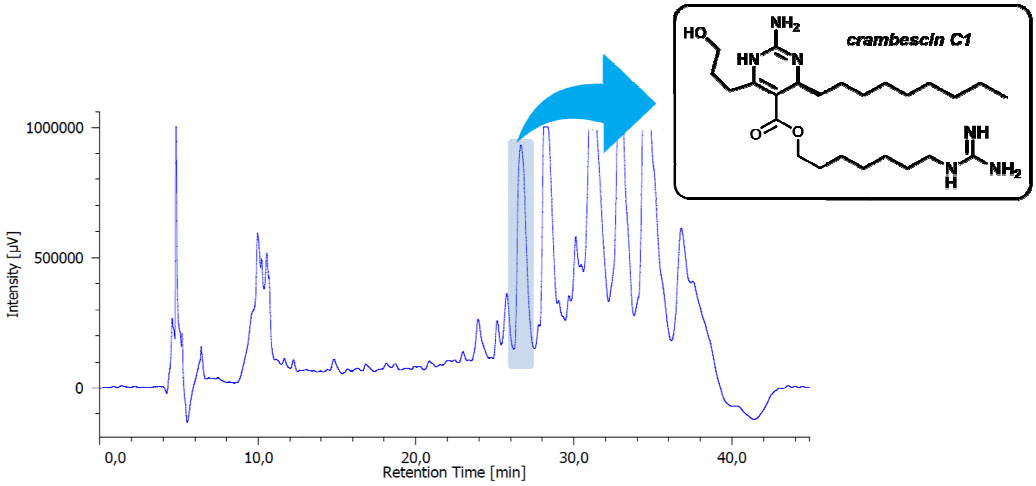

Figure 24. *C. crambe* metabolomic profile of F2 using a RP phenyl-hexyl column at 210 nm. The peak at 24.5 min corresponds to crambescin C1 alkaloid

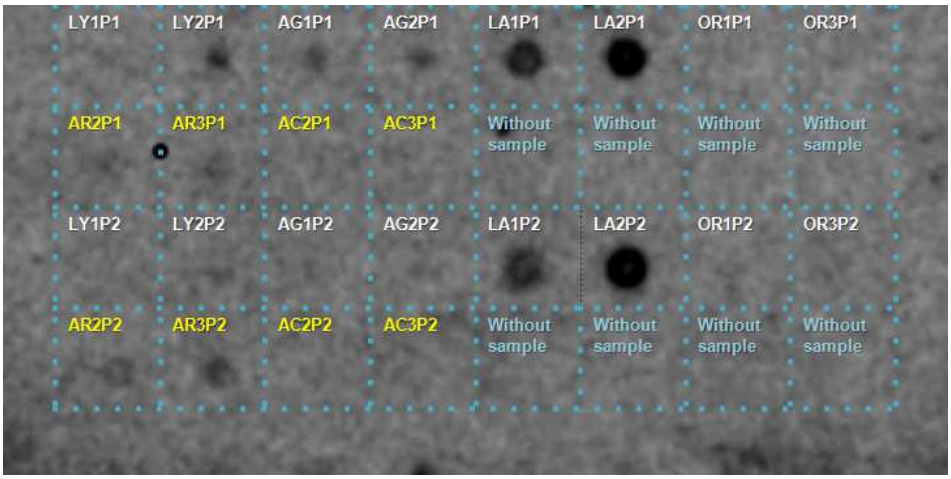

Figure 25. Qualitative beta-imager result

(LY: lysine, AG: agmatine, LA: lauric acid, OR: ornithine, AR: arginine, AC: acetic acid, P1: 1st HPLC purification, P2: 2nd HPLC purification)

According to our biosynthetic hypothesis, arginine can be incorporated into the two crambescin C1 guanidine moieties. Although the autoradiography results are insufficient to conclude the incorporation position, as the L-arginine is labelled on the guanidine position, it is sure that the guanidine moiety is arising from this precursor. Recent reports prove that strains of bacteria[54] and fungi[55] are able to biosynthesize 4-guanidinobutyric acid from L-arginine. Therefore the biosynthesis of the 6-guanidino-hexyl unit might be related to a symbiosis with microorganisms. The fact that agmatine was not incorporated into crambescin C1 can be either an

[54] H. Hong, T. Fill, P. F. Leadlay, *Angew. Chem. Int. Ed.* **2013**, *52*, 13096-13099.

[55] G. Romagnoli, M. D. Verhoeven, R. Mans, Y. Fleury Rey, R. Bel-Rhlid, M. van den Broek, R. Maleki Seifar, A. Ten Pierick, M. Thompson, V. Müller, S. A. Wahl, J. T. Pronk, J. M. Daran, *Mol. Microbiol.* **2014**, *93*, 369-389.

indication that the organism cannot uptake this precursor from the diet into the specific metabolism either that the formation of the iminium does not involve agmatine as an intermediate. In the second scenario, the guanidine cyclic core would be derivate from the way A of Scheme 7.

The high activity of the samples fed with lauric acid indicates that this precursor was incorporated into the aliphatic chain participating on few other metabolic pathways. As lauric acid has the same number of carbons necessary for the construction of the upper crambescin C1 aliphatic chain, this result strongly suggests a direct incorporation of the fatty acid from diet. This hypothesis is in accordance with the variety observed on the upper aliphatic chains of crambescins A1, A2, A3, and analogues (Scheme 4). In nature, the providers for fatty acids might be either microorganisms from micro flora of sponge either exogenous sources from marine environment, allowing a variety of specialized metabolites that is probably related with the availability of substrate on sponges' habitat. Although the high concentration of PGAs in *C. crambe* (about 1% of dry mass) might suggest the sponge as the only responsible for the biosynthesis of its secondary metabolites, our present incorporation results in addition to the report of a predominance of a betaproteobacterium in the microflora of *C. crambe*[56] can suggest the implication of bacteria in the biosynthesis of crambescins and crambescidins.

The lack of activity associated with acetic acid suggests that the upper aliphatic chain is not produced by a *de novo* pathway, although it is important to notice that during the long experiment period the precursors might be involved in many other metabolism/catabolism steps, including primary metabolism.

2. 4 Conclusions

For the first time, biosynthetic experiments with *C. Crambe* allowed the identification of two building blocks involved in the synthesis of crambescin C1: L-arginine and lauric acid. The incorporation of lauric acid or close fatty acids from diet could explain the variety observed on the upper aliphatic side chain of crambescins. The microorganisms apparently play a crucial role on these secondary metabolic pathways, which can be expanded to the biosynthesis of other crambescins and derivatives. The incorporation of L-arginine labelled at the guanidine indicate

[56] J. Croué, N. J. West, M.-L. Escande, L. Intertaglia, P. Lebaron, M. T. Suzuki, *Sci. Rep.* **2013**, *3*, 2583.

that the origin of the guanidine is clearly L-arginine. However agmatine does not seem to be involved in the biosynthesis (way A, Figure 26).

Once more our sponge feeding experiments protocol[30,42] proved to be useful to give initial insights into sponge metabolites biosynthetic pathways. Further studies focusing on the genome and enzymes of sponges would help in the understanding of this intriguing and exciting biochemistry.

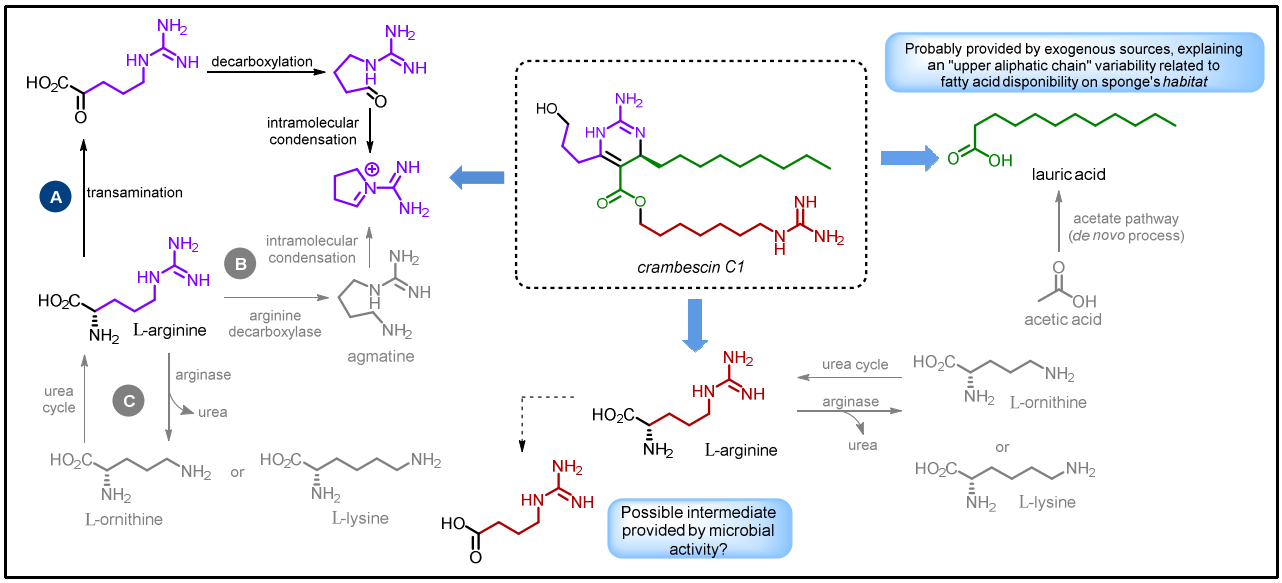

Figure 26. Final conclusions and further questions concerning the biosynthesis of crambescin C1

Chapter 3. Biomimetic Synthesis of Crambescin A2 and Derivatives

3. 1 Introduction

3. 1. 1 "Nature knows best": biomimetic synthesis of natural products

Observing nature to answer human questions is the oldest and most fundamental activity of philosophy and its younger sister: science. Biomimicry, biomimetic or bioinspiration are some terms used to describe the concept of taking advantage of years of evolution in natural materials, substances, and processes to human benefit. Such concept can be applied to all domains: arts, science, fashion, philosophy, survival tactics, etc. When applied to chemistry, topics such as supramolecular chemistry, material chemistry and biomimetic synthesis exploit the concept of biomimicry.[57, 58]

On the brilliant paper "Nature knows best: an amazing reaction cascade is uncovered by design and discovery"[59], Heathcock poses fundamental questions about the advances of organic chemistry synthesis field, hints biomimetic synthesis as the alternative to the development of efficient synthetic pathways and culminates by the description of biomimetic synthesis itself:

"One of the strategies we have been used to look for efficient synthetic routes to complex natural products is to try and figure out how nature has solved the problem. The basic assumption of this approach is that nature is the quintessential process development chemist. We think that the molecular frameworks of most natural products arise by intrinsically favorable chemical pathways - favorable enough that the skeleton could have arisen by a non enzymic reaction in the primitive organism. (...)

A corollary of the foregoing hypothesis is that the coexistence of two structurally related molecules in an organism implies some reasonable chemical pathway from one to the other. (...) A 'biomimetic' synthesis is a laboratory synthesis that is based on such reasoning".

During the development of a biomimetic synthesis strategy, experimental biosynthesis evidence or at least a reasonable biogenic hypothesis will be demanded. Therefore, biomimetic synthesis and biosynthesis are tethered fields on the process of "reverse engineering" nature: on one hand the biosynthesis will inspire putative precursors and reactions to a synthetic strategy, on the other hand the achievement of the biomimetic synthesis will corroborate that putative

[57] in *Biomimetic Organic Synthesis* (Eds.: E. Poupon, B. Nay), Wiley-VCH Verlag GmbH & Co. KGaA, **2011**, pp. I-XXXV.
[58] T. W. Hanks, G. F. Swiegers, in *Bioinspiration and Biomimicry in Chemistry*, John Wiley & Sons, Inc., **2012**, pp. 1-15.
[59] C. H. Heathcock, *P. Natl. Acad. Sci.* **1996**, *93*, 14323-14327.

precursors and intermediate species are prone to react even in a non-enzymatic way. An example of the symbiosis between biomimetic synthesis and biosynthesis is the synthesis of endiandric acids A, D, and E (**3e**, **3a**, and **3c**) (polyketides isolated from the Australian tree *Endiandra introrsa*) achieved by Nicolaou and co-workers and based on the biogenic hypothesis of Black's group (Scheme 9). During these works, endiandric acid D (**3a**) structure was suggested by the biosynthesis hypothesis and biomimicry synthesized even before its detection in the natural source.[34]

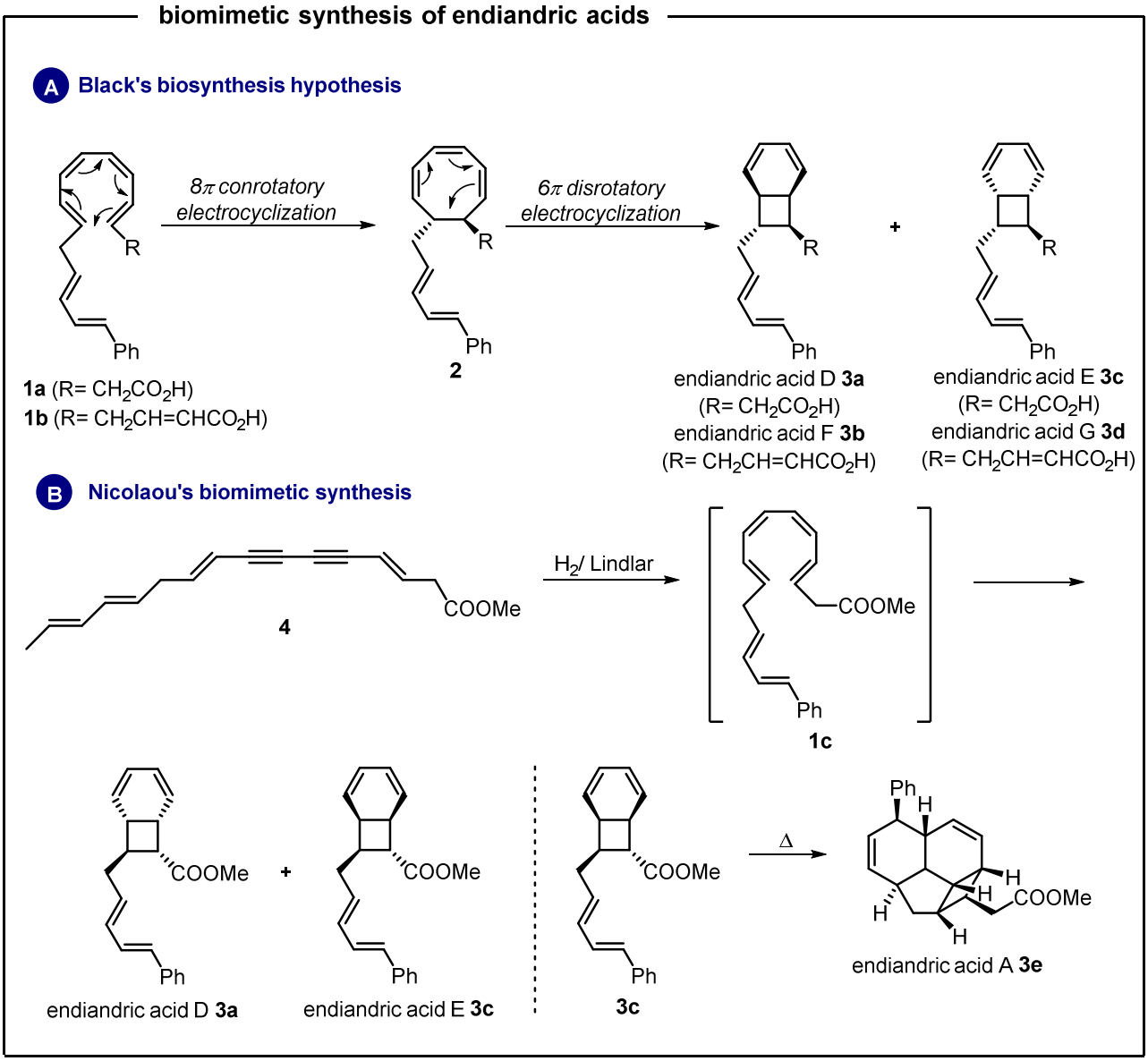

Scheme 9

The "toolbox" of biomimetic synthesis is composed by "classical and old fashion" organic reactions (often revised on a "type" style to replace dangerous chemicals or to include a catalyst)

like aldolization, Claisen condensation, Mannich reaction, and Diels-Alder reaction.[57] Cascade reactions have also been extensively exploited in biomimetic approaches; they basically consist in having a substrate with a required functionality to be converted into the desired species in the same pot.[60]

The combination between the number of steps and the increase in molecular complexity from starting materials to the target molecule is relevant to describe the success of a organic synthesis strategy. A pioneer index to calculate molecular complexity was proposed by Bertz[61] in 1981 and relies on a combination of graphic and information theories to translate what a synthetic chemist could intuitively describe as a "complex structure". In this approach, a molecule is described as a "skeletal" without hydrogen atoms (Scheme 10). The calculation is then based on the sum (C_T) of two coefficients defined as: Cη - the number of connections, which means the amount of adjacent lines; and Cε - the elemental diversity coefficient, namely the number of heteroatoms. The Cη coefficient increases with the presence of multiple bonds, rings, branches and molecular asymmetry. The range in complexity from reactants to products in the course of a reaction is called ΔC_T.[61]

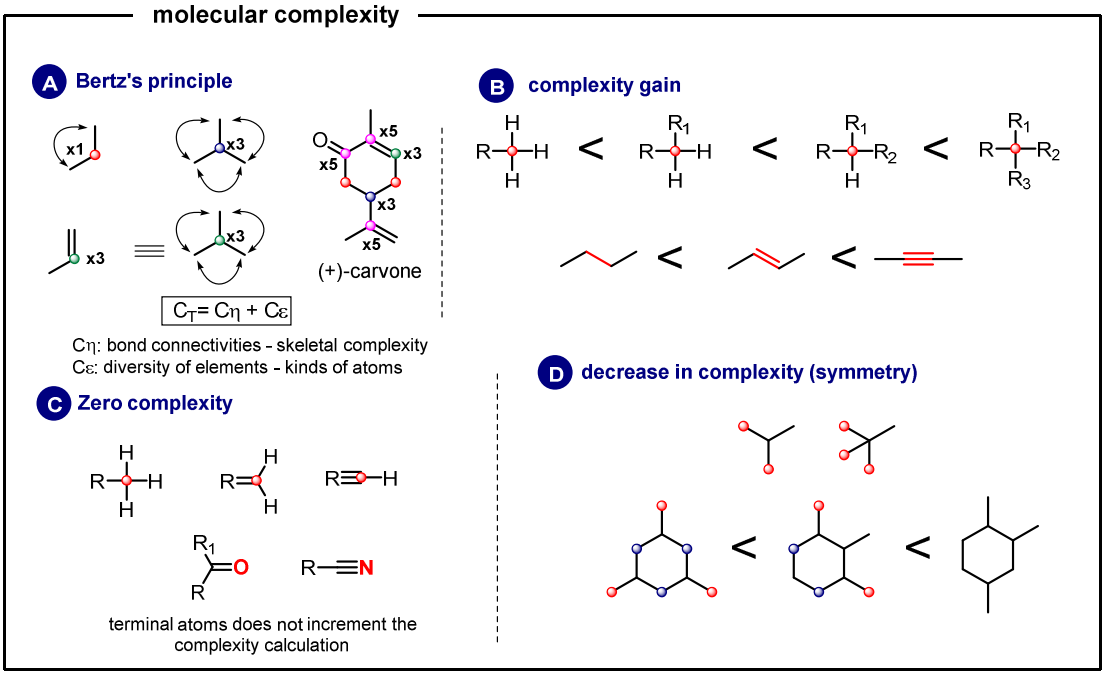

Scheme 10

Bertz's index is the most popular manner to measure molecular complexity and a database

[60] B. Nay, N. Riache, in *Biomimetic Organic Synthesis*, Wiley-VCH Verlag GmbH & Co. KGaA, **2011**, pp. 503-535.
[61] S. H. Bertz, *J. Am. Chem. Soc.* **1981**, *103*, 3599-3601.

containing the C_T of many chemical compounds is publically available on PubChem.[62] Hendrickson proposed a simplified formula of Bertz's index that is adapted to evaluate the atom environments and not linear-three atoms systems (simplifying a studied molecule to units of propane) as in Bertz approach.[63] Besides the limitations, such as not considering the stereochemistry[62], herein we will employ the Bertz-Hendrickson index as an estimation to access the molecular complexity range in the course of the biomimetic synthesis of crambescin A2.

3. 1. 2 The guanidine bicyclic alkaloid crambescin A2 448 and analogues

Crambescin A2 448[64] (**5a**, Figure 27) is a bicyclic guanidine alkaloid isolated from the Mediterranean encrusting sponge *C. crambe*. This alkaloid was initially called "crambine A" however Rinehart's group proposed to rename the whole class of alkaloids to "crambescins"[48] in order to avoid misunderstandings with the protein "crambin" (sometimes spelled as "crambine"), isolated 25 years earlier from the plant *Crambe abyssinica*.[65]

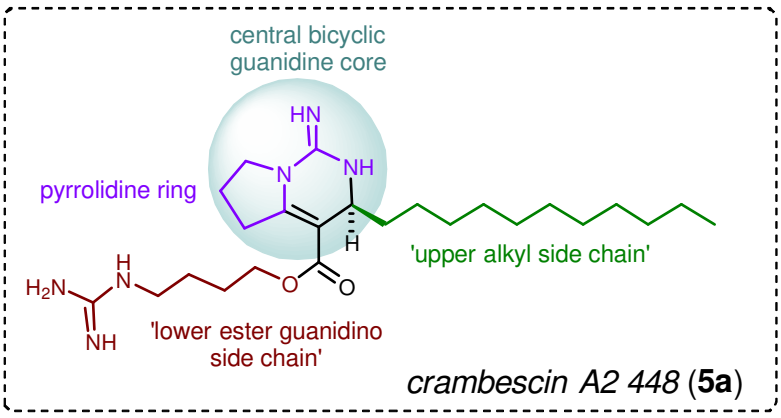

Figure 27. Structure of crambescin A2 448 (**5a**)

Crambescin A2 448 contains a central bicyclic guanidine core containing a pyrrolidine ring and two side chains: an upper alkyl chain possessing 12 carbons and a lower ester guanidino alkyl chain composed by 4 methylene groups. All crambescins A2 have a lower alkyl chain smaller than crambescins from series 1 (A1, B1 or C1). In crambescins A2 this lower alkyl chain has 4 methylene units whereas crambescin A1, for example, has 7 methylene units. Due to difficulties in

[62] T. Böttcher, *J. Chem. Inf. Model.* **2016**, *56*, 462-470.
[63] J. B. Hendrickson, P. Huang, A. G. Toczko, *J. Chem. Inf. Comp. Sci.* **1987**, *27*, 63-67.
[64] R. G. S. Berlinck, J. C. Braekman, D. Daloze, K. Hallenga, R. Ottinger, I. Bruno, R. Riccio, *Tetrahedron Lett.* **1990**, *31*, 6531-6534.
[65] C. H. Van Etten, H. C. Nielsen, J. E. Peters, *Phytochemistry* **1965**, *4*, 467-473.

purification process, crambescin A2 has often been isolated as a mixture of homologues on the upper alkyl side chain, that justifies the need to precise the mass of the molecule after its name (Figure 28).[45] Analogues of crambescin A2 448 had also been isolated from non Crambeidae sponges, as compounds **5e-h**[66], produced by *Pseudaxinella reticulata* (Axinellida, Axinellidae).

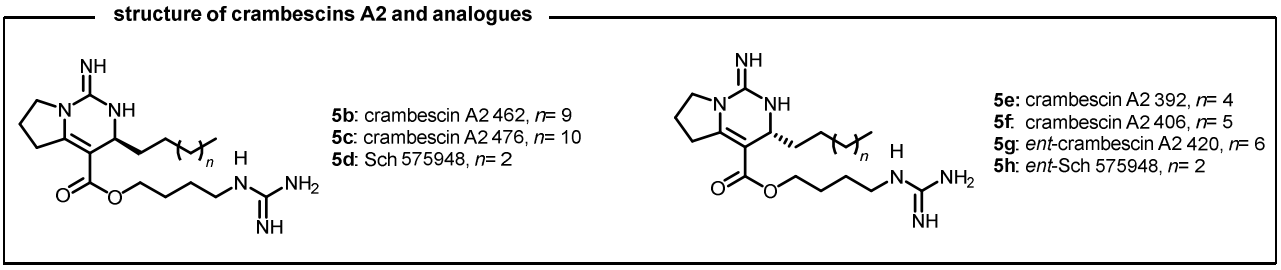

Figure 28. Structure of crambescins A2

Some crambescins A2 presented biological activities such as effect in the voltage-gated calcium channels of neurons[25] and antifungal activity with a potency dependent upon the length of the aliphatic chain[66].

3. 1. 3 Biomimetic synthesis of crambescins

The first and only synthesis of crambescins is a "biomimetic" approach proposed by Snider and Shi on early 90s.[44, 67] The authors designed a retro(bio)synthesis of the crambescins bicyclic guanidine core based on structural similarities between crambescins and two polycyclic guanidine alkaloids previously studied by the team: ptilomycalin A and ptilocaulin (**8a** and **13**), both isolated from the Caribbean sponge *Ptilocaulis spiculifer* (Axinellidae, Axinelida).[68] On their approach, the central moiety arises from a Michael addition of a guanidine derivative (*O*-methylisourea) to an enone, hence considering a **fully polyketide biochemical pathway** (Scheme 11). According to their hypothesis, crambescins B (**6**) would be formed by an acid or base cyclization of crambescins C (**7**). In the same way, crambescins A (**5**) would arise from a conversion of hydroxyl from crambescins C into a good leaving group followed by base-catalyzed cyclization. Summing up, crambescins C would be intermediates towards crambescins A and B.

[66] M. T. Jamison, T. F. Molinski, *J. Nat. Prod.* **2015**, *78*, 557-561.
[67] B. B. Snider, Z. Shi, *J. Org. Chem.* **1992**, *57*, 2526-2528.
[68] B. B. Snider, Z. Shi, *Tetrahedron Lett.* **1993**, *34*, 2099-2102.

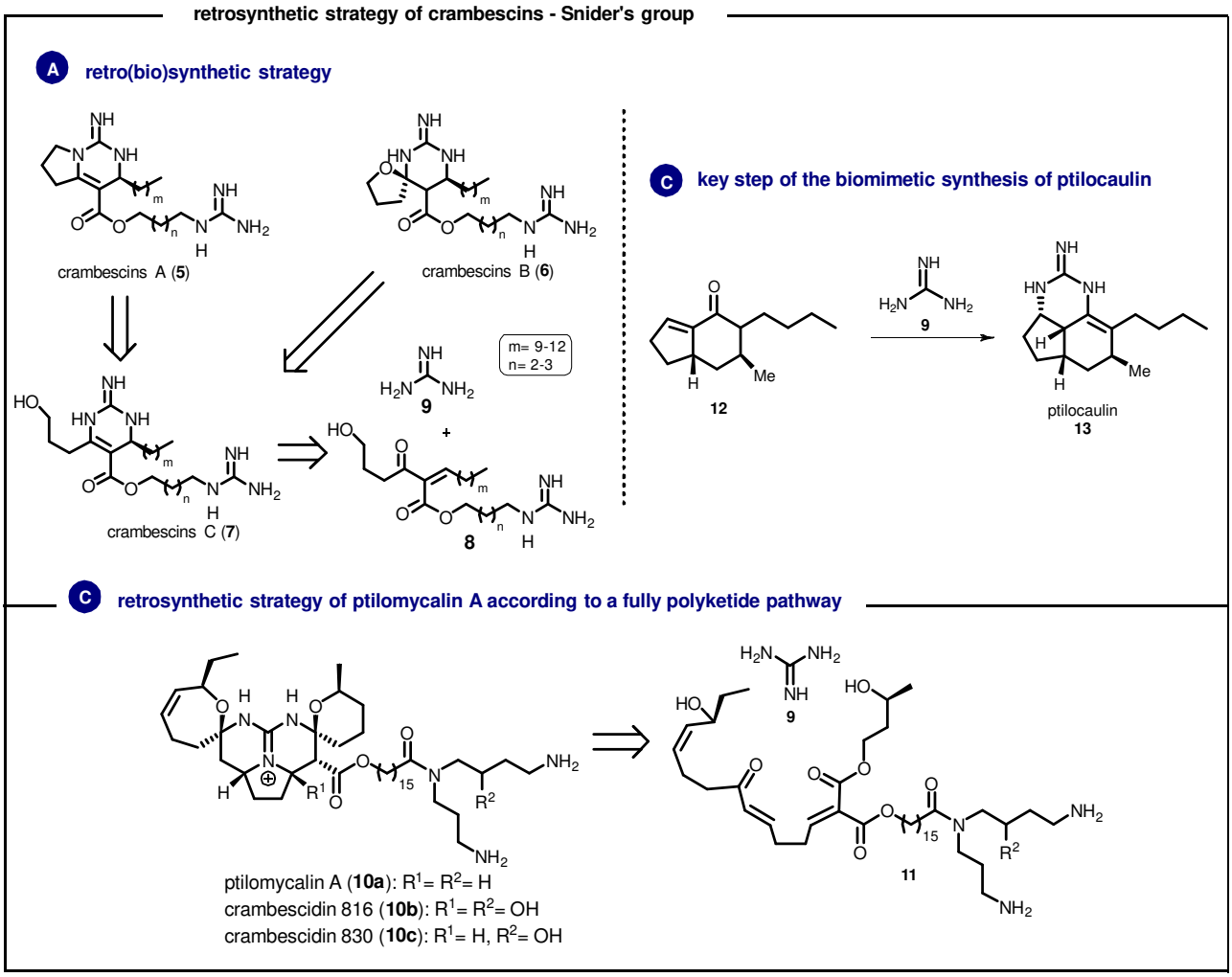

Scheme 11

Finally Snider's group performed a stereospecific biomimetic synthesis of crambescins A2 448 (**5a**, eight step, 22%), B1 (**6c**, eight steps, 19%), C1 (**7b**, seven steps, 21%), and C2 (**7c**, seven steps, 27%), as depicted on Scheme 12.[44]

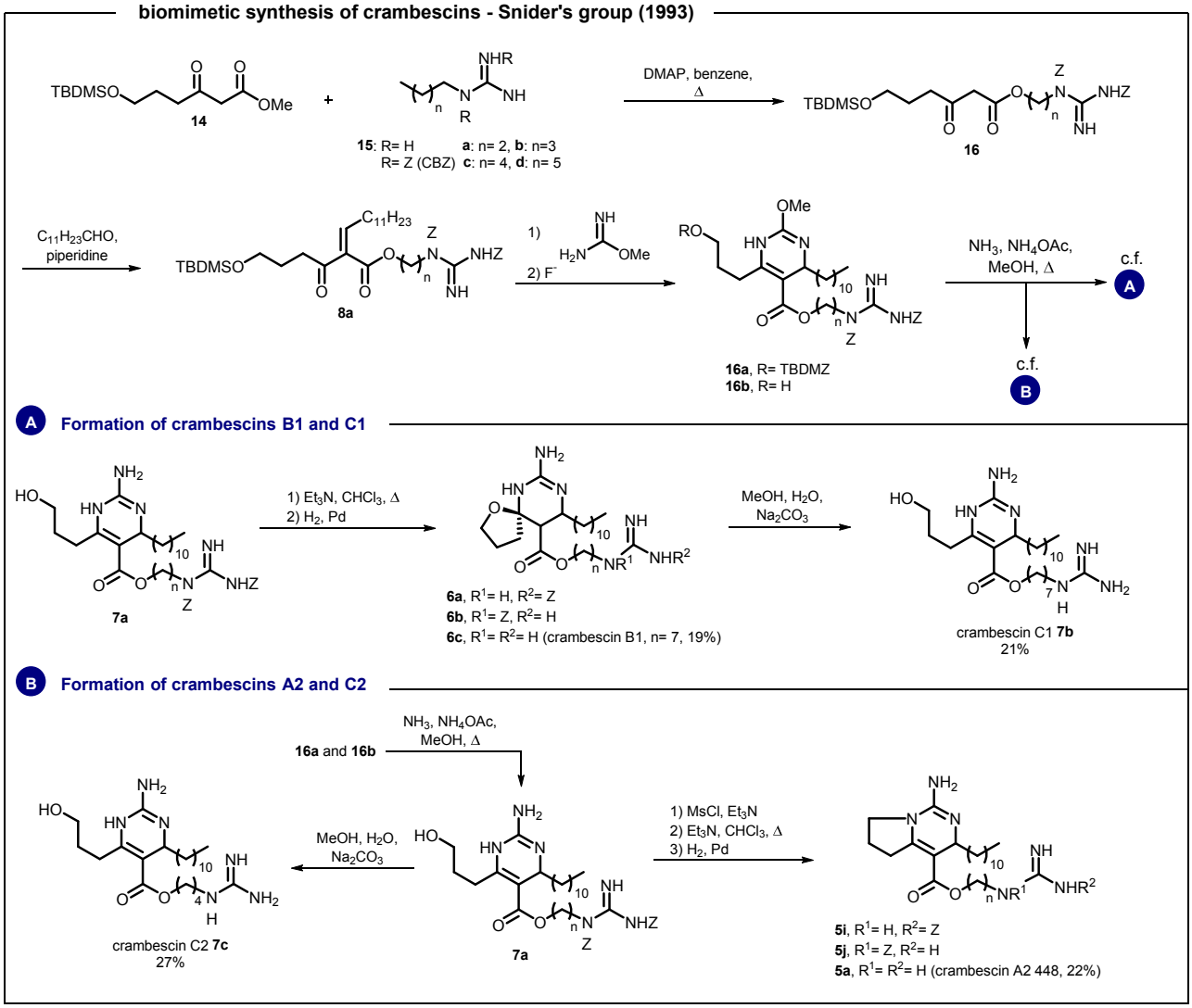

Scheme 12

3. 2 Objectives of this project

This project aims at the synthesis of **crambescin A2 448** based on the results of ^{14}C-feeding experiments with the Mediterranean sponge *C. crambe* (Chapter 2). The retro(bio)synthetic strategy (Scheme 13) has as starting materials: L-arginine (**19**), 4-amino-butan-1-ol (**22**) and lauric acid (**23**). The key-step would be the condensation between the guanidine pyrrolidinium **18** and the enone **17a**, that already encloses the lower ester guanidine moiety chain. The achievement of this synthesis will: i) confirm the intrinsic reactivity of the putative intermediates proposed in the biosynthesis hypothesis, providing additional insights into the biogenic origins of crambescins and derivatives; ii) fully dissect all mechanisms leading to this class of natural substances.

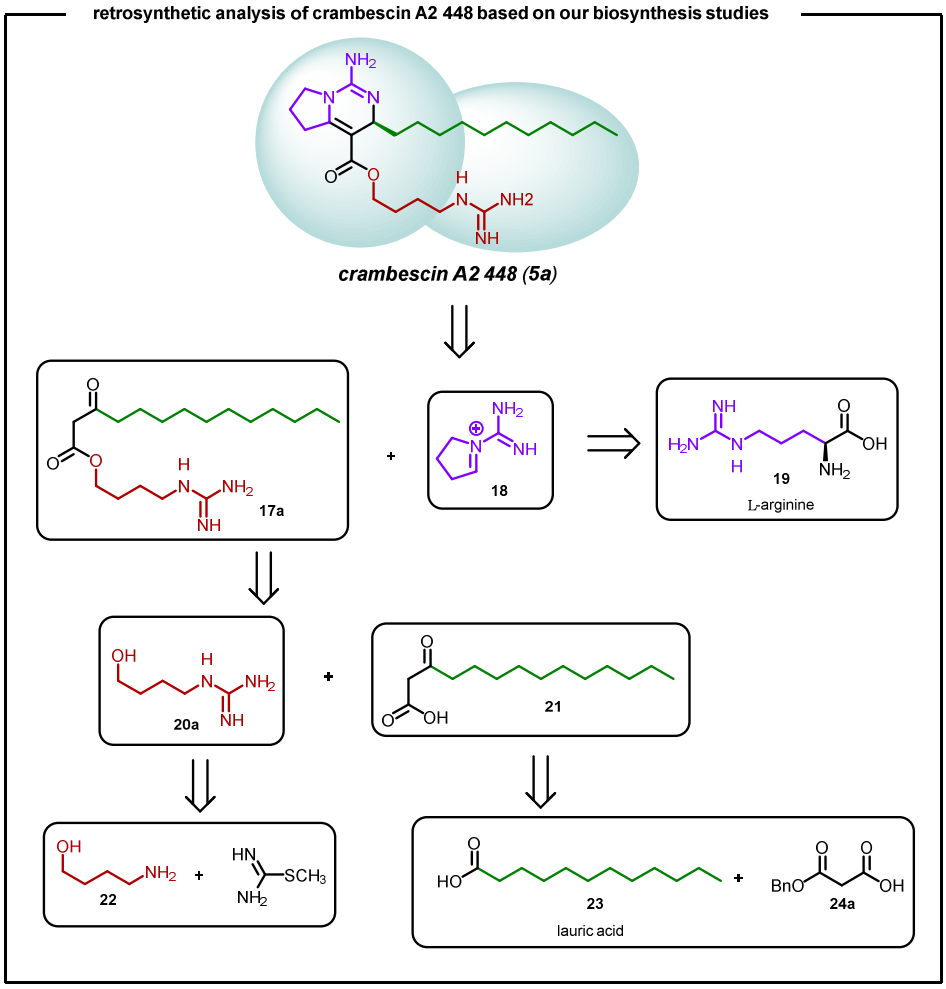

Scheme 13

3. 3 Results and Discussion

3. 3. 1 Synthesis of aliphatic fragment 21

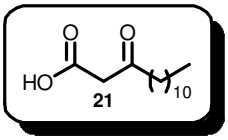

The convergent synthesis of crambescin A2 started with the preparation of the "upper aliphatic fragment", achieved through a *C*-acylation of lauric acid **23** with a malonate magnesium salt[69] (Scheme 14). Two malonates were employed: benzyl malonate and ethyl malonate, furnishing the desired β-keto-fatty ester **25** in similar yields.

[69] D. W. Brooks, L. D. L. Lu, S. Masamune, *Angew. Chem. Int. Edit.* **1979**, *18*, 72-74.

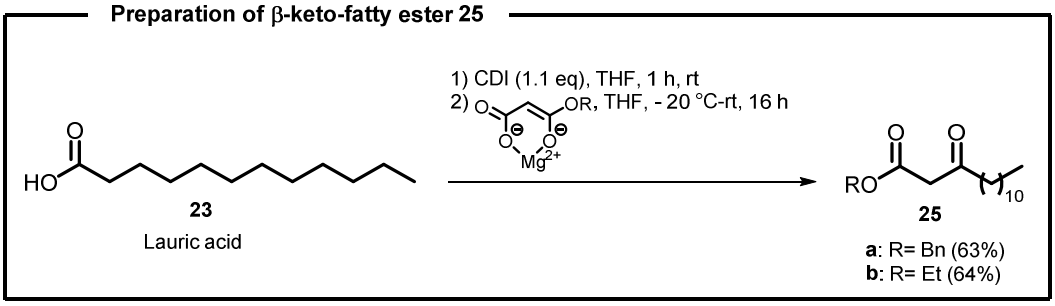

Scheme 14

The first reaction step is the nucleophilic addition of the hydroxy group from carboxylic acid **23** to carbonyl of carbonyldiimidazole (CDI, **26**), forming a sp^3 intermediate **27** (Scheme 15). The sp^2 hybridization is re-established with the departure of imidazole followed by deprotonation of oxonium ion. Subsequently intermediate **28** suffers an intramolecular nucleophilic attack of the imidazole nitrogen on carbonyl group. During this second nucleophilic attack there is a CO_2 liberation, a driving force that shifts all previous equilibriums to formation of **29**, just as in the fundamental steps of polyketide biosynthesis. Suspension containing **29** is then added into malonate magnesium salt mixture and the enol **30** attacks the carbonyl-imidazole **29**. Desired **25** is obtained after a decarboxylation and departure of imidazole as leaving group.

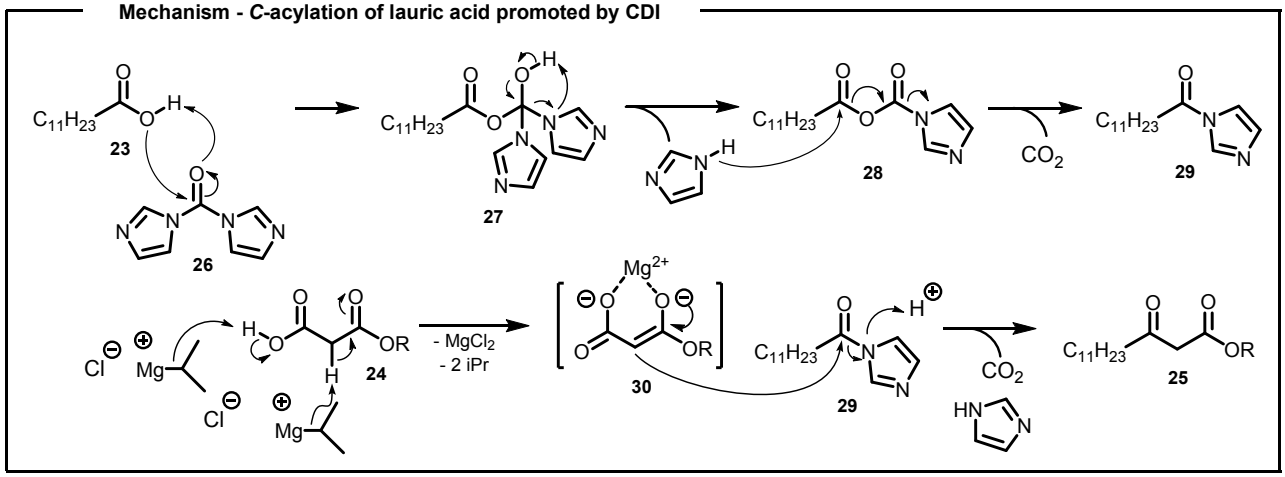

Scheme 15

The β-keto-fatty esters were converted into carboxylic acid **21** by hydrogenation of **25a** catalyzed by Pd/C or saponification of **25b** (Scheme 16). Both ways were effective, furnishing the desired product in excellent yields.

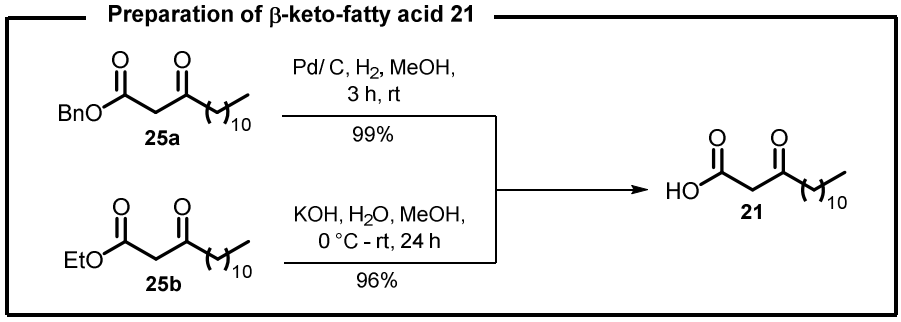

Scheme 16

3. 3. 2 Synthesis of fragment 17

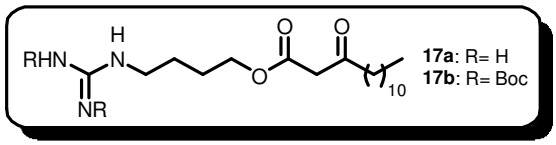

3. 3. 2. 1 Preparation of alcohols 20a and 20c

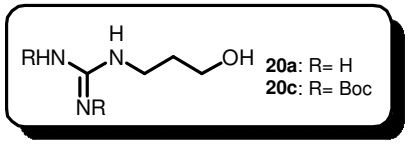

In order to mimic as best as possible the biosynthetic hypothesis, our first attempts were to convert L-arginine **19** into alcohol **20a** by an oxidative decarboxylation followed by a reduction of resulting carboxylic acid **31** into the corresponding alcohol (Scheme 17). This fragment corresponds to a constitutive unit of the "lower ester side chain" of crambescine A2.

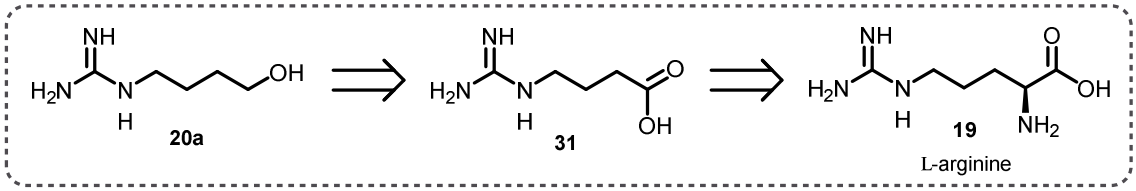

Scheme 17. Retrosynthesis of alcohol **20a** from L-arginine

For this purpose, L-arginine was oxidatively decarboxylated by dimethyl dioxirane generated *in situ*[70] (Scheme 18), giving carboxylic acid **31** with a moderate yield of 49% (literature: 57%).

[70] V. M. Paradkar, T. B. Latham, D. M. Demko, *Synlett* **1995**, *1995*, 1059-1060.

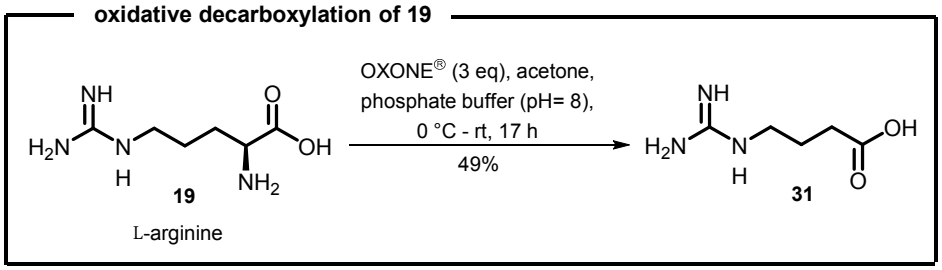

Scheme 18

A proposal of mechanism is presented on Scheme 19[70]. The authors claimed that intermediates **19a**, **19b**, and **32** were produced from the oxidation of amines with dioxirane. Decarboxylation of **19b** by a cyclic transition state leads to oxime **32**, that undergoes a hydrolysis to aldehyde **33** and is further converted into carboxylic acid **31** by an oxidation.

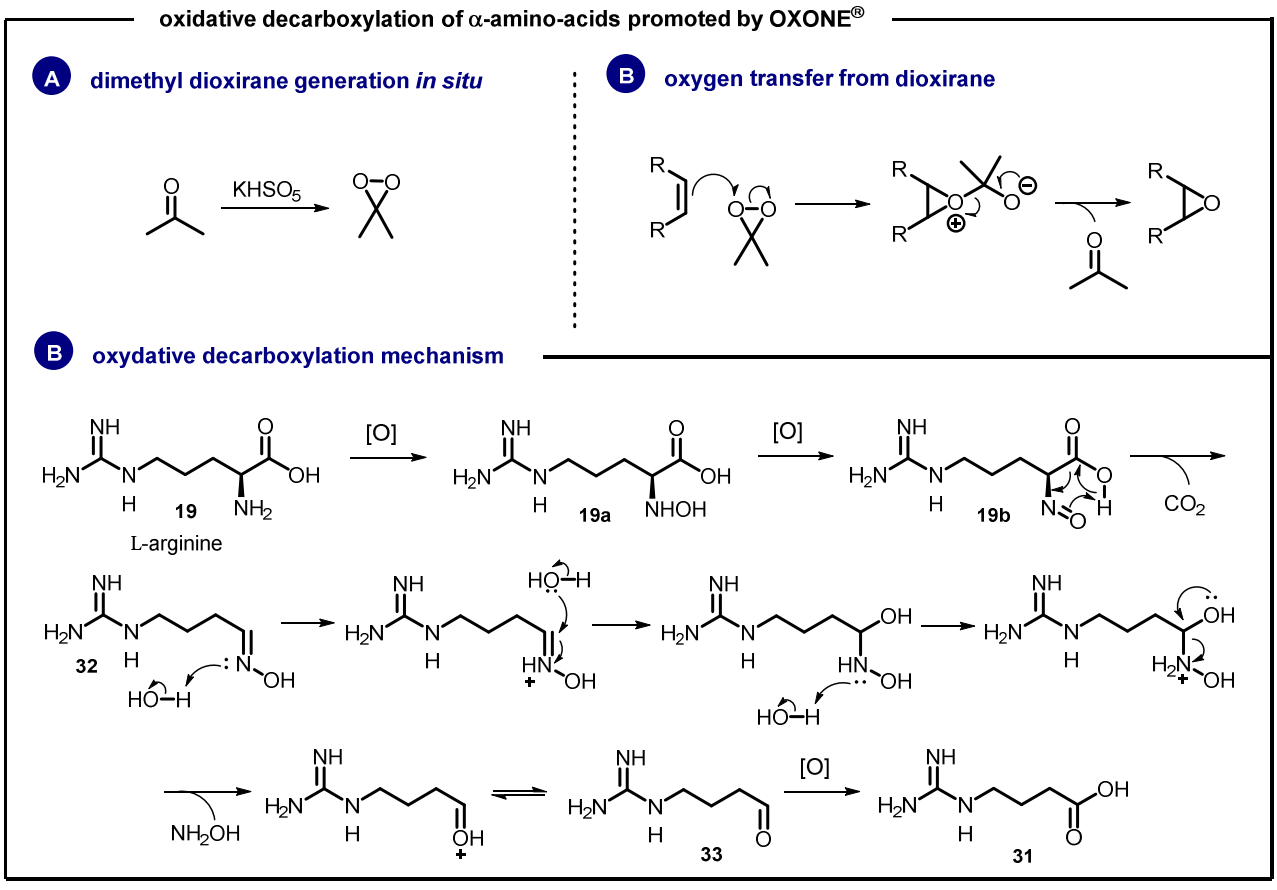

Scheme 19

Compound **31** was submitted to reduction by $LiAlH_4$. Desired alcohol **20a** was identified by HRMS but the product was lost during the purification on Amberlyst® 15.

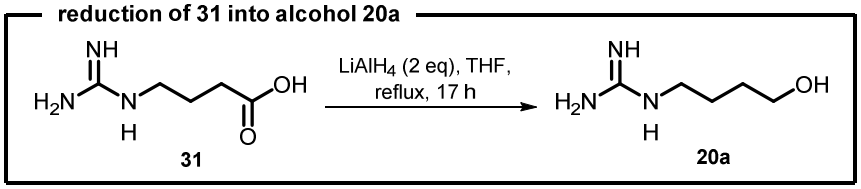

Scheme 20

To reduce the number of steps, we decided to obtain **20a** by guanylation of commercial amino alcohol **22** (Table 4). Two kinds of guanylating agents were tried: a thiourea[71] and a sulfinic acid[72]. Thiourea was the one that furnished desired **20a** in higher yield.

Table 4. Guanylation of amino alcohol **20a**

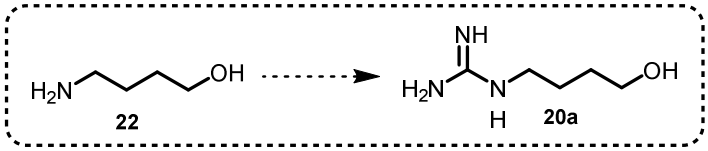

Entry	Conditions	Result
1	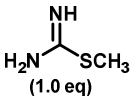 (1.0 eq) DMF, rt, 7 days	**20a** (59%)
2	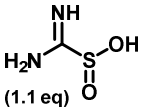 (1.1 eq) TEA, MeOH, H_2O, rt, 21 h	**20a** (38%)

Predicting that protected guanidine could be necessary to obtain chemoselectivity or to simplify purification in the following steps, we also synthesized the *N*,*N*′-bis protected guanidine **20c** by reaction of commercially available *N*, *N*′ bis-Boc-1-guanylpyrazole **9a** with amino alcohol **22** (Scheme 21).

[71] R. G. Linde, N. C. Birsner, R. Y. Chandrasekaran, J. Clancy, R. J. Howe, J. P. Lyssikatos, C. P. MacLelland, T. V. Magee, J. W. Petitpas, J. P. Rainville, W. G. Su, C. B. Vu, D. A. Whipple, *Bioorg. Med. Chem. Lett.* **1997**, *7*, 1149-1152.

[72] O. I. Shmatova, V. N. Khrustalev, V. G. Nenajdenko, *Org. Lett.* **2016**, *18*, 4494-4497.

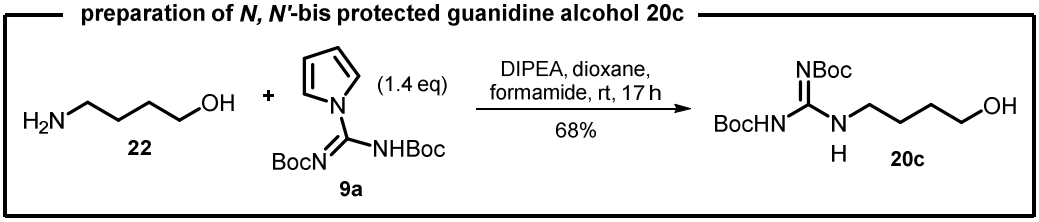

Scheme 21

3. 3. 2. 2 Attempts to the formation of fragment 17 by transesterification

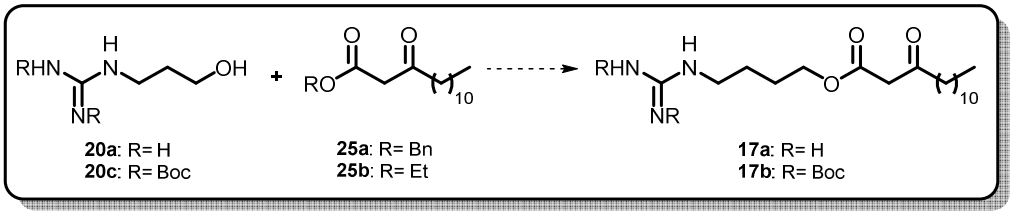

At this stage the alcohol **20** had to be connected to ester **25** in order to produce a fragment containing the "lower" and the "upper" side chains as well as the reactive β-keto-ester function necessary for the biomimetic assembly of the central core of crambescin A2. The initial approach to prepare fragment **17a** was the transesterification of **25a** by alcohol **33** (Scheme 22) promoted by acidic Amberlyst® 15[73]. After 2 days at reflux, the crude mixture was submitted to HRMS analysis where a high intensity peak possessing a *m/z* close to the desired product was identified ($[C_{19}H_{37}N_3O_3+H]^+$ calculated= 356.2908, experimental= 356.2894). Unfortunately, after flash chromatography, any fraction presented the same peak neither a ^{1}H-NMR spectra that could be attributed to the desired product. We decided to keep trying the transesterification with **25b** instead of **25a** because **25b** could generate EtOH as a by-product, an alcohol that could be removed from the reaction by heating and shift the equilibrium to products formation.

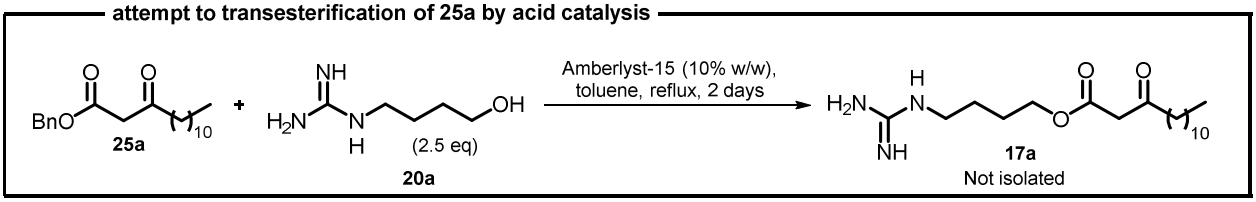

Scheme 22

[73] S. P. Chavan, Y. T. Subbarao, S. W. Dantale, R. Sivappa, *Synthetic Commun.* **2001**, *31*, 289-294.

Chavan and co-authors[74] described a procedure for the transesterification of β-ketoesters promoted by zinc and iodine that was applied to access **17a** (Scheme 23). The HRMS of the crude mixture presented a peak that could correspond to **17a** ($[C_{19}H_{37}N_3O_3+H]^+$ calculated= 356.2908, experimental= 356.2903). One interesting finding was a peak at *m/z* 338.2784, 18 units less than the *m/z* of **17a**, that could be generated by a water elimination on **34** (Scheme 24). This elimination is possible if a formation of a terminal hydroxyl takes place, such as in **34**, so this finding may indicate that the NH from guanidino function of **20a**, instead of the OH, had attacked the carbonyl group. To assure the desired chemoselectivity it was decided to try the transesterification with protected substrate **20c**.

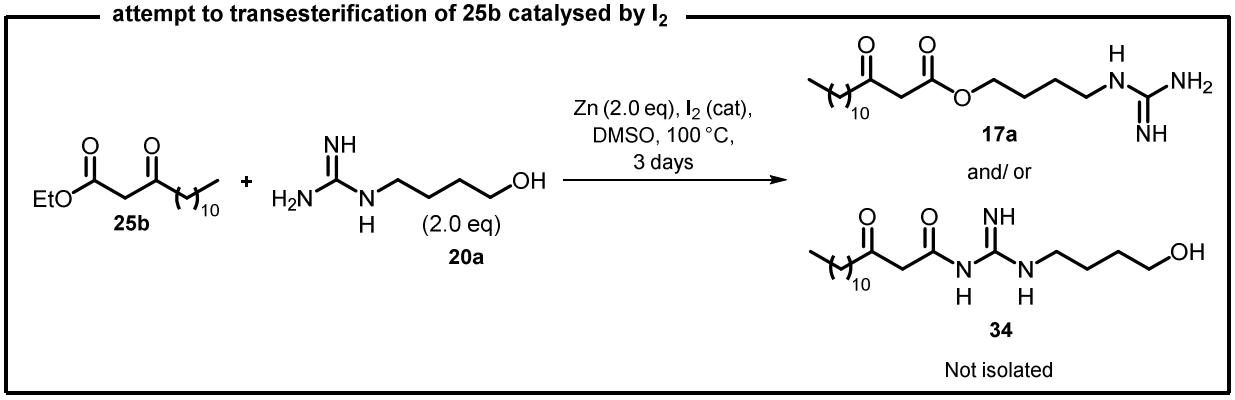

Scheme 23

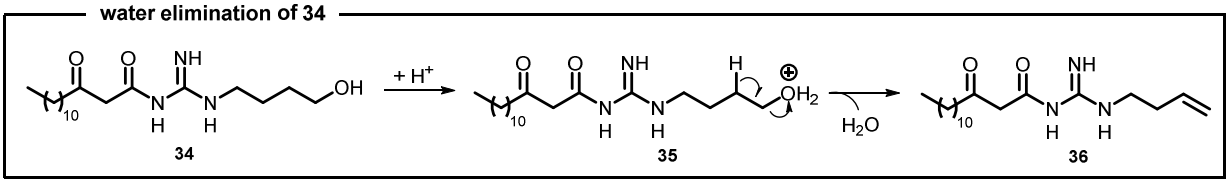

Scheme 24

For this purpose Taber's transesterification[75] of **25b** with **20c** catalyzed by 4-dimethylaminopyridine (DMAP) (Scheme 25) was studied, the same approach as used by Snider's group during their synthesis of crambescins[44]. Despite Snider and Shi had reported a low conversion of starting material into their desired product (77% of recovered starting ester and 33% of yield of expected ester), we decided to try this approach due to the structural similarities shared between **25b** and **20c** and the substrates used by Snider's group. Unfortunately the HRMS of the crude product did not present the peak corresponding to desired product neither its

[74] S. P. Chavan, K. Shivasankar, R. Sivappa, R. Kale, *Tetrahedron Lett.* **2002**, *43*, 8583-8586.
[75] D. F. Taber, J. C. Amedio, Y. K. Patel, *J. Org. Chem.* **1985**, *50*, 3618-3619.

protected version. Instead, it was found a peak of starting ester **25b** ($[C_{16}H_{30}O_3$+ Na$]^+$ calculated: 293.2087, experimental: 293.2125) mixed with the aldol product **37** ($[C_{32}H_{60}O_6$ + Na$]^+$ calculated: 563.4282, experimental: 293.4308). Formation of aldol product can explain the appearance of a spot less polar than starting ester **25b** on TLC analysis.

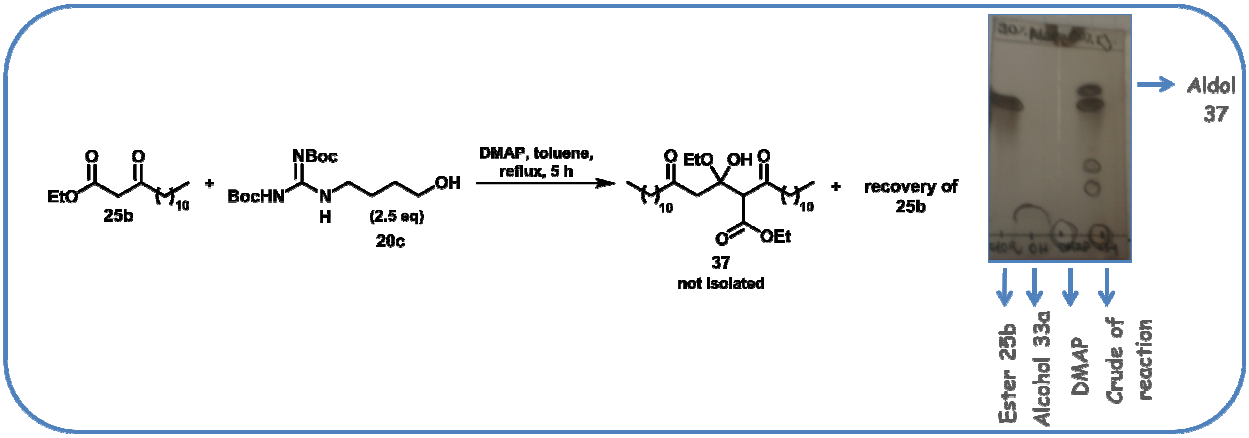

Scheme 25. Attempt of Taber's transesterification of 25b and TLC result

3. 3. 2. 3 Formation of fragment 17 promoted by coupling reagents

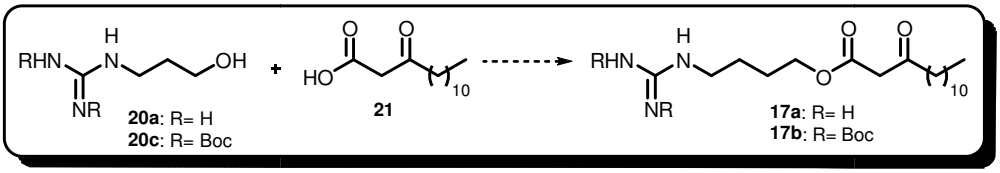

At this point, we considered, as an alternative, a coupling between alcohol **20a** and carboxylic acid **21** instead of a transesterification reaction (Table 5).

It was noticed that **20a** was insoluble in most of organic solvents, explaining the experiments of entries 4-6. Also, the chromatographic purifications were performed with different eluents and at the end the stationary phase was always cleaned with AcOEt or MeOH, a procedure that did not avoid losing the product. Even Sephadex purifications did not allow a good separation. Following the reaction evolution was another problem taking into account that the product is invisible under UV and did not furnish spots in any of tested TLC stains: I_2, vanilline, Dragendorf, sodium nitroprussate / potassium hexacyanoferrate(III), and ninhydrin. As HRMS analysis indicated product formation, we decided to keep trying coupling reactions but using protected substrate **20c**. The Boc groups would also furnish a chromophore to the desired β-ketoester and decrease its

polarity facilitating the purification process.

Table 5. Coupling reactions between **21** and **20a**

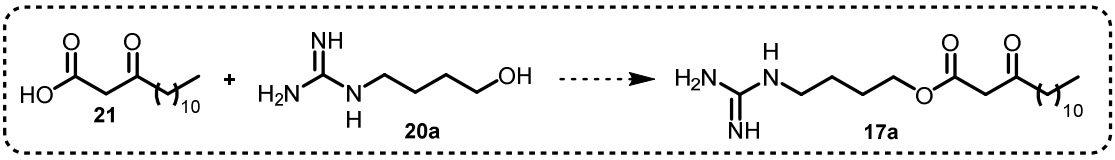

Entry	Conditions	Result
1	EDC (1.1 eq), HOBt (1.8 eq), DIPEA, DMF, **20a** (10 eq), rt - 50°C, 24 h	Decarboxylation of **21**
2	1) **21**, CDI (1.1 eq), THF, O °C, 2 h 2) Addition of **20a** (3 eq) to solution 1, rt, 6 h	Decarboxylation of **21**
3	1) **20a**, CDI (1.0 eq), DIPEA (1 eq.), DCM, 0 °C-rt 2) $CuBr_2$ (cat, 10 mol%), HOBt (10 mol%), DCM, **21** (1.5 eq)	Crude product: HRMS peak corresponding to **17a**. The product was lost during purification on flash chromatography using silica gel 60 HRMS: $[C_{19}H_{37}N_3O_3 + H]^+$ calculated= 356.2908, experimental= 356.2921
4	**20a** (1.0 eq), **21** (1.0 eq), HOBt (1.0 eq), DCC (1.1 eq), ACN, 25 °C, 1 day	Same as entry 3
5	**20a** (1.0 eq), **21** (1.0 eq), HOBt (1.0 eq), DCC (1.0 eq), DMSO : DMF (1 : 2), 25 °C, 2 days	Same as entry 3
6	**20a** (1.0 eq), **21** (1.0 eq), HOBt (1.0 eq), DCC (1.0 eq), H_2O : DMF (1 : 2), 25 °C, 23 h	Same as entry 3

Finally Neises and Steglich esterification[76] between **21** and **20c** allowed the preparation of **17b** in 46% of yield (Scheme 26).

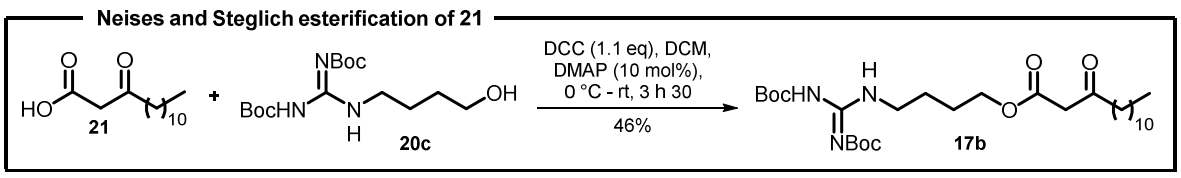

Scheme 26

[76] B. Neises, W. Steglich, *Angew. Chem.Int. Ed. Engl.* **1978**, *17*, 522-524.

The mechanism of this reaction is presented on Scheme 27. The reactivity of the carboxyl function from **21** is enhanced to nucleophilic attack by *N*,*N*′-dicyclohexylcarbodiimide (DCC), forming *O*-acylisourea intermediate **38**. Catalyst DMAP, a stronger nucleophile than alcohols, reacts with protonated intermediate **38** giving amide **39**. The acyl group is then transferred to **20c** by a nucleophilic substitution leading to **17b**.

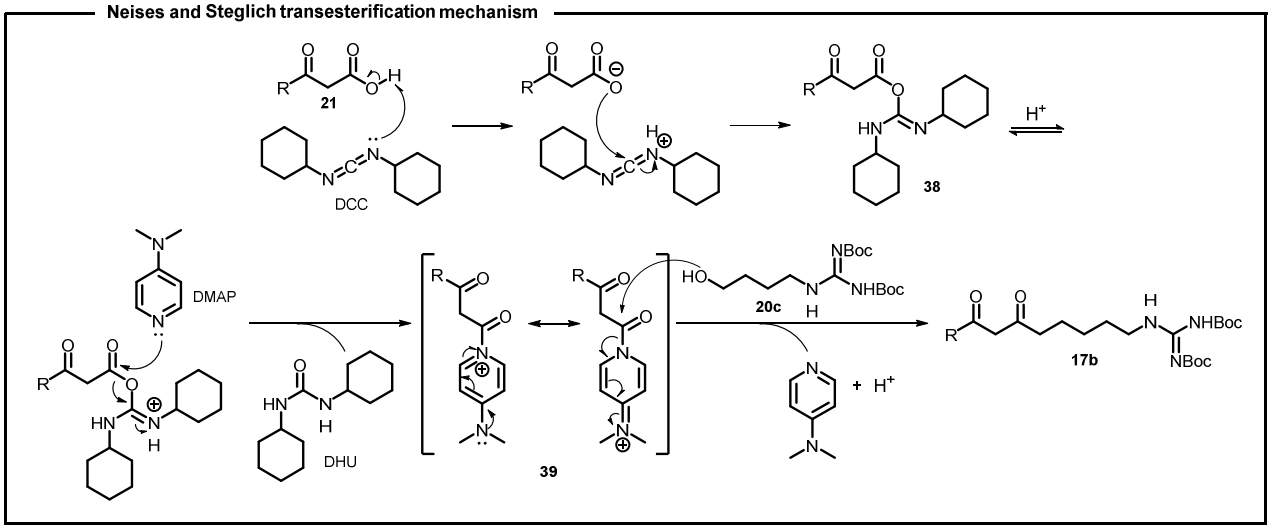

Scheme 27

3. 3. 3 Synthesis of guanidinated pyrrolidinium 18

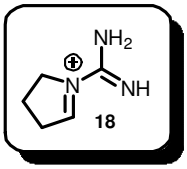

3. 3. 3. 1 Preparation of 18 by sequential reductions of L-arginine

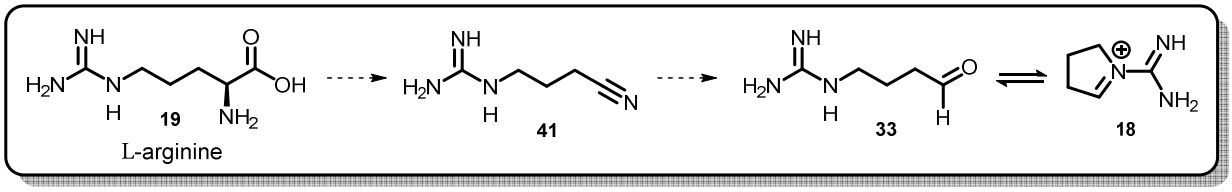

The second task was to convert L-arginine onto the pyrrolidinium **18** necessary for the biomimetic assembly of crambescin A2. The initial strategy to prepare **18** was an oxydative decarboxylation of L-arginine **19** into the aldehyde **33** (Scheme 28). An intramolecular nucleophilic substitution of the amino group from guanidine on the carbonyl of aldehyde would furnish the guanidinated pyrrolidinium **18**. This pyrrolidinium could be trapped by a cyanide or, better, be

used directly as a perfect biosynthetic intermediate.

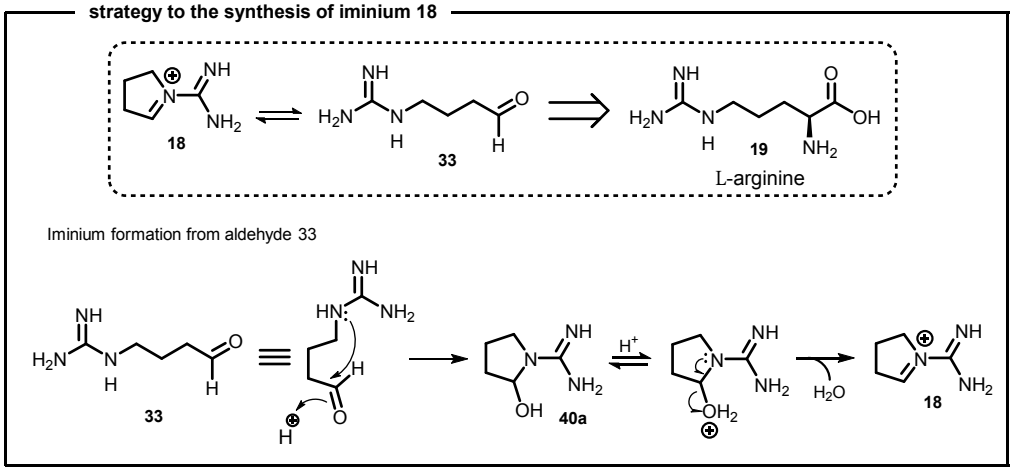

Scheme 28

The decarboxylation of L-arginine promoted by trichloroisocyanuric acid (TCCA)[77] furnished **41** quantitatively (Scheme 29).

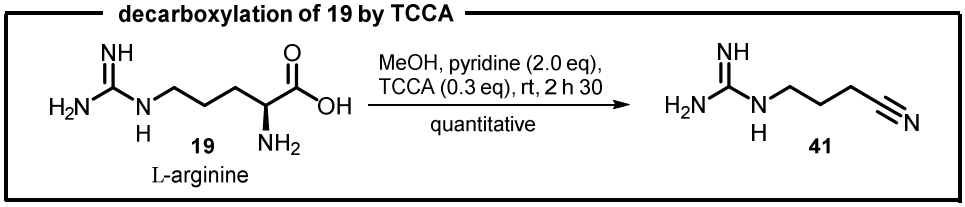

Scheme 29

For the oxidative decarboxylation of L-arginine into nitrile, we propose a mechanism similar to the oxidation of alcohols by TCCA published by van Summeren and co-authors[78] (Scheme 30). The authors suggested that the pyridine and TCCA form a *N*-chloropyridinium cyanide species that acts as an unique oxidation system. While the cyanide species deprotonates the amine function of **19**, the *N*-chloropyridinium promotes the α-CH bond hydride abstraction, performing thereby a concerted mechanism. Further, species **42** decarboxylates giving rise to the desired nitrile **41**.

[77] G. A. Hiegel, J. C. Lewis, J. W. Bae, *Synthetic Commun.* **2004**, *34*, 3449-3453.
[78] R. P. van Summeren, A. Romaniuk, E. G. Ijpeij, P. L. Alsters, *Catal. Sci. Technol.* **2012**, *2*, 2052-2056.

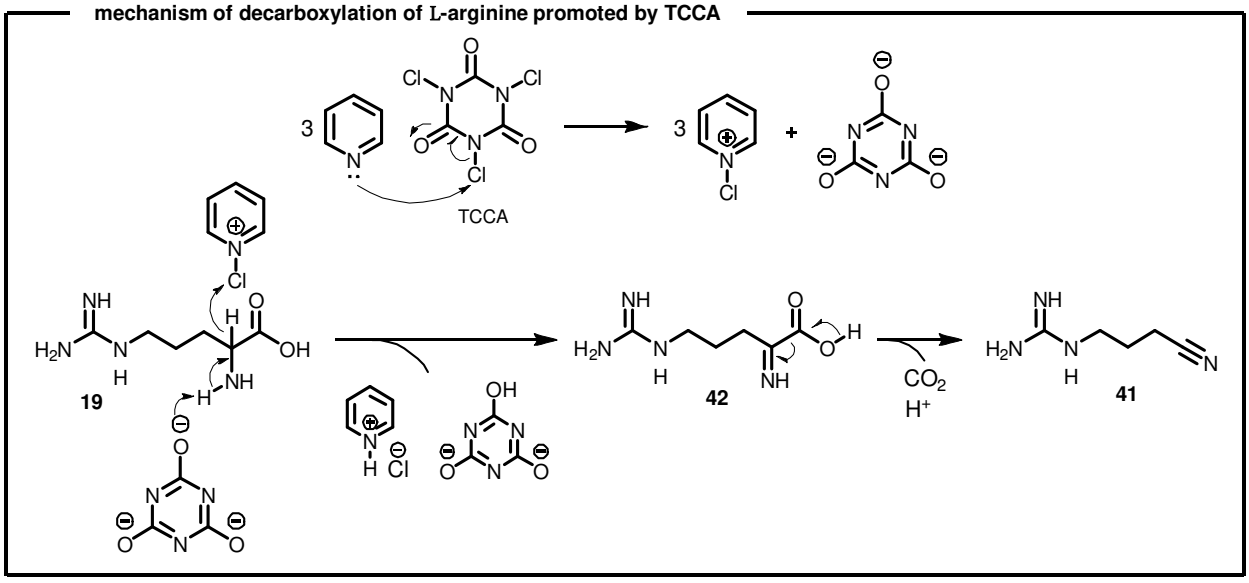

Scheme 30

Next, a reduction of nitrile onto an aldehyde was required. Some approaches often used to reduce nitriles into aldehydes are presented below:[79]

1) The classical Stephen aldehyde synthesis employing HCl gas and anhydrous $SnCl_2$;
2) The catalytic partial hydrogenation promoted by a metal catalyst such as Pd, Pt or Raney nickel and hydrogen gas. The nitrile is converted into an intermediate imine and subsequently hydrolyzed to aldehyde. The addition of a trapping agent such as phenylhydrazine can avoid the overreduction of aldehyde to amine.
3) The partial hydrogenation by a metal hydride, for instance $LiAlH_4$ or $NaBH_4$;
4) The modified Stephen reduction using Raney nickel in aqueous solution of an acid (e.g.: formic acid, acetic acid, H_2SO_4).

In view of these procedures, our first assays to convert **41** into **33** were adapted from the classical reductions promoted by DIBAL-H and Pd/C (entries 1 and 2, Table 6), which resulted in starting material recovery. It was observed that **41** was insoluble in organic solvents, therefore a modified Stephen reduction in aqueous conditions was considered (conditions described on entries 3 to 7). Finally conditions of entry 7 led to the expected aldehyde **33** mixed with iminium **18**.

[79] B. Staskun, T. van Es, *S. Afr. J. Chem.* **2008**, *61*, 144-156.

Table 6. Reduction of nitrile **41** into aldehyde **33**

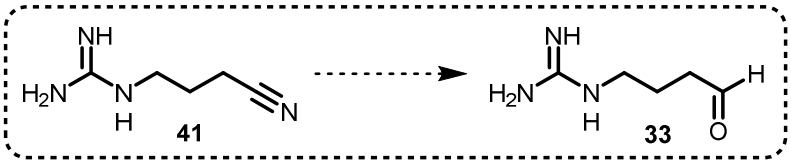

Entry	Conditions	Result
1	DIBAL-H (10 eq), DMSO : THF (1 : 5), - 78 °C, 3 h	Starting material recovery
2	Pd/C (10% w/w), EtOH, rt, H_2, 42 h	Starting material recovery
3[80]	$Et_3NH^+H_2PO^{2-}$. 1.5 H_2O, Ni-Raney (4 : 1, w/w), THF : EtOH (2 : 1), 0 °C, 2 h 30	Starting material recovery(*)
4	$Et_3NH^+H_2PO^{2-}$. 1.5 H_2O, Ni-Raney (25 : 1, w/w), THF : EtOH (1 : 2.5), 0 °C, 7 h	Starting material recovery
5	$Et_3NH^+H_2PO^{2-}$. 1.5 H_2O, Ni-Raney (25 : 1, w/w), EtOH, rt, H_2, 42 h	Starting material recovery
6	Ni-Raney (5 : 1, w/w), HCOOH 75 % (v/v), reflux, 1 h	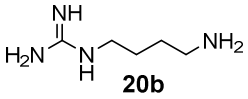 **20b** Checked by HRMS. $[C_5H_{14}N_4+H]^+$calculated: 131.1291, experimental: 131.1297
7[81]	Ni-Raney (1 : 1, w/w), HCOOH 75 % (v/v), reflux, 1 h	**33** and **18** crude checked by ^{1}H-RMN and HRMS

* ^{1}H-NMR presented low intensity peaks corresponding to aldehyde **33**

3. 3. 3. 2 Preparation of 18 by oxidative decarboxylation of L-arginine

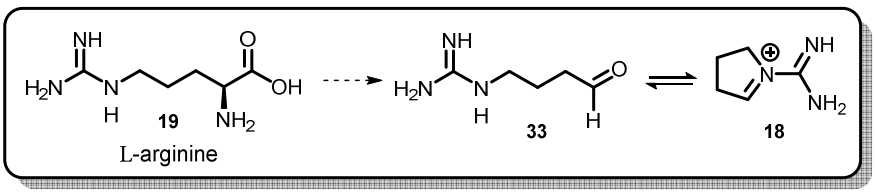

Alternatively, it was also tried to obtain aldehyde **33** in a single step by oxidative decarboxylation of L-arginine promoted by silver(II) picolinate[82,83] (Scheme 31). We were glad to

[80] B. T. Khai, A. Arcelli, *J. Org. Chem.* **1989**, *54*, 949-953.
[81] T. van Es, B. Staskun, *Org. Syn.* **1971**, *51*, 20-23.
[82] T. G. Clarke, N. A. Hampson, J. B. Lee, J. R. Morley, B. Scanlon, *J. Chem. Soc. C* **1970**, 815-817.
[83] T. G. Clarke, N. A. Hampson, J. B. Lee, J. R. Morley, B. Scanlon, *Can. J. Chem.* **1969**, *47*, 1649-1654.

notice that the reaction proceeded exactly as described, with red colour discharging indicating the reduction of silver complex and the end of the reaction. Formation of aldehyde **33** and iminium **18** was confirmed by HRMS.

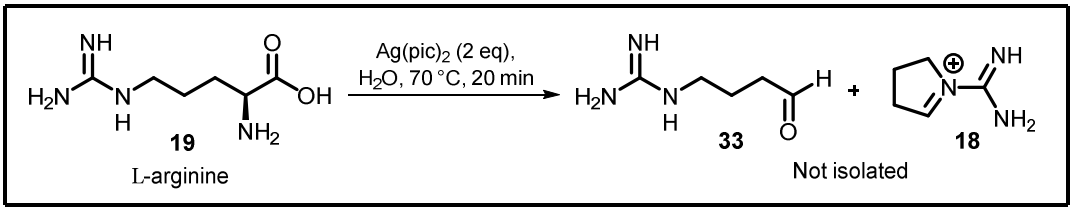

Scheme 31

Efforts were made to convert and to isolate the iminium species as a cyanide (Scheme 32). For this purpose, after the acidification and filtration of reaction mixture with $Ag(pic)_2$ to get rid of silver, KCN (2 eq) was carefully added to the filtrate and submitted to magnetic stirring for 3 h at rt. An extraction with AcOEt and water was tried to separate the picolinic acid (by-product of the oxidative decarboxylation) and inorganic salts from **40b**, but the desired product was identified in the aqueous layer. Both phases were joined and evaporated. Unfortunately the product was obtained mixed with picolinic acid after purification by either flash chromatography on silice 60 or LH-20 Sephadex column.

Having into account the difficulties faced to purify the iminium trapped with cyanide, the crude product of the reaction presented on Scheme 31 was then employed for the next steps without further purification.

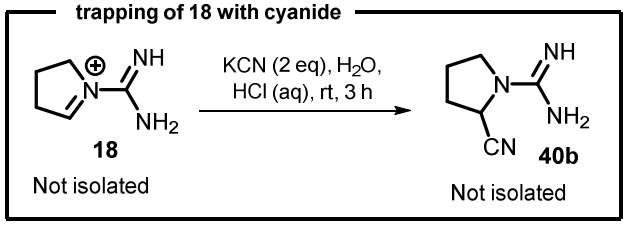

Scheme 32

The oxidative decarboxylation of aminoacids promoted by silver(II) picolinate was found to pass by a cyclic intermediate **19c**, consisting in a eletrocyclic (concerted) mechanism with reduction of silver(II) to its elementary state (Scheme 33).[82, 84] Non reacted silver(II) picolinate immediately reoxidizes Ag° to Ag^{2+}. A radical mechanism does not take place, as proved by

[84] Y. Zelechonok, R. B. Silverman, *J. Org. Chem.* **1992**, *57*, 5787-5790.

trapping experiments.[84] Thereafter hydrolysis of **43** furnishes aldehyde **33**.

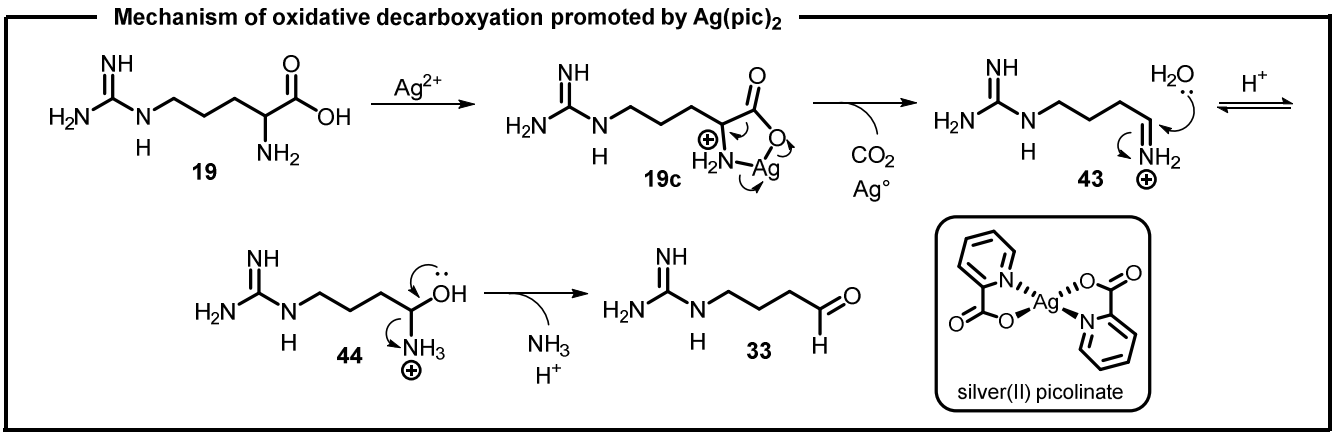

Scheme 33

3. 3. 4 Key-step: formation of the bicyclic guanidine core

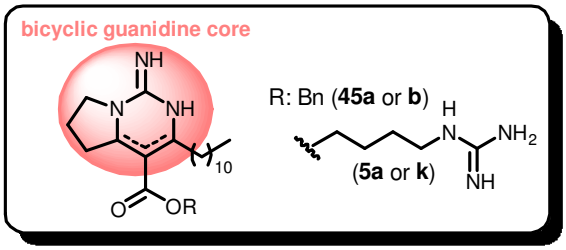

3. 3. 4. 1 Formation of structures 45a and 45b

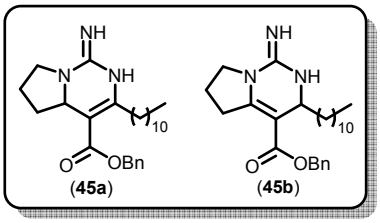

Having prepared the two required fragments **18** and **25**, the study of the biomimetic assembly of the central core of crambescin A2 could be started. Following the biosynthesis hypothesis presented in Chapter 2, Scheme 6, condensations between **18** and **25a** were logically evaluated under Mannich or Biginelli-type conditions to access platform **45** (Table 7).

Table 7. Condensations between **18** and **25a** applying Mannich and Biginelli-type conditions*

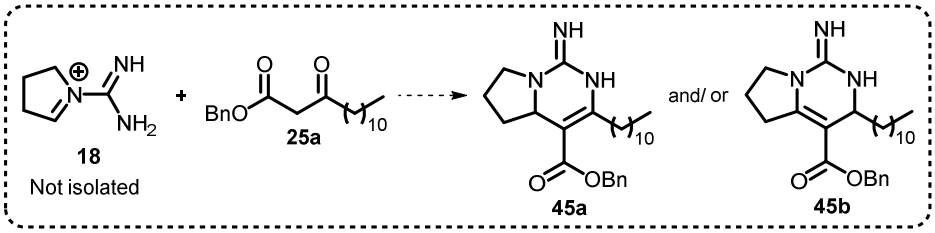

Entry	Conditions	Result
1	H_2SO_4 (5 % v/v), THF, **25a** (1.0 eq), rt, 3 h 30	Starting material recovery
2	AcOH (2.5 eq), **25a** (1.0 eq), Et_2O, MeOH, -20 °C - rt, 17 h	Starting material recovery
3	morpholine (1.1 eq), AcOH (1.1 eq), **25a** (3.0 eq), Na_2SO_4 (3.6 eq), TFE, 60 °C, 2 days	Recovery of starting material
4	morpholine (1.1 eq), AcOH (1.1 eq), **25a** (3.0 eq), Na_2SO_4 (3.6 eq), TFE, 140 °C, sealed tube, 5days	Complex mixture
5	morpholine (1.2 eq), AcOH (1.2 eq), **25a** (3.0 eq), Na_2SO_4 (3.6 eq), TFE, reflux, 5 days	LC-MS: **45** + coupling products transesterified with CF_3O- and MeO-
6	morpholine (1.1 eq), AcOH (1.1 eq), **25a** (3.0 eq), Na_2SO_4 (3.6 eq), TFE, 100 °C, microwave (850 W), 1 h	LC-MS: low intensity peak corresponding to desired product **45**
7	morpholine (1.1 eq), AcOH (1.1 eq), **25a** (3.0 eq), Na_2SO_4 (3.6 eq), TFE, 150 °C, microwave (850 W), 2 h	LC-MS: low intensity peak corresponding to desired product **45**
8	morpholine (1.1 eq), AcOH (1.1 eq), **25a** (3.0 eq), Na_2SO_4 (3.6 eq), TFE, 300 °C, microwave (850 W), 2 h	LC-MS: very low intensity peak corresponding to desired product **45** + many peaks of small intensity

*The equivalents were estimated considering 100% of conversion of **19** into iminium **18**

Despite the long reaction time, entry 5 provides the best conditions to obtain **45**. These conditions correspond to the tethered Biginelli condensation developed by Overman and co-

workers[85, 86, 87] that became a classical approach to access compounds containing 3,4-dihydropyrimidin-2(1*H*)-ones-type cores (DHPMs) such as crambescidins, batzelladines, and monanchocidins (Scheme 34).[88] Despite often mentioned as a possible tool to access crambescins, to the best of our knowledge this is the first time that the tethered Biginelli is employed to build the guanidine core of such family of compounds. It is important to stress out this fact because in comparison with the DHPMs, crambescins have a double bond at positions 7 and 8 (**45b**) that by the mechanism of tetrahedred Biginelli condensation[85] will be formed between positions 7 and 13 (**45a**, Scheme 35), being necessary a further proton displacement in order to access the desired structure **45b**.

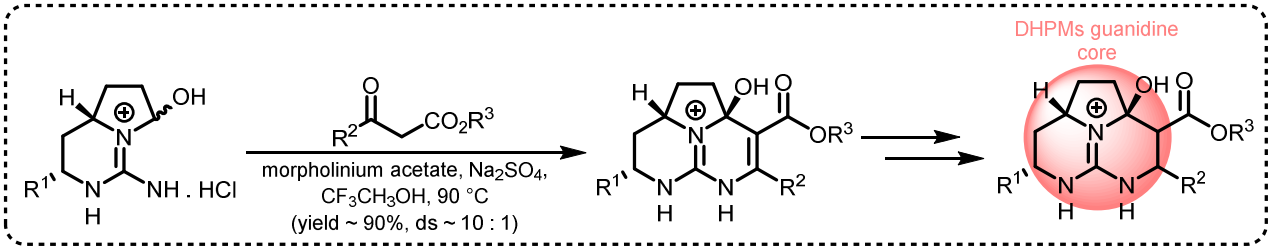

Scheme 34. Tethered Biginelli condensation applied to the construction of tricyclic guanidine core of DHPMs-type alkaloids

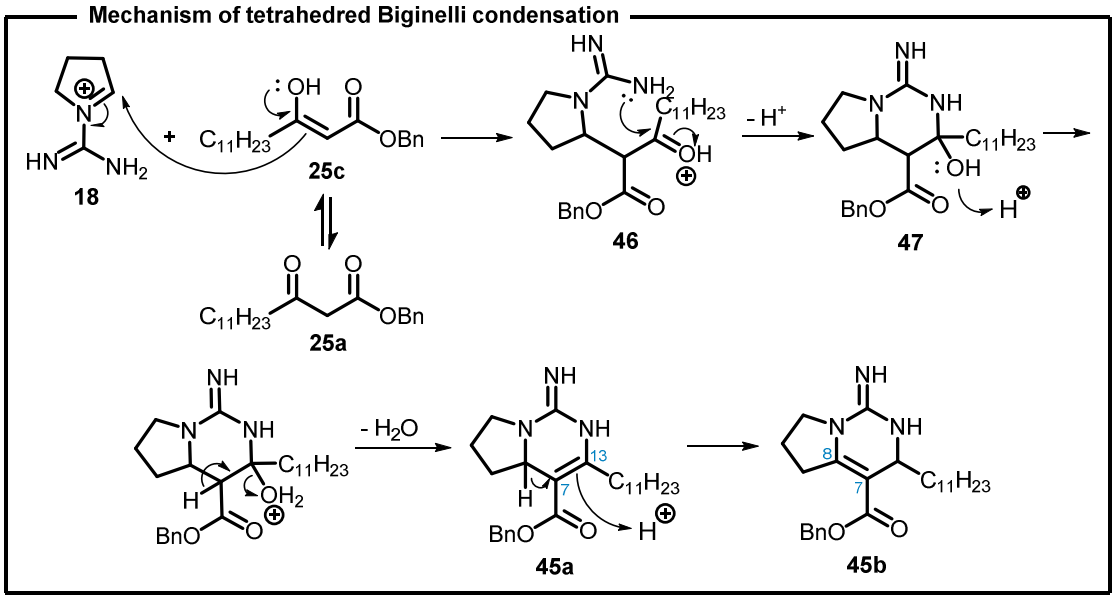

Scheme 35

The crude mixture of the Biginelli-type condensation (Table 7, entry 5) was purified by flash

[85] Z. D. Aron, L. E. Overman, *Chem. Comm.* **2004**, 253-265.
[86] B. L. Nilsson, L. E. Overman, *J. Org. Chem.* **2006**, *71*, 7706-7714.
[87] S. K. Collins, A. I. McDonald, L. E. Overman, Y. H. Rhee, *Org. Lett.* **2004**, *6*, 1253-1255.
[88] C. O. Kappe, *Acc. Chem. Res.* **2000**, *33*, 879-888.

chromatography on silica 60 column, giving a fraction constituted mostly by picolinic acid and a mixture of **45** and **49** and their putative respective aromatized structures **48a** and **48b** (Figure 29). By the analysis of 1D and 2D NMR, it was inferred the formation of both isomers **45a** and **45b**.

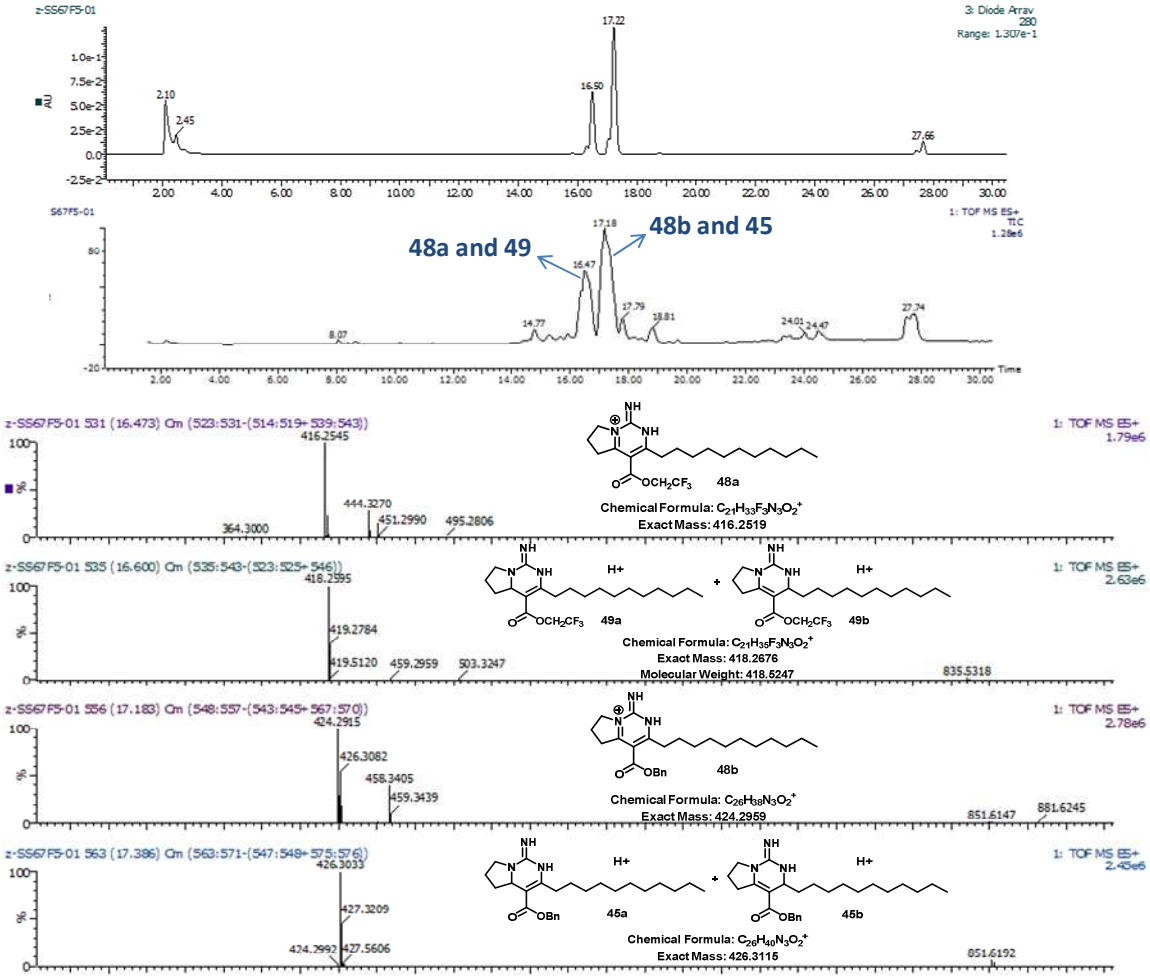

Figure 29. LC-MS of a fraction of the Biginelli-type condensation reaction between **18** and **25a**

In order to obtain only desired **45b**, the product was submitted to acid reflux in DCM (Scheme 36). As a result the counter ion of the guanidinium compounds was exchanged by a triflate and we got rid of the picolinate counter anion signals on NMR spectra (Figure 30). However, a mixture of **45a** and **45b** was still observed.

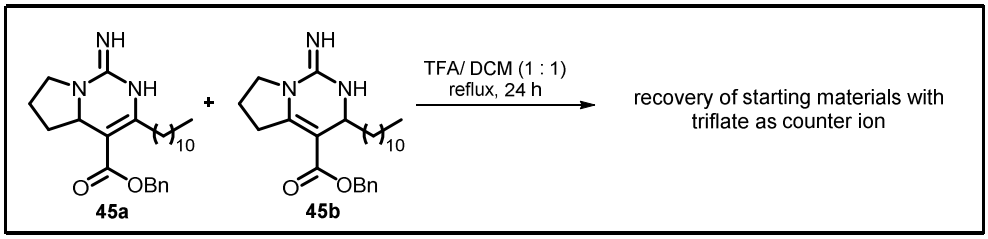

Scheme 36

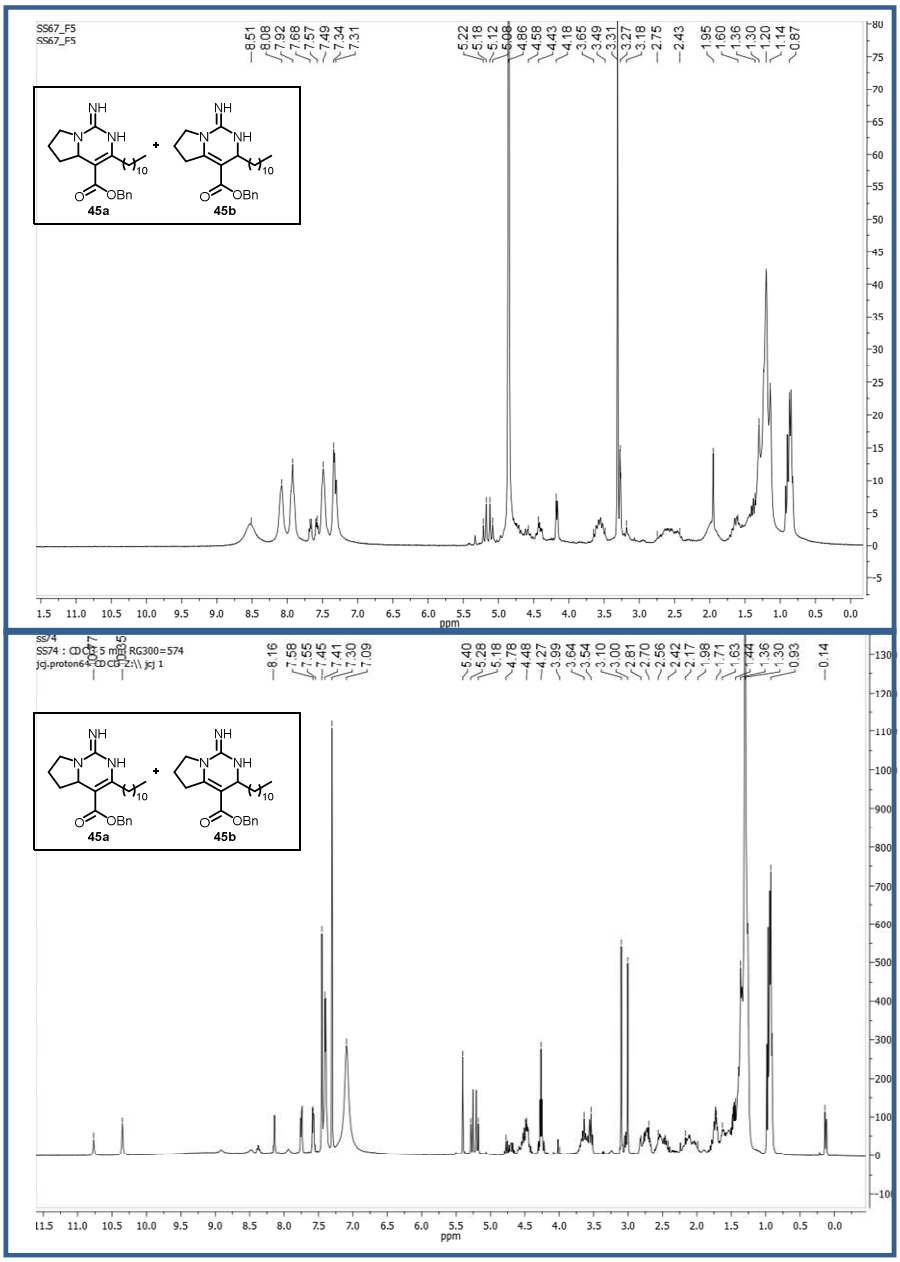

Figure 30. ^{1}H-NMR spectra mixture **45a** and **45b** before (top, in MeOD-d_4) and after reflux in DCM : TFA (9 : 1) (bottom, in $CDCl_3$)

Preliminary assays to achieve an asymmetric isomerization of **45a** into **45b** catalysed by Rh(I) complex or a full aromatization of this mixture promoted by MnO_2 (Scheme 37) were performed using a small amount of substrates. The full aromatization could lead to an analogue of dehydrocrambescin A2 418 (**48c**), a compound recently isolated from a French Polynesian *Monanchora* n. sp. sponge[89]. Surprisingly, the aromatization with MnO_2 gave the starting materials and according to LC-MS, the Rh(I) complex promoted the full aromatization of **45** and **49** instead of

[89] A. El-Demerdash, C. Moriou, M.-T. Martin, A. d. S. Rodrigues-Stien, S. Petek, M. Demoy-Schneider, K. Hall, J. N. A. Hooper, C. Debitus, A. Al-Mourabit, *J. Nat. Prod.* **2016**, *79*, 1929-1937.

the asymmetric isomerization.

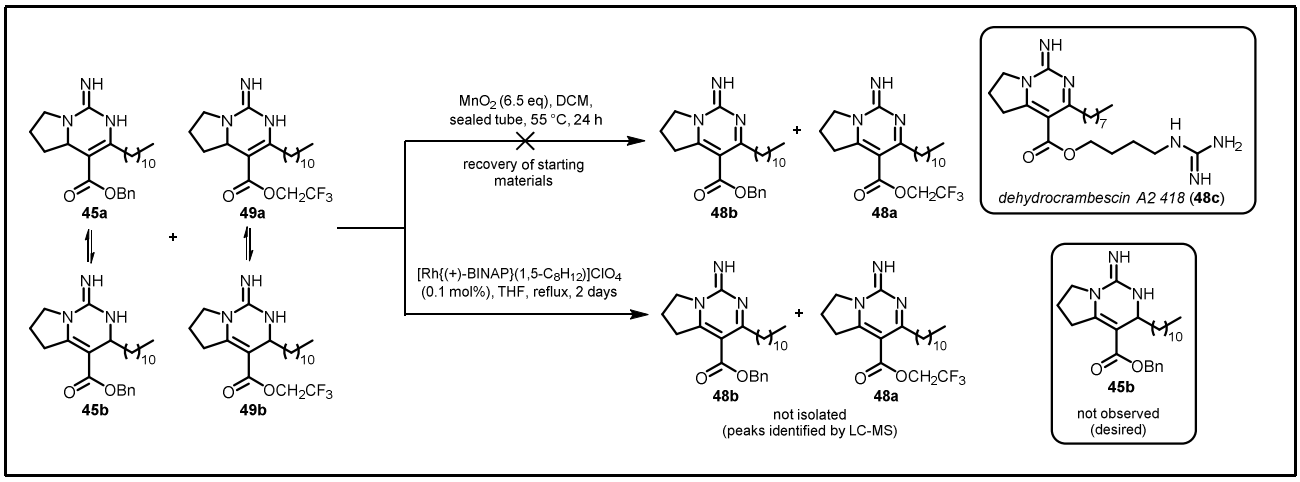

Scheme 37

3. 3. 4. 2 Formation of crambescin A2 448 (5a) and *iso*-crambescin A2 448 (5k)

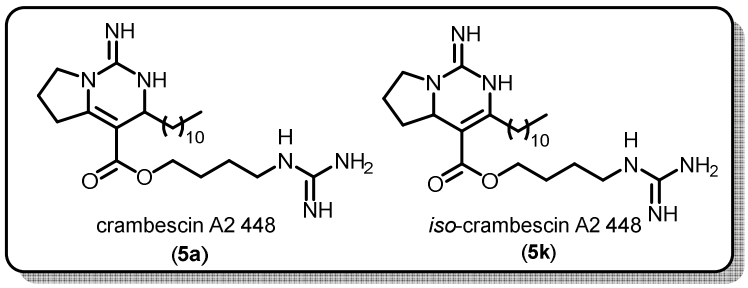

Even with the double bond at a wrong position, we kept on trying to form the crambescin A2 scaffold by the transesterification of the mixture containing **45** and **49** by alcohol **20a**. The conditions assayed are presented bellow (Table 8).

Table 8. Transesterification of the mixture containing **45**

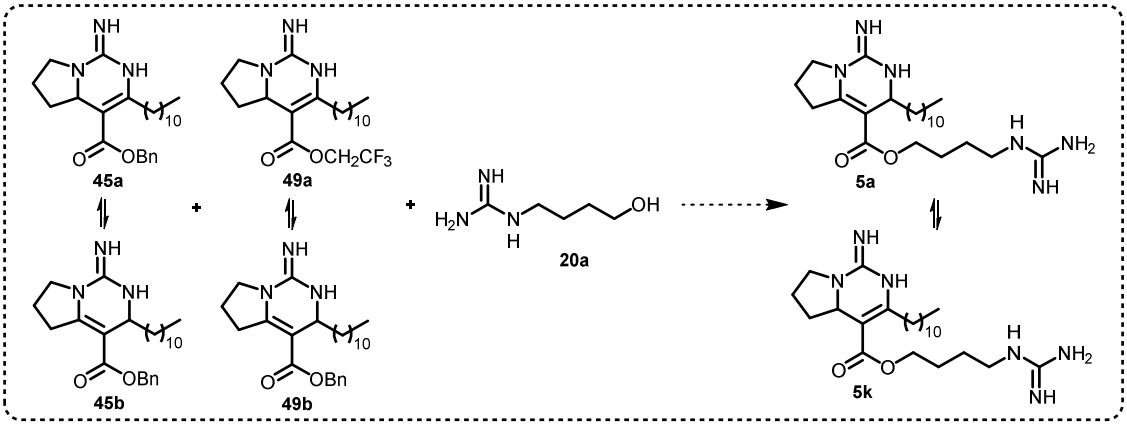

Entry	Conditions	Result
1	Amberlyst 15 (10% w/w), **20a** (1 eq), toluene, reflux, 18 h	Recovery of starting materials
2	K_2CO_3 (0.5 eq), **20a** (3 eq), DMF, 100 °C, 1 day	Recovery of starting materials
3	Amberlyst 15 (10% w/w), **20a** (3.9 eq), toluene, 150 °C, sealed tube, 18 h	Complex mixture
4	Amberlyst 15 (10% w/w), **20a** (3.9 eq), DMF, reflux, 2 days	Complex mixture

As the transesterification did not proceed, the strategy was changed to form the carboxylic acid **50** and to obtain **5a** by an esterification. Unfortunately the desired product **50** was not observed by this approach (Table 9).

Table 9. Saponification of mixture containing **45b**

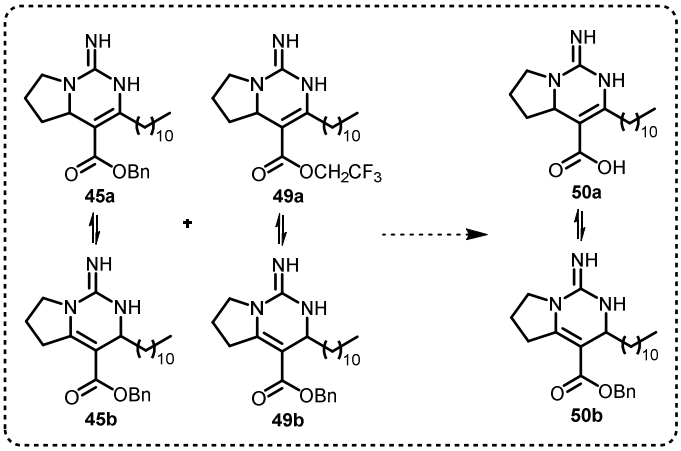

Entry	Conditions	Result
1	KOH (4 M), MeOH, rt, 1 day	LC-MS: **25a** and 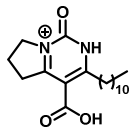 **48d** Chemical Formula: $C_{19}H_{31}N_2O_3^+$ Exact Mass: 335.2329 Found: 335.2332
2	LiOH (2.0 eq), MeOH : H_2O (1 : 1), reflux, 2 h	**25a**

Finding good conditions for the esterification or the transesterification of mixture **45** and **49** was more challenging than expected and was consuming both iminium **18**, β-keto-ester **25a**, alcohol **20a** and time, whereas the condensation takes 5 days to be accomplished. For this reason, we optimized the preparation of substrate **17b**, that contained already the ester moiety, and performed the tethered Biginelli condensation between **18** and this substrate (Scheme 38).

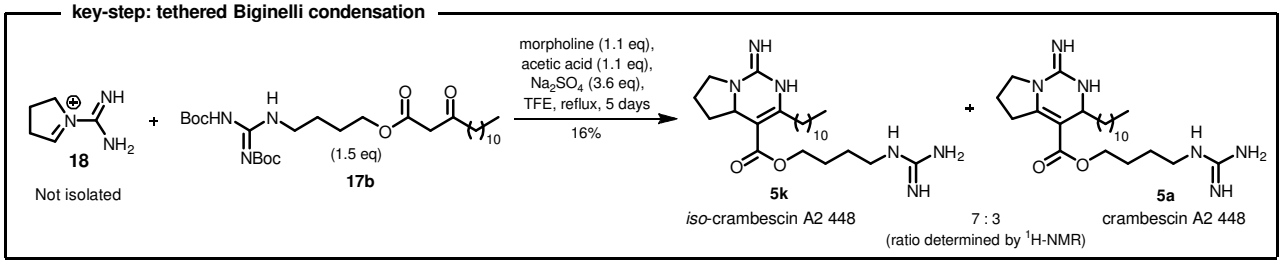

Scheme 38

Thus, using the same conditions as decribed above (section 3. 3. 4. 1), the biomimetic assembly of **17b** and **18** produced in a single step the complete structure of crambescin A2 448 as

a 7 : 3 isomeric mixture of **5k** and **5a**. The mechanism of the tethered Biginelli transformation was already presented on Scheme 35. Conveniently on the course of the reaction the substrate **17b** was deprotected, giving **17a**. This assumption is based on the fact that unconverted **17a** was isolated during the HPLC purification of the crude product and any **17b** nor protected *bis*-Boc **5a** or **5k** were observed. The desprotection of **17b** is showed on Scheme 39.

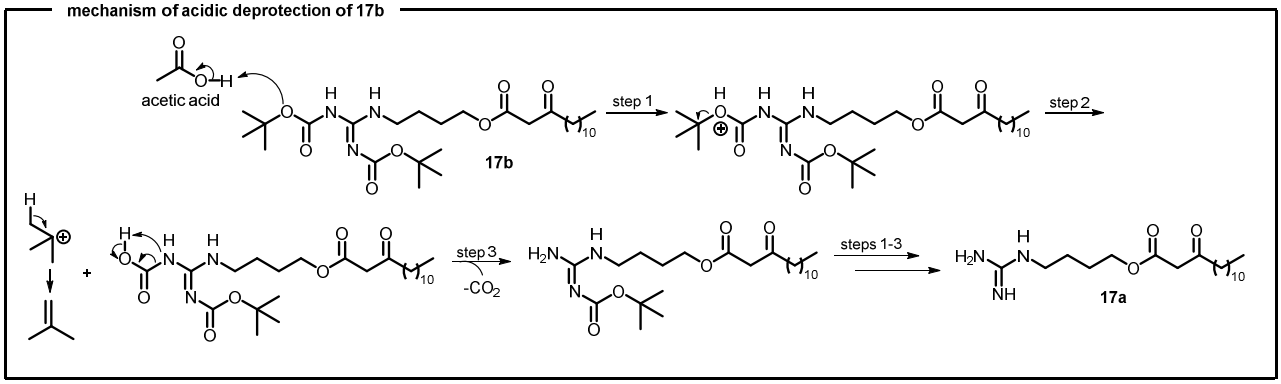

Scheme 39

The comparison of the ^{1}H-NMR spectra of **5k** with crambescin A2 ^{1}H-NMR spectra available in literature[45] differs mainly on the multiplicity of peak at 4.5 ppm (a triplet for crambescin A2 and a double doublet for compound **5k**) as well as in the signals between 2.4 and 3.0 ppm. It is possible to note the signals of crambescin A2 **5a** at 4.4 ppm (*t*, H7) and at 3.1 ppm (*dd*, H9) integrating to 0.3. Unfortunately the mass of the mixture containing crambescin A2 was too low (around 6 mg) and this compound was not isolated and fully characterized to confirm, by instance, its stereochemistry.

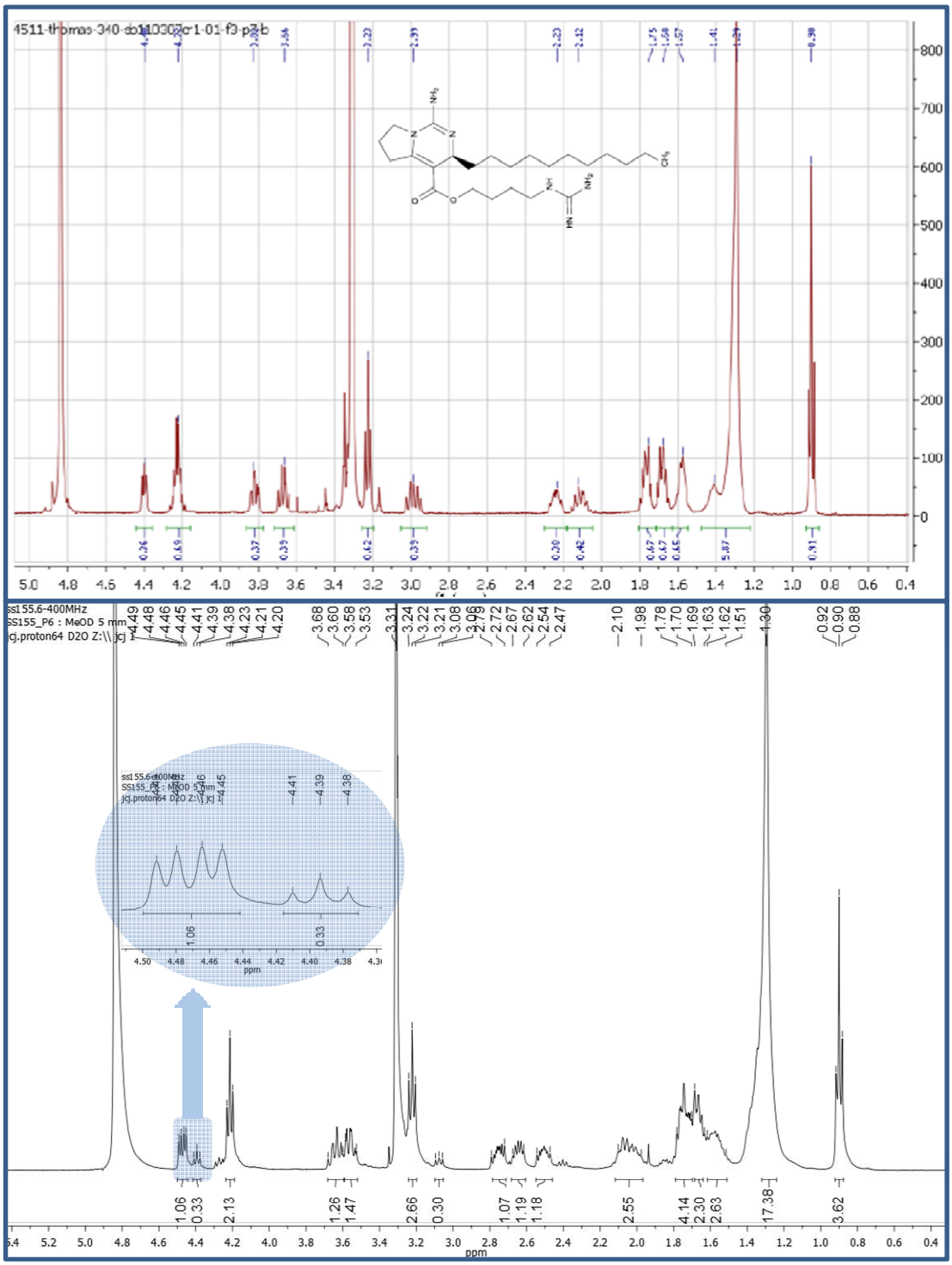

Figure 31. Crambescin A2 448 ^{1}H-NMR spectra[45] (bottom, 500 MHz in MeOH-d_4) and ^{1}H-NMR spectra of *iso*-crambescin A2 448 (**5k**) (down, 400 MHz in MeOH-d_4)

The attribution of compound **5k** is depicted on Figure 32. Existence of a double bond on positions C7-C13 instead of C8-C7 can be confirmed by the COSY correlation of H8 (4.47 ppm) with hydrogens on positions C9 and C10.

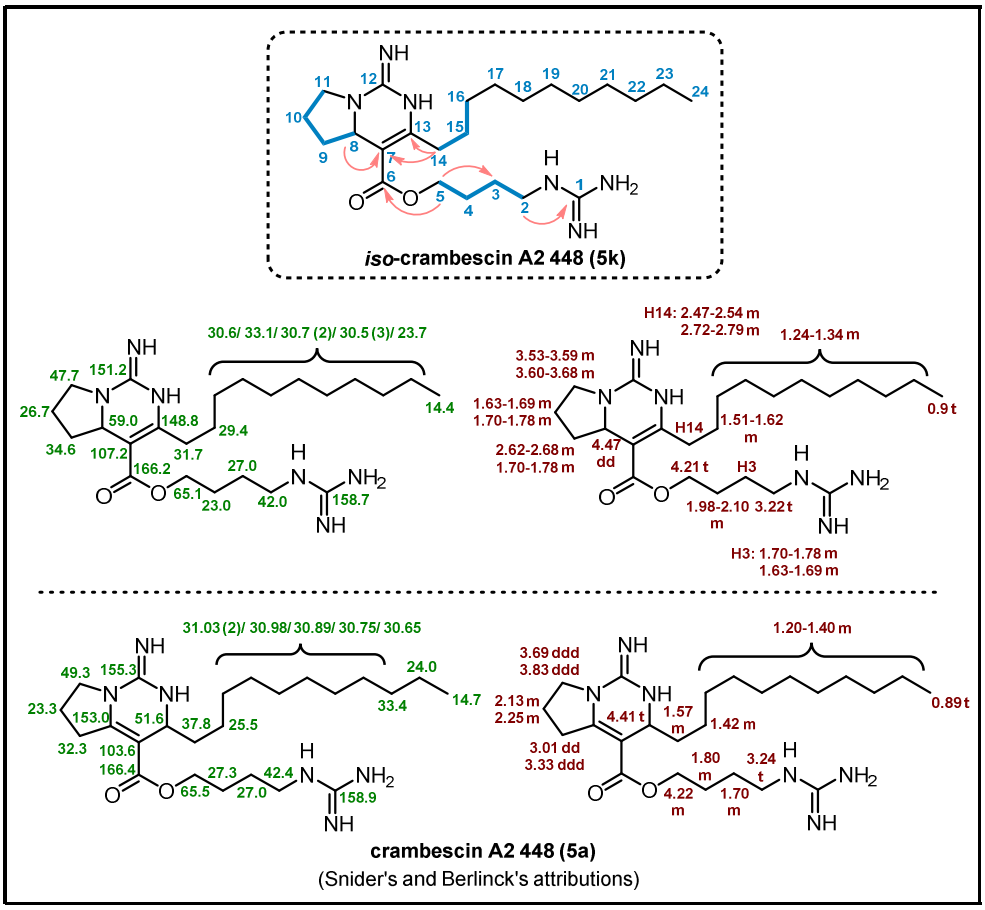

Figure 32. Attributions of *iso*-crambescin A2 (**5k**) in comparison with attributions of crambescin A2 448

The obtainment of *iso*-crambescin A2 448 (**5k**) supports the mechanistic hypothesis concerning both the synthesis and biosynthesis issues. The next efforts will be focused on the conversion of **5k** into crambescin A2 (**5a**) and derivatives, such as dehydrocrambescin A2 (**48c**), and improvement of the Biginelli condensation yield. Presence of crambescin A2 might be an indication of a spontaneous conversion of *iso*-crambescin A2 **5k** into the natural product. Importantly, the isomerization occured spontaneously on the sample kept in the MeOH-d_4 solution. After three weeks, the ration risen from 7 : 3 to 6 : 4 (**5k** : **5a**, respectively). This result had been observed at the end of this work and still under study. The kinetic of this conversion needs to be improved, either by acid catalysis or photo-indution. This hypothesis will be tested by irradiation of mixture containing **5k** with an UV-*vis* lamp system that mimics sunlight.

3. 4 Conclusions and perspectives

Inspired by our results on the biosynthesis experiments with *C. crambe* sponge (Chapter 2), we developed an alternative biomimetic synthesis to access crambescin A2 448 and its derivatives. Up to now, only 4 steps with 3% of overall yield were required to obtain a mixture 7 : 3 of *iso*-crambescin A2 **5k** and crambescin A2 448 (**5a**) (Scheme 40). It is interesting to notice the increase in molecular complexity achieved: the final product is twice more complex than the starting materials and is 1.26 times more complex than the intermediates involved on the Biginelli-type condensation (Figure 33). Further efforts will be performed to enrich the crambescin A2 content on this mixture and to achieve the aromatization of **5a** and **5k** analogues in order to obtain the natural alkaloid dehydrocrambescin A2 (**48c**, Scheme 37).

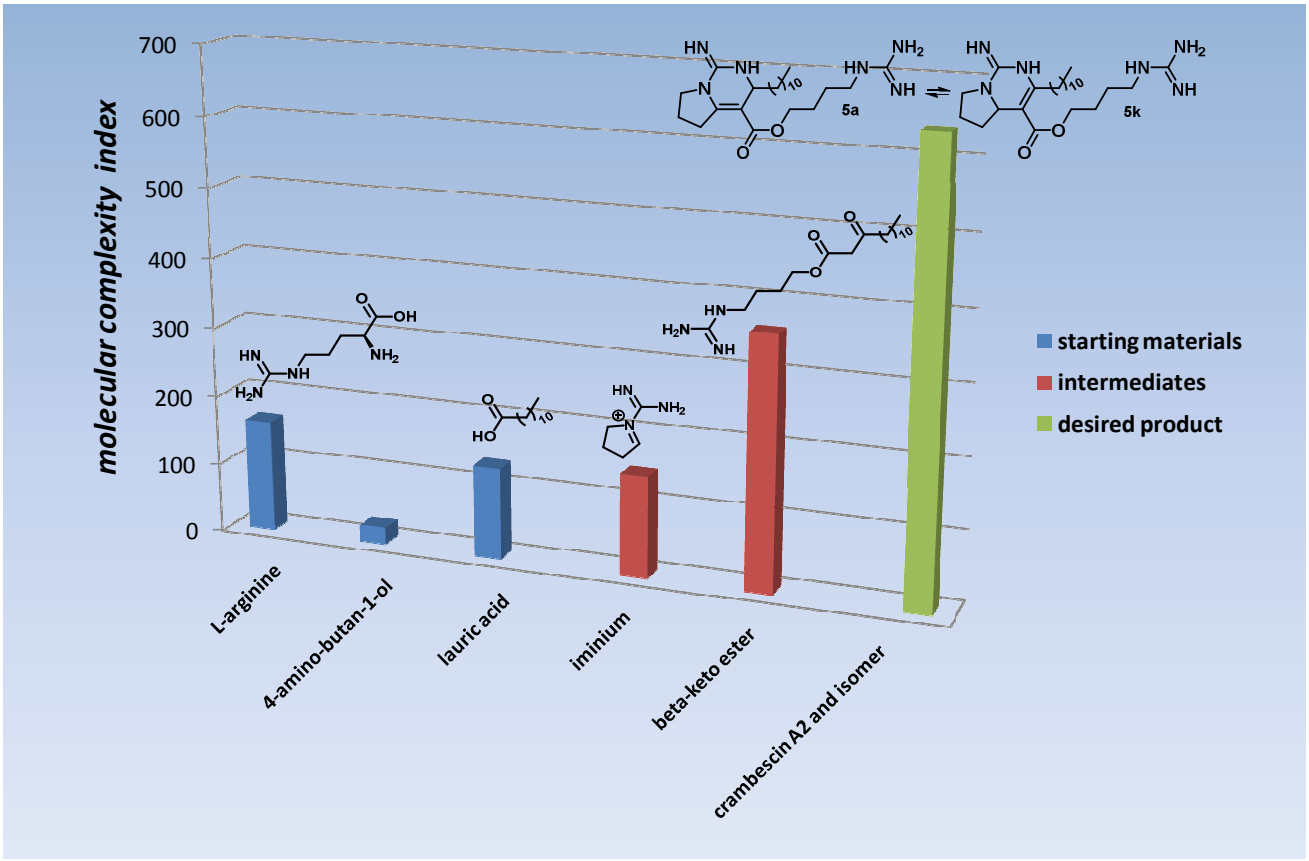

Figure 33. Comparison between the molecular complexity index of species involved on the synthesis of crambescin A2 (**5a**) and its isomer (**5k**)

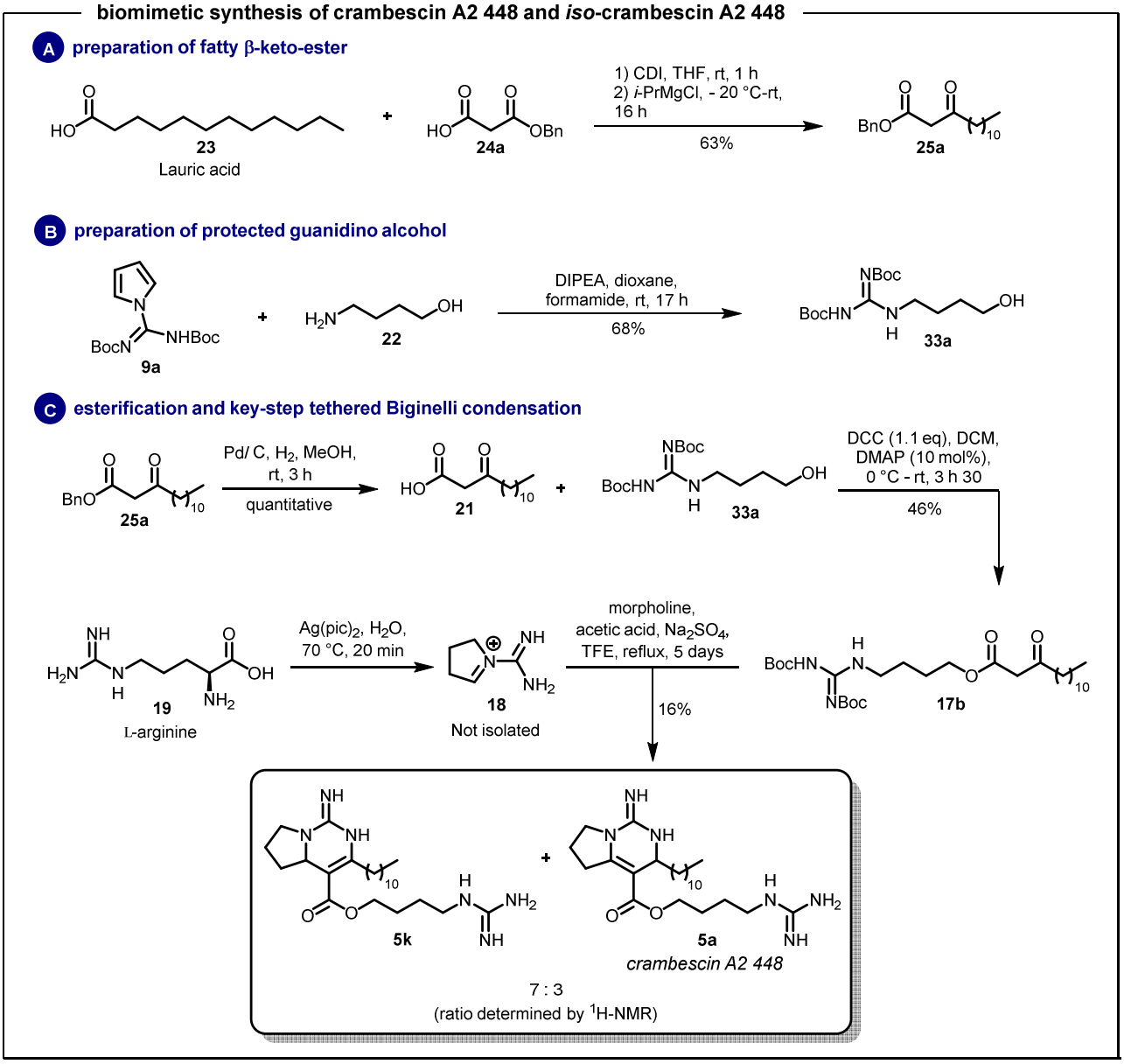

Scheme 40

Even if the crambescin A2 synthesis is not yet fully accomplished, the obtainment of the molecule scaffold confirms that the intrinsic reactivity of the biosynthetic precursors is totally suitable to lead to a common platform to this family of natural products. Summing up, we hope that the set of results presented in Chapters 2 and 3 will contribute to increase the knowledge concerning the chemistry of marine cyclic guanidine alkaloids.

Conclusions and Perspectives

General conclusions and perspectives

This work studied three aspects related with complex marine alkaloids produced by Mediterranean sponges: isolation and structural elucidation, biosynthesis, and biomimetic synthesis.

In the first chapter three species were purified: *Phorbas tenacior*, *Crambe crambe*, and *Crambe tailliezi*. Purification of *P. tenacior* yielded the already described anchinopeptolides A, B, C, and D, as well as the new structure *epi*-anchinopeptolide C. The absolute configuration of already described anchinopeptolides as well as *epi*-anchinopeptolide C will be determined by circular dicroism. Cycloanchinopeptolide C was not found on our purification but it was successfully produced by the photo-cycloaddition of anchinopeptolide C.

The purification of *C. tailliezi* was a challenging task and, unfortunately, we were not able to isolate any new compound. However, we identified crambescidin 816 and crambescidin 800, compounds previously isolated from *C. crambe*, likewise a mixture of new alkaloids containing similar guanidine fragments found in batzelladines, a family never before observed in a Mediterranean sponge.

The purification of *C. crambe* sponge furnished a range of crambescins and crambescidins that valorized the potential biotechnological application of these compounds and furnished standard compounds to our biosynthesis and biomimetic synthesis studies.

The biosynthetic experiments with *C. Crambe* allowed the identification of two building blocks involved in the synthesis of crambescin C1: L-arginine and lauric acid. The incorporation of lauric acid or close fatty acids from diet could explain the variety observed on the upper aliphatic side chain of crambescins. The microorganisms apparently play a crucial role on these secondary metabolic pathways, which can be expanded to the biosynthesis of other crambescins and derivatives. The incorporation of L-arginine labelled at the guanidine indicates that the origin of the guanidine is clearly L-arginine. However agmatine does not seem to be involved in the biosynthesis.

Inspired by our results on the biosynthesis experiments with *C. crambe* sponge, we developed an alternative biomimetic synthesis to access crambescin A2 448 and its analogues. Only 4 steps with 3% of overall yield were required to obtain a mixture 7 : 3 of *iso*-crambescin A2 and crambescin A2 448. Further efforts will be performed to enrich the crambescin A2 content on this mixture and even if the crambescin A2 synthesis is not yet fully accomplished, the obtainment

of the molecule scaffold confirms that the intrinsic reactivity of the biosynthetic precursors is totally suitable to lead to a common platform to this family of natural products.

Finaly, we hope that the set of results presented herein will contribute to increase the knowledge concerning the chemistry of marine cyclic guanidine alkaloids.

Résumé en Français

Introduction

L'objet de ce travail de doctorat est l'étude chimique et biosynthétique d'alcaloïdes guanidiniques d'origine marine provenant d'éponges méditerranéennes. Ce manuscrit est divisé en trois parties complémentaires : i) l'isolement d'alcaloïdes d'éponges marines de l'ordre des Poecilosceridа ; ii) l'étude de la biosynthèse d'alcaloïdes de type crambescine par des études de radiomarquage ; iii) la synthèse biomimétique de la crambescine A.

1. Étude chimique d'éponges marines de l'ordre des Poecilosceridа

Au cours de ce travail, trois éponges marines ont été étudiées : *Phorbas tenacior*, *Crambe crambe* et *Crambe tailliezi*. Ces trois éponges ont pour point commun la présence d'alcaloïdes comportant un motif guanidine. De *Phorbas tenacior*, différents membres de la famille des anchinopeptolides dont un nouveau composé ont été isolés. De plus, par hémisynthèse le cycloanchinopeptolide C a été synthétisé, ce qui permettra ainsi de déterminer sa configuration absolue. Des deux éponges de la famille *Crambeidae*, des alcaloïdes du type crambescines et des batzelladines ont été identifiés.

1. 1 Étude chimique de *Phorbas tenacior*

La première étude chimique de l'éponge P. tenacior a été réalisée par l'équipe du professeur Minale. De cette éponge, une nouvelle famille d'alcaloïdes de nature peptidique a été isolée: les anchinopeptolides (**3a**-**d**), ainsi que le cyclo-anchinopeptolide C (**4c**) comportant un cycle cyclobutane. En plus de ces structures, deux autres composés minoritaires (**5** et **6**), correspondant à des précurseurs ont été isolés.[11, 12, 13] Au cours de notre étude de cette même éponge basée sur un profilage métabolomique, les anchinopeptolides précédemment décrits (**3a**-**d**) ainsi quele composé **5** ont été ré-isolés. Toujours au cours de cette même étude, un nouveau membre de cette famille l'*epi*-anchinopeptolide C (**3e**, Figure 34), épimère du composé **3c** a été isolé et caractérisé.

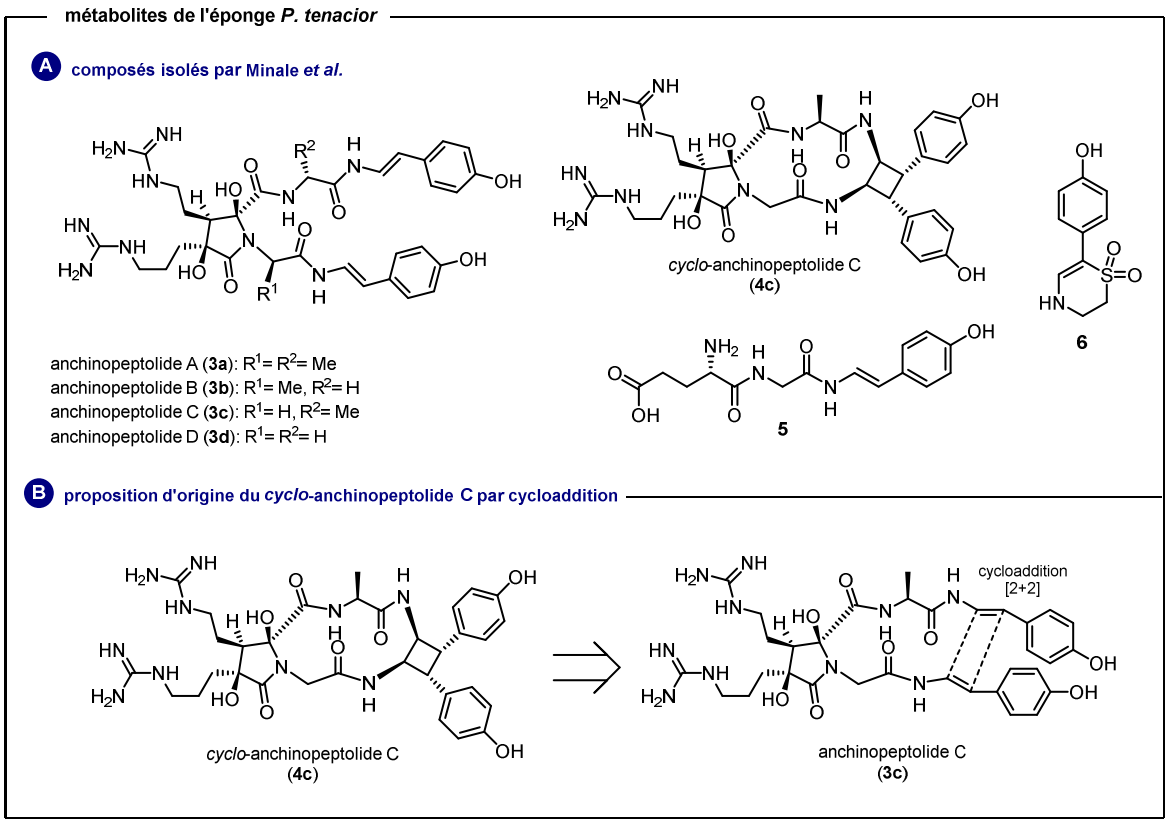

Schéma 1. Structure des anchinopeptolides

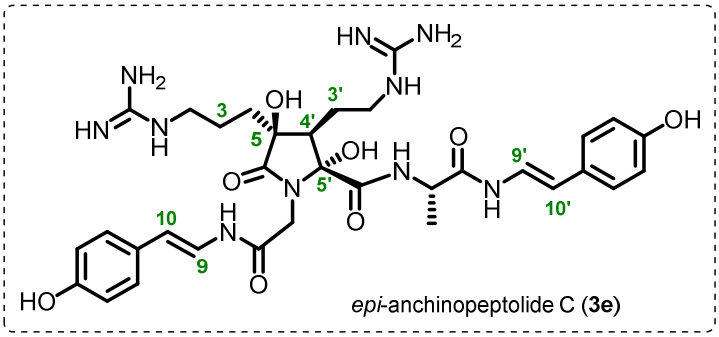

Figure 34. Structure de l'épi-anchinopeptolide C isolé de *P. Tenacior*

De manière intéressante, le composé **4c** n'a pas été détecté au cours de l'étude chimique. Pour comprendre l'origine du composé **4c**, nous en avons réalisé son hémisynthèse par photo-cycloaddition à partir de l'anchinopeptolide C (**3c**). Après irradiation du composé **3c** pendant 23 h par une lampe riche en UV-B mimant la lumière du soleil, le cyclo-anchinopeptolide C (**4c**) a été isolé avec un rendement de 23%. Les données spectrales sont en accord complet avec la littérature (Figure 35). À partir de ce produit la détermination de la configuration absolue par dichroïsme circulaire est en cours. Une origine artéfactuelle de ce composé a été émise.

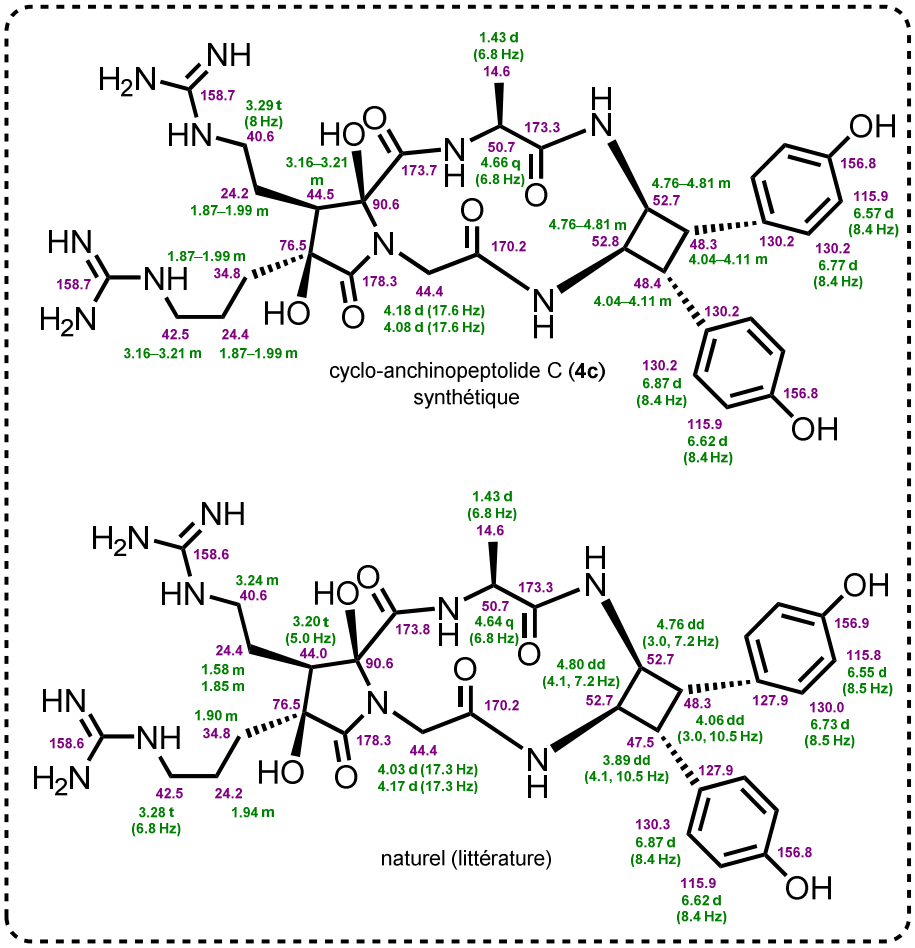

Figure 35. Comparaison des attributions du cyclo-anchinopeptolide C (synthétique versus naturel)

1. 2 Étude chimique de *Crambe tailliezi*

L'éponge *C. Tailliezi* a été décrite en 1982 (Vacelet et Boury-Esnault) et malgréson abondance sur les côtes française,[26] aucune étude chimique pour l'identification de ses métabolites n'est décrite. L'étude a démontré la présence des crambescidines 800 et 816 (**23f** et **23g** respectivement). Des composés nouveaux ont été identifiés par HPLC-HRMS, mais malheureusement des conditions de purification satisfaisantes n'ont pas pu être développées malgré un travail conséquent d'optimisation. Toutefois un composé a été isolé de manière impure et les analyses de RMN et de spectroscopie de masse ont fourni des données partielles sur sa structure. Un premier cycle d'un squelette cyclique central a été identifié avec une substitution similaire à celle de la batzelladine C (Figure 36). Ces données partielles indiquent pour la première fois la présence d'une structure de type batzelladine dans une éponge méditerranéenne, alors qu'actuellement elles ne sont uniquement décrites que dans les éponges des Caraïbes des genres *Monanchora* et *Batzella*.

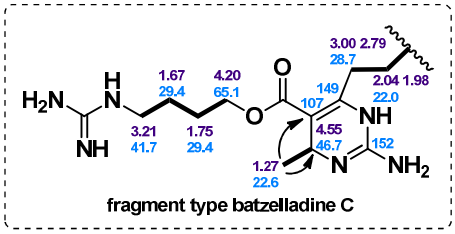

Figure 36. Fragment de la batzelladine découverte dans la *C. taillezi*

1. 3 Étude chimique de *Crambe crambe*

L'éponge *C. crambe* est connue pour la production d'alcaloïdes de type crambescines et crambescidines comportant des unités guanidines et présentant une large diversité d'activités biologiques.[17, 22, 23, 24] De cette éponge, les crambescidines 800, 816 et 830 été isolées en quantités suffisantes pour des évaluations biologiques dans le cadre d'une collaboration. Nos collaborateurs ont identifié pour ces trois molécules une activité importante d'inhibitionde la prolifération de cellules colorectales tumorales dans un modèle *in vivo* chez le poisson-zèbre.[17] De plus, la crambescidine 816 s'est révélée neurotoxique sur des cultures de cellules neuronales.[28] Les crambescines A2 et C1 isolées pendant cette étude ont été utilisées comme standards pour les études de biosynthèse et de synthèse biomimétique réalisées au cours de ce travail de thèse.

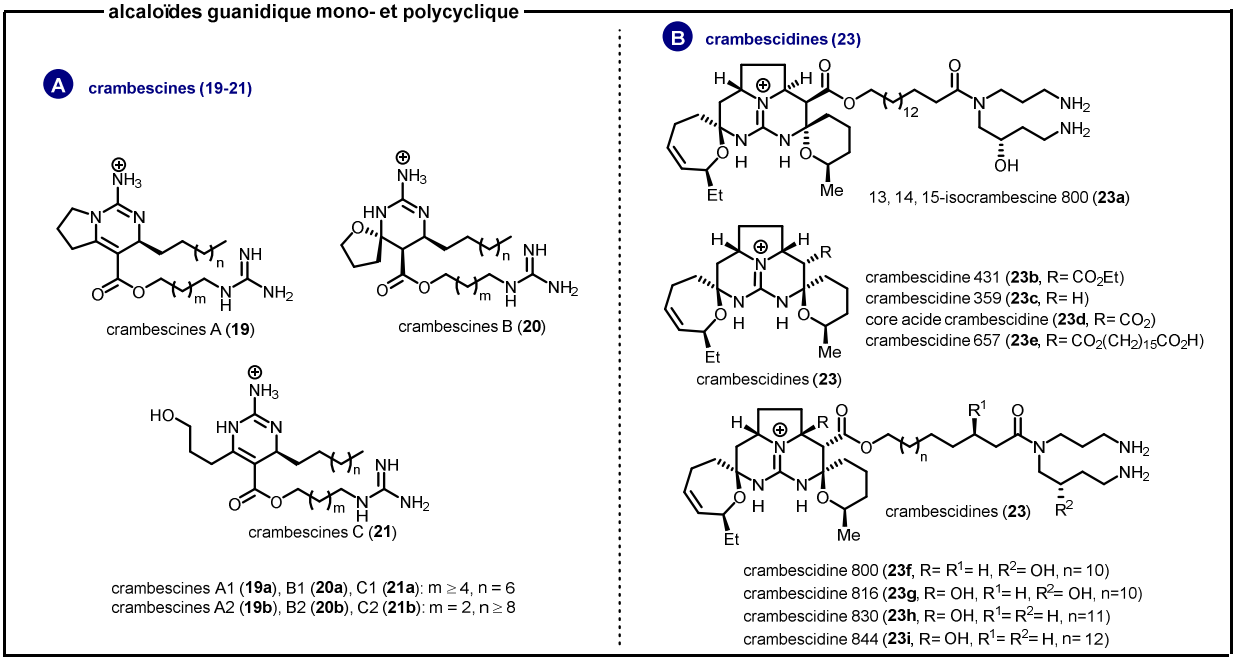

Schéma 2. Structures d'alcaloïdes marins de type crambesine et molécules apparentées

2. Élucidation de la biosynthèse de la crambescine C1 par des études d'incorporation *in vivo* de précurseurs marqués au ^{14}C

La synthèse des crambescines a été décrite dans les années 1990 par le groupe du professeur Snider.[44] L'approche a été dite "biomimétique", bien qu'aucune étude de biosynthèse n'ait confirmé l'hypothèse biosynthétique utilisée (Schéma 3). Selon l'approche de Snider et Shi, le squelette guanidinique serait issu de la condensation d'une l'urée sur un fragment d'origine poly-acétique. Selon nos hypothèses, le squelette guanidinique central serait issu de la condensation d'un acide gras sur d'un pyrrolidinium dérivant de la L-arginine.

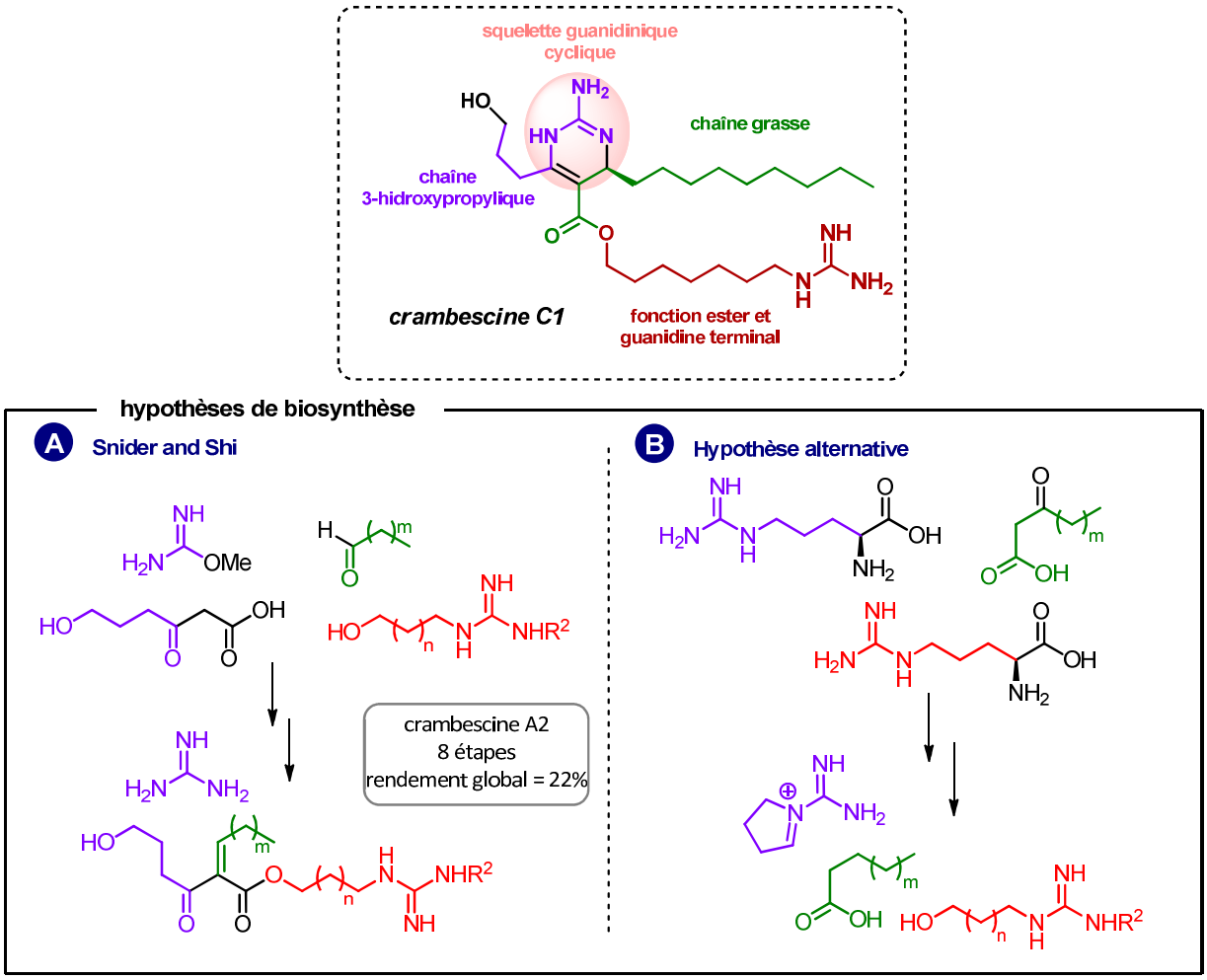

Schéma 3. Hypothèses comparées de biosynthèse des crambescines

Pour démontrer nos hypothèses, nous avons effectué des expériences d'incorporation isotopique par l'éponge *C. Crambe* en utilisant des précurseurs marqués par du carbone-14 (Figure 37). La crambescine C1 a été choisie comme métabolite cible pour étudier les incorporations de radio-éléments (Schéma 3).

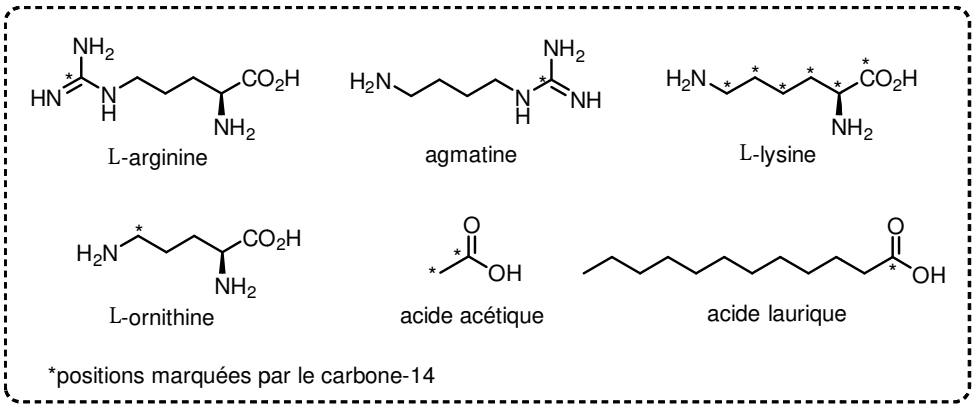

Figure 37. Précurseurs utilisés dans les expériences de radiomarquage

En s'appuyant sur les travaux antérieurs de l'équipe, nous avons utilisé le protocole développé pour l'étude de biosynthèse des métabolites l'éponge *Axinella damicornis*.[30, 42] Ce protocole a montré son efficacité pour contourner de manière optimale les problèmes liés à la manipulationdes éponges en dehors de leur milieu naturel en vue de l'étude d'incorporation.[30, 29, 38] Un résumé est présenté par la Figure 38.

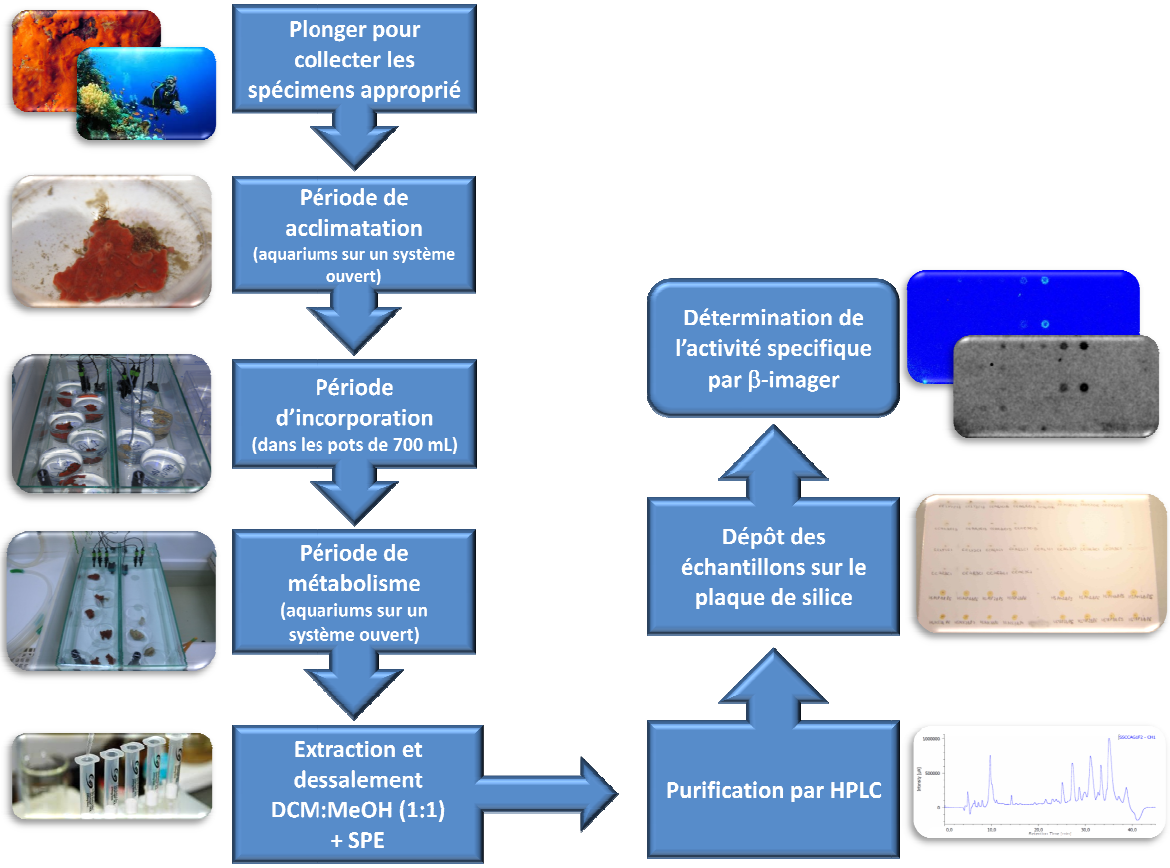

Figure 38. Protocole pour les expériences de biosynthèse *in vivo* avec les éponges

Après les expériences d'incorporation, les éponges ont été extraites par un protocole classique. La crambescine C1 a été choisie comme modèle d'étude car ce métabolite est le plus facile à obtenir à l'état pur. Après deux purifications par HPLC, les échantillons de crambescine C1 purs ont été déposés sur les plaques de silice et ont été analysés par β-imager. L'incorporation de radioéléments a été notée pour les échantillons issus d'éponges alimentées avec de la L-arginine et l'acide laurique marqués (Tableau 10 et Figure 39). Ce résultat a démontré que la guanidine est biosynthétiquement issue de la L-arginine. Le fait que l'acide laurique possède le même nombre de carbones que la chaîne aliphatique ainsi que son incorporation indiquent une incorporation des acides gras nécessaires à la biosynthèse directement par le régime alimentaire. L'absence de radioactivité dans la crambescine C1 provenant des éponges alimentées avec de l'acide acétique marquéne permet pas de conclure. Soit effectivement elle n'est pas incorporée, soit l'acide acétique marqué a été incorporé dans les processus du métabolisme primaire.

Tableau 10. Activitésdescrambescines C1 pures isoléesdesépongesalimentéesavec les précurseurs marqués au carbone-14

Précurseur	Activité mesurée ($x10^{-2}$/ Bq)[a]		Activité spécifique ($x10^{-5}$/ Bq.nmol^{-1})	
	1re purification HPLC	2de purification HPLC	1re purification HPLC	2de purification HPLC
L-[guanidino-^{14}C]arginine	3.15	4.07	7.56	9.78
	3.54	5.25	8.52	12.6
[guanidino-^{14}C]agmatine	3.15	0	7.57	0
	3.41	0	8.20	0
L-[U-^{14}C]-lysine	0	0	0	0
	4.46	0	10.7	0
L-[5-^{14}C]-ornithine	0	0	0	0
	0	0	0	0
acide [U-^{14}C]acétique	0	5.25	0	12.6
	0	0	0	0
acide [1-^{14}C]laurique	10.6	9.71	25.6	23.3
	19.4	21.0	46.7	50.5

[a]Efficience= 12.7% (standard: L-[U-^{14}C]proline)

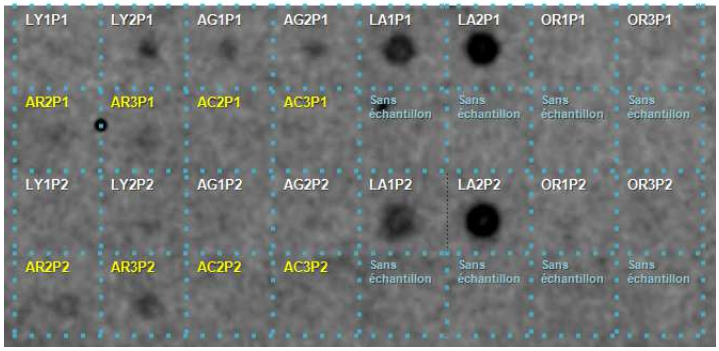

Figure 39. Résultat qualitatif des analyses par β-imager associé aux crambescines C1

(LY: lysine, AG: agmatine, LA: acide laurique, OR: ornithine, AR: arginine, AC: acide acétique, P1: 1re purification par HPLC, P2: 2de purification par HPLC)

3. Synthèse biomimétique de la crambescine A2 448 et molécules apparentées

En prenant en compte les informations sur la voie de biosynthèse des crambescines obtenues par les expériences de radiomarquage, une synthèse biomimétique de la crambescine A2 448 a été développée (Schéma 4). Un β-céto-acide **21** obtenu à partir de l'acide laurique ainsi qu'un pyrrolidinium obtenu de l'arginine ont été mis en réaction pour produire en une étape le squelette des crambescines.

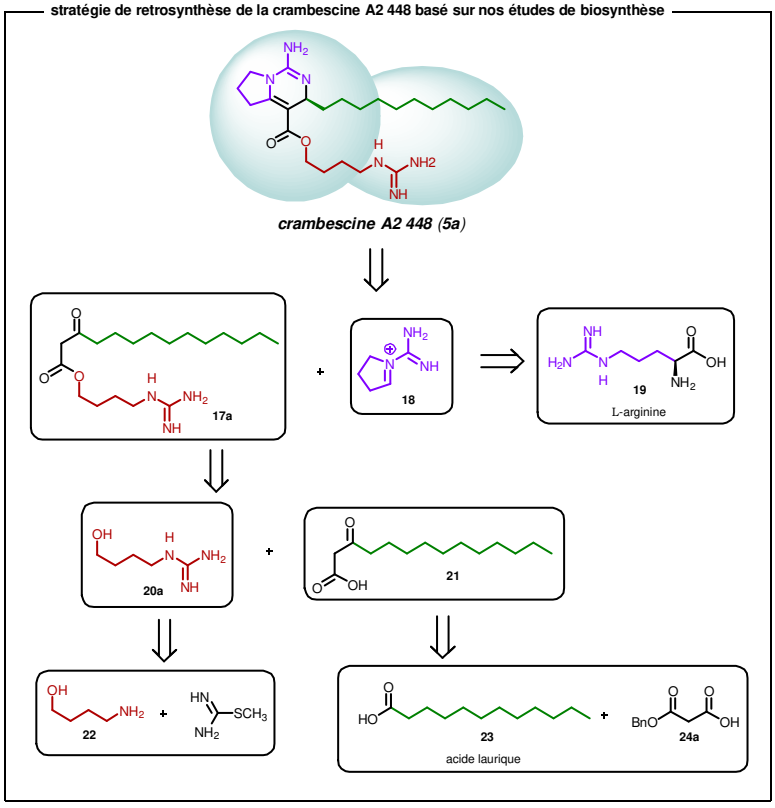

Schéma 4. Rétrosynthèse de la crambescine A2 448

3. 1. Synthèse des fragments pour la synthèse biomimétique de la crambescine A2 448

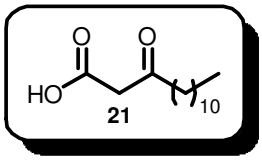

Synthèse du fragment β-céto-acide : Le fragment **21** a été préparé à partir de l'acide laurique par homologation biomimétique par un malonate de magnésium (Schéma 5). Le β-céto-ester a ensuite été converti soit par hydrogénolyse soit par saponification par la soude en β-céto-acide **21** (Schéma 6).

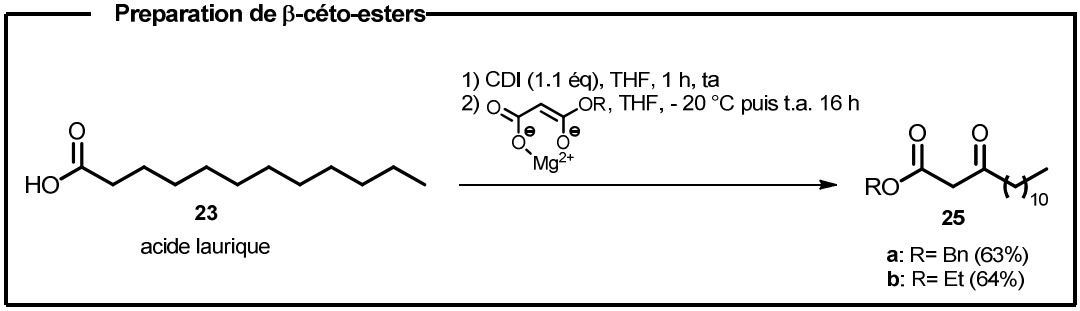

Schéma 5. Homologation biomimétique de l'acide laurique

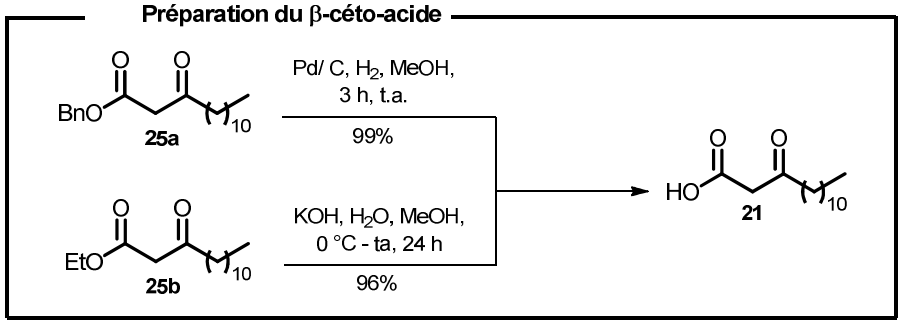

Schéma 6. Réduction et saponification de β-céto-esters

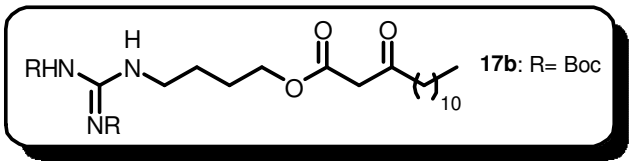

Synthèse du fragment 17b : Le fragment **17b** comporte à la fois la chaîne « acide gras » et la chaîne latérale de type ester de la crambescine A2 448. Dans un premier temps, une fonction guanidine protégée a été transférée sur le 4-amino-butanol (Schéma 7). Le choix de cette version protégée a permis d'améliorer la solubilité et les purifications par comparaison avec son équivalent non protégé.

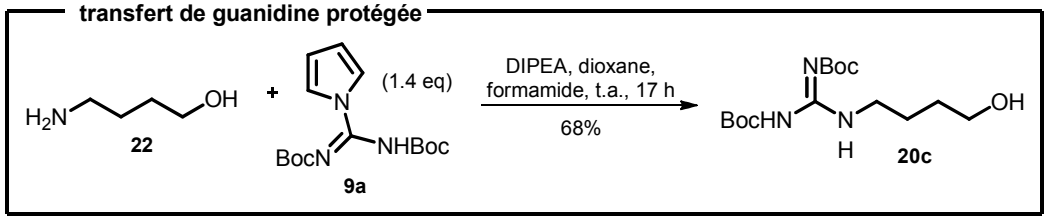

Schéma 7. Transfert de guanidine protégée

Ensuite, le couplage de **20c** avec **21a** été réalisé par une estérification de Neises et Steglich (Schéma 8), fournissant le fragment **17b** avec 46% de rendement.

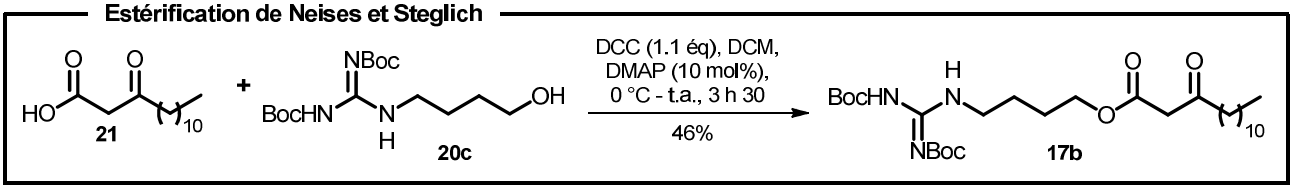

Schéma 8. Couplage de deux chaînes des crambescines

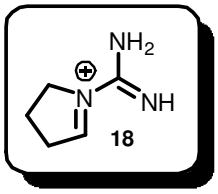

Synthèse biomimétique la plateforme pyrrolidinium : De manière identique à la voie de biosynthèse proposée, l'iminium **18** est l'entité réactive sur lequel le fragment **17b** doit venir s'ancrer pour former le cœur des crambescines. Le pyrrolidinium **18** a été obtenu par décarboxylation oxydante de la L-arginine initiée par le picolinate d'argent(II) (Schéma 9). Le produit brut a été directement utilisé sans purification pour réaliser l'étape suivante d'assemblage biomimétique.

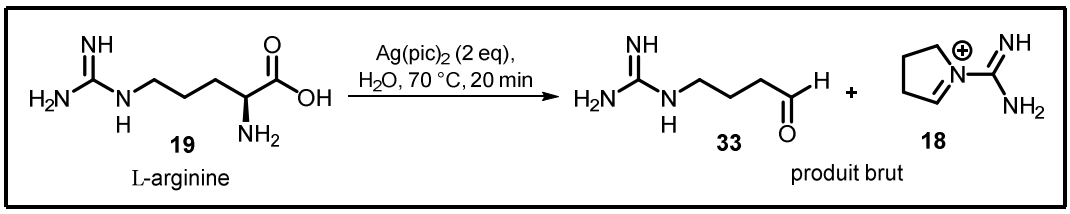

Schéma 9. Décarbolylation oxydante de l'arginine

3. 2. Étape-clé: assemblage biomimétique du cœur des cambescines

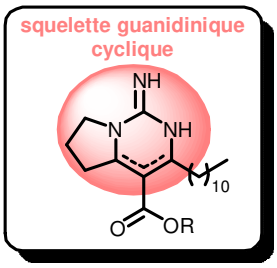

L'assemblage biomimétique du cœur central des crambescines a été réalisé par une condensation du type Biginelli modifiée entre le β-céto-ester **25a** et le pyrrolidinium **18**. Le produit a été obtenu sous la forme d'un mélange de deux isomères, soit avec la double liaison entre les carbones C7 et C13 soit avec la double liaison entre les carbones C7 et C8. De plus un phénomène de transestérification partiel avec le trifluoroéthanol a été observé (Schéma 10).

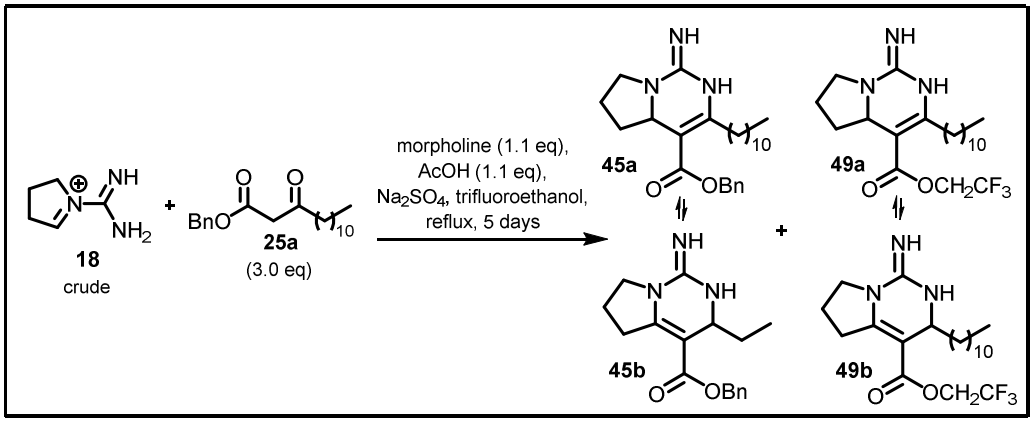

Schéma 10. Assemblage biomimétique du cœur des crambescines

Les tentatives d'introduction de la chaîne latérale ester pour achever la synthèse de la crambescine A2 448 ont été infructueuses. Les essais ont été réalisés soit par transestérification du mélange de produits **45** et **49** avec l'alcool guanidinique **20a**, soit par une séquence de saponification suivie d'une estérification (Schéma 11). La stratégie a été alors modifiée en utilisant directement le fragment **17b**, contenant déjà la bonne chaîne latérale pour réaliser l'assemblage biomimétique de la crambescine A2 448.

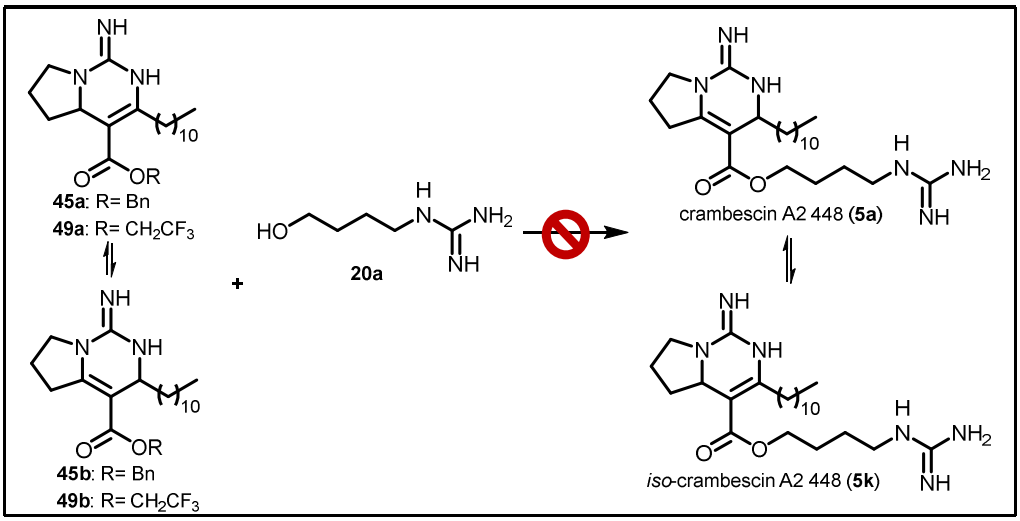

Schéma 11. Tentatives de transestérification de **45** et **49**

3. 3. Assemblage biomimétique de la crambescine A2 448 et de son isomère

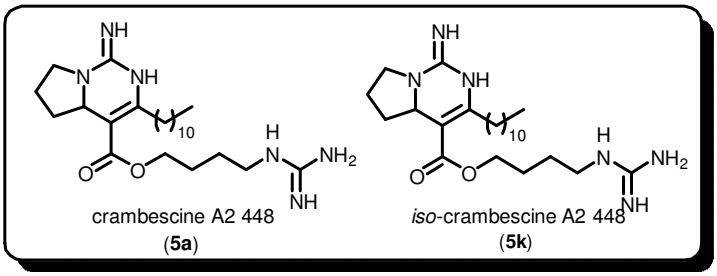

En réalisant l'assemblage biomimétique directement entre le fragment **17b** et l'iminium **18**, la crambescine A2 448 (**5a**) a été obtenue en mélange avec l'*iso*-crambescine A2 448 (**5k**) avec un ratio de 7 pour 3 en défaveur de l'isomère « naturel » (Schéma 12 et Schéma 13). Ainsi en une étape la structure complète comportant le cœur bicyclique et les chaînes latérales a été obtenue avec un rendement de 16 % et la synthèse totale de la crambescine A2 448 a été réalisée avec un total de 4 étapes et un rendement total de 3% (Schéma 14).

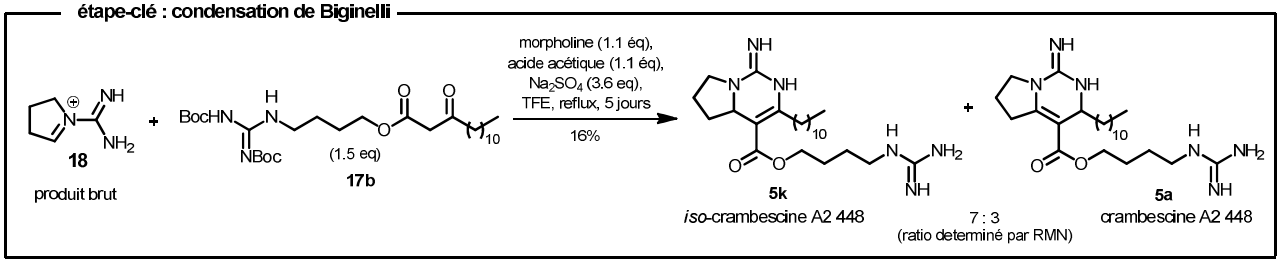

Schéma 12. Synthèse de la crambescine A2 448

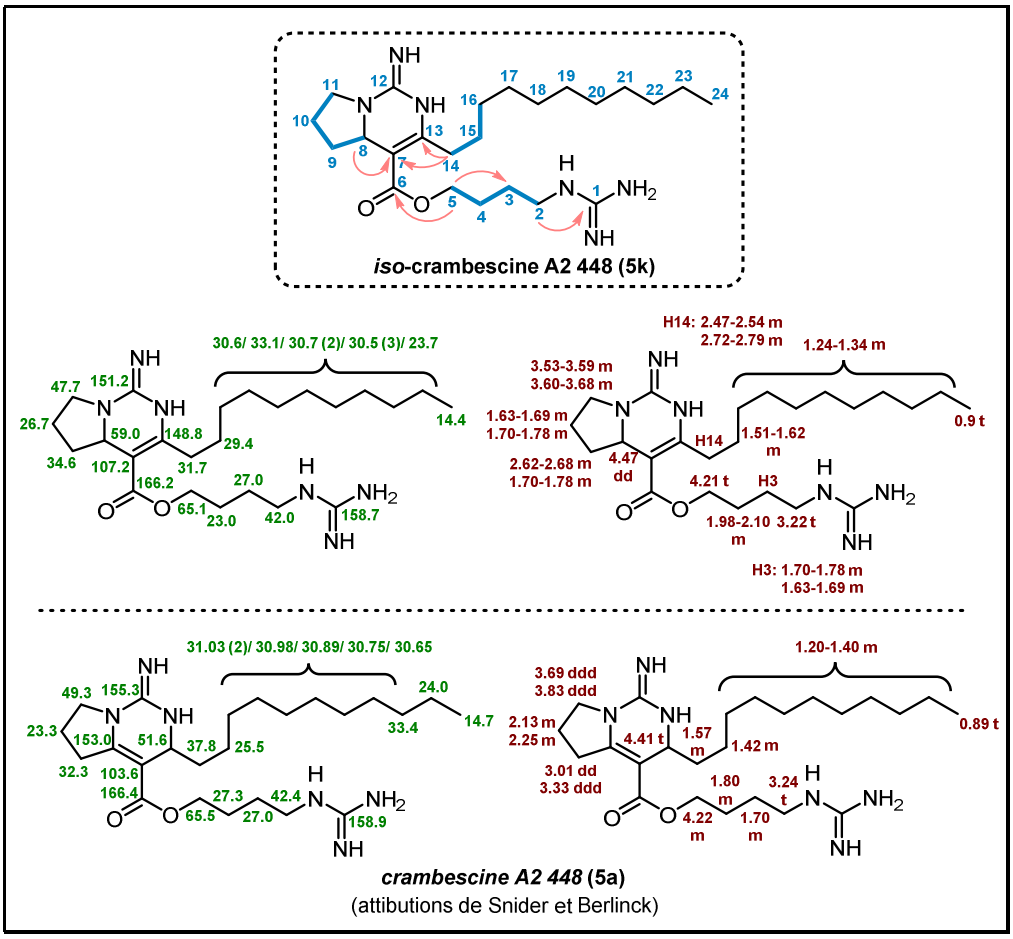

Schéma 13. Analyse RMN de la crambescine A2 448 et de son isomère

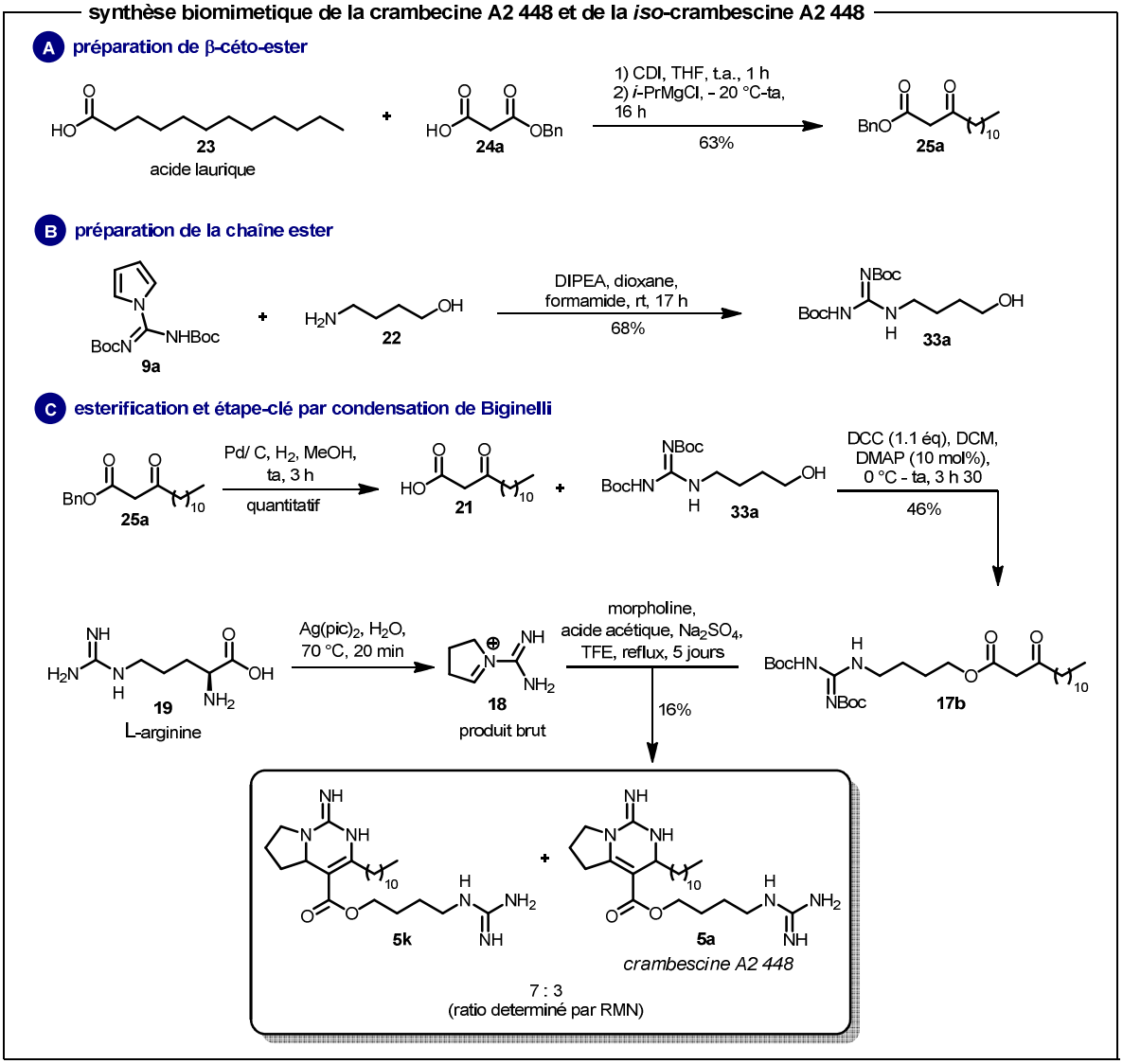

Schéma 14. Bilan de la synthèse biomimétique de la crambescine A2 448

Experimental Section

1. General Information

All purchased chemicals were used without further purification. Compounds names were attributed following IUPAC recommendations or as specified on literature. Each chapter has its own compounds numeration.

Moisture sensitive reactions were performed under argon atmosphere. The glassware was keep at 110 °C at least 2 h. The reaction flasks were flame dried with a heating gun before the use and flushed with argon. Anhydrous THF was obtained distilling the commercial solvent over metallic sodium and using benzophenone as indicator[90]. The other dried solvents were obtained from a PureSolv MD-5 (Inovative Technology) drying apparatus.

Analytical HPLC analysis were recorded on a Agilent 1260 Infinity (detector: UV-visible DAD) or Waters 600E (detector: UV-visible PDA 2996) equipments. Semi-preparative HPLC purification was carried on a Jasco LC-2000 Plus system (detectors: Jasco UV-2075 Plus or ELSD SEDEX 85 Sedere LT-ELSD). Preparative purifications were performed with a DeltaPrep Waters HPLC (detector: UV-visible PDA). High resolution mass analysis were acquired on a HPLC Alliance 2695 coupled to a MS-TOF LCT Premier from Waters. UPLC analysis were performed on a Ultimate 3000 Dionex equipment with an Ultimate 3000 Autosampler Dionex injector using as detectors a Agilent Technologies 380-ELSD as well as a diode array Ultimate 3000 Dionex selected on wavelengths 210, 254, and 290 nm. The stationary phase was a column Phenomenex Kinetex 1.7 µm RP phenyl-hexyl (100 x 2.10 mm) employing H_2O : ACN : TFA as mobile phase following the elution sequence: isocratic 0 - 2 min (90 : 10 : 0.1), gradient 2 - 8 min (from 90 : 10 : 0.1 to 0 : 100 : 0.1), isocratic 8 - 10 min (0 : 100 : 0.1), and gradient 10 - 14 min (from 0 : 100 : 0.1 to 90 : 10 : 0.1) (flow: 0.5 $mL.min^{-1}$, volume of injection: 5 µL, sample concentration: ~ 10 $mg.mL^{-1}$ in MeOH).

NMR experiments were recorded on a Bruker ARX 200 spectrometer (frequency of 200 MHz for ^1H) or on a Bruker Avance 300, 400 or 500 spectrometers (frequencies of 300, 400 or 500 MHz for ^1H, respectively). The NMR chemical shifts (δ) are reported in ppm and were referenced on residual proton signals of the solvent applied (^1H-NMR: δ $CDCl_3$ 7.26, DMSO-d_6 2.50, MeOH-d_4 3.31, D_2O 4.79 ppm, acetone-d_6 2.05; ^{13}C-NMR: δ $CDCl_3$ 77.0, DMSO-d_6 39.50, MeOH-d_4 49.0 ppm, acetone-d_6 29.84). The deuterated solvents were supplied by Sigma-Aldrich or Euriso-top.

The following precursors were used in the feeding experiments: [U-^{14}C]acetic acid sodium salt (American Radiolabeled Chemicals, 110 $mCi.mmol^{-1}$ in EtOH), L-[U-^{14}C]lysine (Hartmann

[90] W. L. F. Armarego, C. L. L. Chai, in *Purification of Laboratory Chemicals (Sixth Edition)*, Butterworth-Heinemann, Oxford, **2009**, pp. 1-60.

Analytic, 297 mCi.mmol^{-1} in 2 EtOH : 98 H_2O), L-[5-^{14}C]ornithine (American Radiolabeled Chemicals, 55 mCi.mmol^{-1} in 0.01 N HCl), L-[guanido-^{14}C]arginine (American Radiolabeled Chemicals, 55 mCi.mmol^{-1} in 0.01 N HCl), [guanido-^{14}C]agmatine (American Radiolabeled Chemicals, 55 mCi.mmol^{-1} in 0.01 N HCl) and [1-^{14}C]lauric acid (American Radiolabeled Chemicals, 55 mCi.mmol^{-1} in EtOH). During the feeding experiments, the activity of the water column surrounding the sponges was measured by a liquid scintillation analyser Tri-Carb 2900TR, Perkin Elmer. Sponge extracts were desalted by solid phase extraction (SPE) using silica cartridges Chromabond® C18, 2000 mg. The samples for beta-radioactivity thin layer (TLC) and autoradiography beta-imager analyses were applied on Merck silica gel 60 F_{254} aluminium plates 20 x 20 cm. The beta-radioactivity TLC (radio-TLC) analysis was performed by Rita Star equipment (Raytest) and the autoradiography was recorded by a beta-imager Biospace Lab.

The IR experiments were obtained using a Bruker Vector 22 spectrometer. The samples were solubilized in MeOH or $CHCl_3$, placed on the cell of the equipment and let to evaporate, forming a film. The wavenumbers (ν) are described in cm^{-1}.

Analytical TLC were carried on Merck silica gel 60 F_{254} aluminium plates. After elution, the plates were observed under UV light at 254 nm and stained with sulfuric vanillin solution or Dragendorff's reagent followed by gentle heating. For silica gel chromatography, the flash chromatography was used, with Merck silica gel 60 (230-400 mesh) p.a. grade.

2. Isolation and Structure Elucidation of Specialized Metabolites from Poecilosclerida Mediterranean Sponges

2. 1 Isolation of metabolites from *P. tenacior* sponge

Isolation of metabolites

The specimen of *P. tenacior* was collected manually by SCUBA diving on the Coast of Villefranche-Sur-Mer (France) on July of 2014 at 50 m deep.

The sample was freeze-dried and grated, furnishing a yellow solid (46.1 g). The powder was exhaustively extracted by MeOH : DCM (1 : 1, 3 x 150 mL) and sonication bath (15 min to each extraction) followed by filtration. The filtrates were combined and evaporated under reduced pressure at 40 °C, giving a brown solid (7.00 g). This solid was adsorbed over silica gel RP-18 (7.00 g) and desalted by VLC using the following elution gradient: H_2O (400 mL, fraction F1, 1.67 g),

MeOH (500 mL, fraction F2, 2.01 g), MeOH : DCM (1 : 1, 400 mL, fraction F3, 1.74 g) and DCM (400 mL, fraction F4, 0.472 g). Fractions F2 to F4 were analyzed by UPLC and ^{1}H-NMR and the fraction F2 was purified twice by HPLC.

On the first time, 300 mg of F2 was purified by HPLC on semi-preparative mode (column: Macherey-Nagel VP 250/10 Nucleodur C18 HTec, 5 μm) using a mixture of H_2O : ACN : TFA according to the following elution sequence: isocratic 0 - 25 min (80 : 20 : 0.1), gradient 25 - 27 min (80 : 20 : 0.1 to 40 : 60 : 0.1), isocratic 27 - 30 min (40 : 60 : 0.1), gradient 30 - 32 min (from 40 : 60 : 0.1 to 80 : 20 : 0.1), and isocratic 32 - 35 min (80 : 20 : 0.1) (flow: 4.0 mL.min^{-1}, injection volume: 200 μL, sample concentration: 150 mg.mL^{-1} in MeOH, detection at 210 nm). There were obtained 12 fractions named as: F2P1 (r_t= 2.5 - 4.0 min, 285 mg), F2P2 (r_t= 5.5 min, 1.14 mg, pure **5**), F2P3 (r_t= 9.5 min, 4.44 mg, anchinopeptolide A**3a**), F2P4 (r_t= 11.0 - 12.5 mi, 20.4 mg), F2P5 (r_t= 12.5 - 13.5 min, 3.30 mg), F2P6 (r_t= 13.5 - 14.5 min, 2.82 mg), F2P7 (r_t= 14.5 - 15.5 min, 4.19 mg), F2P7a (r_t= 15.5 - 16.5 min, 1.49 mg), F2P8 (r_t= 17 - 18 min, 1.59 mg), F2P9 (r_t= 22.5 - 24.5 min, 2.09 mg), F2P10 (r_t= 26 min, 6.32 mg, *epi*-anchinopeptolide C, **3e**), and F2P11 (r_t= 30 - 31 min, 6.56 mg). Fraction F2P4 was purified by HPLC on semi-preparative mode (column: Phenomenex Gemini 5 μm C6 - phenyl 110 A, 250 x 10 mm) employing a mixture of H_2O : ACN : TFA with a elution gradient of H_2O : ACN : TFA 0 - 25 min (from 82 : 18 : 0.1 to 75 : 25 : 0.1) (flow: 3 mL.min^{-1}, injection volume: 50 μL, sample concentration: 41 mg.mL^{-1} in MeOH, detection at 254 nm). There were obtained 3 fractions: F2P4_P1 (r_t= 16.5 min, 4.93 mg, anchinopeptolide C, **3c**), F2P4_P2 (r_t= 17.5 min, 2.35 mg, anchinopeptolide D, **3d**), and F2P4_P3 (r_t= 18.5 min, 0.63 mg). An analytical sample of anchinopeptolide B was obtained from purification of F2P5 by HPLC (column: Waters - X-Select CSH phenyl-hexyl 5 μm, 6 x 250 mm) employing a mixture of H_2O : ACN : TFA according to the following elution gradient: isocratic 0-20 min (85 : 15 : 0.1), gradient 20 - 22 min (from 85 : 15 : 0.1 to 10 : 90 : 0.1), isocratic 22 - 24 min (10 : 90 : 0.1), gradient 24 - 26 min (from 10 : 90 : 0.1 to 85 : 15 : 0.1), and isocratic 26 - 30 min (85 : 15 : 0.1) (flow: 1 mL.min^{-1}, injection volume: 50 μL, sample concentration: 6.6 mg.mL^{-1} in MeOH, detection at 254 nm). Pure anchinopeptolide B **3b** was obtained at r_t= 18.5 min (0.8 mg).

The second purification was performed envisaging the obtainment of a largest amount of anchinopeptolide C (**3c**) for the photo-cycloaddition reaction. An amount of 700 mg of F2 was purified by preparative HPLC (column: C18 Sunfire Waters, 30 x 150 mm, 5 μm) using a mixture of (H_2O + 0.2% TFA) : ACN following a gradient elution of 15 - 25% of ACN in 25 min (flow: 42.0 mL.min^{-1}, injection volume: 500 μL, sample concentration: 350 mg.mL^{-1} in MeOH). There were

obtained 14 fractions assigned as: F2P1 (r_t= 1.5 - 2.5 min, 300 mg), F2P2 (r_t= 2.7 min, 5.4 mg), F2P3 (r_t= 3.3 min, 8.0 mg), F2P4 (r_t= 7.5 min, 66.4 mg), F2P5 (r_t= 9.0 min, 131.9 mg), F2P6 (r_t= 10.3 min, 39.3 mg), F2P7 (r_t= 11.0 - 11.5 min, 29.4 mg), F2P7a (r_t= 12.3 min, 7.8 mg), F2P7b (r_t= 13.0 min, 5.6 mg), F2P8 (r_t= 15.5 min, 63.5 mg), F2P8a (r_t= 17.0 min, 3.2 mg, anchinopeptolide A, **3a**), F2P8b (r_t= 19.0 min, 18.2 mg), F2P9 (r_t= 21.5 min, 17.7 mg), and F2P10 (r_t= 23.3 min, 2.2 mg). Samples F2P4, F2P5, and F2P8 were purified on HPLC. Fraction F2P4 was purified using as eluent (H_2O + 0.2% TFA) : ACN and applying a gradient of 15 - 35% of ACN in 20 min (column: C18 Sunfire Waters 19 x 150 mm, 5 μm; flow: 17 $mL.min^{-1}$; concentration: 66.4 $mg.mL^{-1}$ in MeOH, injection volume: 200 μL; detection at 254 nm). Pure anchinopeptolide A (9.0 mg, **3a**) was eluted at r_t = 8.2 min. Sample F2P5 was purified using as eluent (H_2O + 0.2% TFA) : MeOH and employing a gradient of 30 - 45% of MeOH in 20 min (column: C18 Sunfire Waters 30 x 150 mm, 5 μm; flow: 42 $mL.min^{-1}$, concentration: 131.9 $mg.mL^{-1}$ in MeOH, injection volume: 200 μL, detection at 254 nm). Pure anchinopeptolide D (**3d**) (r_t= 9.0 min, 36.1 mg) and anchinopeptolide C (**3c**) (10.2 min, 67.6 mg) were isolated. Fraction F2P8 was purified using as eluent (H_2O + 0.2% TFA) : ACN and applying a gradient of 15 - 35% of ACN in 30 min (column: C18 Sunfire Waters 19 x 150 mm, 5 μm; flow: 17 $mL.min^{-1}$; concentration: 63.5 $mg.mL^{-1}$ in MeOH, injection volume: 200 μL; detection at 254 nm). Pure *epi*-anchinopeptolide C (**3e**) (r_t= 15.0 min, 10.6 mg; r_t= 15.5 min, 8.6 mg) was obtained.

(*S,E*)-4-amino-5-((2-((4-hydroxystyryl)amino)-2-oxoethyl)amino)-5-oxopentanoic acid[12] (5)

^{1}H-NMR (500 MHz, MeOH-d_4) δ: 7.25 (d, *J* = 14.5 Hz, 1H), 7.15 (d, *J* = 8.5 Hz, 2H), 6.74 (d, *J* = 8.5 Hz, 2H), 6.18 (d, *J* = 14.5 Hz, 1H), 4.25 (m, 1H), 3.96 (s, 2H), 2.53–2.40 (m, 2H), 2.36–2.29 (m, 1H), 2.19–2.13 (m, 1H)

Data are consistent with those reported in literature

anchinopeptolide A[11] (3a)

^{1}H-NMR (500 MHz, MeOH-d_4) δ: 7.15 (d, *J* = 15 Hz, 2H), 7.02 (d, *J* = 8.5 Hz, 4H), 6.63 (d, *J* = 8.5 Hz, 2H), 6.62 (d, *J* = 8.5 Hz, 2H), 6.19 (d, *J* =14.5 Hz, 1H), 6.04 (d, *J* = 14.5 Hz, 1H), 4.42 (q, *J* = 7.0 Hz, 1H), 4.12 (q, *J* =7.0 Hz, 1H), 3.28–3.16 (m, 2H), 3.14 (t, *J* = 5.0 Hz, 2H), 2.70 (t, *J* = 7.5 Hz, 1H), 1.99 – 1.92 (m, 2H), 1.85–1.72 (m, 2H), 1.56 (d, *J* = 7 Hz, 3H), 1.49 (d, *J* =7.0 Hz, 3H), 1.46–1.40 (m, 1H)

^{13}C-NMR (125 MHz, MeOH-d_4) δ: 177.0, 174.7, 172.1, 170.2, 159.1, 159.0, 158.0, 157.9, 129.3, 129.2, 128.2 (2C), 128.1 (2C), 121.7, 121.5, 116.9 (2C), 116.8 (2C), 116.3, 115.3, 92.5, 77.2, 53.8, 52.1, 46.9, 42.8, 41.0, 34.8, 25.1, 24.7, 17.9, 15.0

$[\alpha]_D^{20}$= -40 (*c*= 0.05, MeOH) (literature[11]: $[\alpha]_D^{20}$= -103.6, *c*= 4, MeOH)

HRMS (ESI) *m/z*, calcd for $[C_{34}H_{47}N_{10}O_8]^+$: 723.3573, found: 723.3627

Data are consistent with those reported in literature

anchinopeptolide B[13] (3b)

^{1}H-NMR (500 MHz, MeOH-d_4) δ: 7.26 (d, *J* = 15, 1H), 7.21 (d, *J* = 14.5, 1H), 7.16 (d, *J* = 8.5, 2H), 7.11 (d, *J* = 8.5, 2H), 6.71 (d, *J* = 8.5, 2H), 6.68 (d, *J* = 9, 2H), 6.20 (d, *J* = 14.5, 1H), 6.05 (d, *J* = 14.5, 1H), 4.28 (d, *J* = 16, 1H), 4.01 (q, *J* = 7, 1H), 3.90 (d, *J* = 16, 1H), 3.63–3.59 (m, 1H), 3.45–3.41 (m, 1H), 3.14–3.10 (m, 2H), 2.64 (dd, *J* = 5.5 and 9.0, 1H), 2.09–1.94 (m, 4H), 1.77–1.70 (m, 2H), 1.55 (d, *J* = 6.5, 3H)

HRMS (ESI) *m/z*, calcd for $[C_{33}H_{45}N_{10}O_8]^+$: 709.3416, found: 709.3497

Data are consistent with those reported in literature

anchinopeptolide C[13](3c)

^{1}H-NMR (500 MHz, MeOH-d_4) δ: 7.22 (d, *J* = 14.5, 1H), 7.21 (d, *J* = 14.5, 1H), 7.15 (d, *J* = 8.5, 1H), 7.12 (d, *J* = 8.5, 2H), 6.69 (d, *J* = 8.5, 2H), 6.68 (d, *J* = 8.5, 2H), 6.19 (d, *J* = 14.5, 1H), 6.16 (d, *J* = 14.5, 1H), 4.37 (q, *J* = 7.3, 1H), 4.17 (d, *J* = 17, 1H), 3.28–3.24 (m, 2H), 3.22–3.19 (m, 2H), 2.72 (m, 1H), 2.09–1.94 (m, 3H), 1.60–1.54 (m, 1H), 1.46 (d, *J* = 7, 3H)

^{13}C-NMR (100 MHz, MeOH-d_4) δ: 177.9, 172.6, 172.0, 168.0, 158.7 (2C), 157.8, 157.7, 128.7, 128.9, 127.9 (2C), 127.8 (2C), 121.1, 120.8, 116.5 (4C), 116.1, 115.8, 90.9, 76.6, 51.3, 46.5, 44.9, 42.5, 40.6, 34.9, 24.6, 24.4, 17.7

$[\alpha]_D^{20}$= -35 (*c*= 0.09, MeOH) (literature[13]: $[\alpha]_D^{20}$= -6.3, *c*= 1, MeOH)

HRMS (ESI) *m/z*, calcd for $[C_{33}H_{45}N_{10}O_8]^+$: 709.3416, found: 709.3365

Data are consistent with those reported in literature

anchinopeptolide D[13] (3d)

^{1}H-NMR (500 MHz, MeOH-d_4) δ: 7.23 (d, *J* = 14.5, 1H), 7.21 (d, *J* = 14.5, 1H), 7.14 (d, *J* = 8.5, 4H), 6.18 (d, *J* = 14.5, 1H), 6.17 (d, *J* = 14.5, 1H), 4.22 (d, *J* = 16.5, 1H), 4.12 (d, *J* = 16.5, 1H), 3.91 (d, *J* = 16.5, 1H), 3.89 (d, *J* = 16.5, 1H), 3.49–3.43 (m, 1H), 3.27–3.22 (m, 1H), 3.21–3.15 (m, 2H), 2.68 (dd, *J* = 4.5 and 10.3, 1H), 2.10–2.01 (m, 1H), 1.89–1.83 (m, 2H), 1.82–1.74 (m, 2H), 1.58–1.50 (m, 1H)

^{13}C-NMR (100 MHz, MeOH-d_4) δ: 177.8, 173.6, 168.3, 168.0, 158.7, 157.8, 128.7, 128.7, 127.9 (2C), 127.8 (2C), 121.0, 120.8, 116.6 (4C), 116.1, 115.6, 91.1, 76.6, 46.7, 45.0, 43.4, 42.5, 40.8, 34.6, 24.6, 24.0

$[\alpha]_D^{20}$= +86 (*c*= 0.07, MeOH) (literature[13]: $[\alpha]_D^{20}$= +11.4, *c*= 1, MeOH)

HRMS (ESI) *m/z*, calcd for $[C_{32}H_{43}N_{10}O_8]^+$: 695.3260, found: 695.3225

Data are consistent with those reported in literature

***epi*-anchinopeptolide C (3e)**

IR (film) ν/cm^{-1} 3400 (O-H), 1673 (C=C and N-H), 1466 (C-N), 1242 and 1204 (C-O)

HRMS (ESI) *m/z*, calcd for $[C_{33}H_{45}N_{10}O_8]^+$: 709.3416, found: 709.3445

$[\alpha]_D^{20}$= -54 (*c*= 0.5, MeOH)

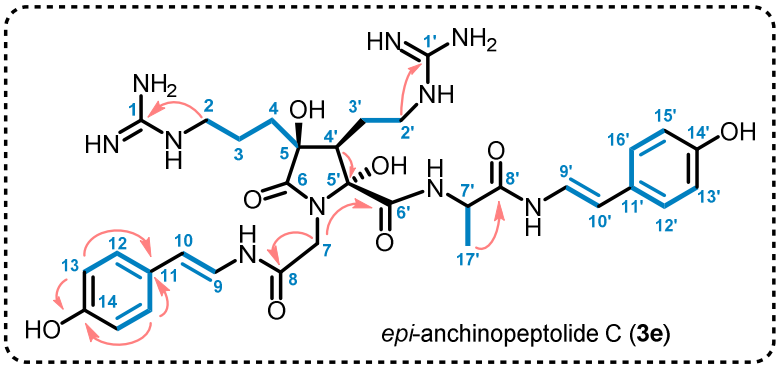

Table 11. ^{1}H- and ^{13}C-NMR data of compound **3e** in MeOH-d_4

attribution	δ (ppm) ^{1}H	multiplicity	J (Hz)	integration	δ (ppm) ^{13}C
1	-	-	-	-	158.7
2	3.23	t	7	2	42.3
3	1.64–1.77	m	-	2	24.6
4	1.74–1.88	m	-	2	32.1
5	-	-	-	-	77.9
6	-	-	-	-	176.3
7a	4.10	d	16	1	43.0
7b	3.82	d	16	1	43.0
8	-	-	-	-	167.3
9	7.23	d	15	1	120.9
10	6.22	d	15	1	115.8
11	-	-	-	-	128.8
12, 16	7.15	d	8.5	2	127.8
13, 15	6.71	d	8.5	2	116.6
14	-	-	-	-	157.8
1'	-	-	-	-	158.6
2'	3.38	m	-	1	41.1
3'	1.77-1.82	m	-	-	24.7
4'	2.37	dd	4.0 and 10.0	1	51.2
5'	-	-	-	-	92.1
6'	-	-	-	-	171.6
7'	4.43				51.0
8'	-	-	-	-	171.9
9'	7.24	d	14.5	1	121.1
10'	6.19	d	14.5	1	115.8
11'	-	-	-	-	128.9
12', 16'	7.17	d	8.5	2	127.9
13', 15	6.71	d	8.5	2	116.6
14'	-	-	-	-	157.8
17'	1.48	d	7.5	3	17.9

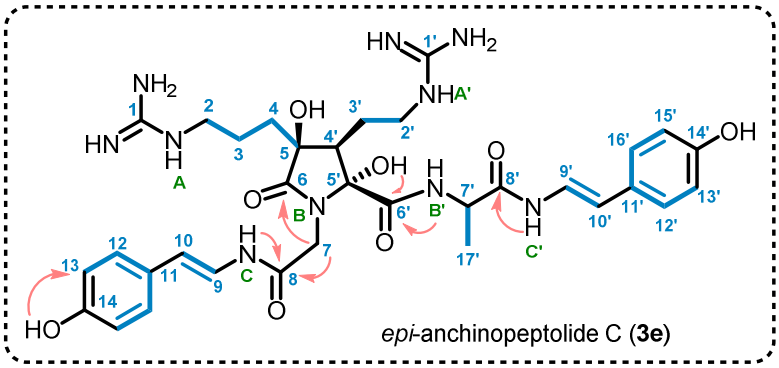

Table 12. ^{1}H- and ^{13}C-NMR data of compound **3e** in DMSO-d_6

attribution	δ (ppm) ^{1}H	multiplicity	J (Hz)	integration	δ (ppm) ^{13}C
1	-	-	-	-	157.4
2	3.14–3.10	m	-	2	40.8
3a	1.66–1.60	m	-	1	23.3
3b	1.41–1.45	m	-	1	23.3
4a	1.69–1.68	m	-	1	31.2
4b	1.56–1.50	m	-	1	31.2
5	-	-	-	-	76.1
6	-	-	-	-	174.3
7a	3.97	d	16	1	41.7
7b	3.63	d	15.5	1	41.7
8	-	-	-	-	165.9
9	7.13	s	-	1	120.3
10	6.11	d	14.5	1	112.6
11	-	-	-	-	127.8
12, 16	7.16	s	-	2	126.4
13, 15	6.69	d	8.5	2	115.5
14	-	-	-	-	157.0
N_A-H	7.56	br t	5.5	1	-
N_C-H	10.14	d	10	1	-
5-OH	5.52	s	-	1	-
14-OH	9.40	s	-	1	-
1'	-	-	-	-	156.7
2'	3.24–3.20	m	-	2	39.2
3'a	1.56–1.50	m	-	1	23.4
3'b	1.66–1.60	m	-	1	23.4
4'	2.30	dd	5.5 and 10.5	1	48.4
5'	-	-	-	-	90.7
6'	-	-	-	-	171.0
7'	4.33	t	6.5	1	49.2
8'	-	-	-	-	169.5
9'	7.17	s	-	1	120.6
10'	6.14	s	15	1	112.9
11'	-	-	-	-	127.8
12', 16'	7.16	s	1	2	126.4
13', 15	6.69	d	8.5	2	116.0

attribution	δ (ppm) ^{1}H	multiplicity	J (Hz)	integration	δ (ppm) ^{13}C
14'	-	-	-	-	157.0
17'	1.36	d	7	3	17.6
$N_{A'}$-H	7.43	br t	5.5	1	-
$N_{B'}$-H	8.59	d	7	1	-
$N_{C'}$-H	10.22	d	9.5	1	-
5'-OH	7.36	s	-	1	-
14'-OH	9.40	s	-	1	-

Hemisynthesis of cycloanchinopeptolide C (4c)

A sample of anchinopeptolide C (**3c**, 13.8 mg) in a quartz tube was dissolved into 0.70 mL of D_2O and exposed to an irradiation chamber (lamps ReptiSun 10.0 ZOOMED® UV-B (10%) 26W). The evolution of the reaction was followed by ^{1}H-NMR and after 23 h the solution was evaporated at 40 °C under reduced pressure. The crude was purified by preparative HPLC [column: C18 Sunfire Waters 19 x 150 mm, 5 µm; mobile phase: (H_2O + 0.2% TFA) : ACN; method: gradient of 10-30% of ACN in 20 min; flow: 17 mL.min^{-1}; volume of injection: 200 µL, concentration: 10 mg.mL^{-1} in MeOH, detection at 254 nm]. The fraction with r_t= 9.8 min corresponded to pure cycloanchinopeptolide C (**4c**, 2.3 mg, white solid, 17% of yield).

cycloanchinopeptolide C (4c)

IR (film) ν/cm^{-1} 3307 (O-H), 2916 (C-H), 2850 (C-H), 1678 (C=C), 1203 and 1138 (C-O)

HRMS (ESI) *m/z*, calcd for $[C_{33}H_{45}N_{10}O_8]^+$: 709.3416, found: 709.3364

$[\alpha]_D^{20}$= -44 (*c* 0.09, MeOH) (literature[13]: $[\alpha]_D^{20}$= +18.6°, *c*= 0.5 , MeOH)

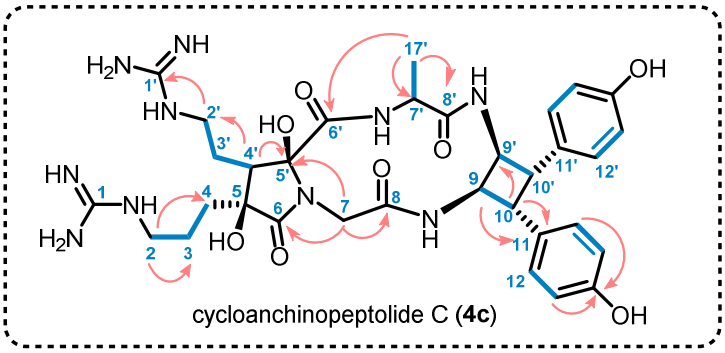

Table 13. ^{1}H- and ^{13}C-NMR data of compound **4c** in MeOH-d_4

attribution	δ (ppm) ^{1}H	multiplicity	J (Hz)	integration	δ (ppm) ^{13}C
1	-	-	-	-	158.7
2	3.16 – 3.21	m	-	2	42.5
3	1.87 – 1.99	m	-	2	24.4
4	1.87 – 1.99	m	-	2	34.8
5	-	-	-	-	76.5
6	-	-	-	-	178.3
7a	4.18	d	17.6	1	44.4
7b	4.08	d	17.6	1	44.4
8	-	-	-	-	170.2
9	4.76 – 4.81	m	-	1	52.8
10	3.93	dd	3.6 and 10.0	1	47.7
11	-	-	-	-	130.2
12, 16	6.87	d	8.4	1	130.2
13, 15	6.62	d	8.4	1	115.9
14	-	-	-	-	156.8
1'	-	-	-	-	158.7
2'	3.29	t	8.0	2	40.6
3'	1.87 – 1.99	m	-	2	24.2
4'	3.16 – 3.21	m	-	1	44.5
5'	-	-	-	-	90.6
6'	-	-	-	-	173.7
7'	4.66	q	6.8	1	50.7
8'	-	-	-	-	173.3
9'	4.76 – 4.81	m	-	1	52.7
10'	4.04 – 4.11	m	-	1	48.3
11'	-	-	-	-	130.2
12', 16'	6.87	d	8.4	-	130.2
13', 15	6.62	d	8.4	-	115.9
14'	-	-	-	-	156.8
17'	1.43	d	6.8	3	14.6

Table 14. NMR shifts of synthetic and natural cycloanchinopeptolide (**4c**) in MeOH-d_4

	Hemisynthetic	Natural product[13]		Hemisynthetic	Natural product[13]	
attribution	δ (ppm) ^{1}H		Δ ppm	δ (ppm) ^{13}C		Δ ppm
1	-		-	158.7	158.6	0.1
2	3.19	3.28	-0.09	42.5	42.5	0.0
3	1.93	1.94	-0.01	24.4	24.2	0.2
4	1.93	1.90	-0.03	34.8	34.8	0.0
5	-	-	-	76.5	76.5	0.0
6	-	-	-	178.3	178.3	0.0
7a	4.18	4.03	0.15	44.4	44.2	0.2
7b	4.08	4.17	-0.09	44.4	44.2	0.2
8	-	-	-	170.2	170.2	0.0
9	4.79	4.80	0.01	52.8	52.7	0.1
10	3.93	3.89	0.04	48.4	47.5	0.9
11	-	-	-	130.2	127.9	2.3
12, 16	6.87	6.85	0.02	130.2	130.3	-0.1
13, 15	6.62	6.59	0.03	115.9	115.9	0.0
14	-	-	-	156.8	156.8	0.0
1'	-	-	-	158.7	158.6	0.1
2'	3.29	3.24	0.05	40.6	40.6	0.0
3'a	1.93	1.58	0.08	24.2	24.4	-0.2
3'b	1.93	1.85	0.08	24.2	24.4	-0.2
4'	3.19	3.20	-0.01	44.5	44.0	0.5
5'	-	-	-	90.6	90.6	0.0
6'	-	-	-	173.7	173.8	-0.1
7'	4.66	4.64	0.02	50.7	50.7	0.0
8'	-	-	-	173.3	173.4	-0.1
9'	4.79	4.76	0.03	52.7	52.7	0.0
10'	4.08	4.06	0.02	48.3	48.3	0.0
11'	-	-	-	130.2	127.9	2.3
12', 16'	6.87	6.73	0.14	130.2	130.0	0.2
13', 15	6.62	6.55	0.07	115.9	115.8	0.1
14'	-	-	-	156.8	156.9	-0.1
17'	1.43	1.43	0.00	14.6	14.6	0.0

2. 2 Isolation of metabolites from *C. taillezi* sponge

The specimens of *C. taillezi* were collected manually by SCUBA diving on the Coast of Villefranche-Sur-Mer (France) on January of 2015 between 10 and 30 m deep.

The samples were freeze-dried and grated, yielding a hard orange solid (20.8 g) that was exhaustively extracted with a mixture DCM : MeOH (1 : 1). After the solvent removal by reduced pressure, the extract yielded a brown oil (8.5 g) that was adsorbed in Silice RP-18 and fractionated

by VLC using the following elution gradient: H_2O (500 mL, F1 fraction, 4.42 g), MeOH (650 mL, F2 fraction, 1.72 g), MeOH : DCM (1 : 1, 500 mL, F3 fraction, 656 mg), and DCM (900 mL, F4 fraction, 429 mg). Fractions F2 - F4 were analysed by UPLC and F2 (400 mg) was submitted to HPLC purification by semi-preparative mode (column: X-Select CSH C18, 5 µm, flow: 10 $mL.min^{-1}$, concentration: 100 $mg.mL^{-1}$) applying H_2O : ACN : TFA according the elution sequence: isocratic 0 - 3 min (65 : 35 : 0.1),gradient 3 - 15 min (from 65 : 35 : 0.1 to 60 : 40 : 0.1), gradient 15 - 17 min (from 60 : 40 : 0.1 to 40 : 60 : 0.1), isocratic 17 - 20 min (40 : 60 : 0.1), gradient 20 - 22 min (from 40 : 60 : 0.1 to 65 : 35 : 0.1), isocratic 22 - 25 min (65 : 35 : 0.1). The chromatogram profile was divided in 14 peaks. Crambescidins were identified on peaks F2P10 - P14, crambescidin 800 (**23f**) was identified in F2P12 (52.9 mg) and F2P14 yielded crambescidin 816 (**23g**) (25.8 mg).

crambescidin 800[91] **(23f)**

^{1}H-NMR (500 MHz, MeOH-d_4) δ: 5.71 (br t, *J* = 9, 2H), 5.50 (br d, *J* = 11, 1H), 4.45–4.38 (m, 1H), 4.37–4.30 (m, 1H), 4.17–4.11 (m, 2H), 3.97–3.90 (m, 1H), 3.69–3.59 (m, 1H), 3.50–3.59 (m, 1H), 3.44–3.36 (m, 1H), 3.16–3.06 (m, 2H), 2.97–2.94 (m, 1H), 2.91–2.84 (m, 1H), 2.64 (dd, *J* = 5 and 13, 1H), 2.51–2.37 (m, 4H), 2.19–2.13 (m, 1H), 2.05–1.80 (m, 9H), 1.73–1.56 (m, 10H), 1.43 (t, *J* = 12.5, H), 1.38–1.28 (m, 24H), 1.13 (d, *J* = 6, 3H), 0.88 (t, *J* = 7.5, 3H)

HRMS (ESI) *m/z*, calcd for $[C_{45}H_{81}N_6O_6]^+$: 801.6212, found: 801.6225

Data are consistent with those reported in literature

crambescidin 816 (23g)

^{1}H-NMR (500 MHz, MeOH-d_4) δ: 5.72 (br t, *J* = 8.5, 1H), 5.52 (br d, *J* = 11, 1H), 4.45 (br d, *J* = 9.5, 1H), 4.37–4.32 (m, 1H), 4.18–4.14 (m, 2H), 3.96–3.93 (m, 2H), 3.68 (quint, *J* = 7.0, 1H), 3.47 (s, 1H), 3.45–3.44 (m, 1H), 3.42–3.37 (m, 1H), 3.14–3.09 (m, 2H), 2.92–2.84 (m, 2H), 2.65 (dd, *J* = 5 and 13, 1H), 2.55-2.49 (m, 2H), 2.44-2.40 (m, 3H), 2.21–2.15 (m, 2H), 2.06–2.01 (m, 2H), 1.98–1.96 (m, 1H), 1.92–1.88 (m, 4H), 1.74–1.71 (m, 3H), 1.68–1.65 (m, 4H), 1.61–1.59 (m, 1H), 1.51–1.48 (m, 1H), 1.44 (t, *J* = 12.5, 1H), 1.35–1.36 (m, 1H), 1.31–1.29 (m, 24H), 1.14 (d, *J* = 6.5, 3H), 0.89 (t, *J* = 7, 3H)

^{13}C-NMR (125 MHz, MeOH-d_4) δ: 177.5, 168.8, 149.7, 134.2, 131.2, 90.6, 85.2, 84.6, 72.4, 70.0,

[91] N. C. Gassner, C. M. Tamble, J. E. Bock, N. Cotton, K. N. White, K. Tenney, O. R. P. St, M. J. Proctor, G. Giaever, R. W. Davis, P. Crews, T. R. Holman, R. S. Lokey, *J. Nat. Prod.* **2007**, *70*, 383-390.

68.7, 67.1, 56.1, 54.7, 54.1, 43.8, 38.5, 38.0, 37.6, 37.4, 34.1, 32.8, 32.7, 32.4, 30.9, 30.8, 27.0, 26.6, 26.5, 24.5, 21.7, 19.0, 11.0

HRMS (ESI) *m/z*, calcd for $[C_{45}H_{81}N_6O_7]^+$: 817.6161, found: 817.6134

Data are consistent with those reported in literature

2. 3 Isolation of metabolites from *C. crambe* sponge

Specimens of *Crambe crambe* were manually collected by SCUBA diving on the coast of Villefranche-Sur-Mer (France) on November 2014 at deeps ranging from 10 to 25 m and kept frozen until used. The sponges were freeze-dried and grated, furnishing a red solid (24.2 g). This powder was purified according to the procedure described on literature[45]. Compounds sent to biological assays were identified by NMR and HRMS (95% of purity, determined by HPLC).

3. ^{14}C-Feeding Experiments with *C. crambe* Sponge: Initial Insights into the Biosynthesis of Crambescin C1

3. 1. Sponges Collection and *in vivo* feeding experiments with ^{14}C-labelled precursors

C. Crambe sponges were collected at 50 m deep of the Coast of Villefranche-Sur-Mer (France) by SCUBA diving, on June 2015. The specimens were acclimatized in open system aquaria supplied with sea water during 3 weeks (average values for water parameters: pH= 8.11, T= 18°C, dissolved oxygen= 105.3%), being daily fed with phytoplankton *Isochrysis Galbana*. For the feeding experiments, the sponges were placed in 700 mL round plastic boxes in presence of the radiolabelled precursor (37 kBq= 1 μCi per spike, 10 μL of precursor each one) during 18 h. The activity of a 1 mL sample of the water column surrounding the sponge was analysed by liquid scintillation just after injecting the precursor and just before opening the water system to the metabolization period in order to follow the percentage of activity disappearance. After the incubation with the precursor, the sponges were removed from the plastic boxes, fed with phytoplankton and let in open water system aquaria during at least 6 hours. After 10 cycles of incubations followed by metabolization period (8 cycles for acetate), the sponges were freeze, lyophilized and extract 3 times with 30 mL of MeOH under ultrasound during 15 minutes. The

samples were centrifuged and the supernatants were concentrated under reduced pressure at 40°C and fractionated by SPE by a step gradient of H_2O (F1), H_2O : MeOH 1:1 v/v (F2), H_2O : MeOH 1:3 v/v (F3), and MeOH (F4). Fraction F2 was purified by semi-preparative HPLC (RP column Phenomenex Luna phenyl-hexyl, 250 x 10 mm, 5 μm) eluted with H_2O/ACN/TFA as following: isocratic elution 0-3 min (90 : 10 : 0.1), gradient elution 3-5 min (from 90 : 10 : 0.1 to 65 : 35 : 0.1), isocratic elution 5-10 min (65 : 35 : 0.1), gradient elution 10-30 min (from 65 : 35 : 0.1 to 55 : 45 : 0.1), isocratic elution 30-34 min (55 : 45 : 0.1), gradient elution 34-36 min (from 55 : 45 : 0.1 to 90 : 10 : 0.1), and isocratic 36-45 min (90 : 10 : 0.1), applying a flow rate of 3 $mL.min^{-1}$, to give 7 fractions, named as: F2P1 (r_t= 9.0-11.0 min), F2P2 (r_t= 26-27 min), F2P3 (r_t= 28.0-29.5 min), F2P4 (r_t= 30-32 min), F2P5 (r_t= 32-34 min), F2P6 (r_t= 34-36 min) and F2P7 (r_t= 36.5-39 min). The F2P2 was identified by NMR as crambescin C1[45] and was submitted to further HPLC purification (RP column C18 HTec, 250 x 4.6 mm, 5 μm, analytical column) applying an isocratic elution of H_2O : ACN : TFA (57 : 43 : 0.1) during 20 min, which afforded the pure compound (r_t= 11 min).

crambescin C1[45]

^{1}H-NMR (500 MHz, MeOH-d_4) δ: 4.41 (dd, *J* = 4.5 and 7.0, 1H), 4.24–4.13 (m, 2H), 3.62 (t, *J* = 6.5, 2H), 3.17 (t, *J* = 7, 2H), 2.88–2.76 (m, 2H), 1.81 (quint, *J* = 6.5, 2H), 1.73–1.70 (m, 2H), 1.62–1.58 (m, 5H), 1.45–1.38 (m, 8H), 1.36–1.26 (m, 14H), 0.90 (t, *J* = 6.5, 3H).

Data are consistent with those reported in literature.

3. 2. Radioactivity TLC and autoradiography beta-imager analyses

F2, F3 and F4 (1 mg of each one) were adsorbed on small spots of a silica TLC plate and had the beta-radioactivity measured by a radio-TLC equipment was accumulated for 1 hour. To access the specific activity, a standard curve of L-[U-^{14}C]proline was used.

Pure crambescins C1 (0.2 mg) were adsorbed on small spots of a silica TLC plate and measured during 46 hours on a autoradiography beta-imager equipment. It was determined an efficiency of 12.7% applying L-[U-^{14}C]proline as standard.

3. 3. Control Experiments

Into a 700 mL box containing sea water, distilled water, sea water with 2 mL 10% NaClO solution or sea water with 2 mL 10% NaClO and a sponge rock support, it was introduced 37 kBq (1 μCi) of a radiolabelled precursor (lauric acid or agmatine). To avoid external contamination, the samples were let inside a covered box during 20 days and during this period had the beta-radioactivity of the water column evaluated by liquid scintillation (1 mL of sample was collected to each essay). After 17 days, the sample containing sea water with NaClO and agmatine was split into two and to the second box was added 2 mL of 10% NaClO solution. The radioactivity of these samples were also analysed by liquid scintillation.

4. Biomimetic Synthesis of Crambescin A2 and Derivatives

4. 1. Preparation of benzyl 3-oxotetradecanoate (25a)

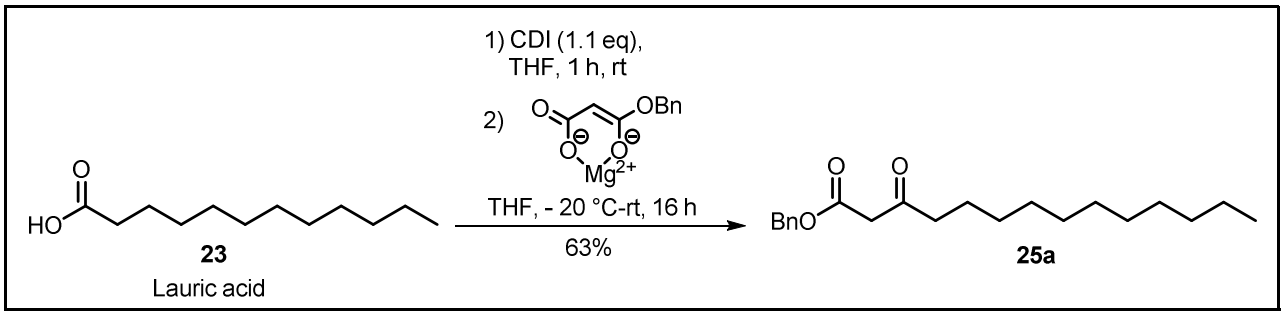

A mixture of dodecanoic acid (**23**) (1.01 g, 5.00 mmol) and CDI (0.901 g, 5.50 mmol) in anhydrous THF (30 mL) was stirred under inert atmosphere during 1 h at 0 °C. In another round bottom flask a solution of mono-benzyl malonate (1.08 g, 5.50 mmol) and isopropyl magnesium chloride (2 M in THF, 5.00 mL, 11.0 mmol) in anhydrous THF (20 mL) was stirred 1 h at 0 °C under inert atmosphere. Afterwards the magnesium salt solution was cooled to - 20 °C and the reaction containing **23** was poured dropwise into this solution. After 45 min, the mixture was brought to rt. After 16 h of stirring, the reaction was quenched with saturated aq. NH_4Cl solution (30 mL) and H_2O (30 mL). The aqueous layer was extracted with Et_2O (3 x 50 mL). The combined organic phases were dried over Na_2SO_4, filtered and the solvent was removed under reduced pressure at 40 °C. The crude product was purified by flash chromatography (cyclohexane : AcOEt, 4 : 1) to furnish the

desired product **25a**[92, 93] as a white solid (1.05 g, 3.15 mmol, 63%).

^{1}H-NMR (300 MHz, $CDCl_3$) δ: 7.39 – 7.33 (m, 5H, Ar), 5.17 (s, 2H, C*H*$_2$Ph), 3.48 (s, 2H, H-2), 2.50 (t, *J* = 7.4 Hz, 2H, H-4), 1.57 (t, *J* = 6.8 Hz, 2H, H-5), 1.30 – 1.21 (m, 16 H), 0.88 (t, *J*= 6.5 Hz, 3H, H-14)

^{13}C-NMR (75 MHz, $CDCl_3$) δ: 202.8 (C-1), 167.2 (C-3), 135.4, 128.7, 128.5 (2C), 128.3 (2C), 67.2 (*C*H_2Ph), 49.3 (C-2), 43.2 (C-4), 32.0, 29.7 (2C), 29.6 (2C), 29.5, 29.1, 23.6, 22.8, 14.2 (*C*H_3)

IR (film) ν/cm^{-1} 1218 (C-O), 1716 (C=O), 1743 (C=O), 2853 (CH_3), 2923 (CH_2)
HRMS (ESI) *m/z*, calcd for $[C_{21}H_{32}O_3Na]^+$: 355.2249, found: 412.1182

Data are consistent with those reported in literature

4. 2. Preparation of ethyl 3-oxotetradecanoate (25b)

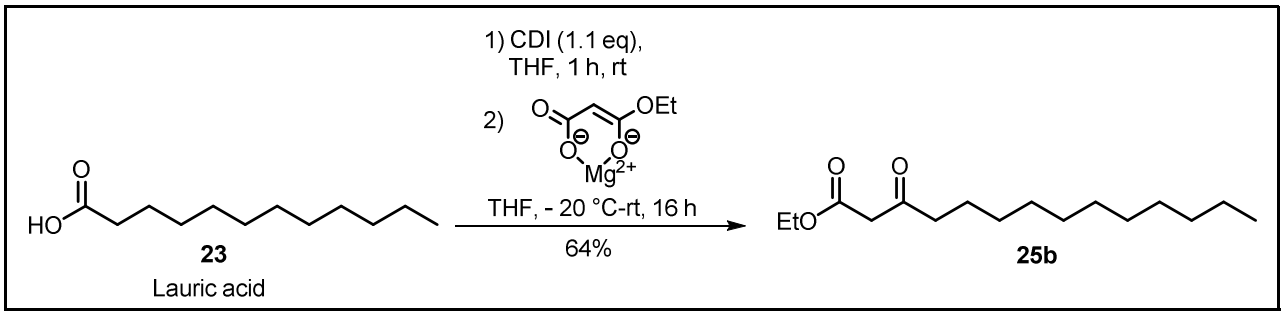

Compound **25b** was prepared by the same procedure as described on item 4. 1 using a mixture of dodecanoic acid **23** (1.00 g, 4.99 mmol) and CDI (0.890 g, 5.49 mmol) in anhydrous THF (20 mL) and a solution of mono-ethyl malonate (0.731 g, 5.49 mmol) and isopropyl magnesium chloride (2 M in THF, 1.10 mL, 11.0 mmol) in anhydrous THF (10 mL). The crude product was purified by flash chromatography (cyclohexane : AcOEt, 4 : 1) leading to **25b** as a colorless oil (0.861 g, 3.18 mmol, 64%).

[92] W. J. Christ, L. D. Hawkins, T. Kawata, D. P. Rossignol, S. Kobayashi, O. Asano, Eisai Co., Ltd., USA . **1996**, pp. 92 pp., Cont.-in-part of U.S. Ser. No. 776,100, abandoned.

[93] W. J. Christ, T. Kawata, L. D. Hawkins, S. Kobayashi, O. Asano, D. P. Rossignol, Eisai Co., Ltd., Japan . **1993**, p. 213 pp.

^{1}H-NMR (300 MHz, $CDCl_3$) δ: 4.19 (q, *J* = 7.2 Hz, 2H, OCH_2), 3.42 (s, 2H, H-2), 2.52 (t, *J* = 7.2 Hz, 2H, H-4), 1.60 – 1.56 (m, 2H, H-5), 1.27 – 1.25 (m, 17H), 0.87 (t, *J* = 6.3 Hz, 3H, H-14)

^{13}C-NMR (75 MHz, $CDCl_3$) δ: 202.9 (C-3), 167.2 (C-1), 61.3 (OCH_2), 49.3 (C-2), 43.0 (C-4), 31.9, 29.6 (2C), 29.4, 29.3 (2C), 29.0, 23.5, 22.7, 14.1 (2C, C-14, CH_3CH_2O)

IR (film) ν/cm^{-1}1232 (C-O), 1717 (C=O), 1746 (C=O), 2853 (CH_3), 2923 (CH_2)

HRMS (ESI) *m/z*, calcd for $[C_{16}H_{30}O_3Na]^+$: 293.2093, found: 293.2094

4. 3. Preparation of 3-oxotetradecanoic acid (21)

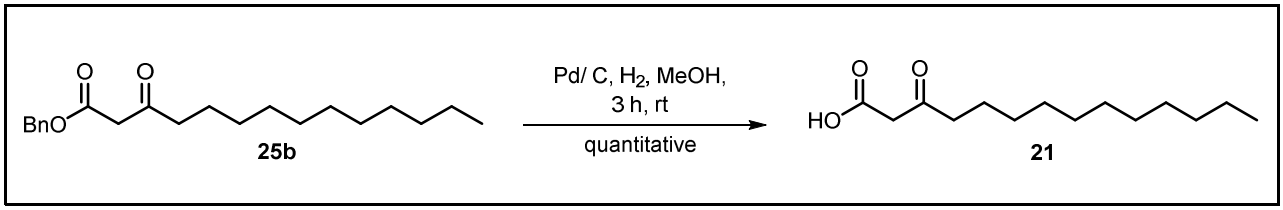

To a solution of **25b** (0.808 g, 2.43 mmol) in MeOH (10 mL) was added Pd/C 10% w/w (60.0 mg) and then the reaction was flushed with H_2. The suspension was stirred for 3 h, filtered under a small column of Celite®, washed with MeOH and the solvent was evaporated under reduced pressure at 40 °C yielding pure **21**[94] (0.582, 2.40 mmol, 99 %, white solid). The product was stored at - 6 °C to avoid decarboxylation.

^{1}H-NMR (300 MHz, acetone-d_6) δ: 3.49 (*br s*, 2H, H-2), 2.60 (*t*, *J* = 7.2 Hz, 2H, H-4), 1.60 – 1.52 (*m*, 2H, H-5), 1.30 – 1.20 (*m*, 16H), 0.88 (*t*, *J* = 6.5 Hz, 3H, H-14)

HRMS (ESI) *m/z*, calcd for $[C_{14}H_{25}O_3]^-$: 241.1809, found: 241.1800

Data are consistent with those reported in literature

[94] M. A. Mitz, A. E. Axelrod, K. Hofmann, *J. Am. Chem. Soc.* **1950**, *72*, 1231-1232.

4. 4. Preparation of 4-guanidinobutanoic acid (31)

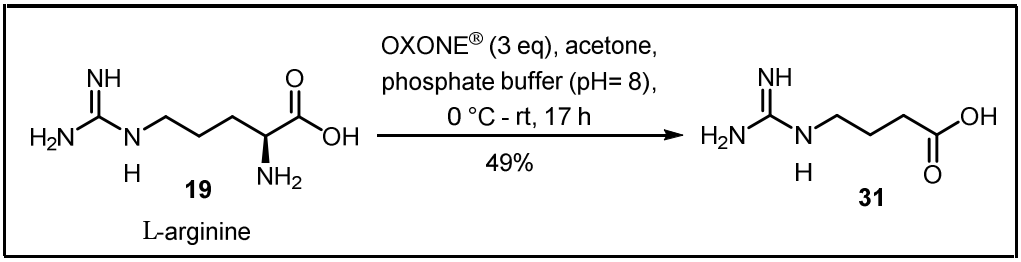

A mixture of L-arginine (179 mg, 1.03 mmol) and acetone (2 mL) in phosphate buffer (pH= 8, 15 mL) was cooled to 0 °C. Then, a solution of OXONE® (1.85 g, 3.00 mmol) in water (10 mL) was added dropwise. During the addition the pH was maintained between 7.5 and 8.5 by addition of a 0.1 M aq. NaOH solution. The reaction mixture was stirred at rt for 17 h. The excess of oxidant was quenched by addition of Na_2SO_3 (≈ 50 mg) and the pH was adjusted to 2 with a 2 M aq. HCl solution. The mixture was concentrated under reduced pressure and 45 °C and the residue was washed with BuOH (4 x 2.5 mL). The organic extracts were evaporated under reduced pressure to yield **31**[70*] as a white solid (70.5 mg, 49 %).

*Reference 70 reports preparation of compound **31** but does not describe experimental spectroscopic data. IR, ^{1}H- and ^{13}C-NMR spectra provided by BIORAD Laboratories are available on SciFinder (access: 06/19/2017).

^{1}H-NMR (300 MHz, MeOH-d_4) δ: 3.25 – 3.20 (t, *J* = 7.2 Hz, 2H, H-4), 2.41 – 2.37 (t, *J* = 7.2 Hz, 2H, H-2), 1.91 – 1.81 (*quint*, *J* = 7.2 Hz, 2 H, H-3)

^{13}C-NMR (75 MHz, MeOH-d_4) δ: 177.1 (C-1), 158.7 (C-5), 41.7 (C-4), 31.8 (C-2), 25.3 (C-3)

HRMS (ESI) *m/z*, calcd for $[C_5H_{12}N_3O_2]^+$: 146.0930, found: 146.0927

Data are consistent with those reported in literature

4. 5. Preparation of 1-(4-hydroxybutyl)guanidine (20a)

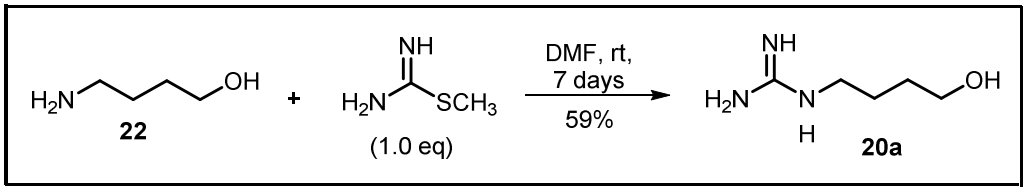

To a solution of **22** (45.0 mg, 0.500 mmol) in DMF (1 mL) was added *S*-methylisothiourea hemisulfate salt (76.0mg, 0.500 mmol). The white suspension was stirred during 7 days. After evaporation, the crude was suspended in EtOH (2 mL) centrifuged and the supernatant was discarded. This procedure was repeated twice and the remaining solid was dried under reduced pressureto yield **20a**[*] as a white powder (38.6mg, 0.294 mmol, 59%).

[*]The compound is described but there is any experimental spectroscopic data available.

^{1}H-NMR (300 MHz, D_2O) δ: 3.61 (t, *J* = 6.0 Hz, 2H, H-1), 3.20 (t, *J* = 6.6 Hz, 2H, H-4), 1.69 – 1.53 (br s, 4H, H-2, H-3)

^{13}C-NMR (75 MHz, D_2O) δ: 156.7 (C-5), 61.1 (C-1), 40.9 (C-4), 28.4 (C-3), 24.5 (C-2)

IR (film) ν/cm^{-1}1204 (CH_2), 1455 (N-H), 1612 (C=N), 2468 (O-H), 3415 (NH_2)

HRMS (ESI) *m/z*, calcd for $[C_5H_{14}N_3O]^+$: 132.1137, found: 132.1132

4. 6. Preparation of 4-(*N*,*N'*-di-*t*-butoxycarbonylguanidino)-butan-1-ol (20c)

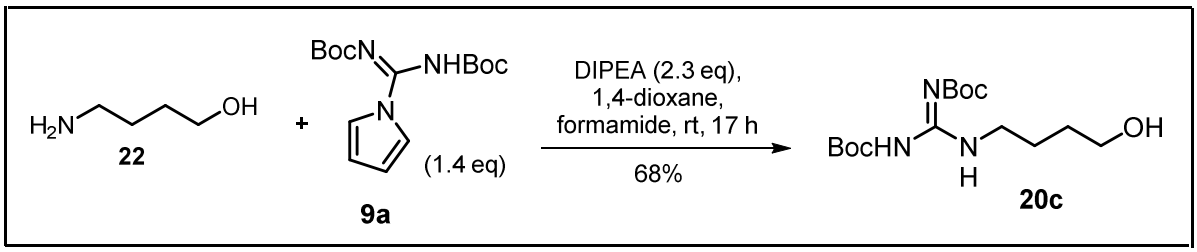

To a solution of **22** (0.100 g, 1.10 mmol) in a mixture of formamide (3.00 mL) and 1,4-dioxane (3 mL) was added DIPEA (0.450 mL, 2.60 mmol) and **9a** (0.484 g, 1.50 mmol). After 17 h of stirring at rt, the reaction mixture was acidified with a 10% aq. HCl solution (5 mL), extracted with AcOEt (4 x 10 mL) and the combined organic phases were washed with brine (10 mL), dried over Na_2SO_4, filtrated and evaporated under reduced pressure at 40 °C. The crude was purified by flash

chromatography (DCM : MeOH : formic acid, 16 : 1 : 0.1) yielding **20c**[95] as a white solid (0.246 g, 0.75 mmol, 68%).

^{1}H-NMR (300 MHz, $CDCl_3$) δ: 11.48 (*s*, 1H, N*H*), 8.38 (*s*, 1H, N*H*Boc), 3.69 (*t*, *J* = 5.9 Hz, 2H, H-1), 3.44 (*m*, 2H, H-4), 1.70 – 1.59 (*m*, 4H, H-2, H-3), 1.55 – 1.44 (*m*, 18 H, *t*Bu)

^{13}C-NMR (75 MHz, $CDCl_3$) δ: 163.0 (C-5), 156.4 (*C*=O), 153.4 (C=O), 83.6 (O*C*$(CH_3)_3$), 80.0 (O*C*$(CH_3)_3$), 62.2 (C-1), 40.6 (C-4), 29.2 (C-2), 28.3 (3C, *C*H_3), 28.2 (3C, *C*H_3), 25.8 (C-3)

IR (film) ν/cm^{-1} 1291 (C-O), 1646 (CH_2), 1720 (C=O), 2980 (N-H), 3330 (O-H)

HRMS (ESI) *m/z*, calcd for $[C_{15}H_{30}N_3O_5]^+$: 332.2180, found: 332.2133

Data are consistent with those reported in literature

4. 7. Synthesis of 4-(2,3-*bis*(*tert*-butoxycarbonyl)guanidino)butyl 3-oxotetradecanoate (17b)

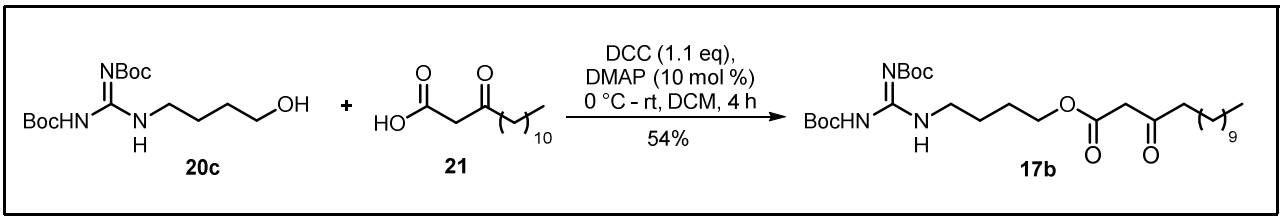

To a solution of **21** (0.214g, 0.880 mmol) in DCM was added **20c** (0.292g, 0.880 mmol) and DMAP (11.0 mg, 10 mol %). The temperature was cooled to 0 °C and DCC (0.206 g, 0.970 mmol) was added. The mixture was stirred 5 min at 0 °C and 4 h at rt. By-product urea was removed by filtration and the filtrate was concentrated under reduced pressure. The crude product was purified by flash chromatography (AcOEt : MeOH, 9 : 1) yielding **17b** (0.281 g, 0.506 mmol, 54 %) as a colorless oil.

^{1}H-NMR (300 MHz, $CDCl_3$) δ: 11.49 (s, 1H, N*H*), 8.31 (m, 1H, N*H*), 4.15 (t, *J* = 5.9 Hz, H-1), 3.42 – 3.48 (m, 4H, H-4, H-2'), 2.52 (t, *J* = 7.4 Hz, 2H, H-4'), 1.71 – 1.56 (m, 6H, H-2, H-3, H-5'), 1.49 (d, *J* =

[95] V. Rerat, G. Dive, A. A. Cordi, G. C. Tucker, R. Bareille, J. Amédée, L. Bordenave, J. Marchand-Brynaert, *J. Med. Chem.* **2009**, *52*, 7029-7043.

2.4 Hz, 18 H, C(C*H*$_3$)$_3$), 1.30 – 1.20 (m, 16H), 0.87 (t, *J* = 6.5 Hz, 3H, H-14')

^{13}C-NMR (75 MHz, $CDCl_3$) δ: 203.0 (C-3'), 167.4 (C-1'), 163.7 (C-5), 156.3 (*C*=O(Boc)), 153.5 (*C*=O(Boc)), 83.3 (*C*(CH$_3$)$_3$), 79.4 (*C*(CH$_3$)$_3$), 65.0 (C-1), 49.3 (C-2'), 43.3 (C-4'), 40.5 (C-4), 32.1 (2C), 29.7 (2C), 29.6, 29.5, 29.2, [28.4 (3C), 28.4 (3C), C(*C*H$_3$)$_3$], 26.0, 25.8, 23.6, 22.8, 14.3 (C-14')

IR (film) ν/cm^{-1} 1132 (C-O), C=O (1640), C=O (1718), CH_2 (2925), N-H (3341)

HRMS (ESI) *m/z*, calcd for $[C_{29}H_{54}N_3O_7]^+$: 556.3956, found: 556.3959

4. 8. Preparation of 1-carbamimidoyl-3,4-dihydro-2H-pyrrol-1-ium (18)

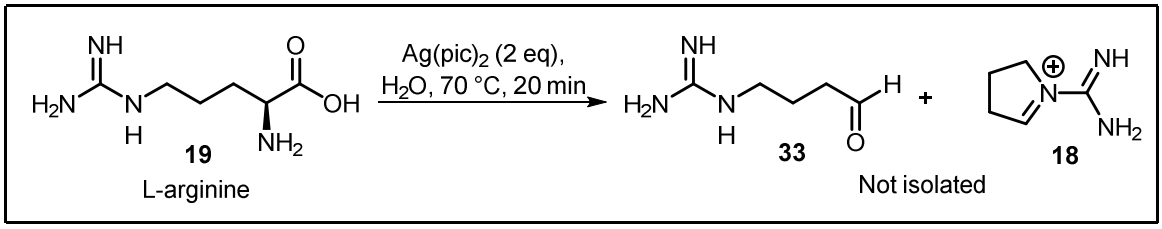

The complex silver(II) picolinate was prepared according to the protocol available in the literature.[83]

A suspension of **19** (179 mg, 1.02 mmol) and Ag(pic)$_2$ (709 mg, 2.00 mmol) in strictly degassed water (15 mL, ultrasound, 15 min, flushed with Ar) was brought to 70 °C in a flask protected from the light and under inert atmosphere. After 20 min the reaction color faded from red to pale yellow. After cooling to rt, the reaction mixture was acidified with aq. 2M HCl (5 mL), filtered and evaporated under reduced pressure. The resulting pink solid was employed without further purification.

18: HRMS (ESI) *m/z*, calcd for $[C_5H_{10}N_3]^+$: 112.0869, found: 112.0869

33: HRMS (ESI) *m/z*, calcd for $[C_5H_{12}N_3O]^+$: 130.0975, found: 130.0974

4. 9. Synthesis of crambescin A2 448 (5a) and *iso*-crambescin A2 (5k)

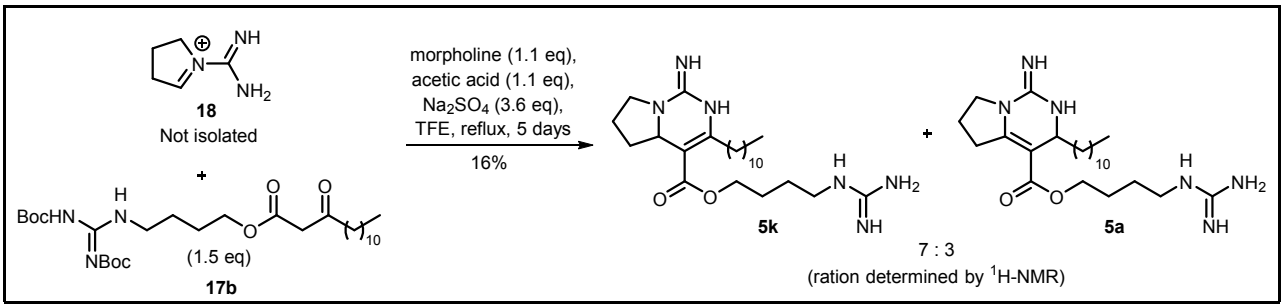

To a solution of **18** (72.3 mg, 0.080 mmol*) and **17b** (59.2 mg, 0.12 mmol) in TFE (15 mL) was added Na_2SO_4 (41.8 mg, 0.29 mmol), AcOH (6.0µL, 0.10 mmol), and morpholine (8.0µL, 0.10 mmol).The mixture was brought to reflux for 5 days. Sodium sulfate was removed by filtration and the filtrate was concentrated under reduced pressure. The crude product was purified by preparative HPLC [column: C18 Sunfire Waters 30 x 150 mm 5 µm; mobile phase: (H_2O + 0.2% TFA) : ACN; method: gradient of 30-80% of ACN in 20 min; flow: 42 $mL.min^{-1}$; volume of injection: 300 µL, concentration: 287 $mg.mL^{-1}$ in MeOH, detection at 280 nm]. The fraction with r_t= 9.25 min corresponded to a mixture 7 : 3 of **5k** and **5a** (5.7 mg, 0.013 mmol, 16%, white solid).

*Estimated number of mols considering 100% of L-arginine (**19**) conversion into **18**.

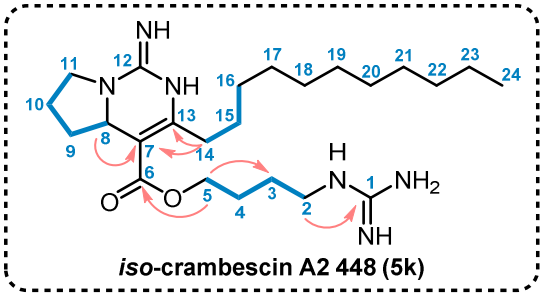

Table 15. ^{1}H- and ^{13}C-NMR of compound **5k** in MeOH-d_4

attribution	δ (ppm) ^{1}H	multiplicity	J (Hz)	integration	δ (ppm) ^{13}C
1	-	-	-	-	158.7
2	3.22	t	7.0	2	42.0
3a	1.63 – 1.69	m	-	2	27.0
3b	1.70 – 1.78	m	-	4	27.0
4	1.98 – 2.10	m	-	2	23.0
5	4.21	t	6.4	2	65.1
6	-	-	-	-	166.2
7	-	-	-	-	104.2

attribution	δ (ppm) ^{1}H	multiplicity	J (Hz)	integration	δ (ppm) ^{13}C
8	4.47	dd	5.0/ 11.0	1	59.0
9a	2.62 – 2.68	m	-	1	34.6
9b	1.70 – 1.78	m	-	4	34.6
10a	1.63 – 1.69	m	-	2	26.7
10b	1.70 – 1.78	m	-	4	26.7
11a	3.68 – 3.60	m	-	1	47.7
11b	3.59 – 3.53	m	-	1	47.7
12	-	-	-	-	151.2
13	-	-	-	-	148.8
14a	2.72 – 2.79	m	-	1	31.7
14b	2.47 – 2.54	m	-	1	31.7
15	1.51 – 1.62	m	-	2	29.4
16-23	1.30	bs	-	17	30.6/ 33.1/ 30.7
24	0.90	t	6.8	3	14.4

IR (film) ν/cm^{-1} 1135 (C-N), 1204 (C-O), 1681 (C=O and C=N), 2855 (N-H), 2926 (N-H)

HRMS (ESI) *m/z*, calcd for $[C_{24}H_{45}N_6O_2]^+$: 449.3599, found: 449.3628

4. 10. Molecular complexity calculation

The molecular complexity index was calculated by Excel using the formula developed by Bertz-Hendrickson[61, 63]:

$$C = C_\eta + C_E$$

$C_\eta = 2\eta \log_2\eta - \Sigma_i (S_k)_i$ =>

C_η: coeficient related to skeletal complexity as a function of bond conectivities (η)

η: sum of all bonds connectivities

$\eta = {}^1/_2(4\text{-}h)(3\text{-}h)$

h: number of hydrogens bonded to the atom

S_k: symmetry term according to symmetry type (k)

$k = (3 - h)(2 - h) + R$

R: number of repetitions of bonds to identical attached atoms on studied atom A (either σ- or π-bonds). E.g.: R= 0 if all bonds from A are to different atoms; R= 1 if all bonds goes to the same or to two identical attached atoms; etc

Values of S_k are available on reference 63 to help hand calculations.

$C_E = E \log_2 E - \Sigma_j E_j \log_2 E_j$ =>

C_E: coeficient related to the diversity of elements (kinds of atoms)

E: sum of non hydrogen atoms

E_j: term related to symmetry. If all atoms attached to a given atom A are of the same type, so C_E= 0.

NMR Spectra

(*S*,*E*)-4-amino-5-((2-((4-hydroxystyryl)amino)-2-oxoethyl)amino)-5-oxopentanoic acid (**5**) (^{1}H-NMR, 500 MHz, MeOH-d_4)

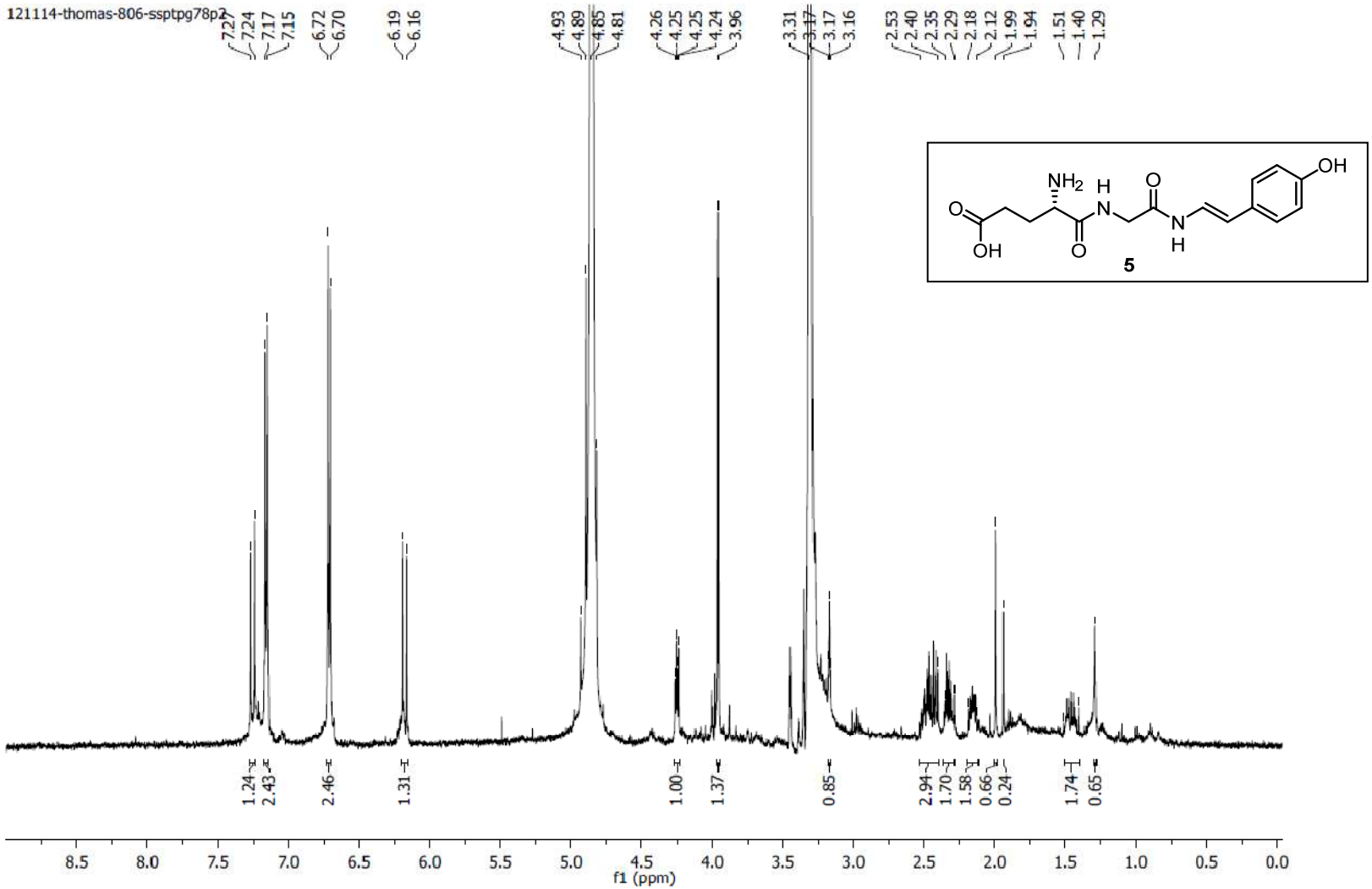

Anchinopeptolide A (**3a**) (^{1}H-NMR, 500 MHz, MeOH-d_4)

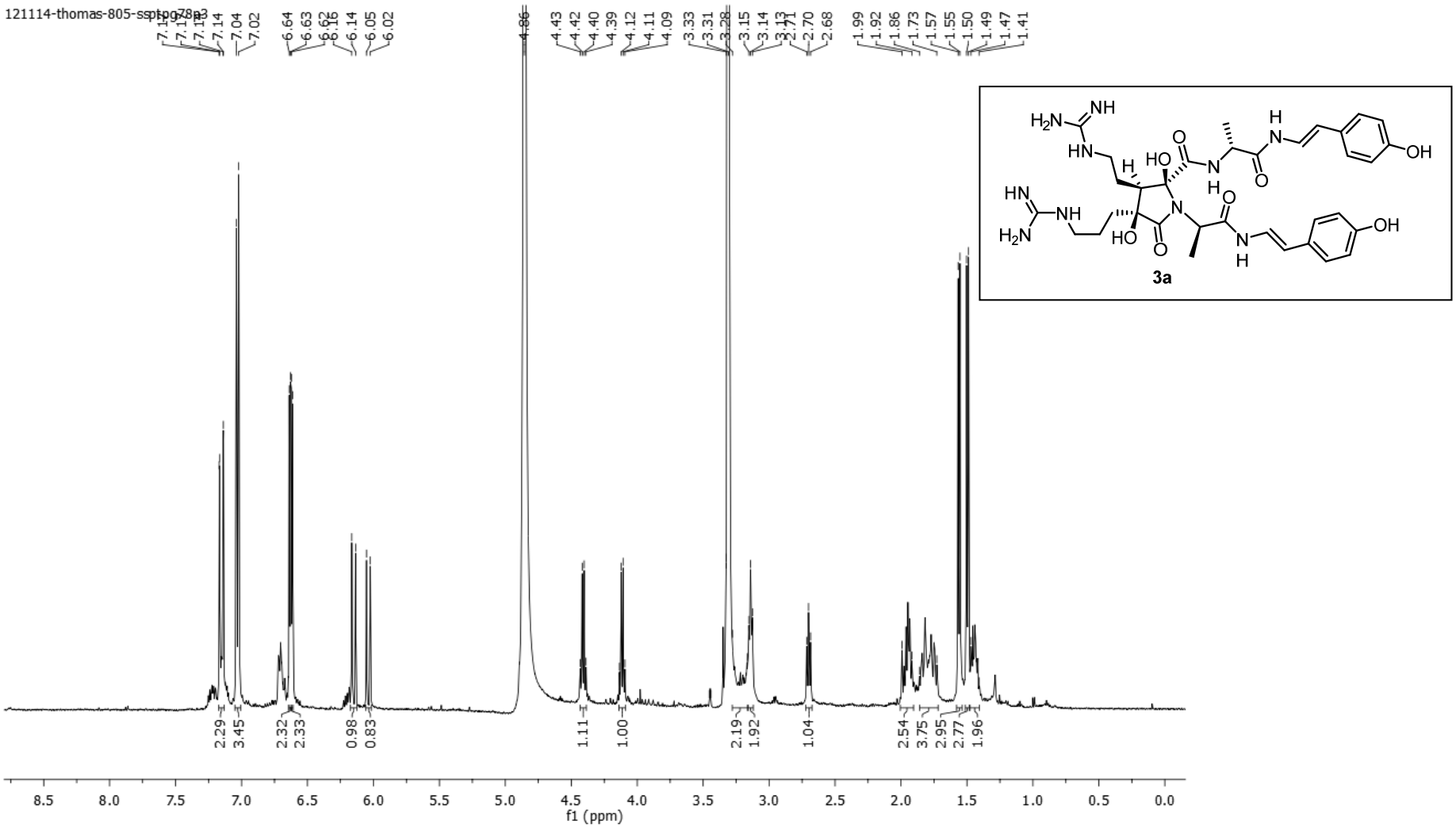

Anchinopeptolide A (**3a**) (^{13}C-NMR, 125 MHz, MeOH-d_4)

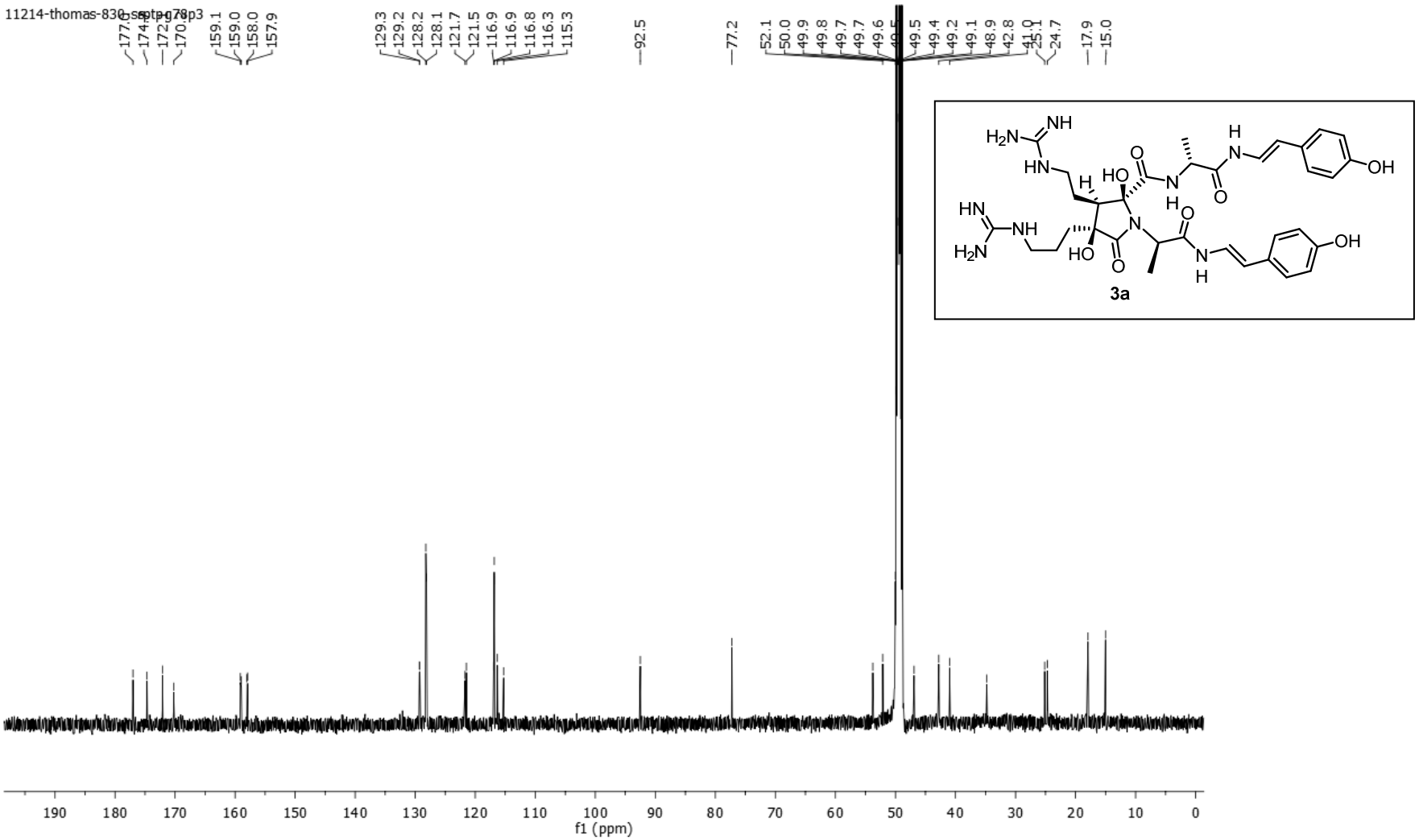

Anchinopeptolide B (**3b**) (^{1}H-NMR, 500 MHz, MeOH-d_4)

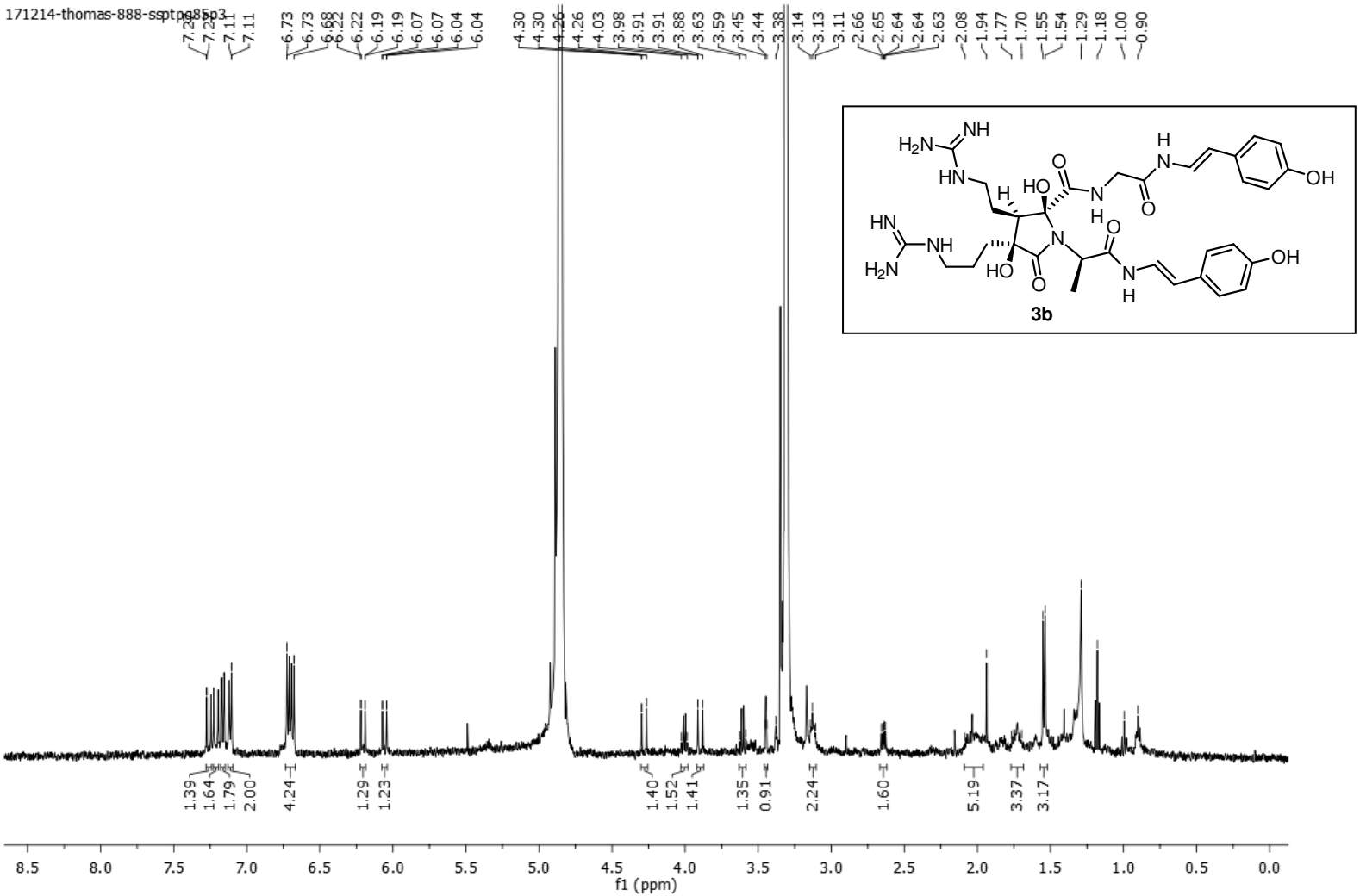

Anchinopeptolide C (**3c**) (^{1}H-NMR, 500 MHz, MeOH-d_4)

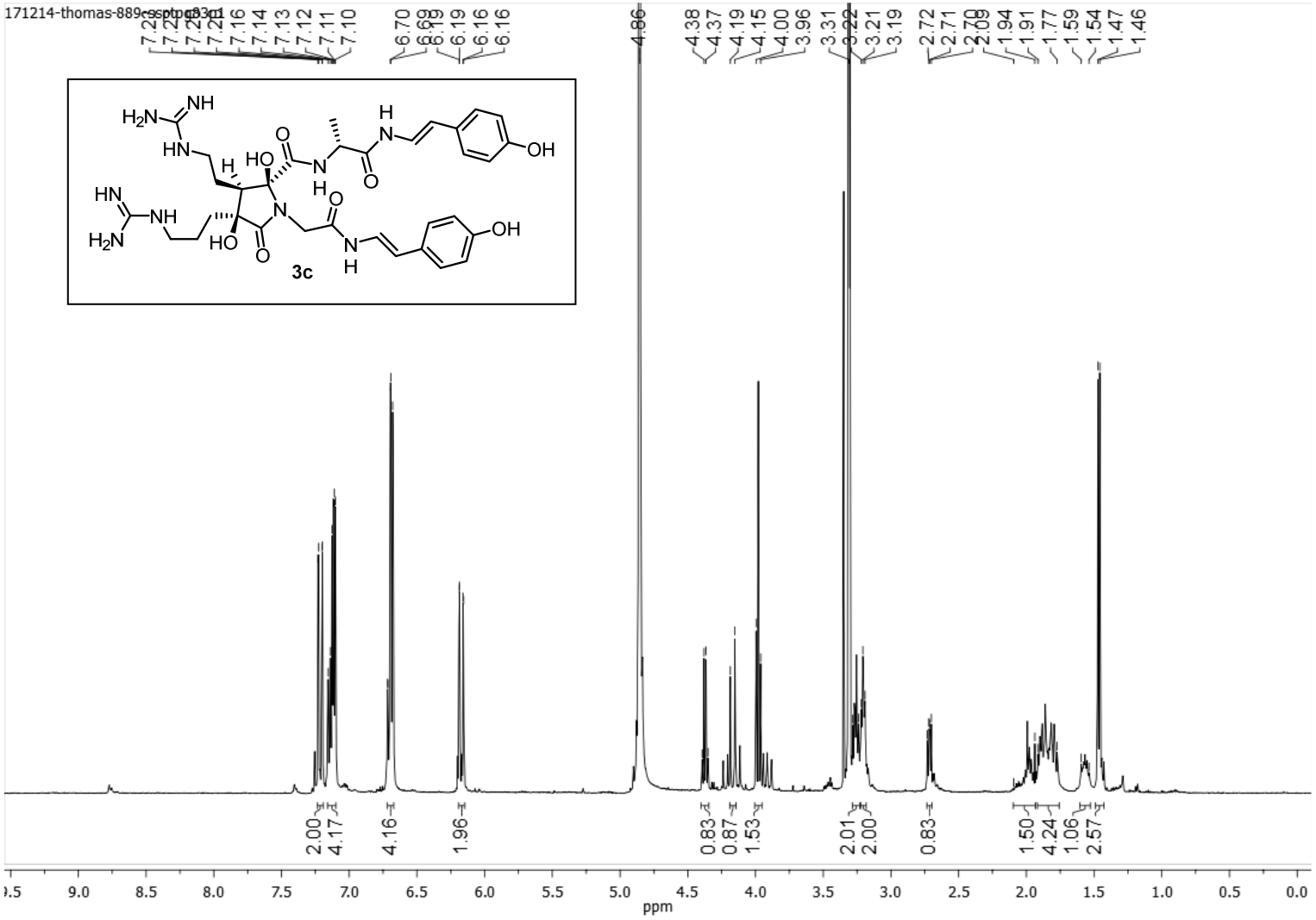

Anchinopeptolide C (**3c**) (^{13}C-NMR, 100 MHz, MeOH-d_4)

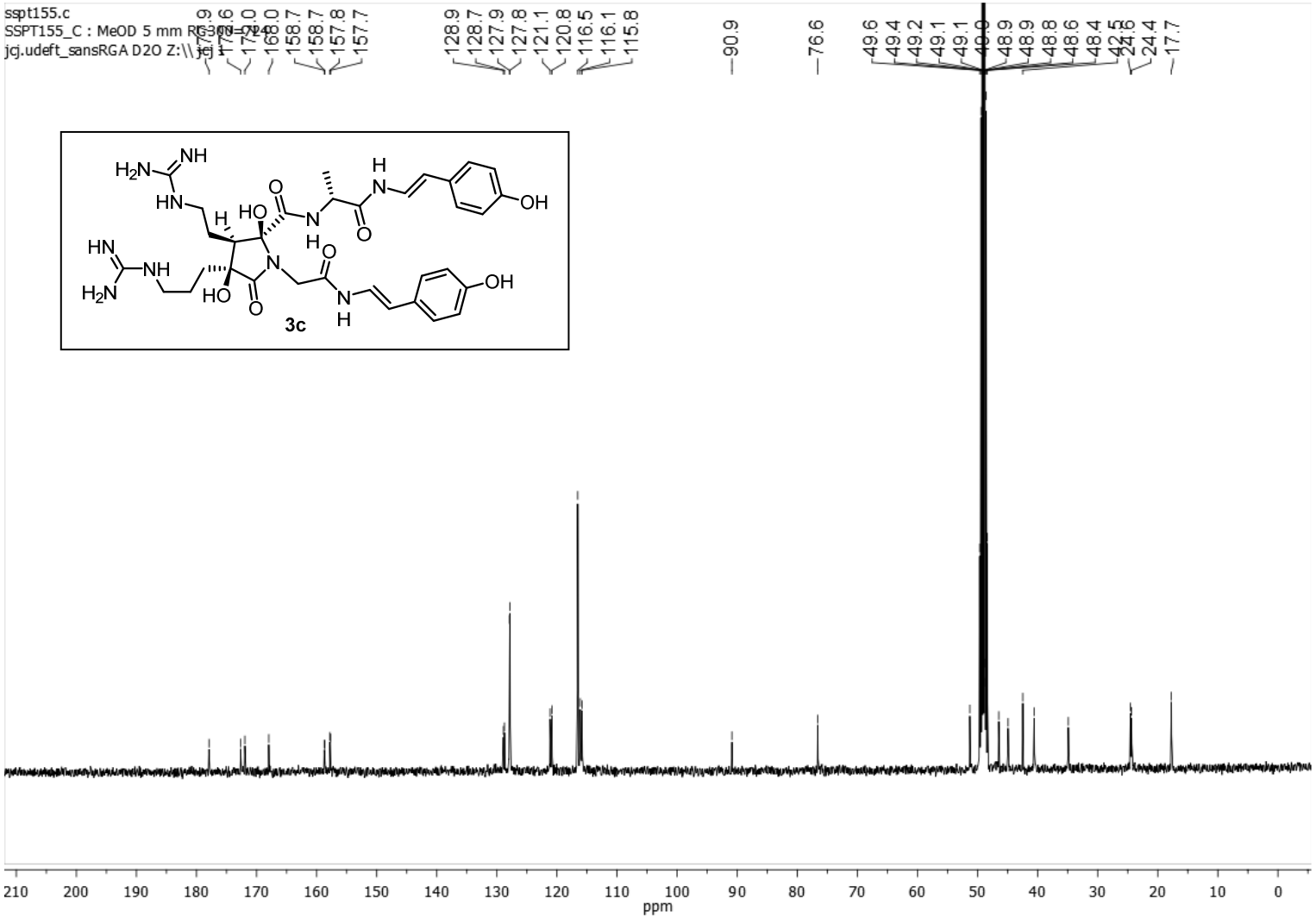

Anchinopeptolide D (**3d**) (^{1}H-NMR, 500 MHz, MeOH-d_4)

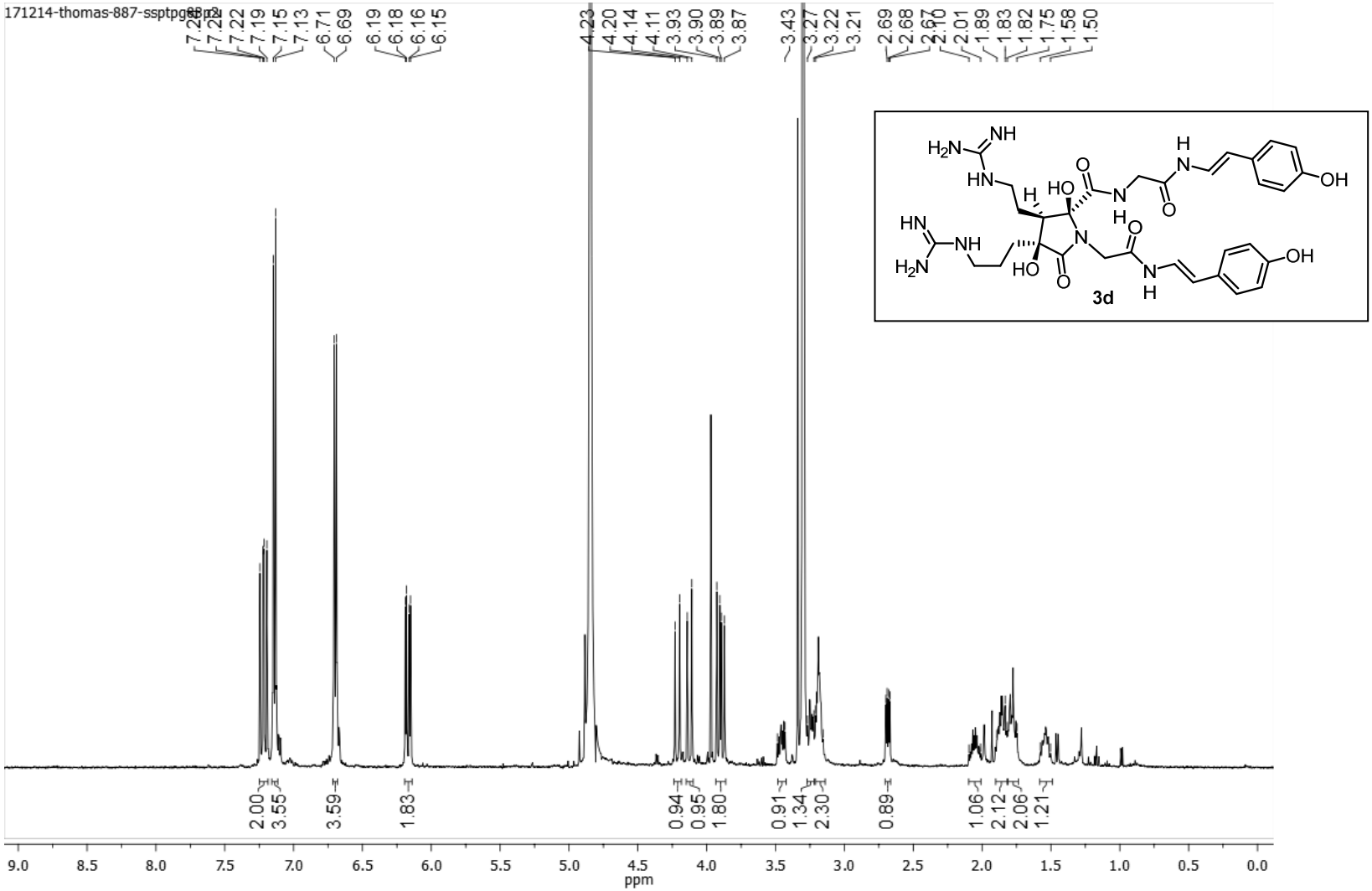

Anchinopeptolide D (**3d**) (^{13}C-NMR, 100 MHz, MeOH-d_4)

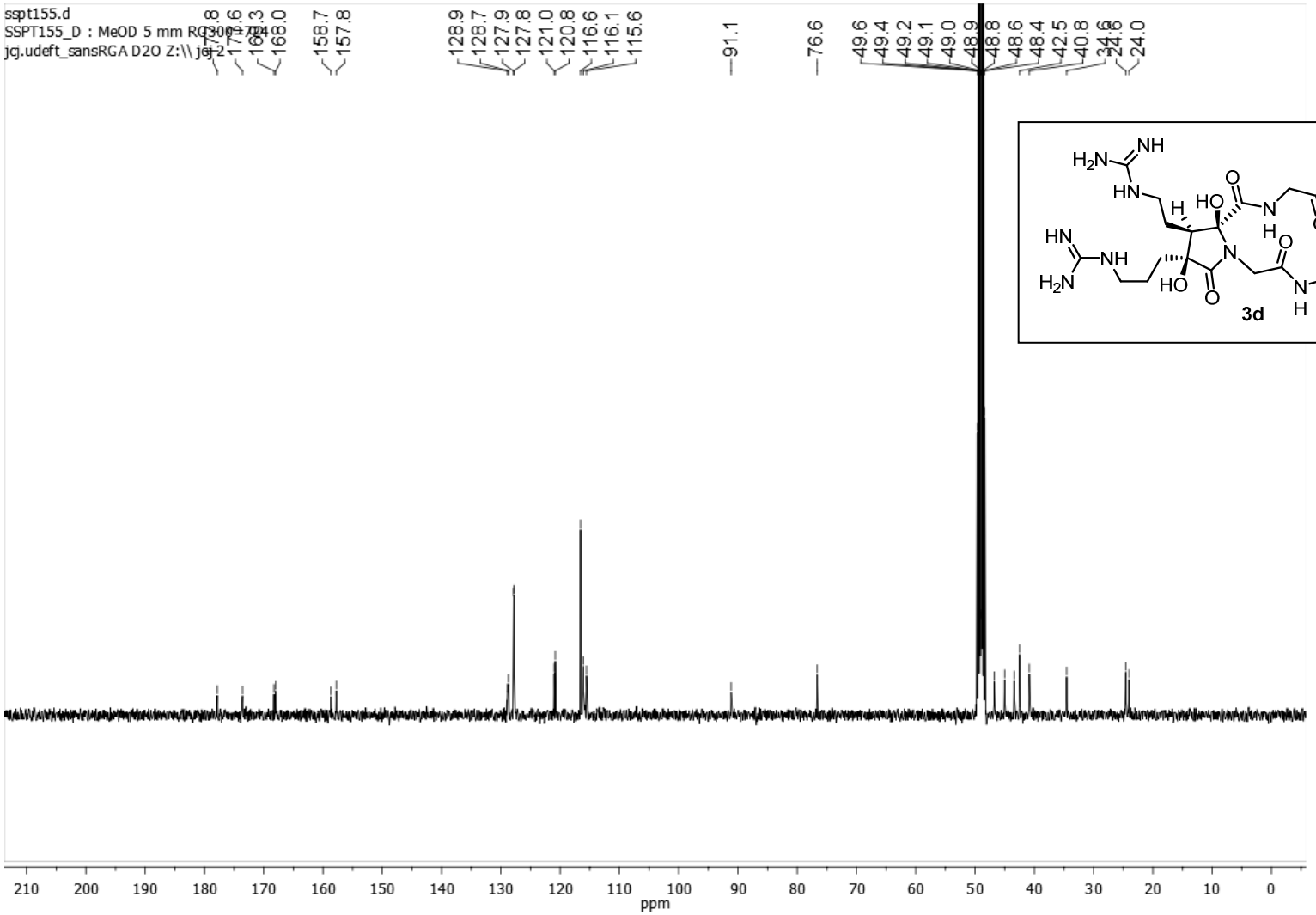

Epi-anchinopeptolide C (**3e**) (^{1}H-NMR, 500 MHz, MeOH-d_4)

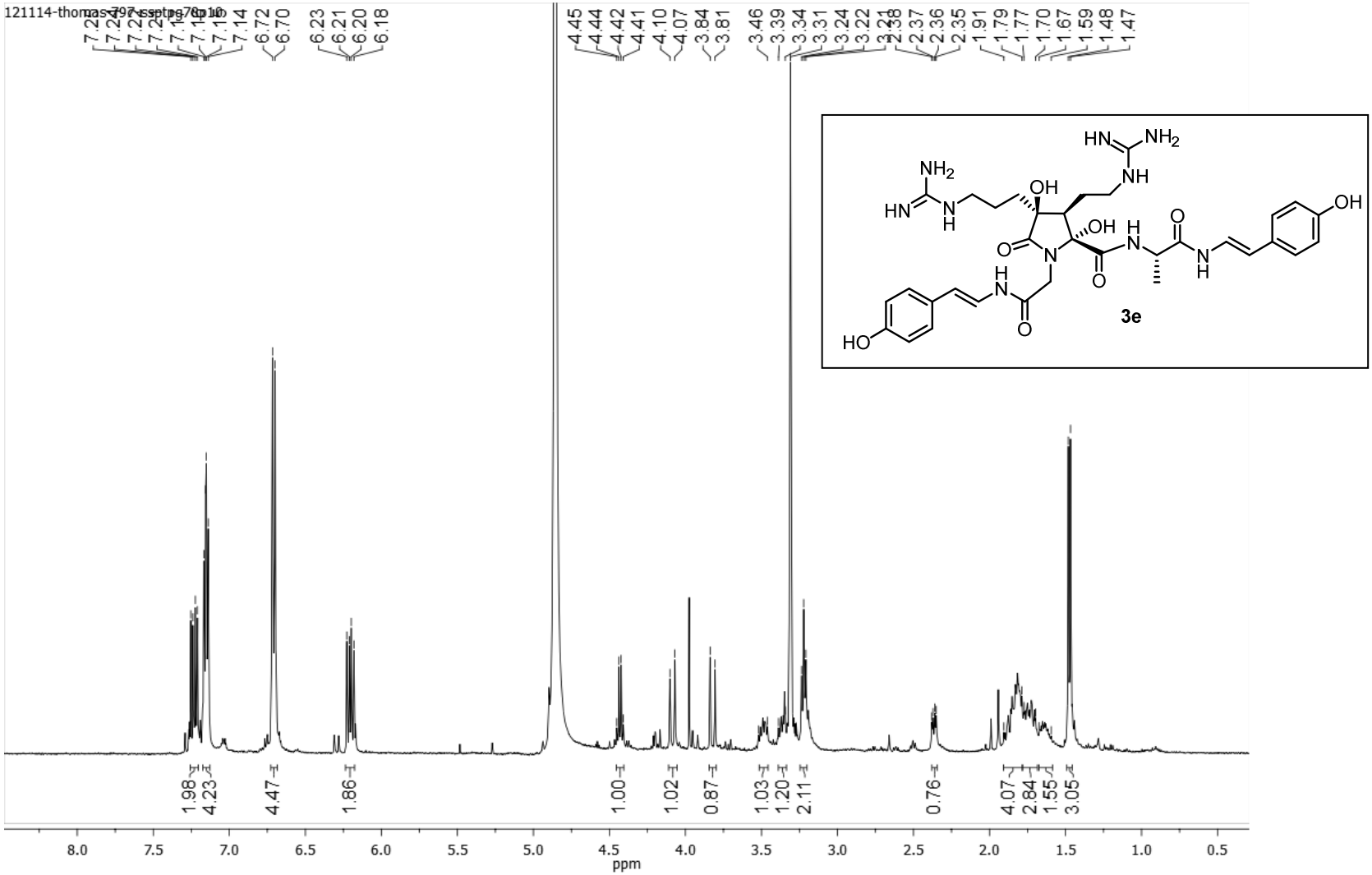

Epi-anchinopeptolide C (**3e**) (^{13}C-NMR, 125 MHz, MeOH-d_4)

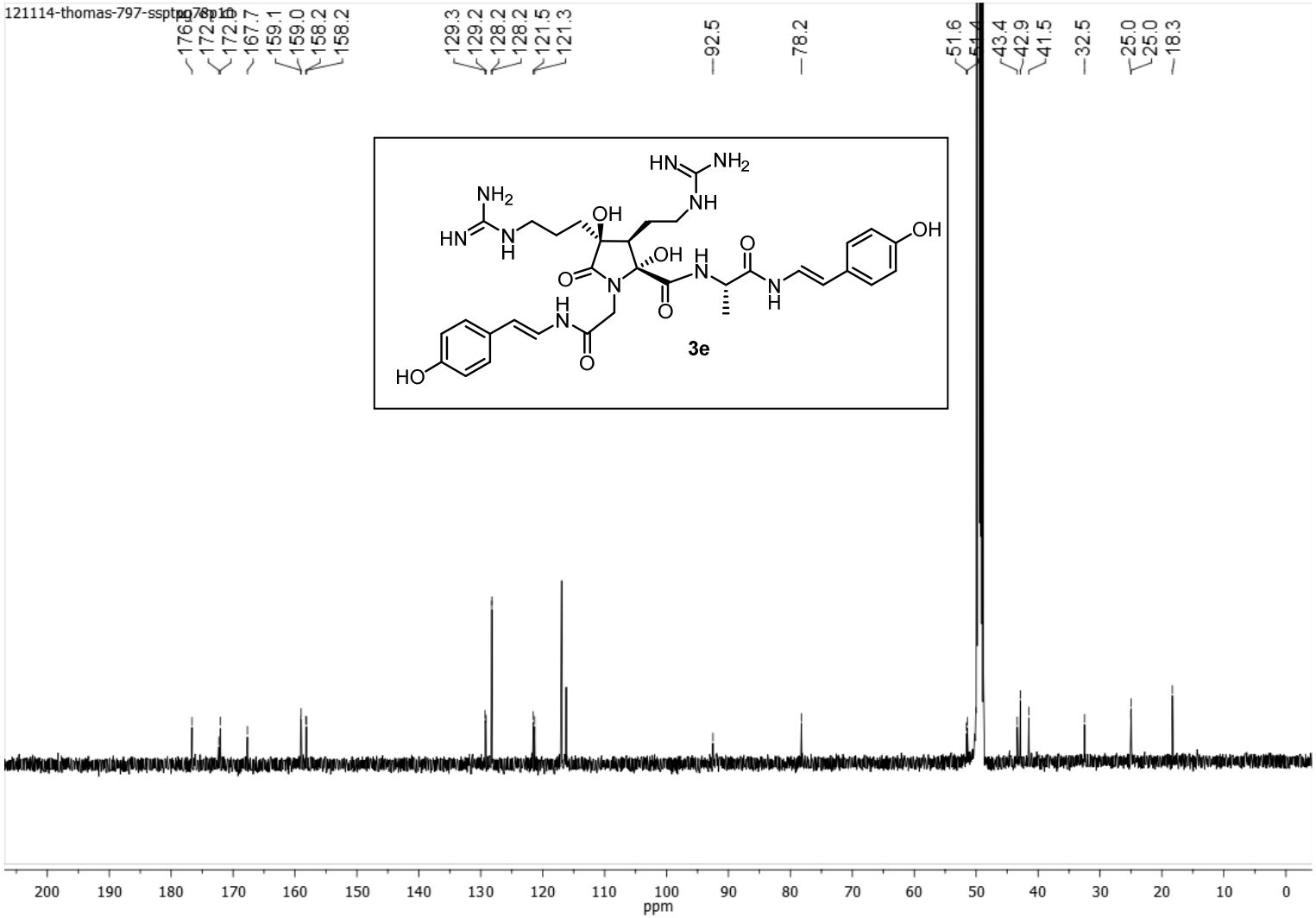

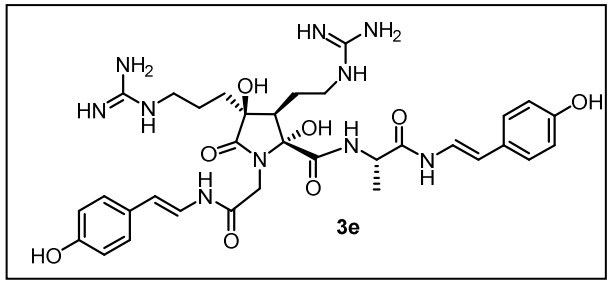

Epi-anchinopeptolide C (**3e**) (COSY-2D-^{1}H-NMR, 500 MHz, MeOH-d_4)

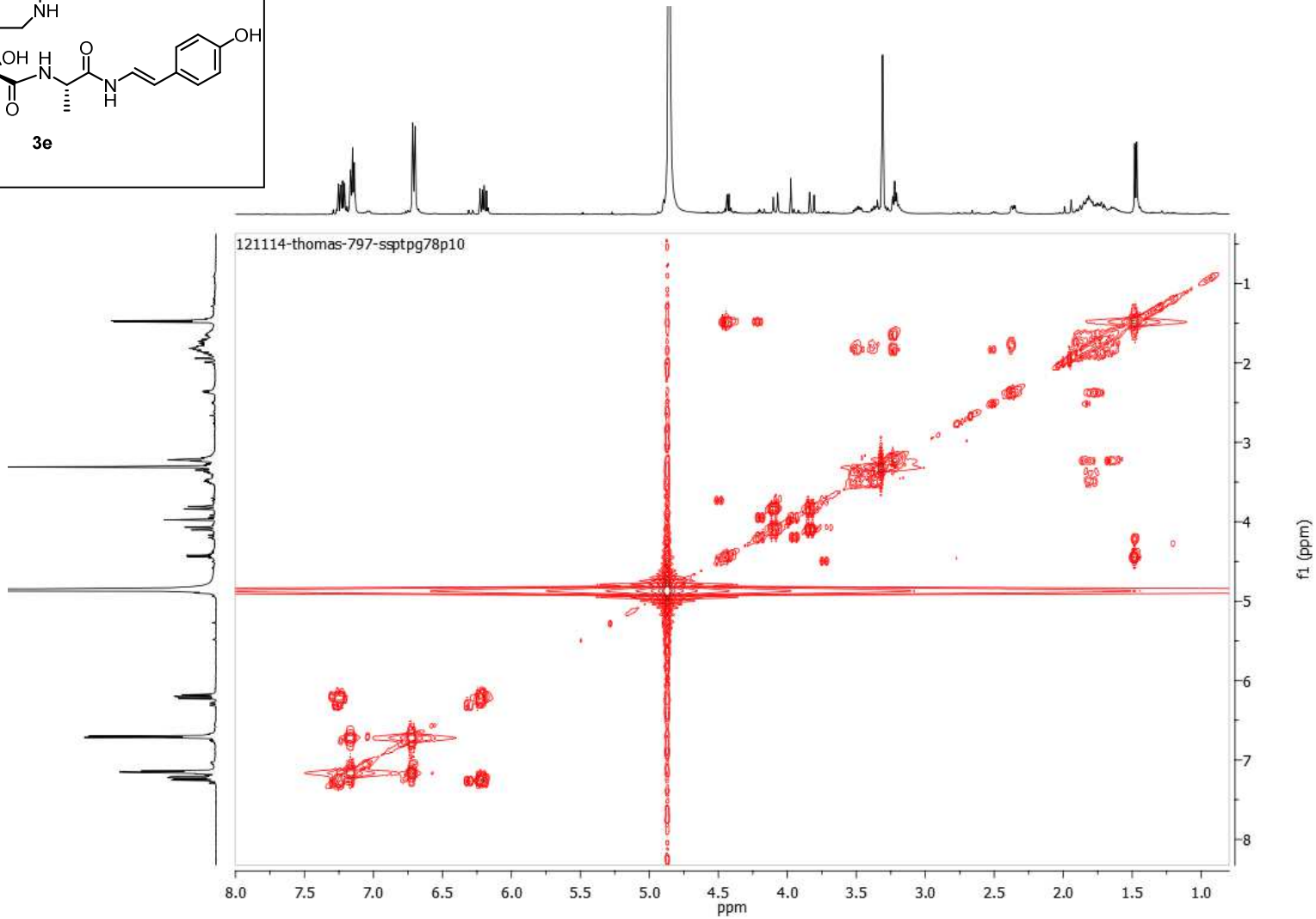

Epi-anchinopeptolide C (**3e**) (HSQC-2D-^{1}H and ^{13}C-NMR correlations, 500 MHz to ^{1}H nucleus, MeOH-d_4)

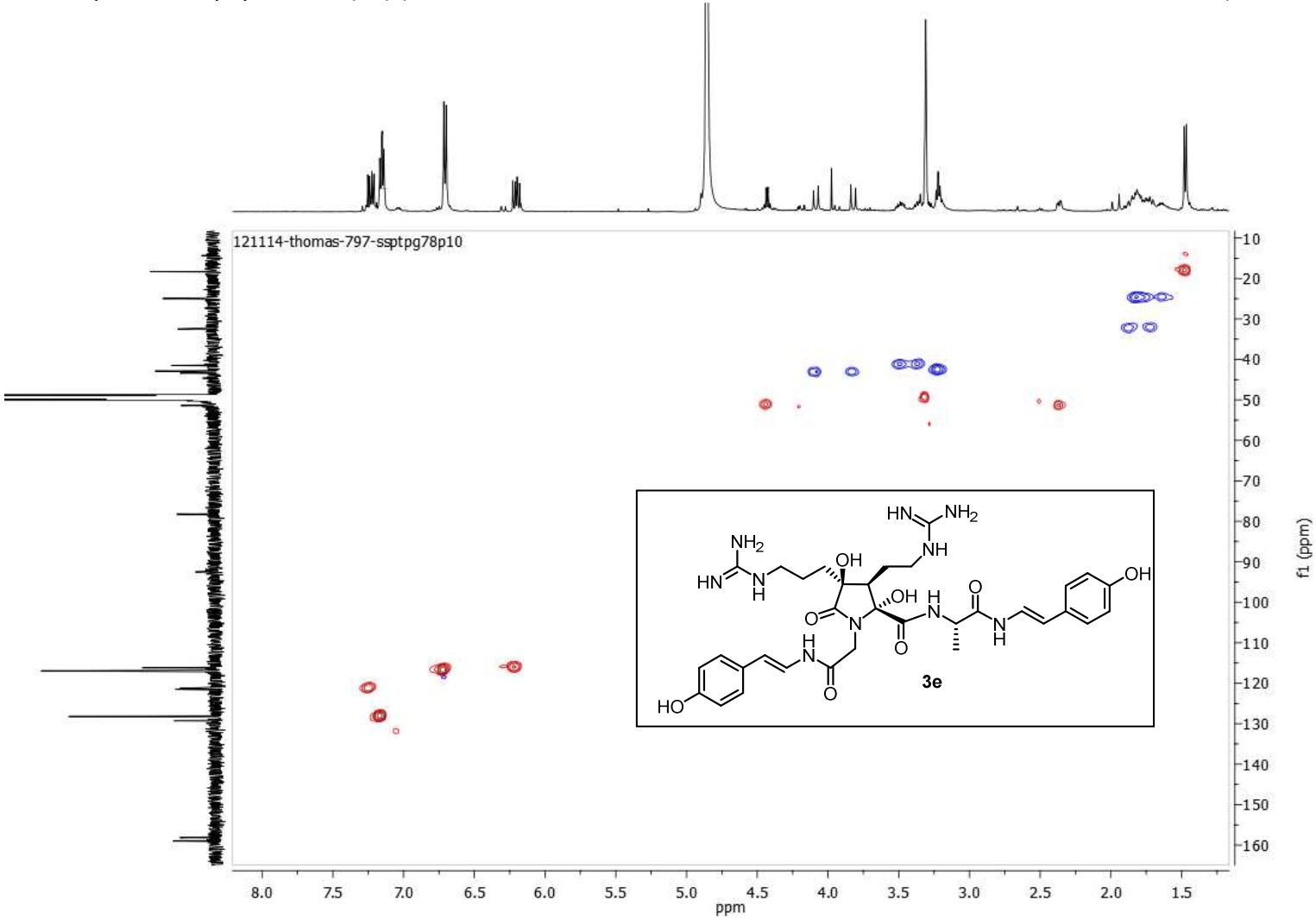

Epi-anchinopeptolide C (**3e**) (HMBC-2D-^{1}H and ^{13}C-NMR correlations, 500 MHz to ^{1}H nucleus, MeOH-d_4)

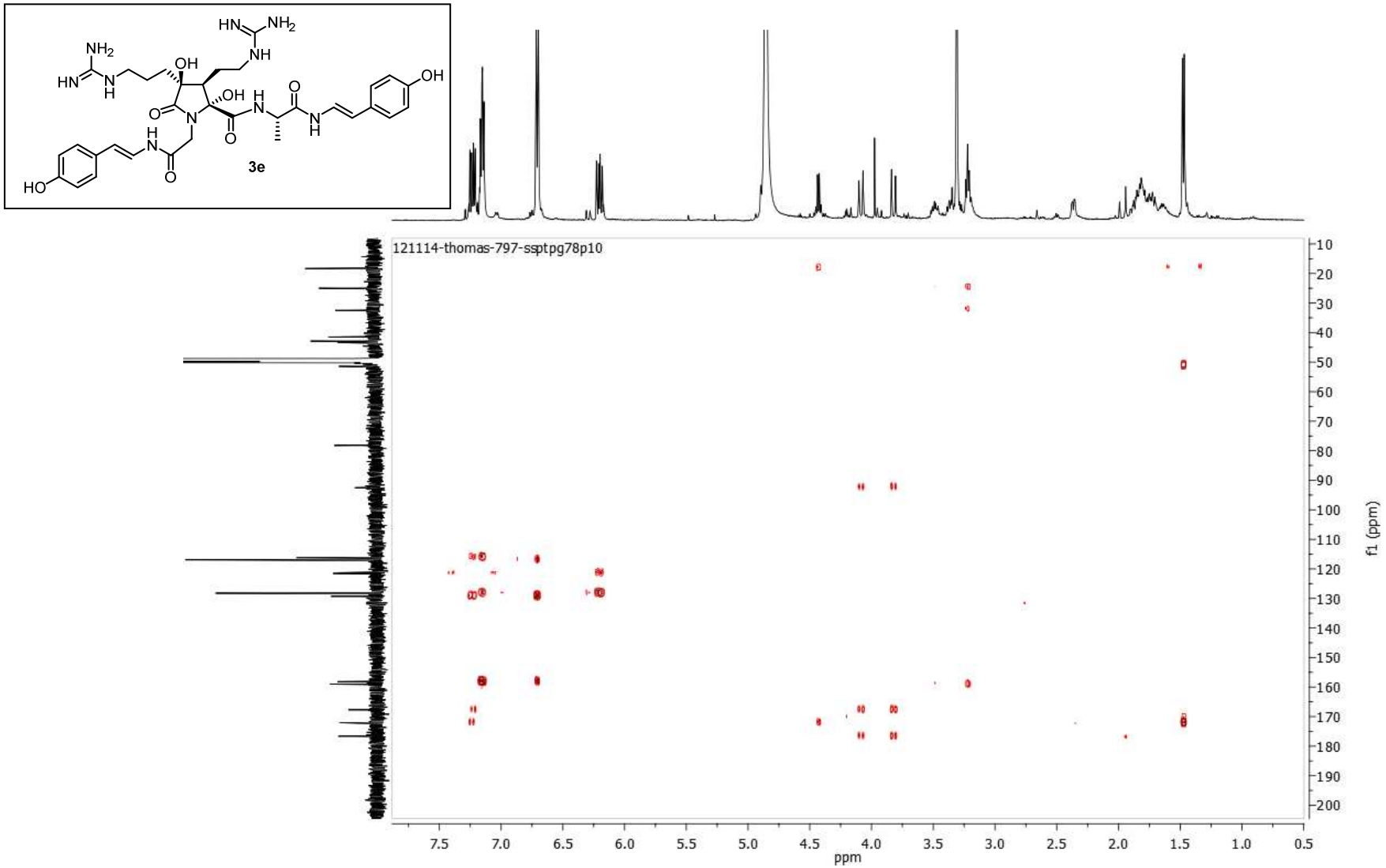

Epi-anchinopeptolide C (**3e**) (NOESY-2D-^{1}H NMR, 500 MHz, MeOH-d_4)

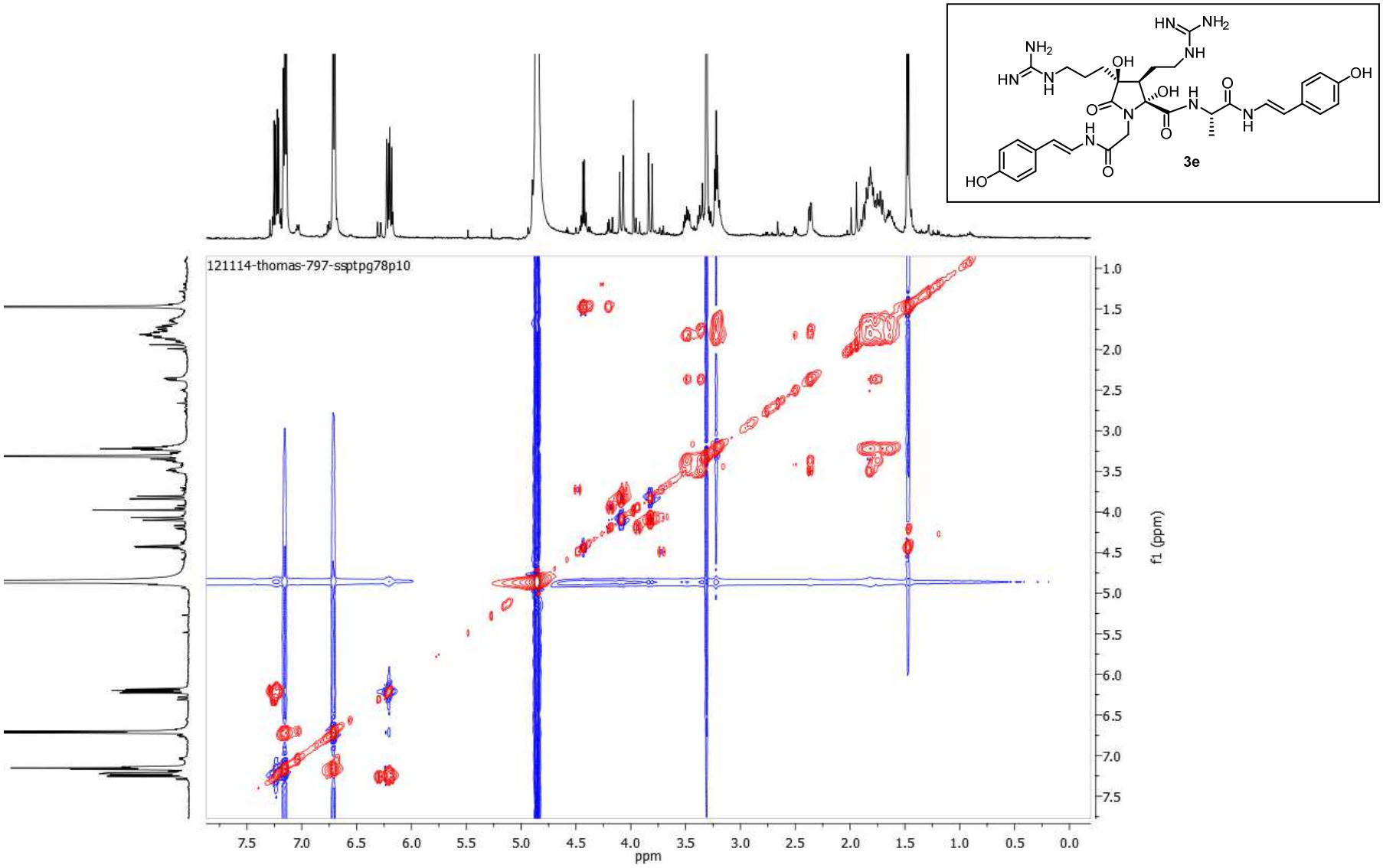

Epi-anchinopeptolide C (**3e**) (^{1}H-NMR, 500 MHz, DMSO-d_6)

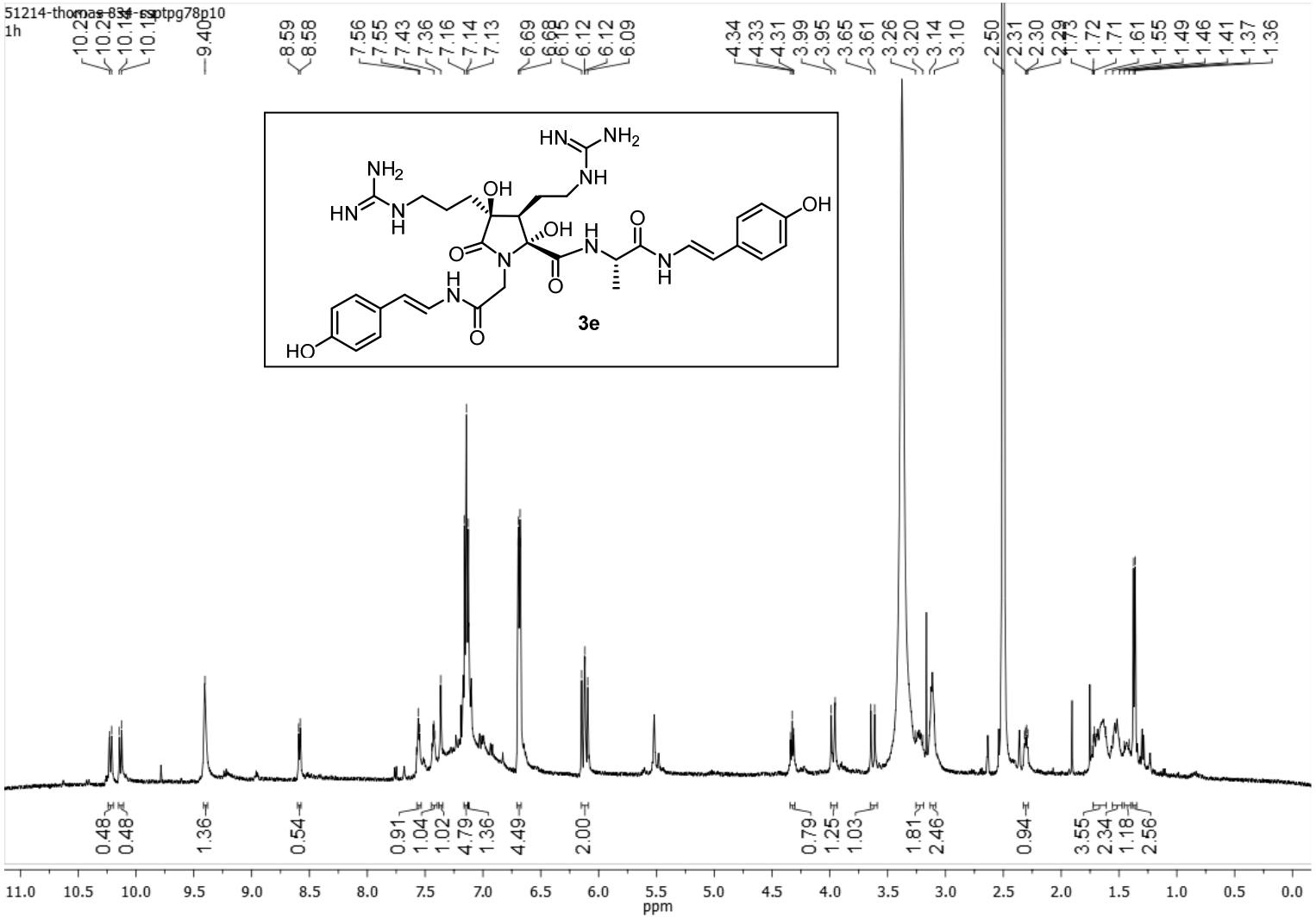

Epi-anchinopeptolide C (**3e**) (^{13}C-NMR, 125 MHz, DMSO-d_6)

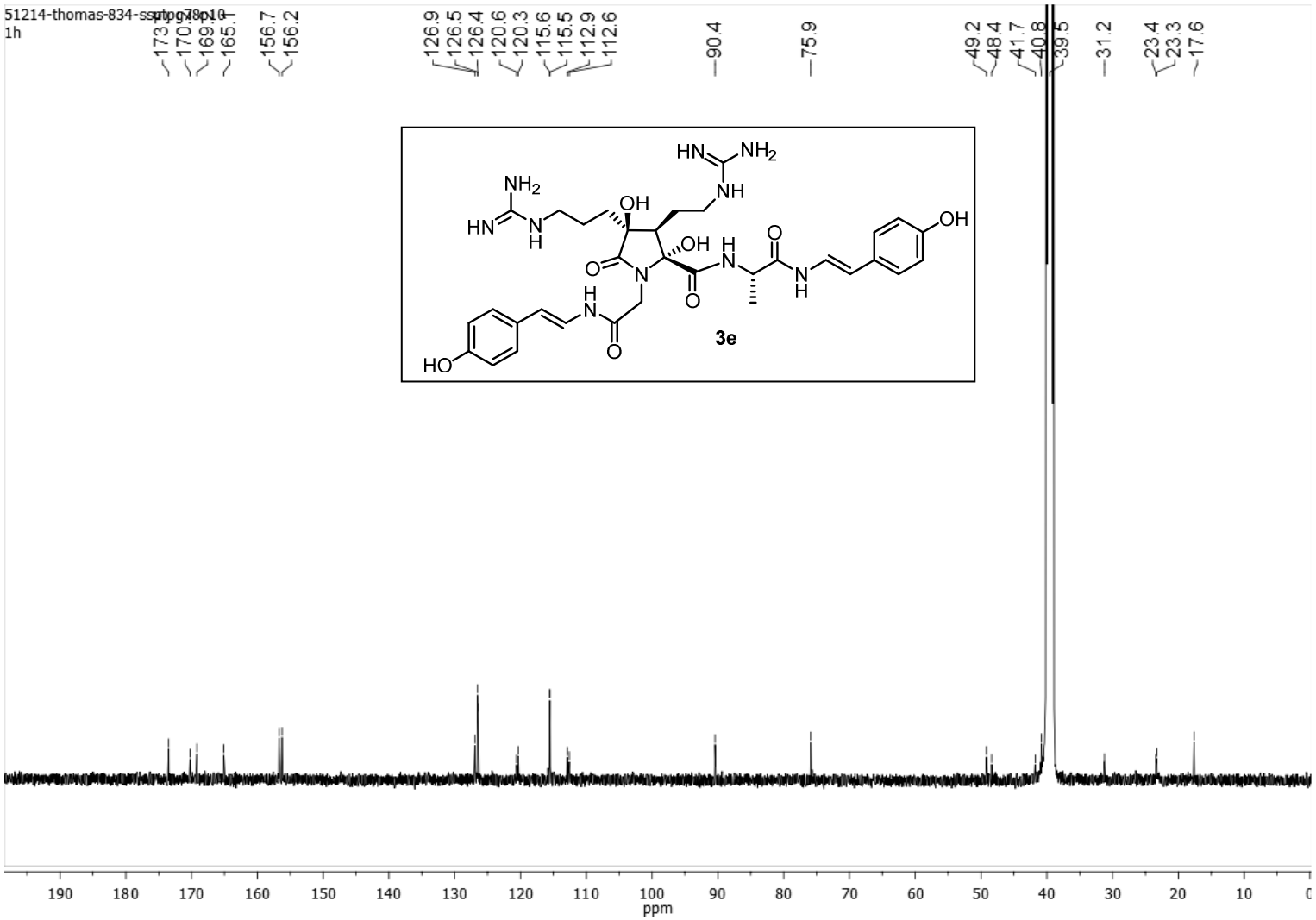

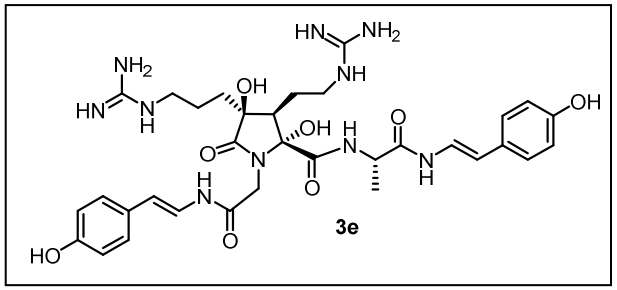

Epi-anchinopeptolide C (**3e**) (COSY-2D-^{1}H-NMR, 500MHz, DMSO-d_6)

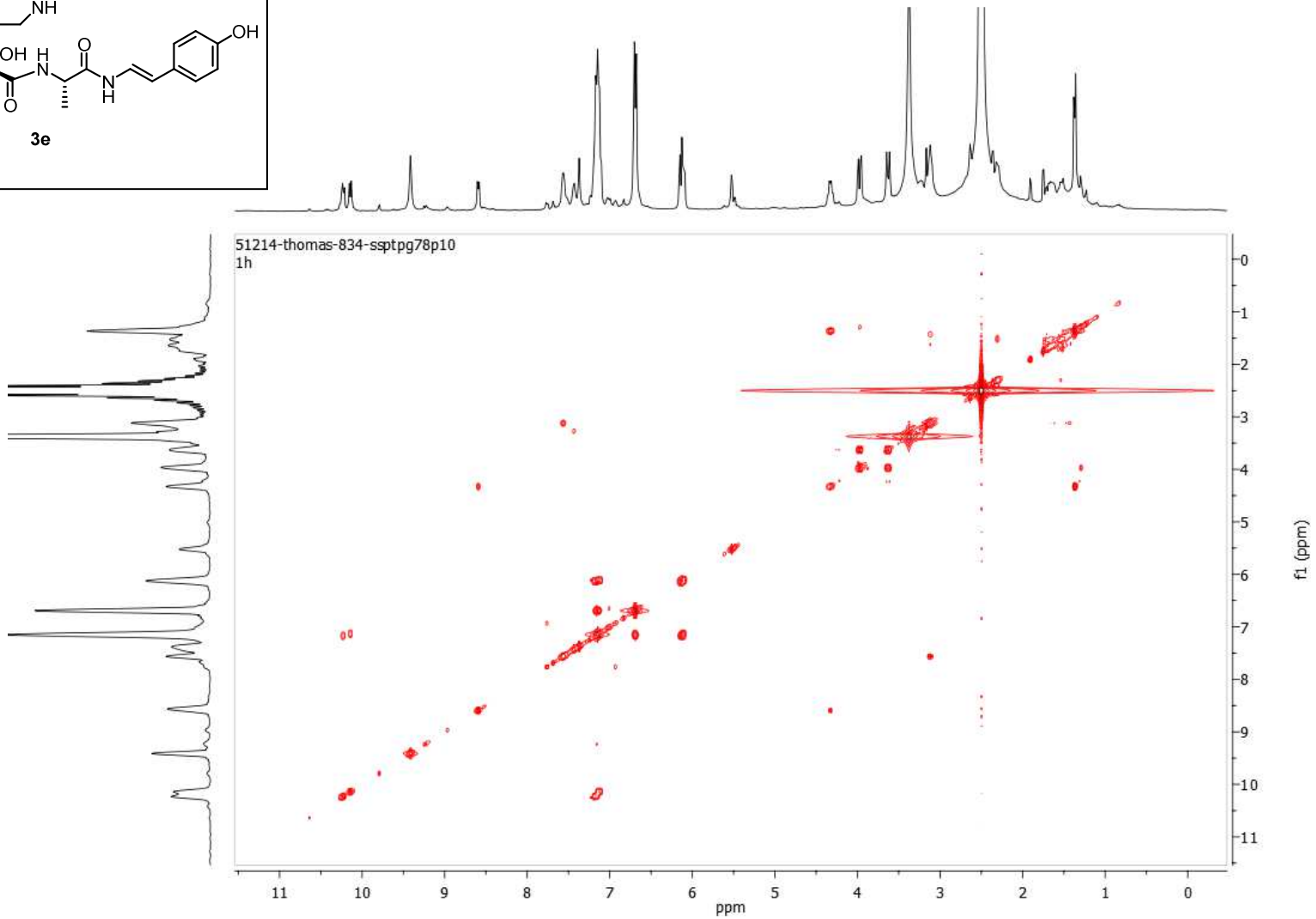

Epi-anchinopeptolide C (**3e**) (HSQC-2D-^{1}H and ^{13}C-NMR correlations, 500 MHz to ^{1}H nucleus, DMSO-d_6)

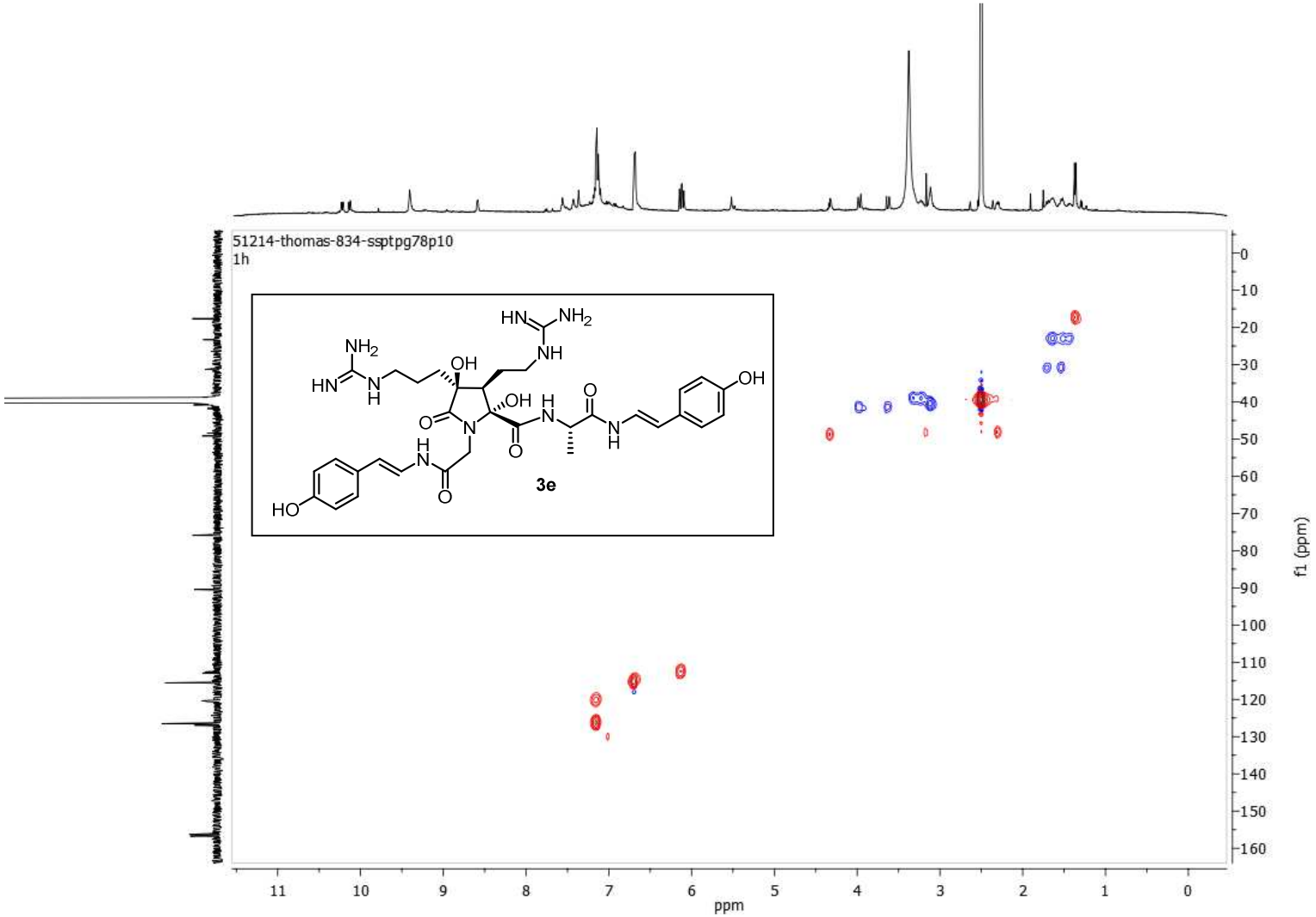

Epi-anchinopeptolide C (**3e**) (HMBC-2D-^{1}H and ^{13}C-NMR correlations, 500 MHz to ^{1}H nucleus, DMSO-d_6)

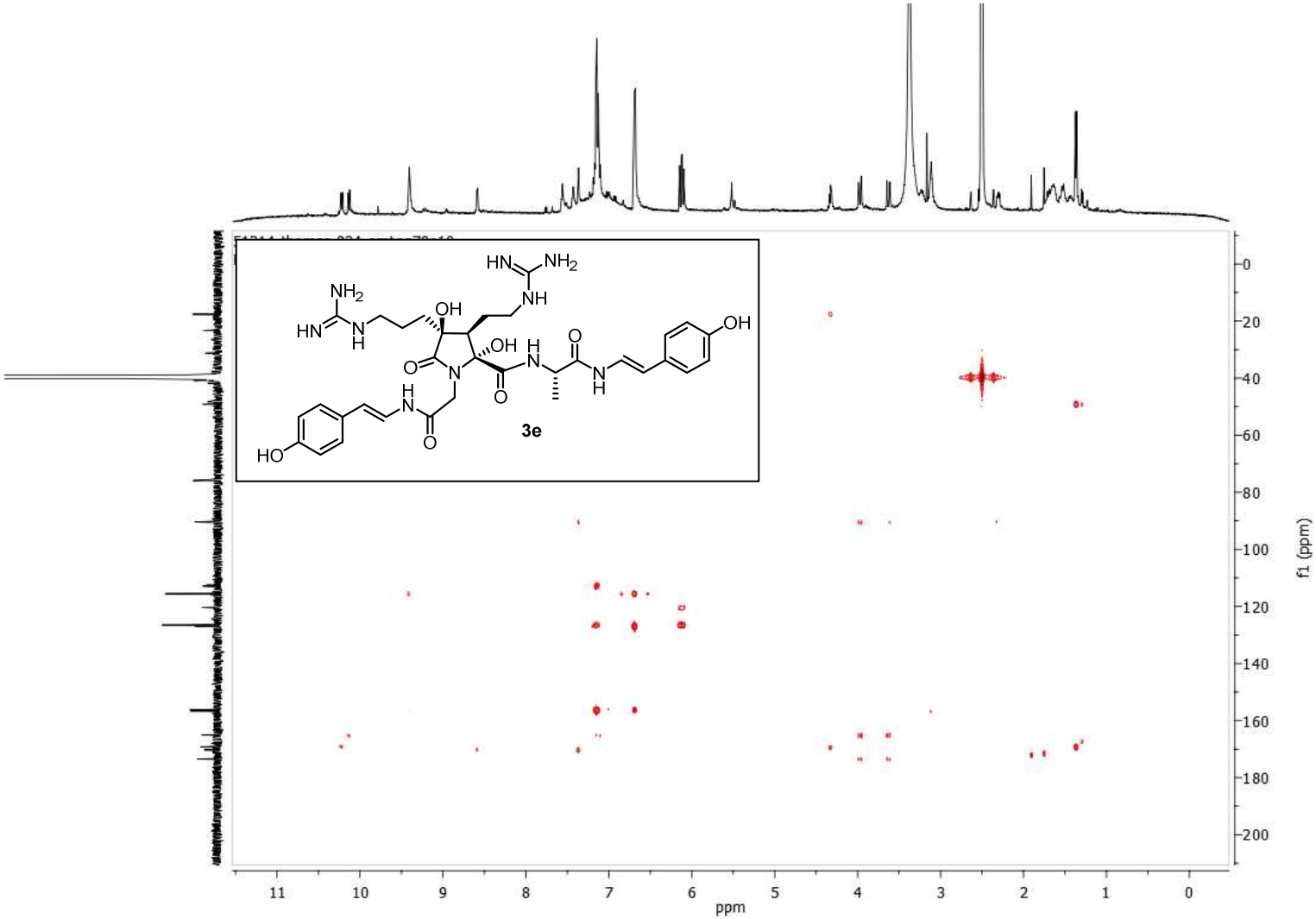

Epi-anchinopeptolide C (**3e**) (NOESY-2D-^{1}H NMR, 500 MHz, DMSO-d_6)

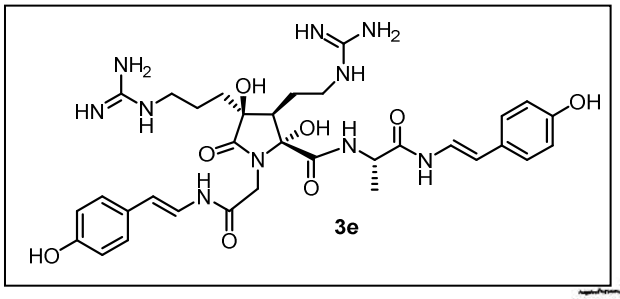

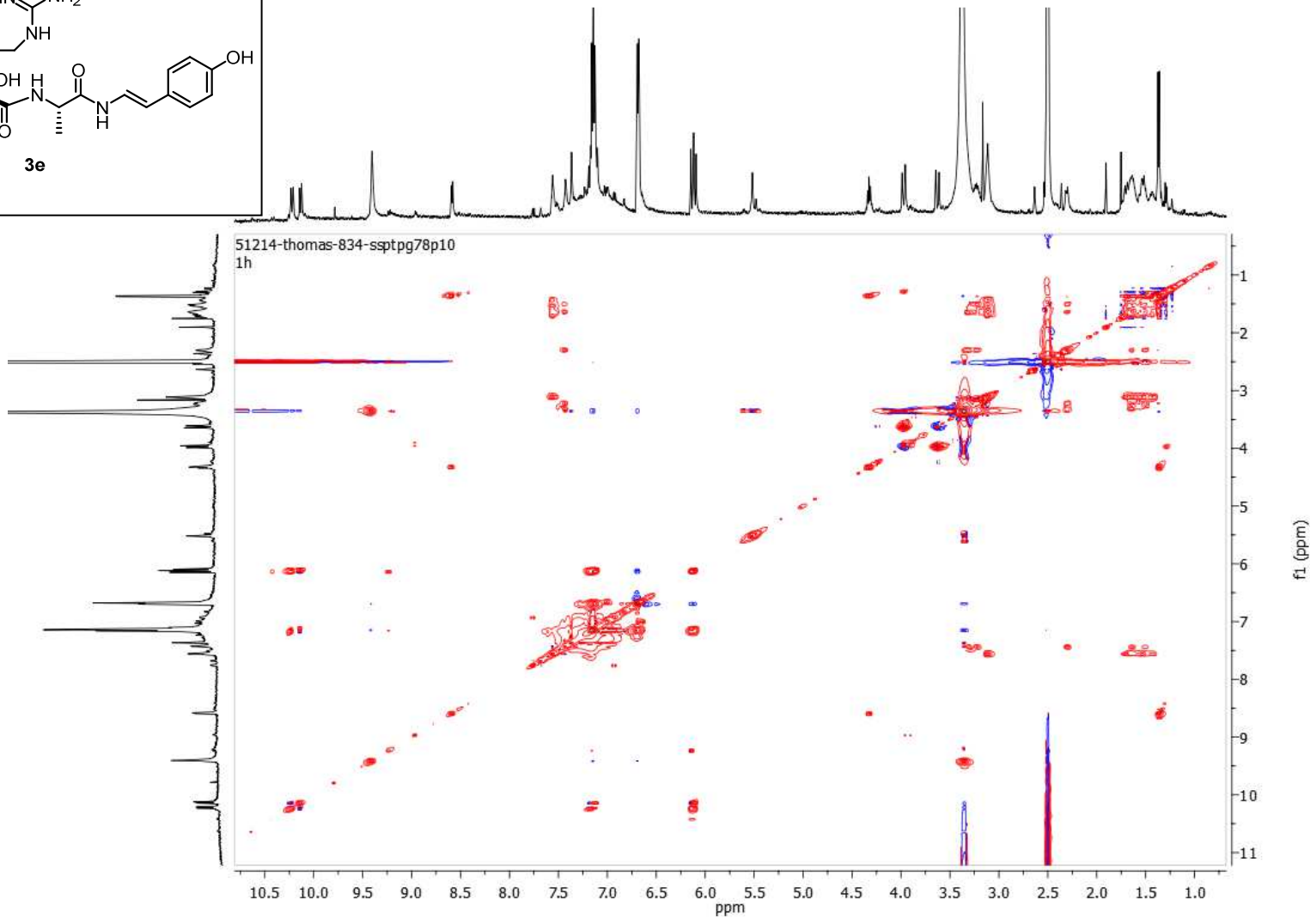

Cycloanchinopeptolide C (**4c**) (^{1}H-NMH, 400 MHz, MeOH-d_4)

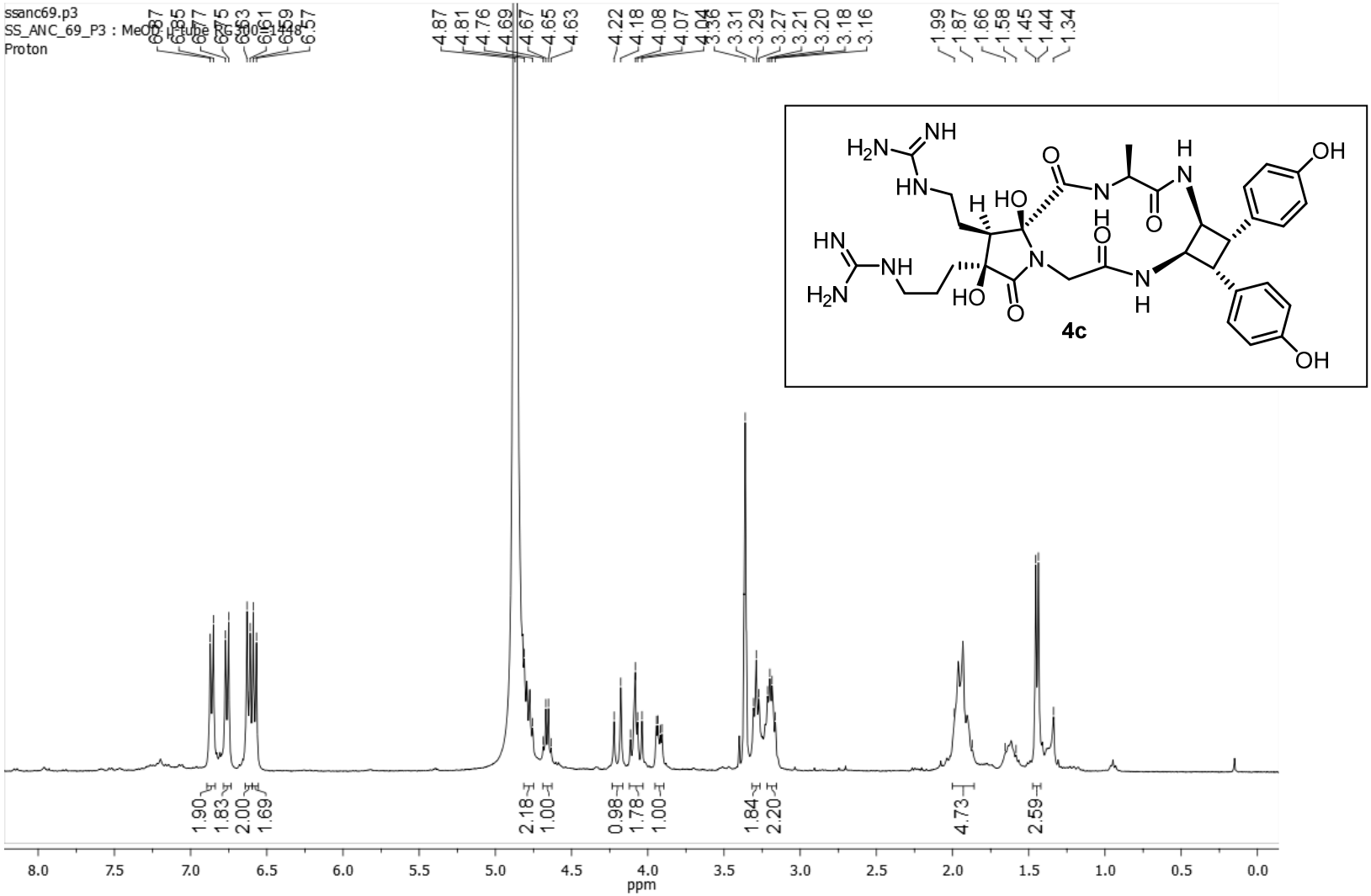

Cycloanchinopeptolide C (**4c**) (^{13}C-NMH, 100 MHz, MeOH-d_4)

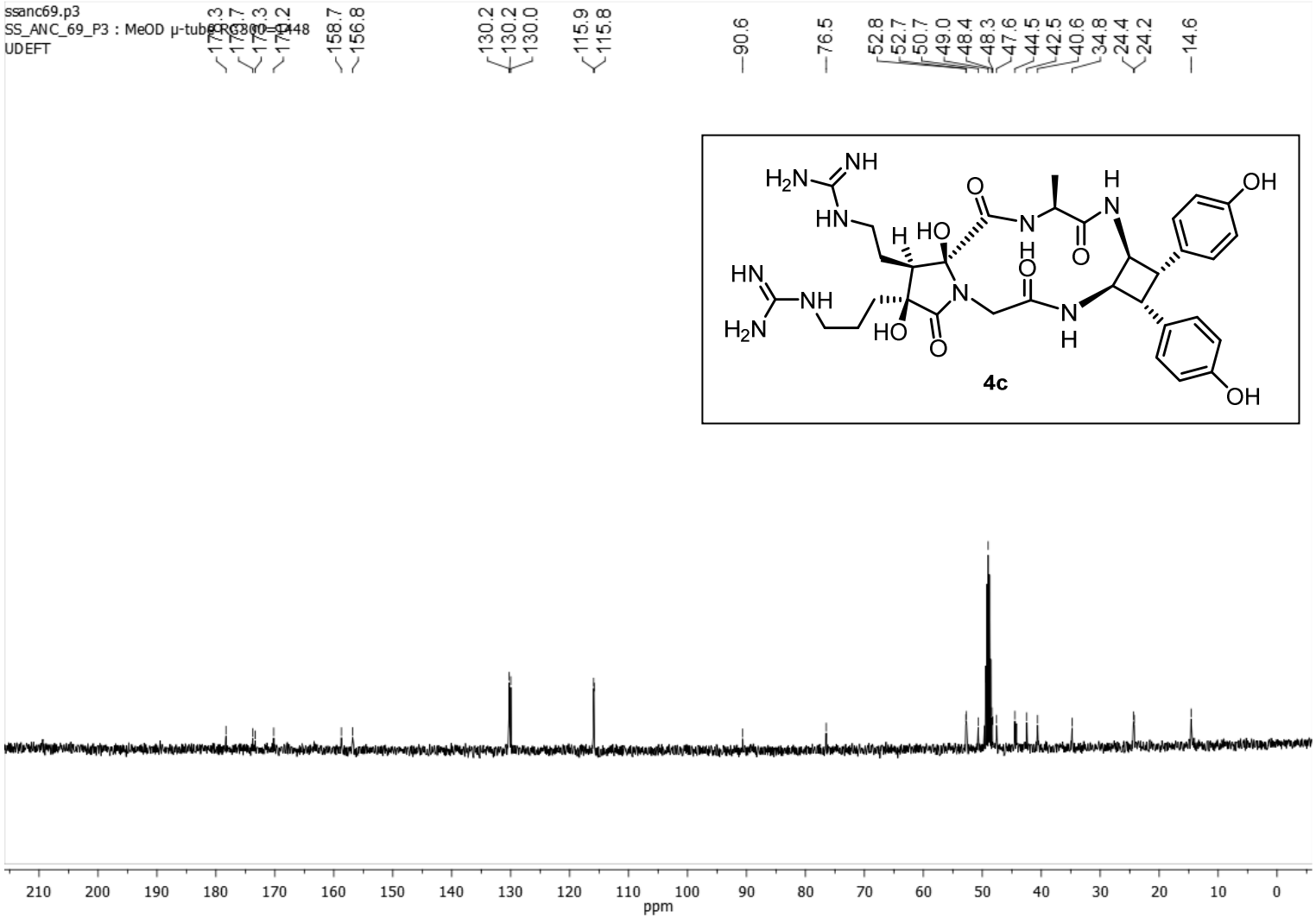

Cycloanchinopeptolide C (**4c**) (COSY-2D-^{1}H-NMR, 400MHz, MeOH-d_4)

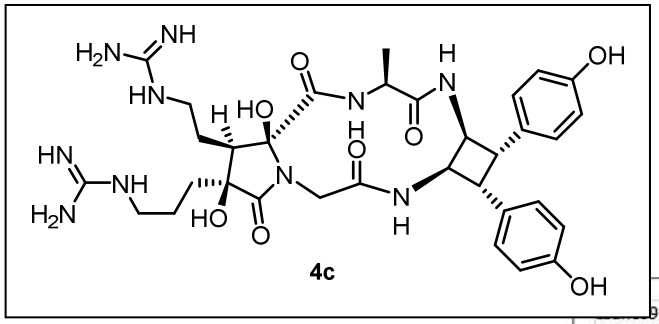

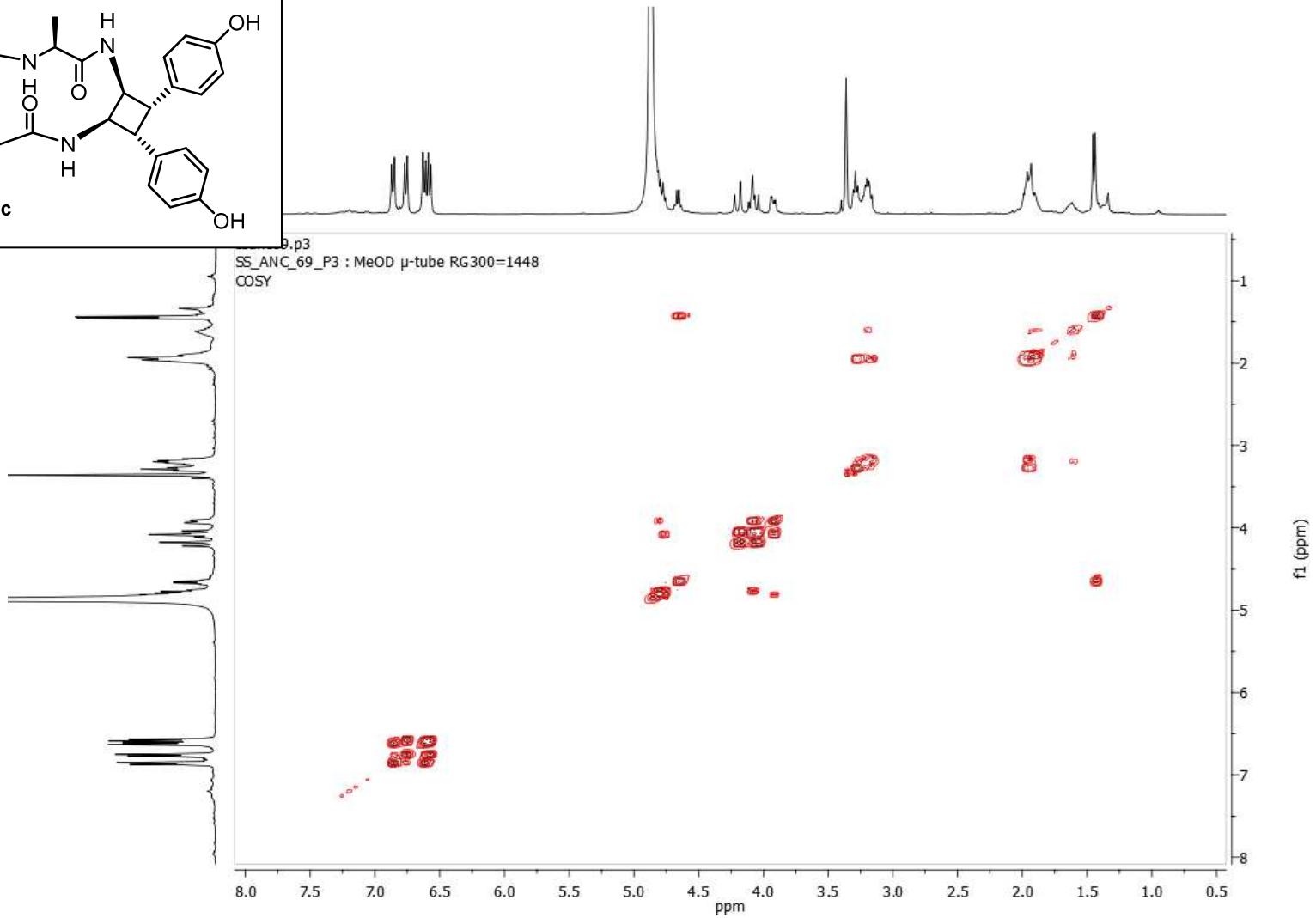

Cycloanchinopeptolide C (**4c**) (HSQC-2D-^{1}H and ^{13}C-NMR correlations, 400 MHz to ^{1}H nucleus, MeOH-d_4)

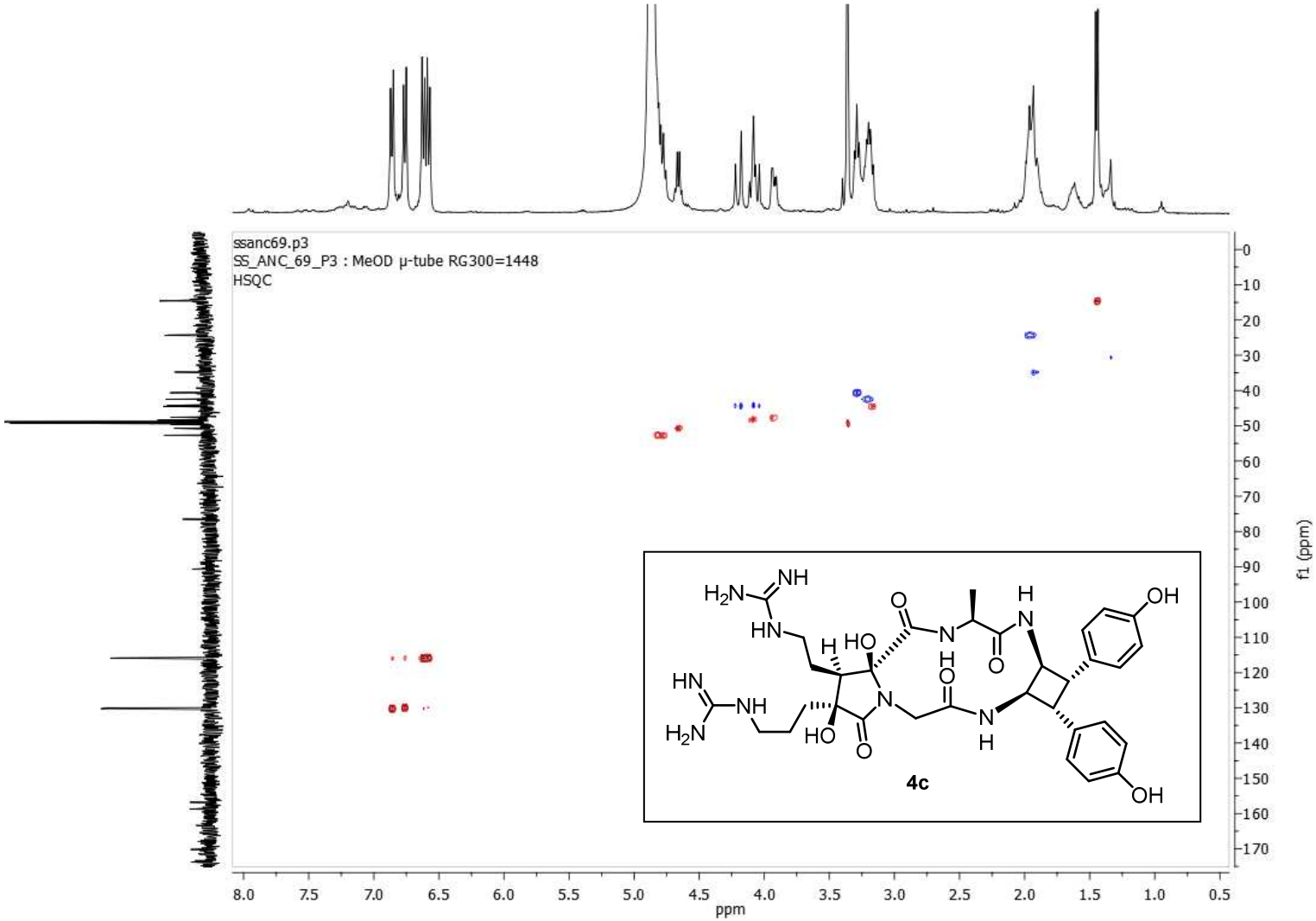

Cycloanchinopeptolide C (**4c**) (HMBC-2D-^{1}H and ^{13}C-NMR correlations, 400 MHz to ^{1}H nucleus, MeOH-d_4)

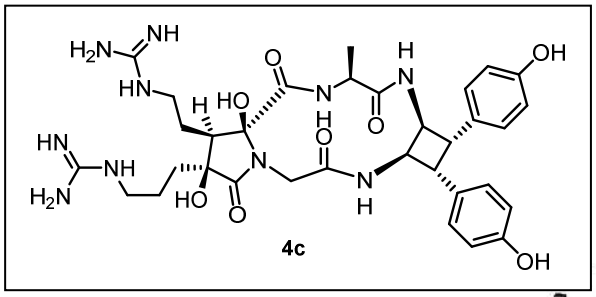

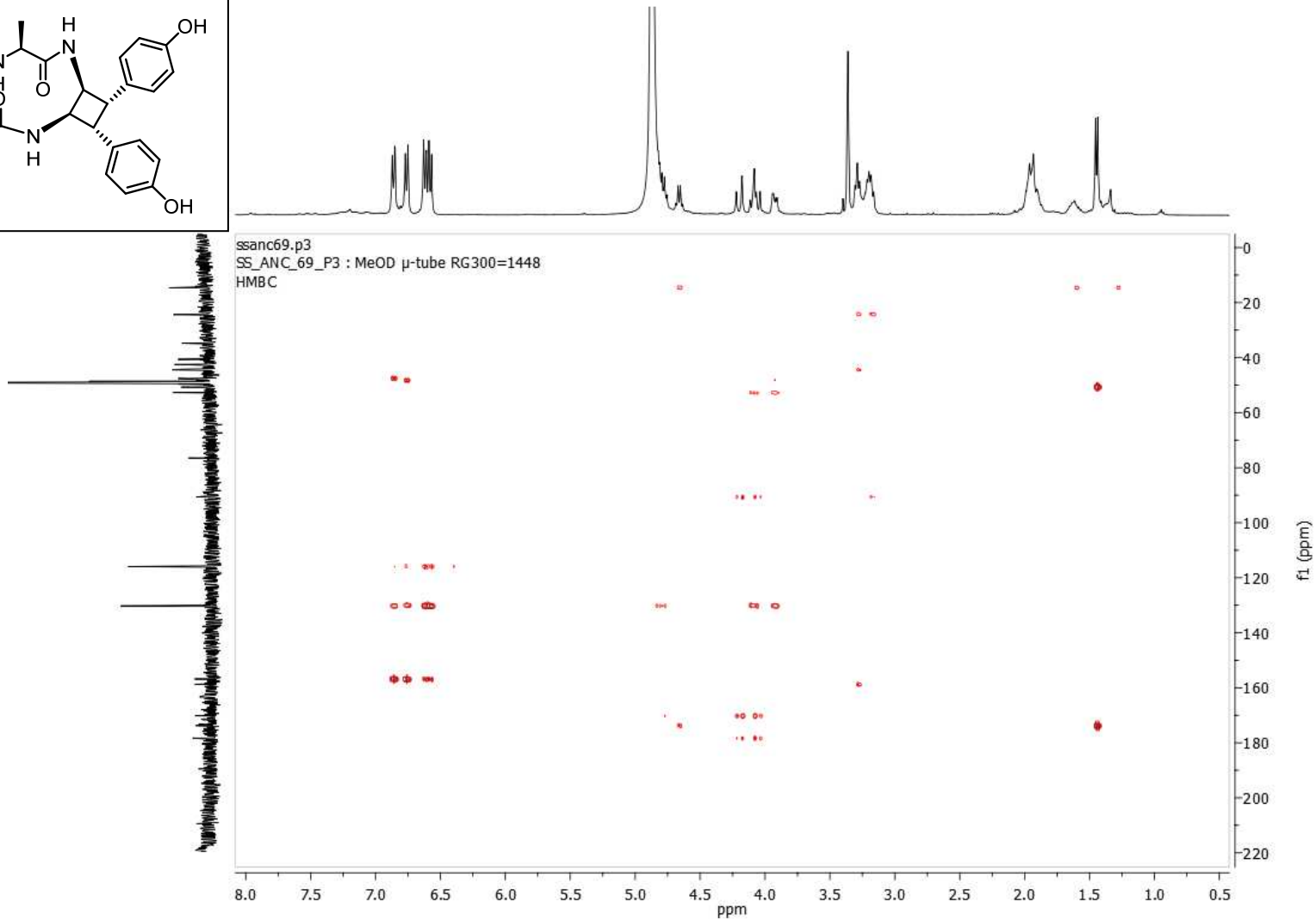

Cycloanchinopeptolide C (**4c**) (NOESY-2D-^{1}H NMR, 500 MHz, MeOH-d_4)

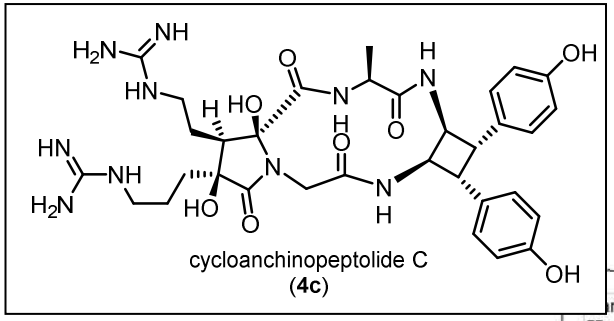

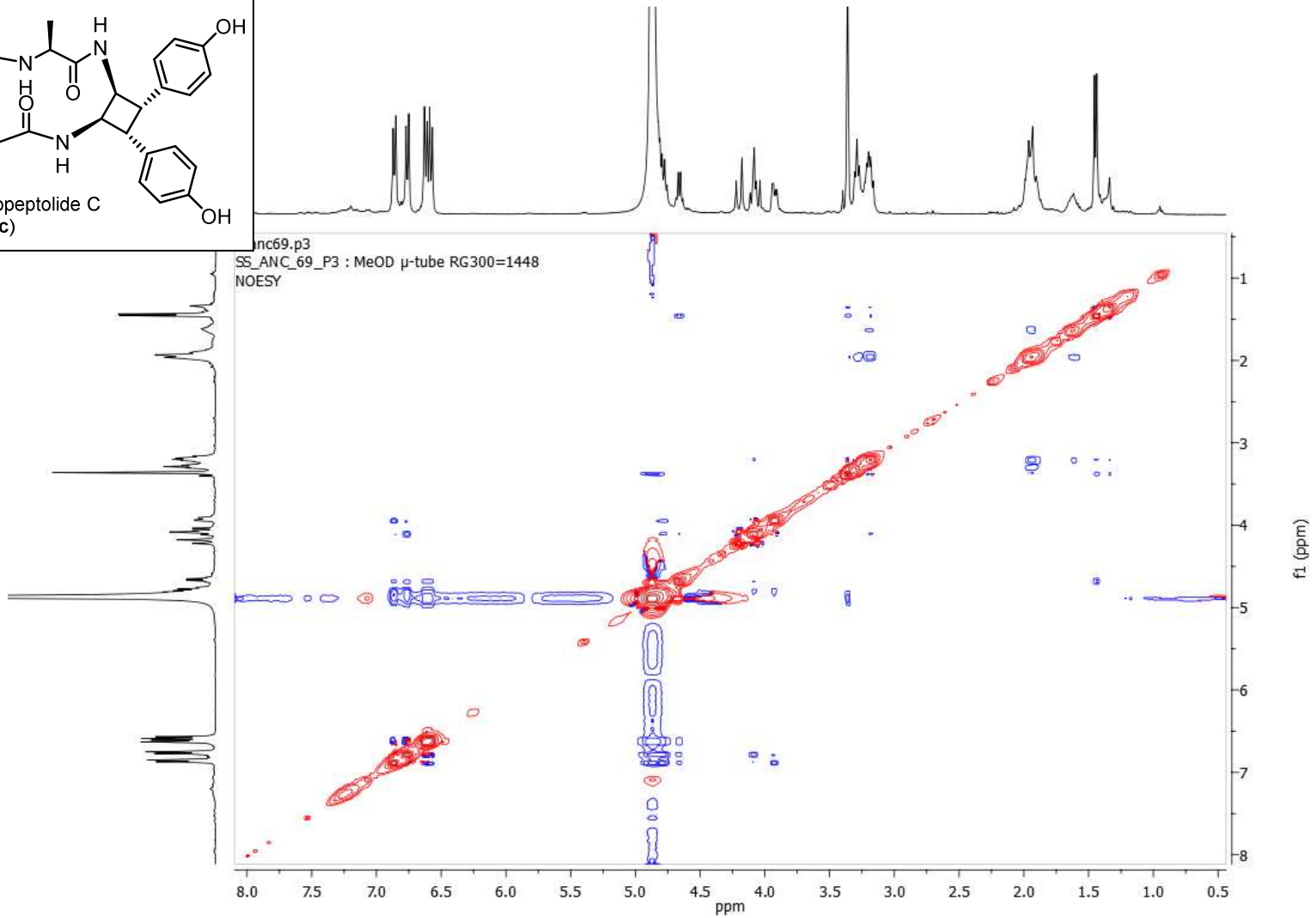

Crambescidin 800 (**23f**) (^{1}H-NMR, 500 MHz, MeOH-d_4)

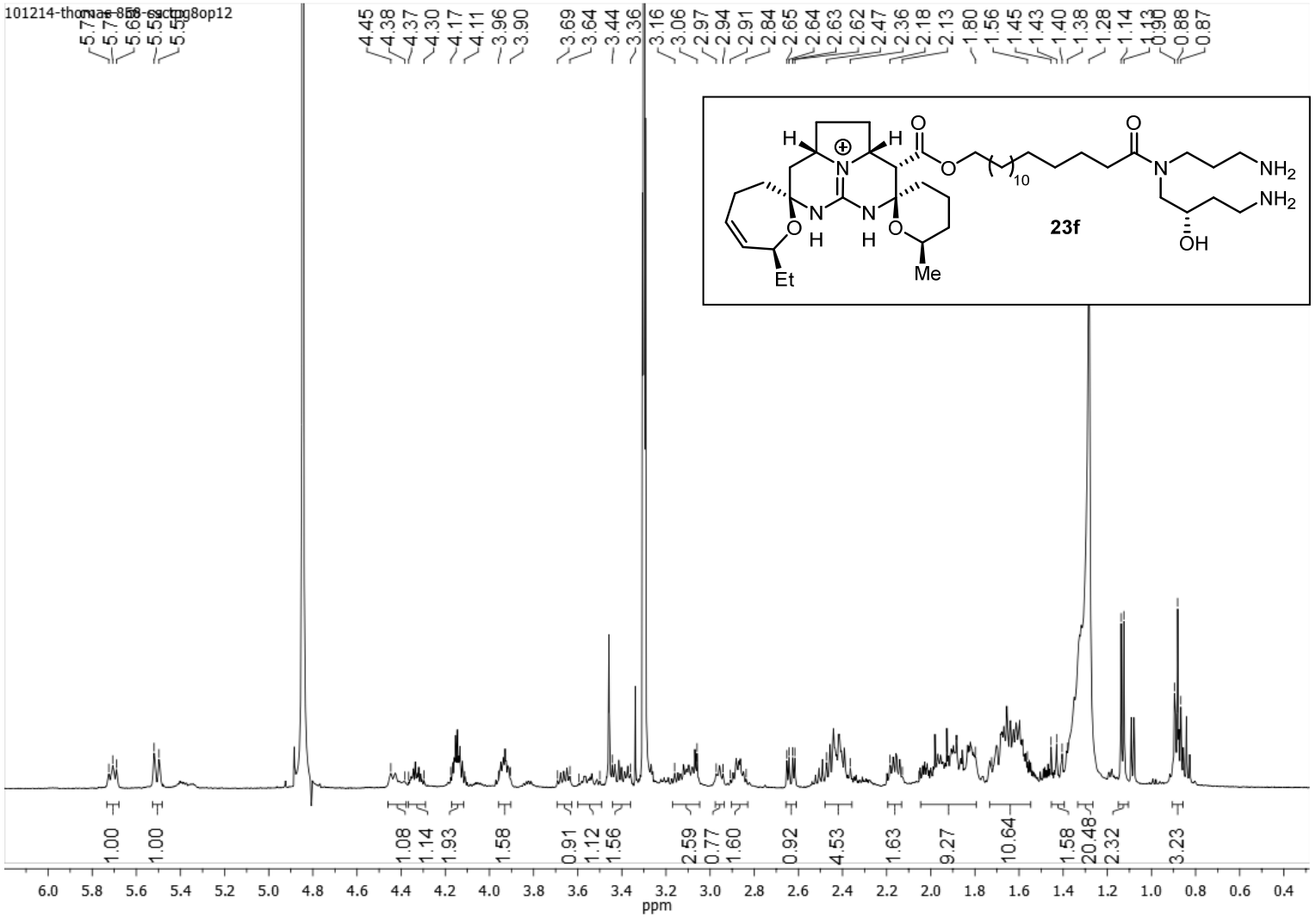

Crambescidin 816 (**23g**) (^{1}H-NMR, 500 MHz, MeOH-d_4)

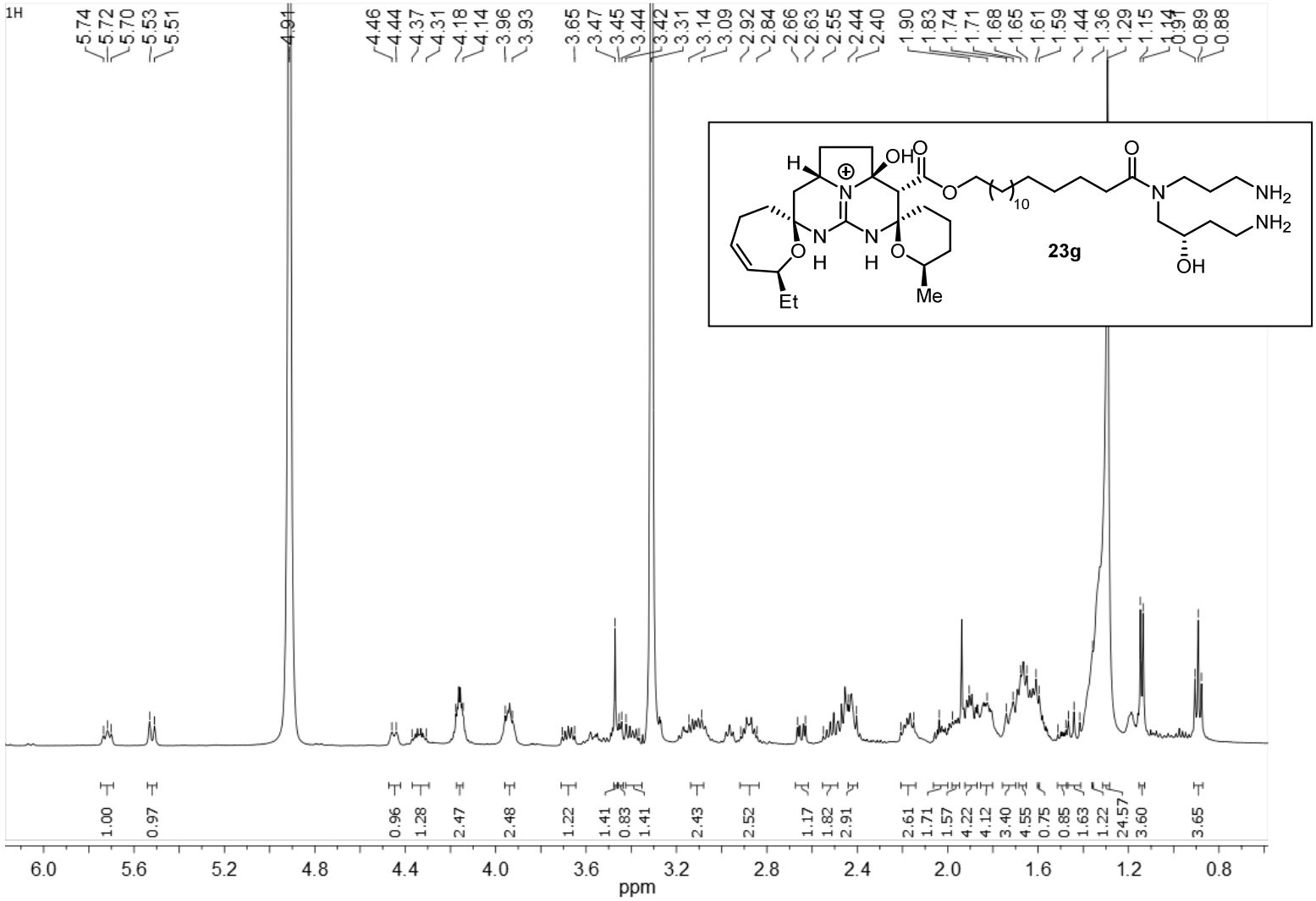

Crambescidin 816 (**23g**) (^{13}C-NMR, 125 MHz, MeOH-d_4)

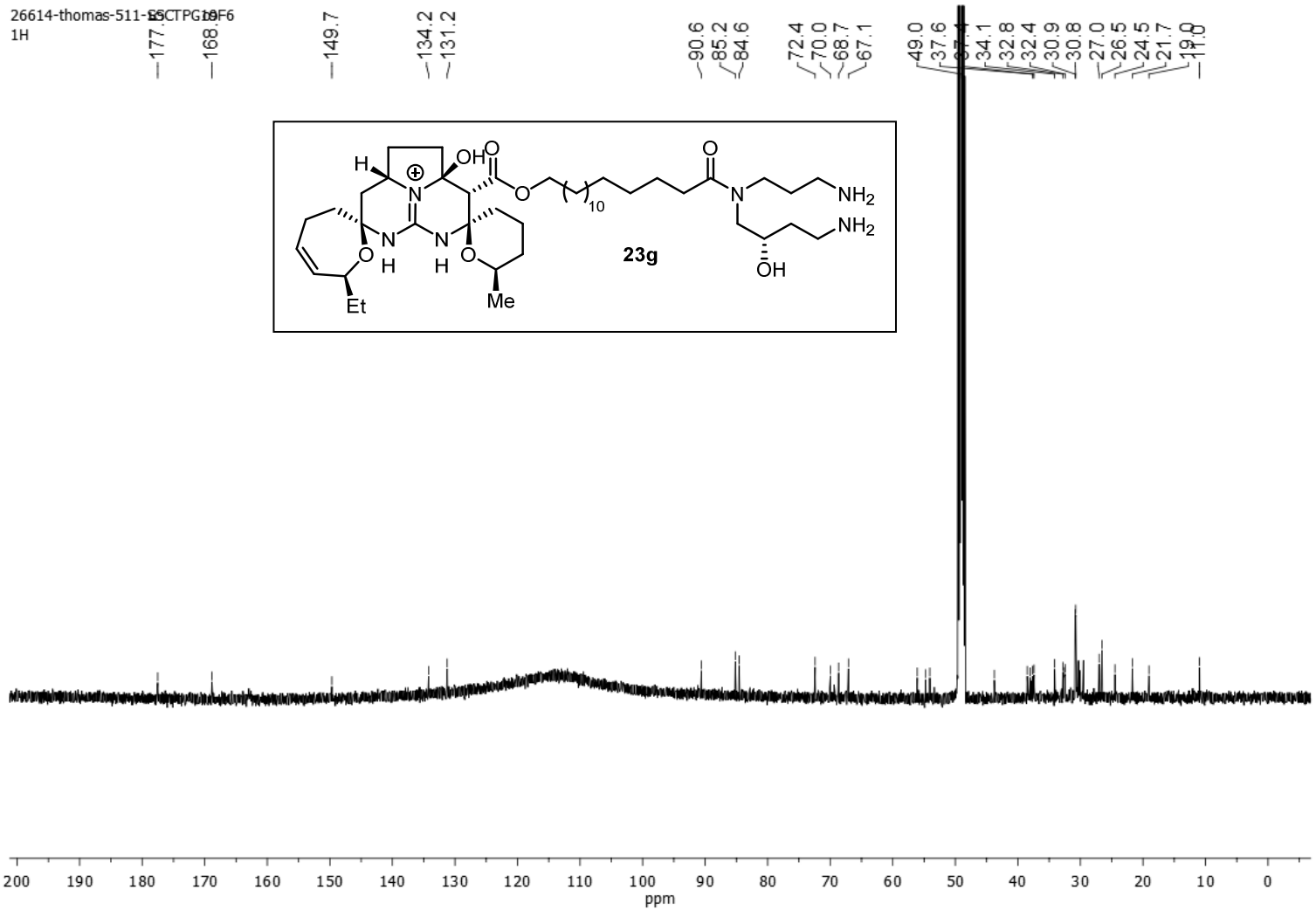

C. tailliezi F3P3 (^{1}H-NMR, 500 MHz, MeOH-d_4)

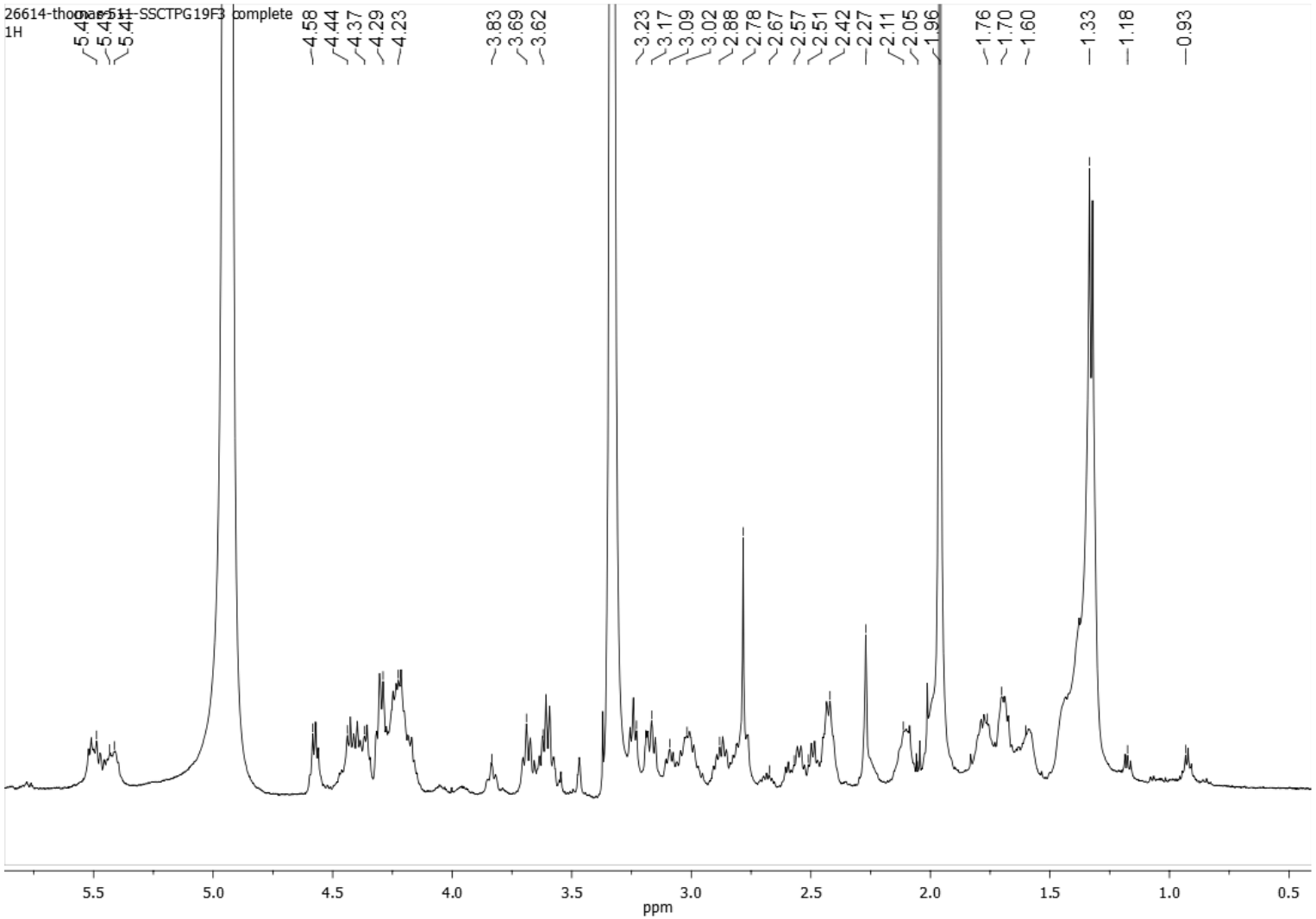

C. tailliezi F3P3 (^{1}C-NMR, 125 MHz, MeOH-d_4)

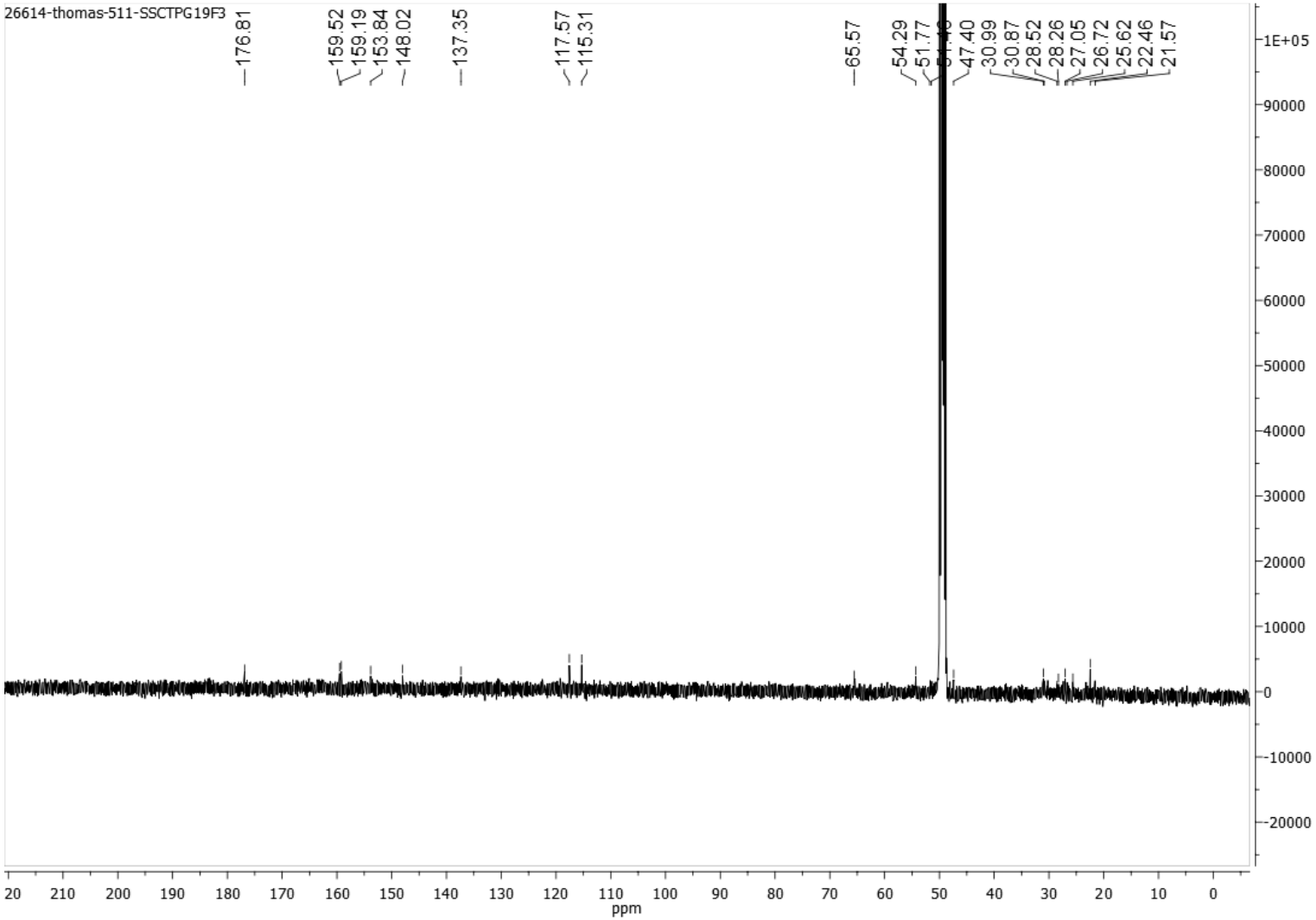

C. tailliezi F3P3 (COSY-2D-^{1}H-NMR, 500 MHz, MeOH-d_4)

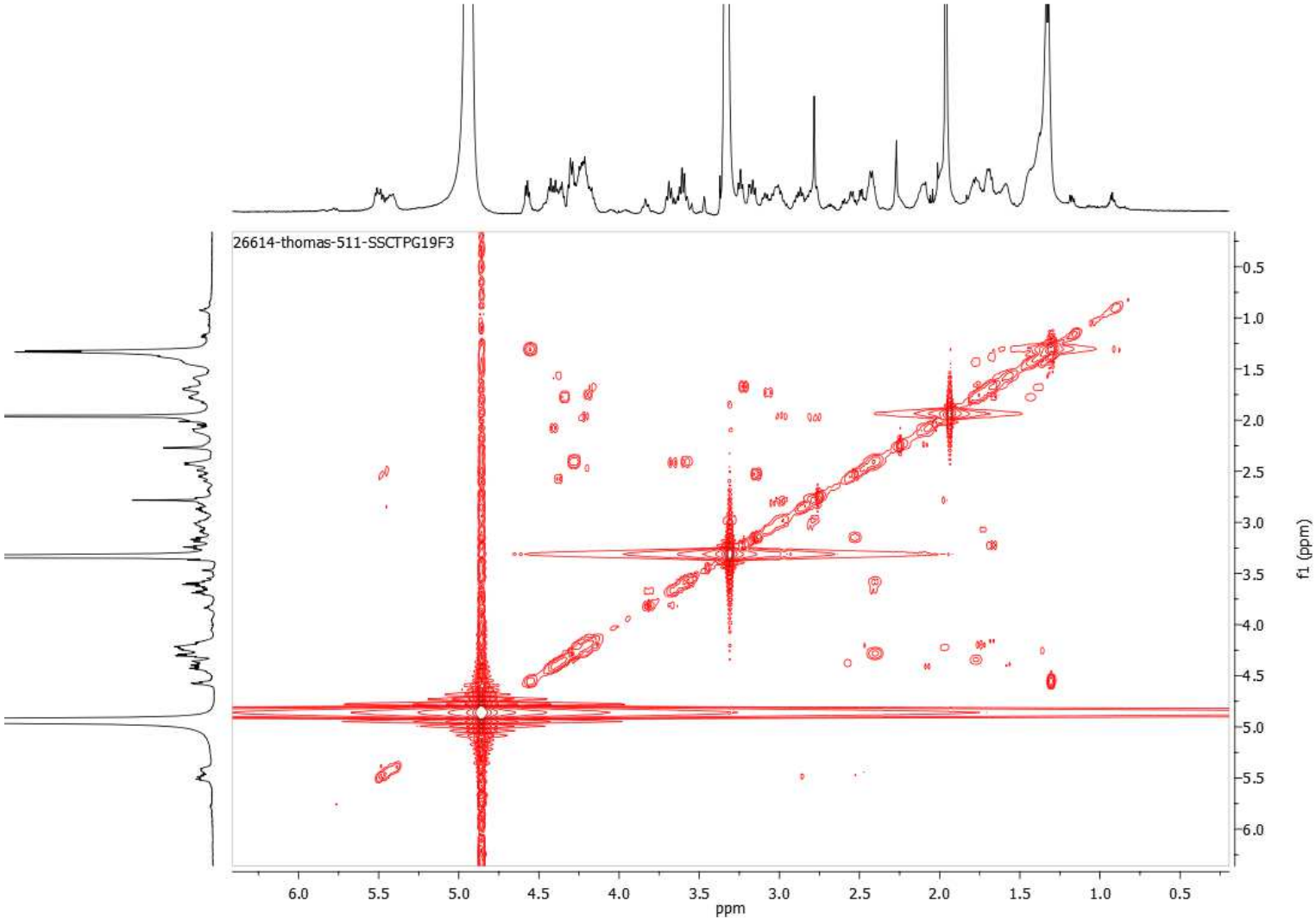

C. tailliezi F3P3 (HSQC-2D-^{1}H and ^{13}C-NMR correlations, 500 MHz to ^{1}H nucleus, MeOH-d_4)

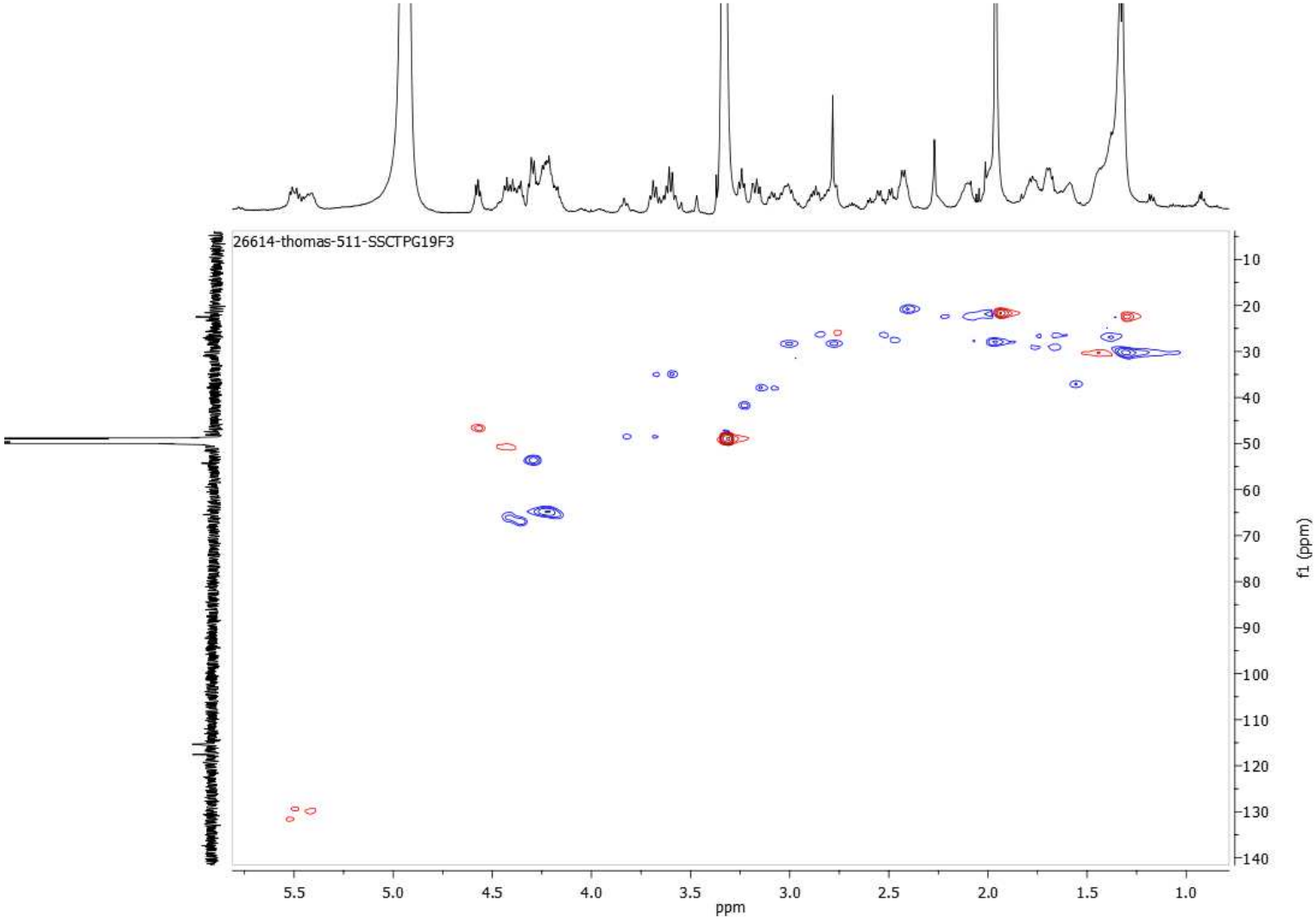

C. tailliezi F3P3 (HMBC-2D-^{1}H and ^{13}C-NMR correlations, 500 MHz to ^{1}H nucleus, MeOH-d_4)

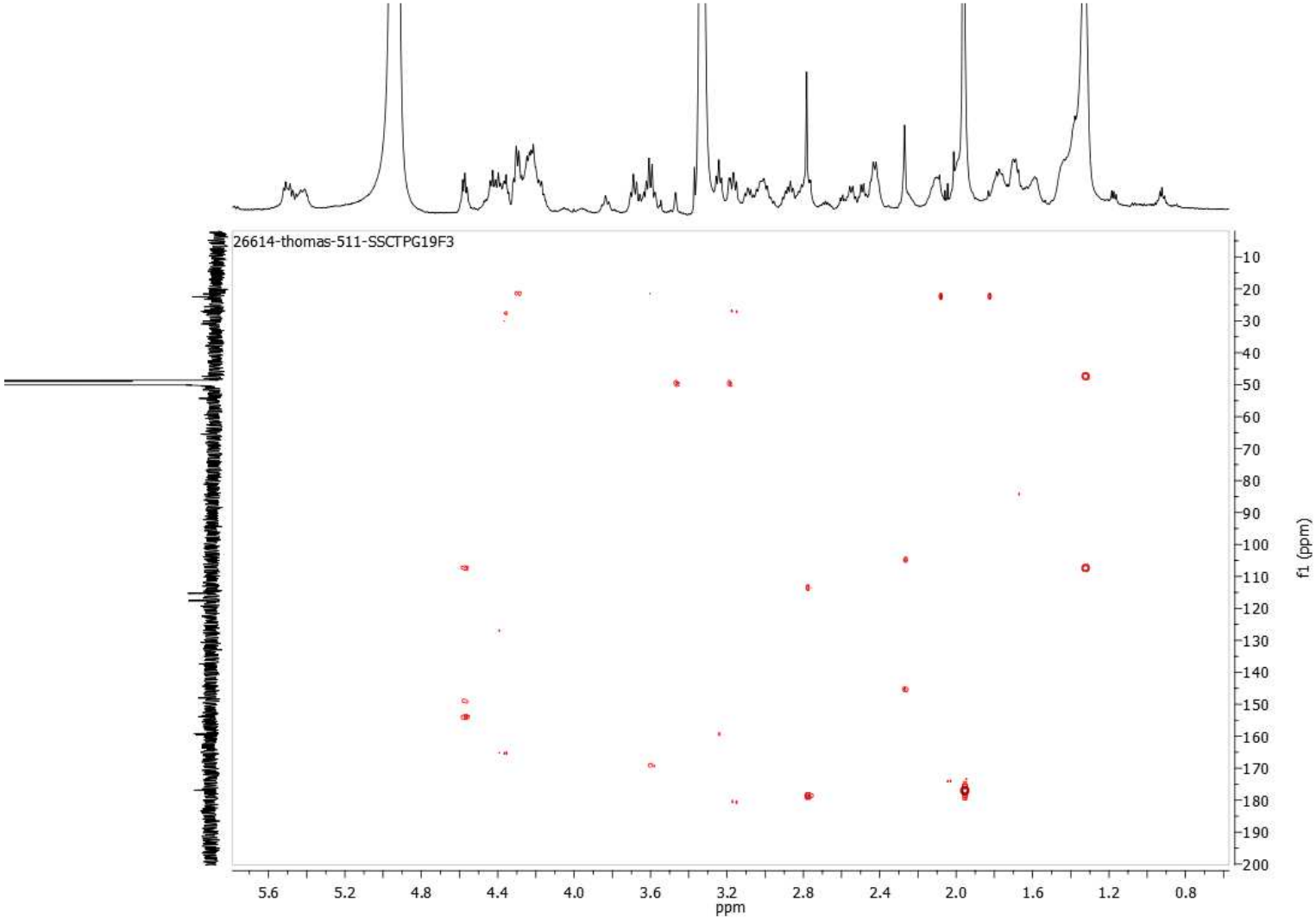

Crambescin C1 (^{1}H-NMR, 500 MHz, MeOH-d_4)

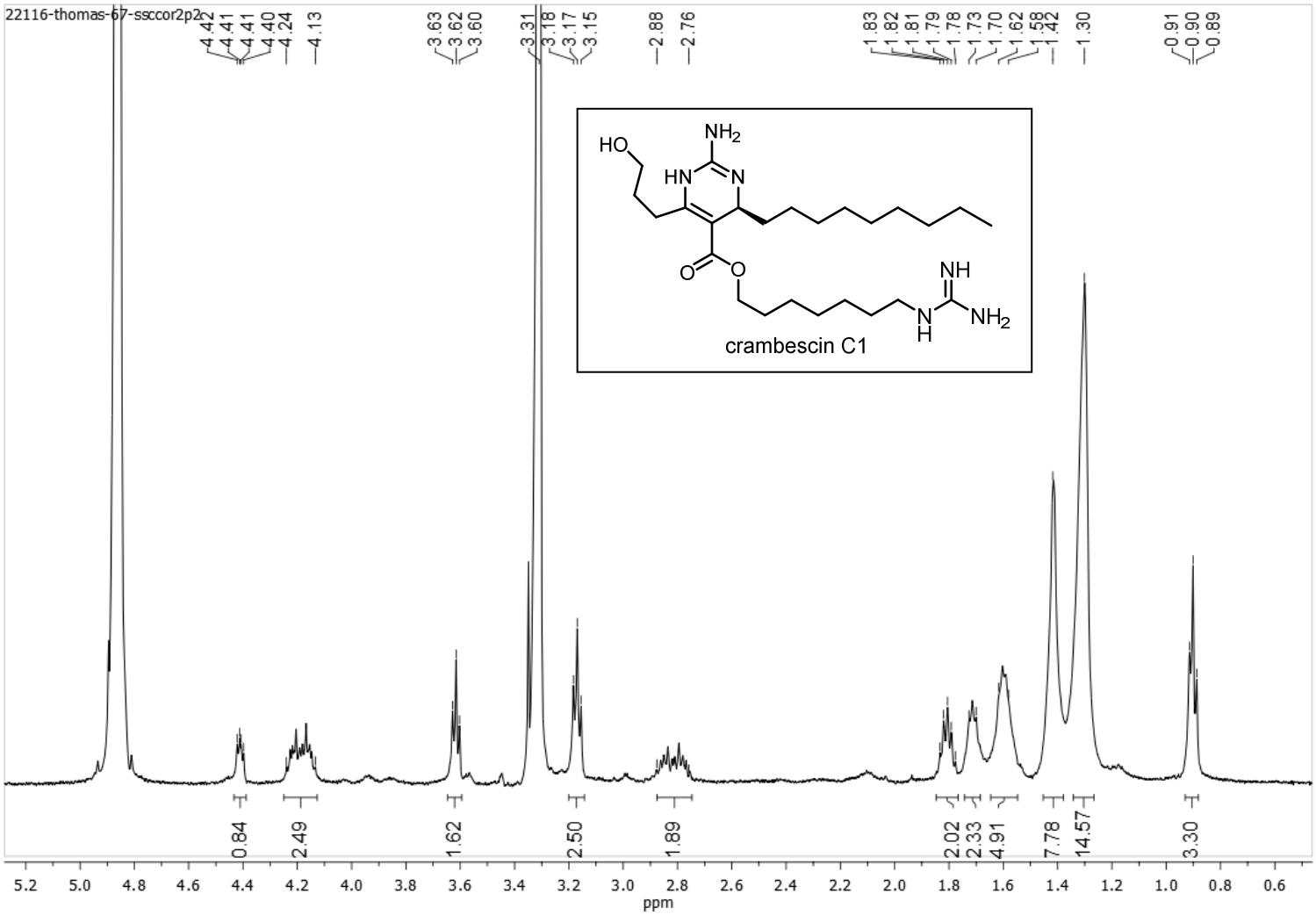

benzyl 3-oxotetradecanoate (**25a**) (^{1}H-NMR, 500 MHz, $CDCl_3$)

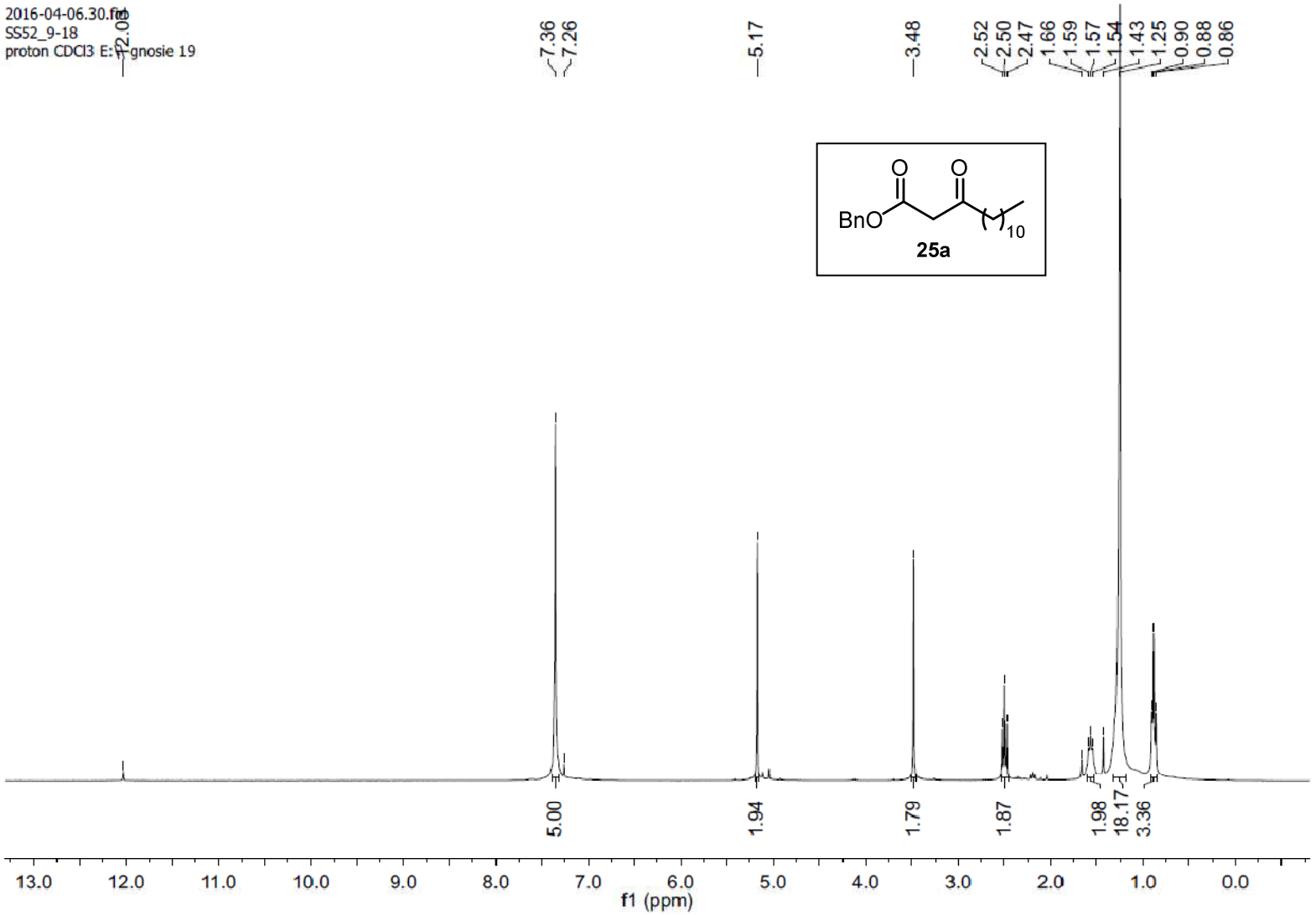

benzyl 3-oxotetradecanoate (**25a**) (JMOD-^{13}C-NMR, 300 MHz, $CDCl_3$)

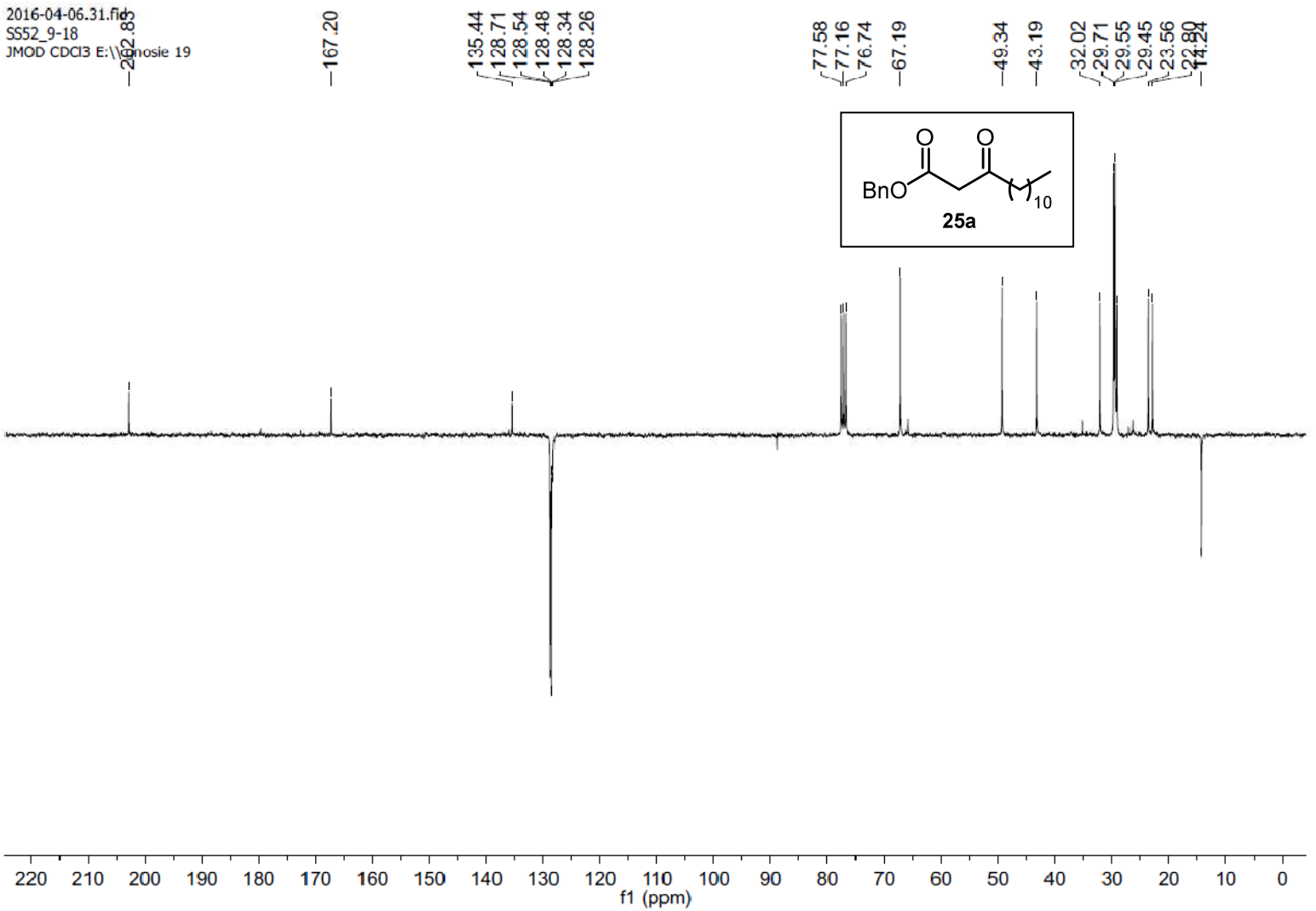

ethyl 3-oxotetradecanoate (**25b**) (^{1}H-NMR, 300 MHz, $CDCl_3$)

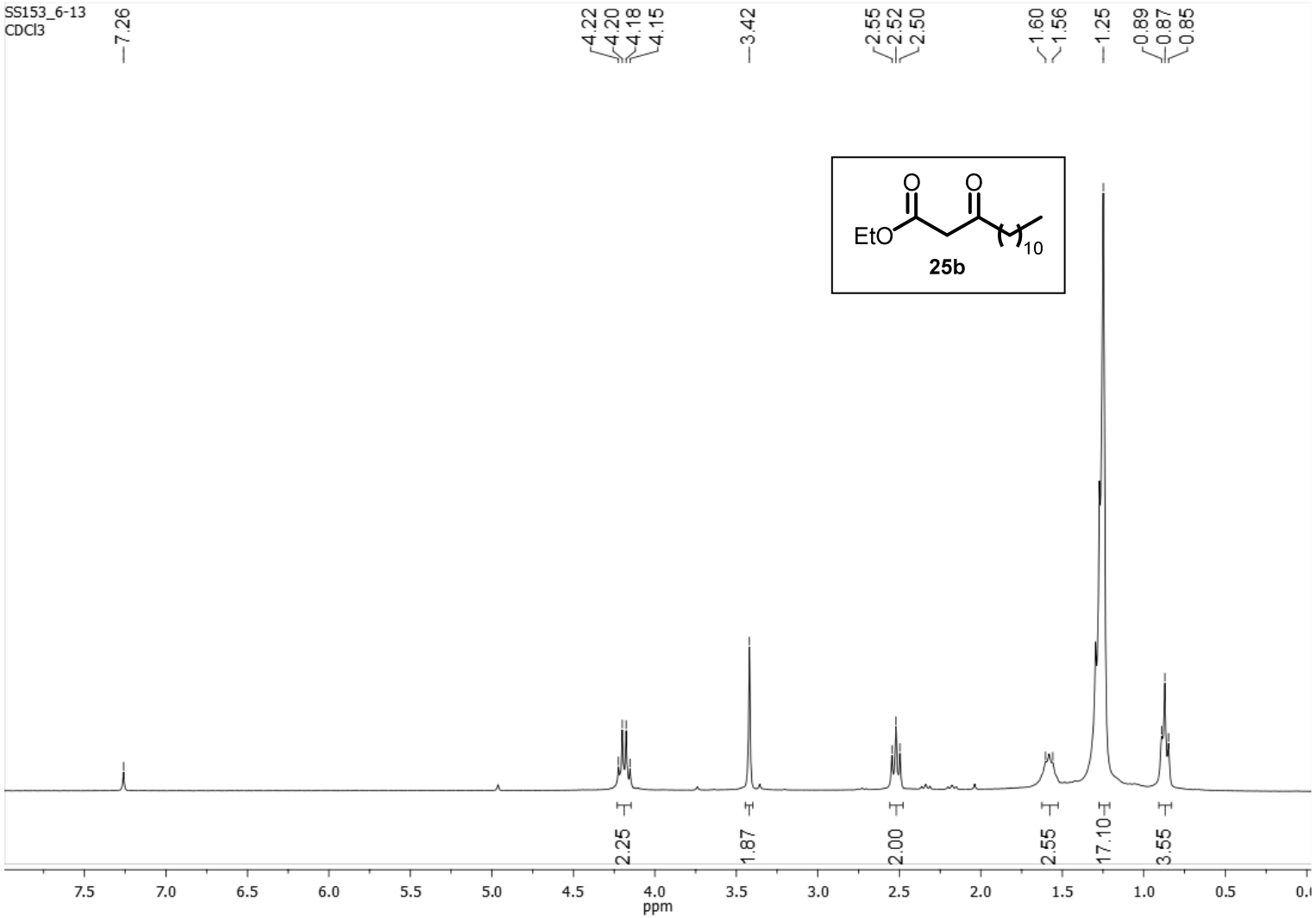

ethyl 3-oxotetradecanoate (**25b**) (JMOD-^{13}C-NMR, 75 MHz, $CDCl_3$)

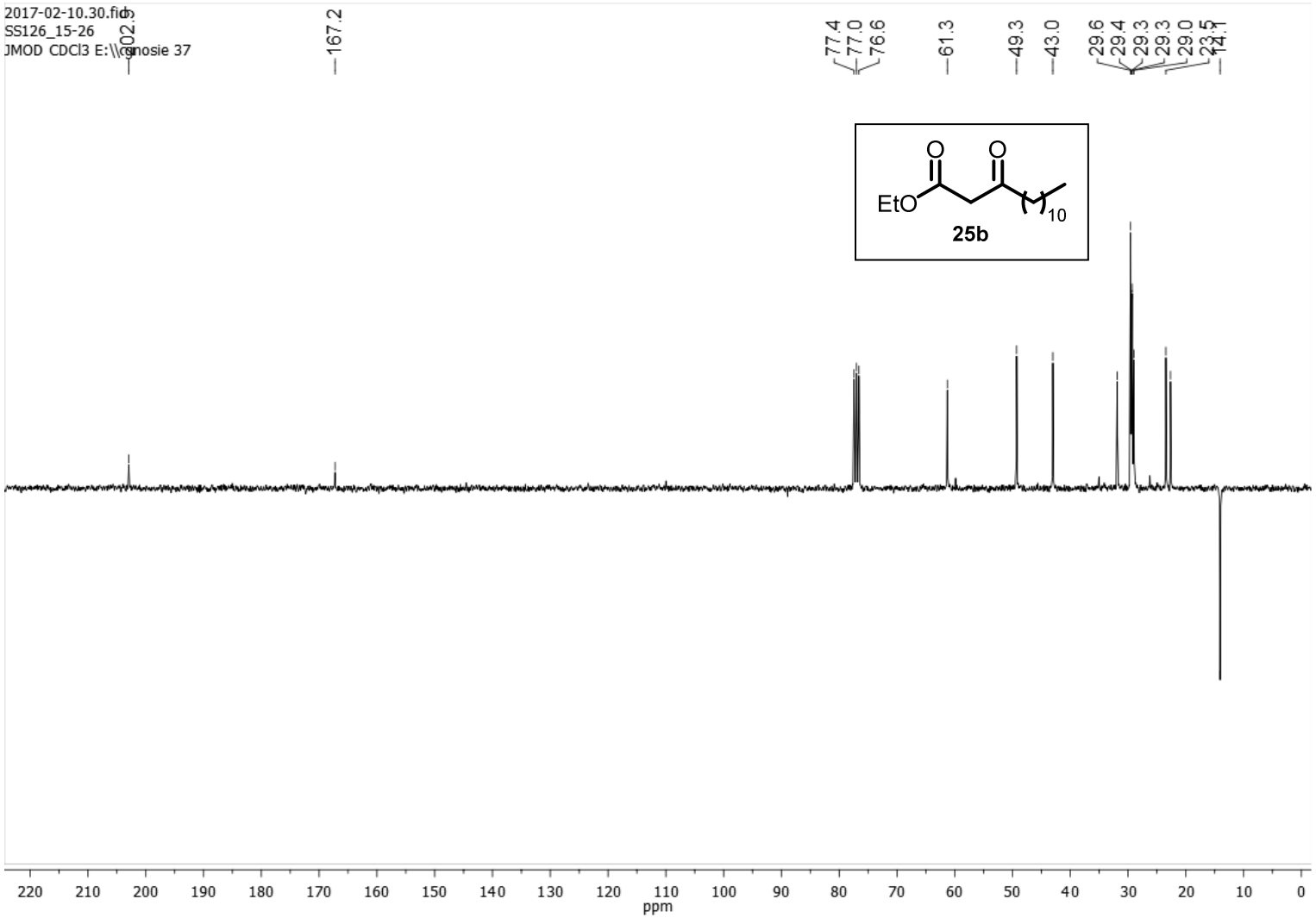

3-oxotetradecanoic acid (**21**) (^{1}H-NMR, 300 MHz, acetone-d_6)

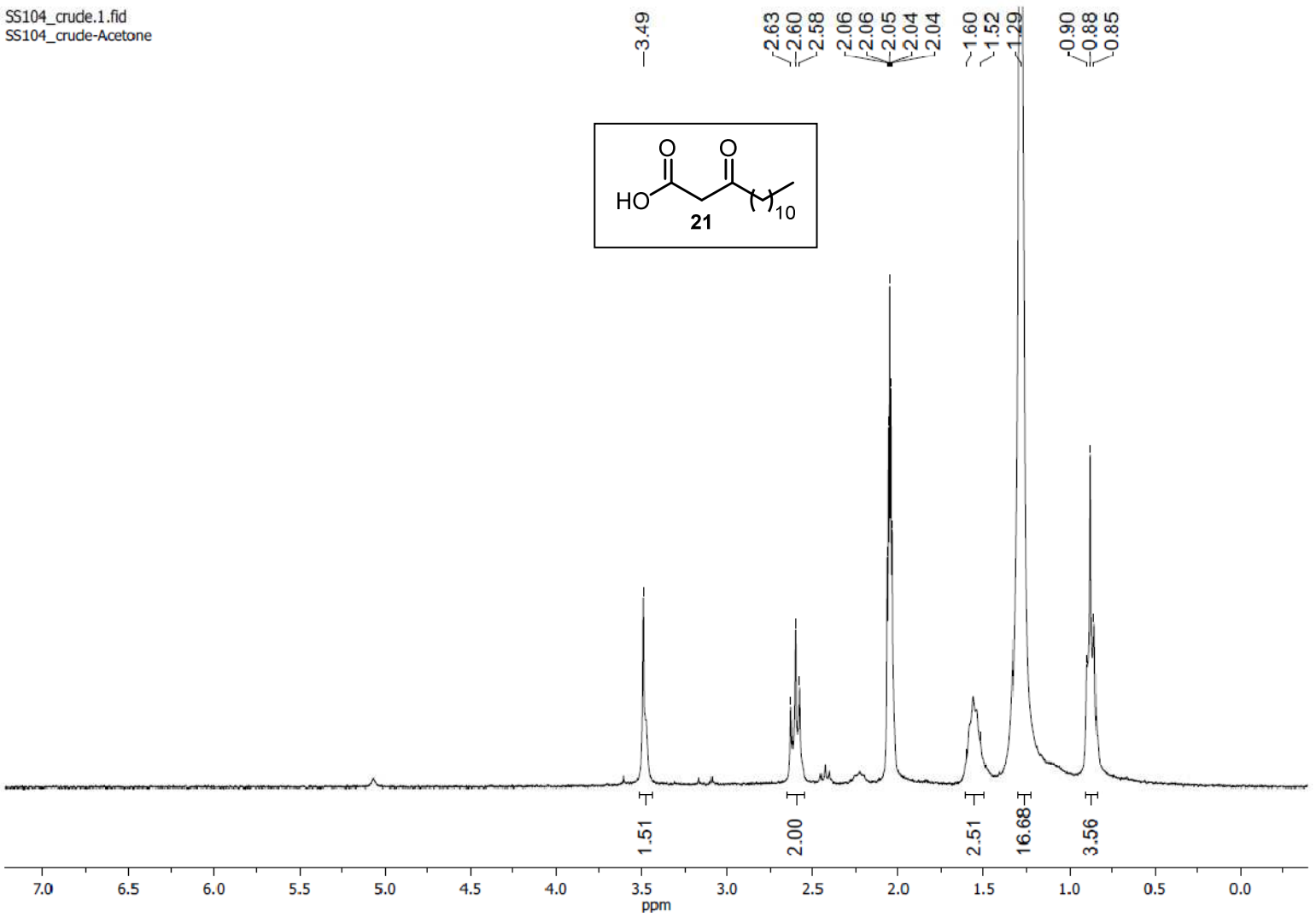

4-guanidinobutanoic acid (**31**) (^{1}H-NMR, 300 MHz, MeOH-d_4)

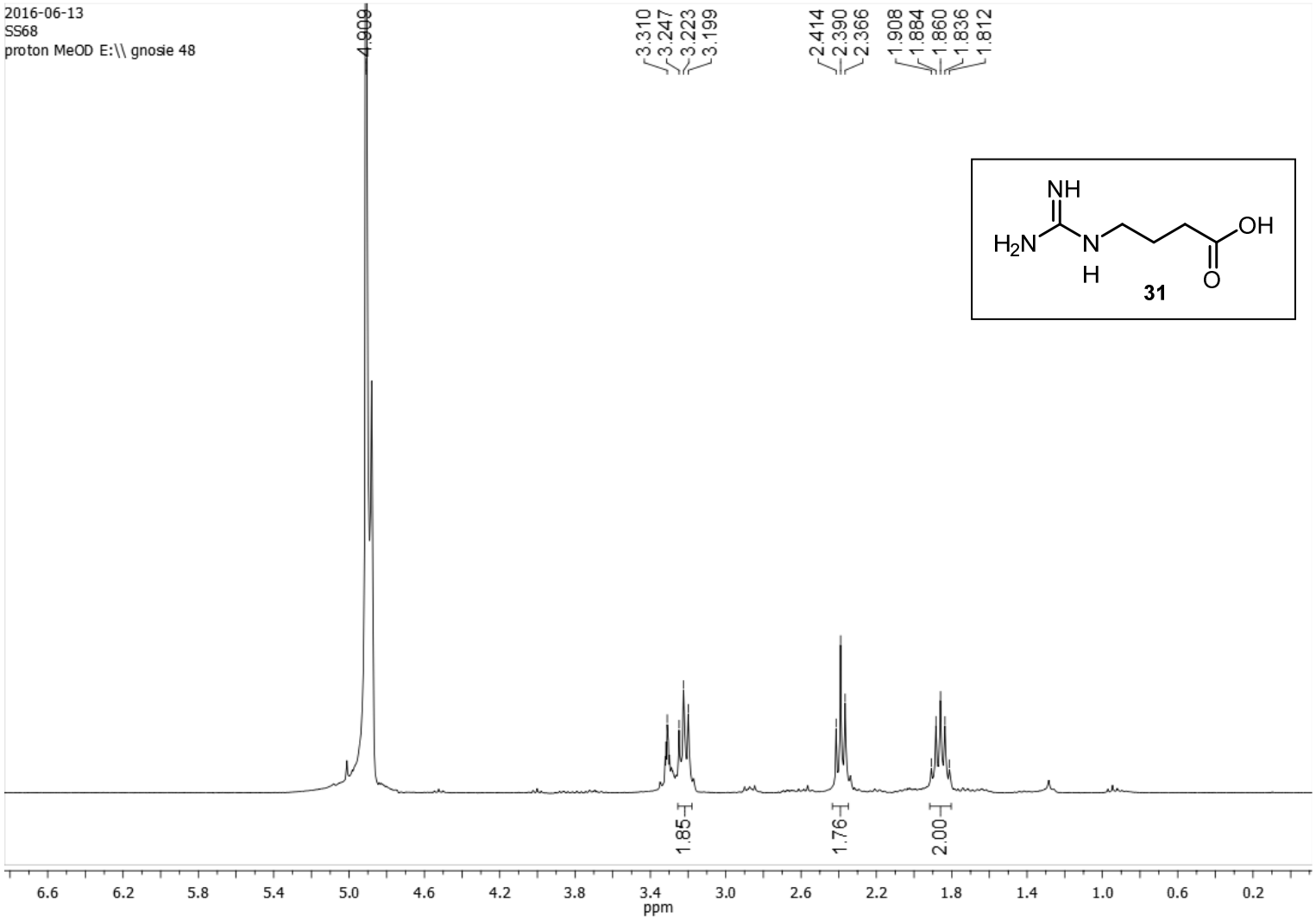

4-guanidinobutanoic acid (**31**) (JMOD-^{13}C-NMR, 75 MHz, MeOH-d_4)

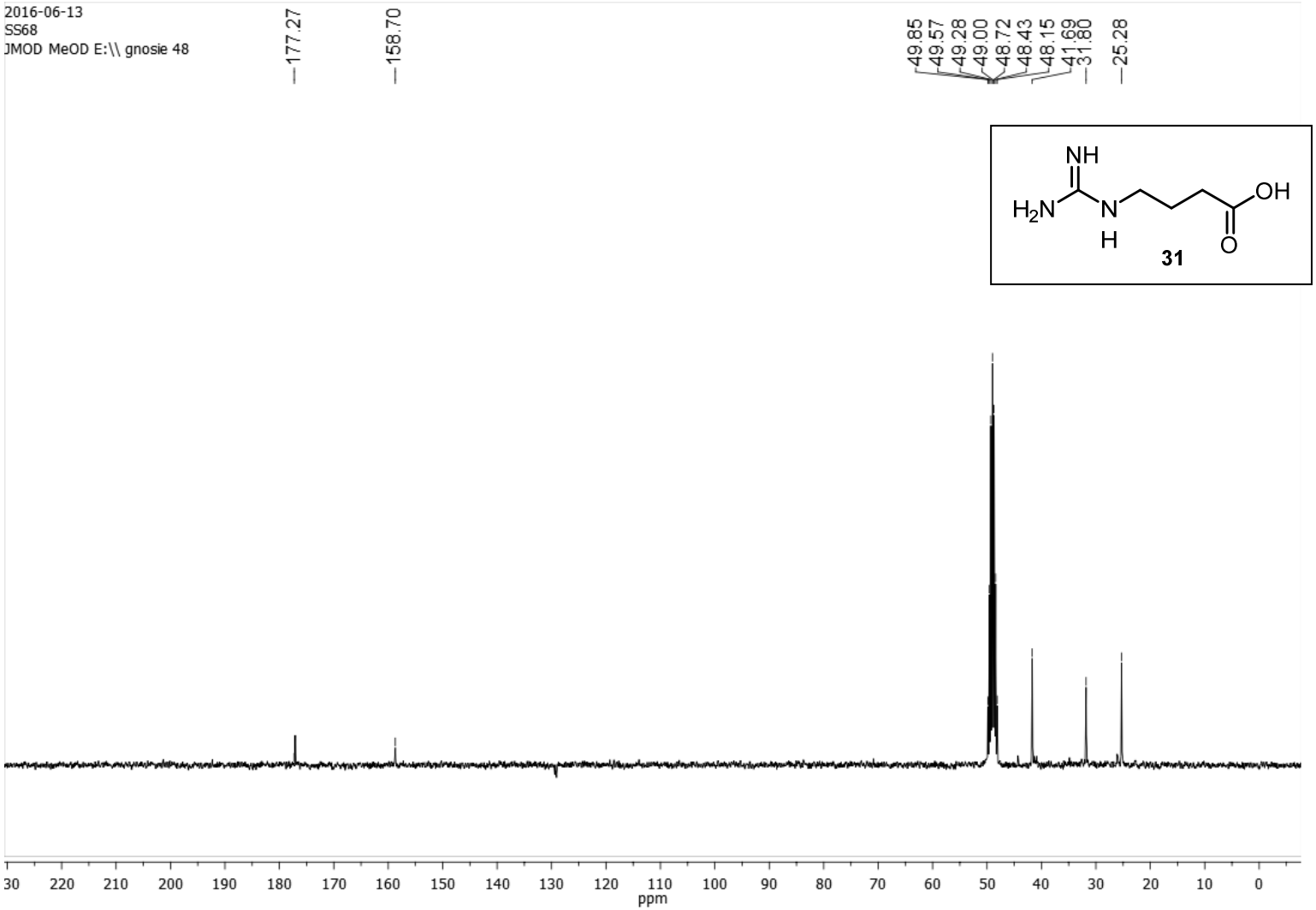

1-(4-hydroxybutyl)guanidine (**20a**) (^{1}H-NMR, 300 MHz, D_2O)

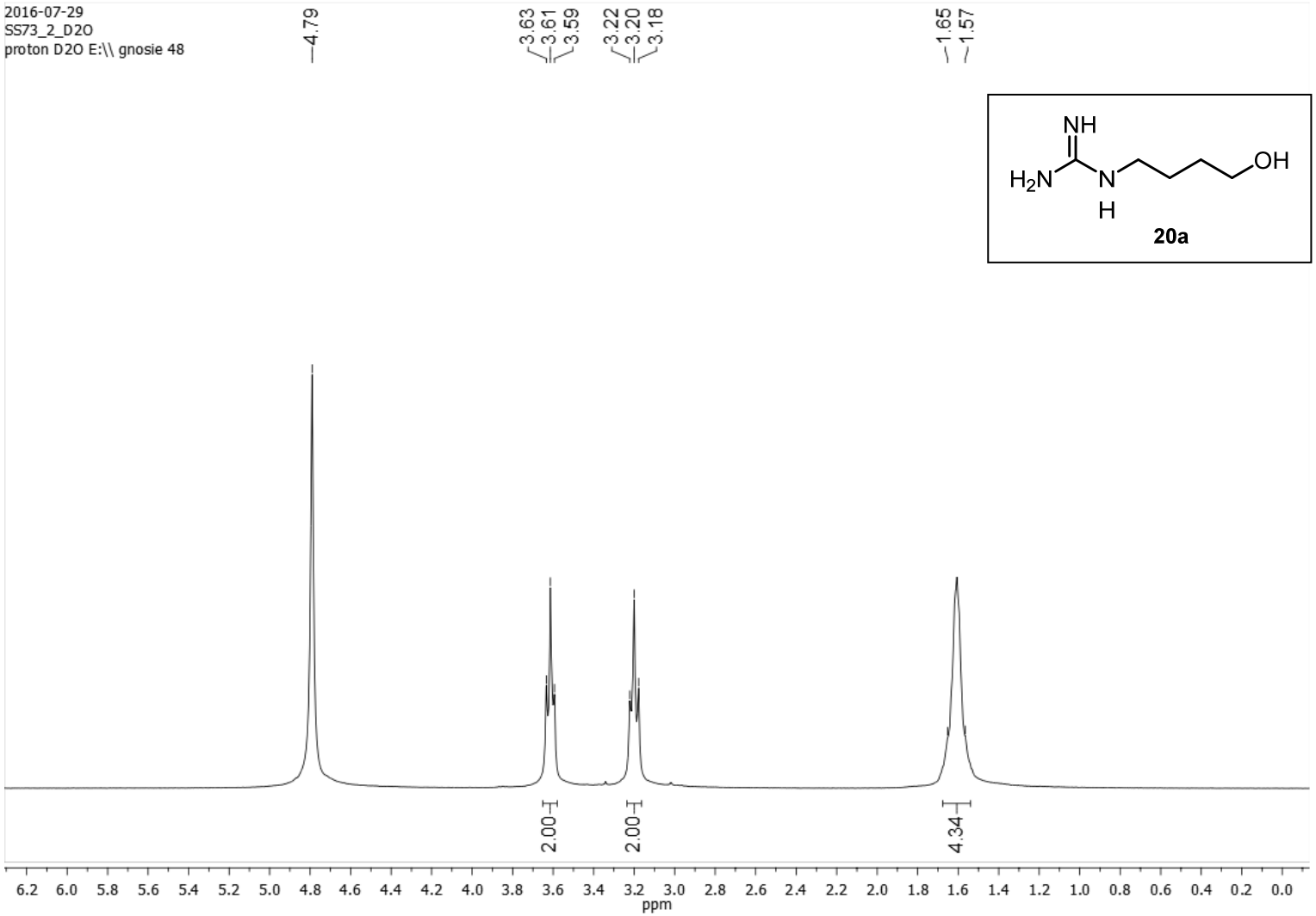

1-(4-hydroxybutyl)guanidine (**20a**) (JMOD-^{13}C-NMR, 75 MHz, D_2O)

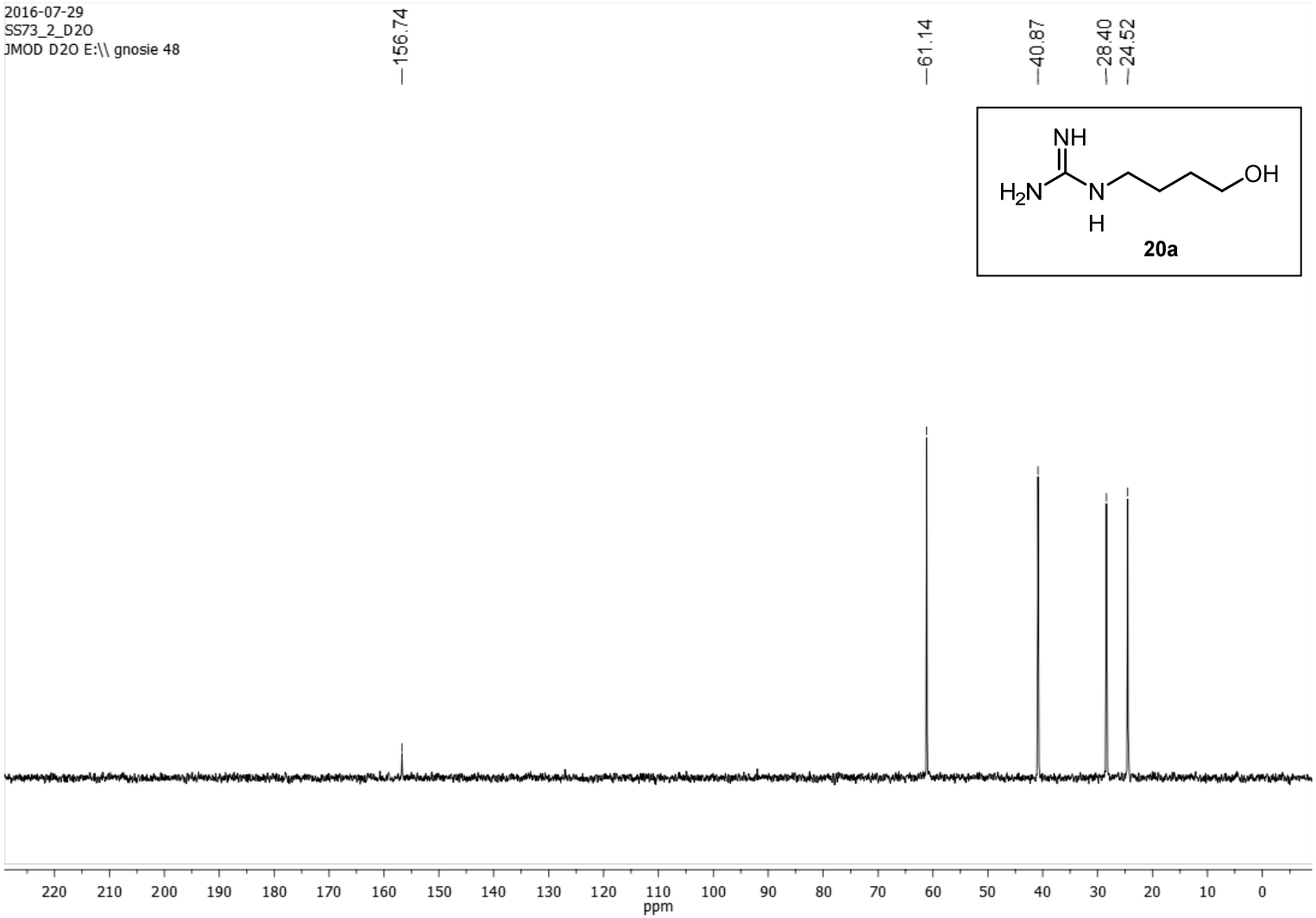

4-(*N*,*N*'-di-*t*-butoxycarbonylguanidino)-butan-1-ol (**20c**) (^{1}H-NMR, 300 MHz, $CDCl_3$)

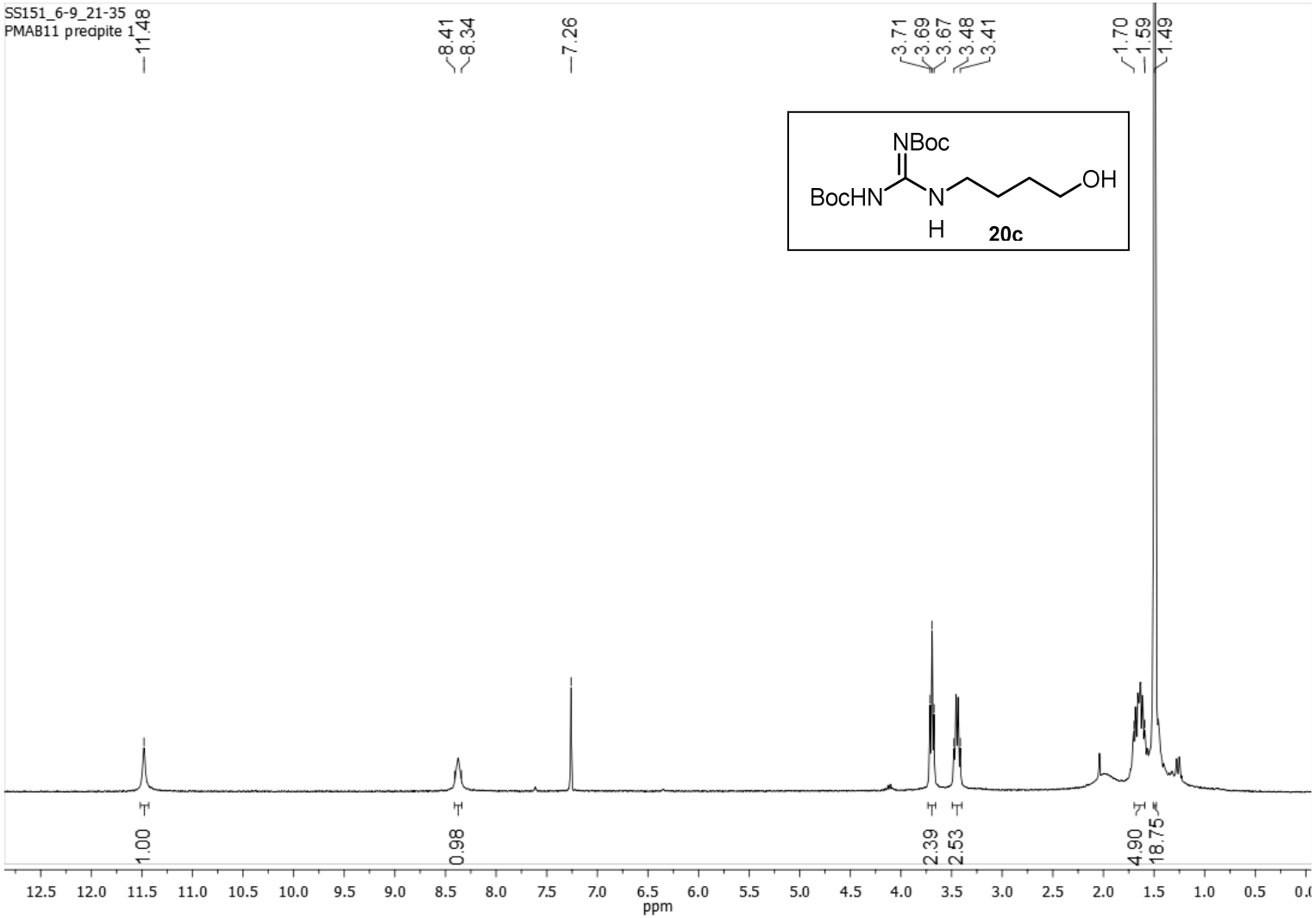

4-(*N*,*N*'-di-*t*-butoxycarbonylguanidino)-butan-1-ol (**20c**) (^{13}C-NMR, 75 MHz, $CDCl_3$)

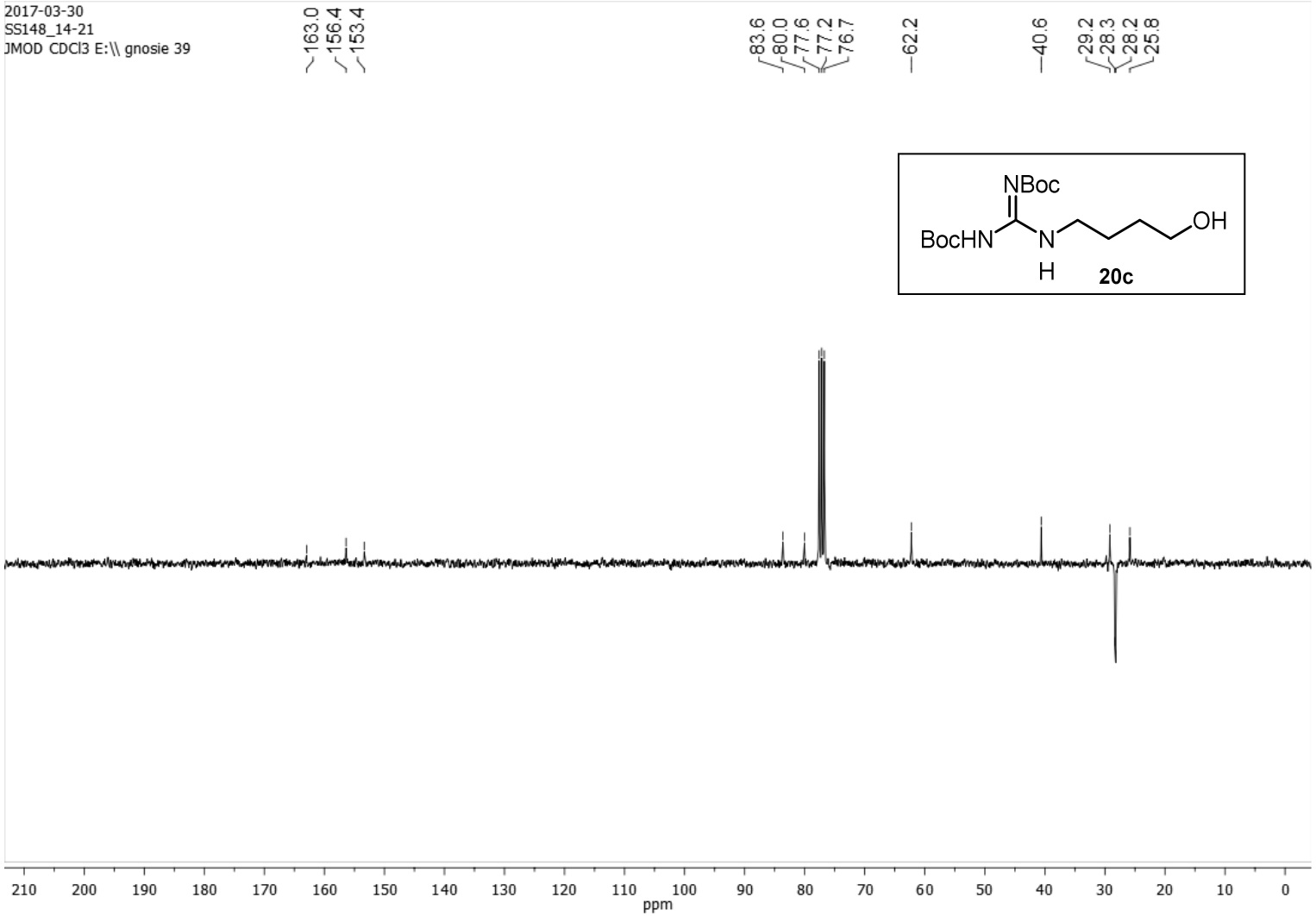

4-(2,3-bis(*tert*-butoxycarbonyl)guanidino)butyl 3-oxotetradecanoate (**17b**) (^{1}H-NMR, 300 MHz, $CDCl_3$)

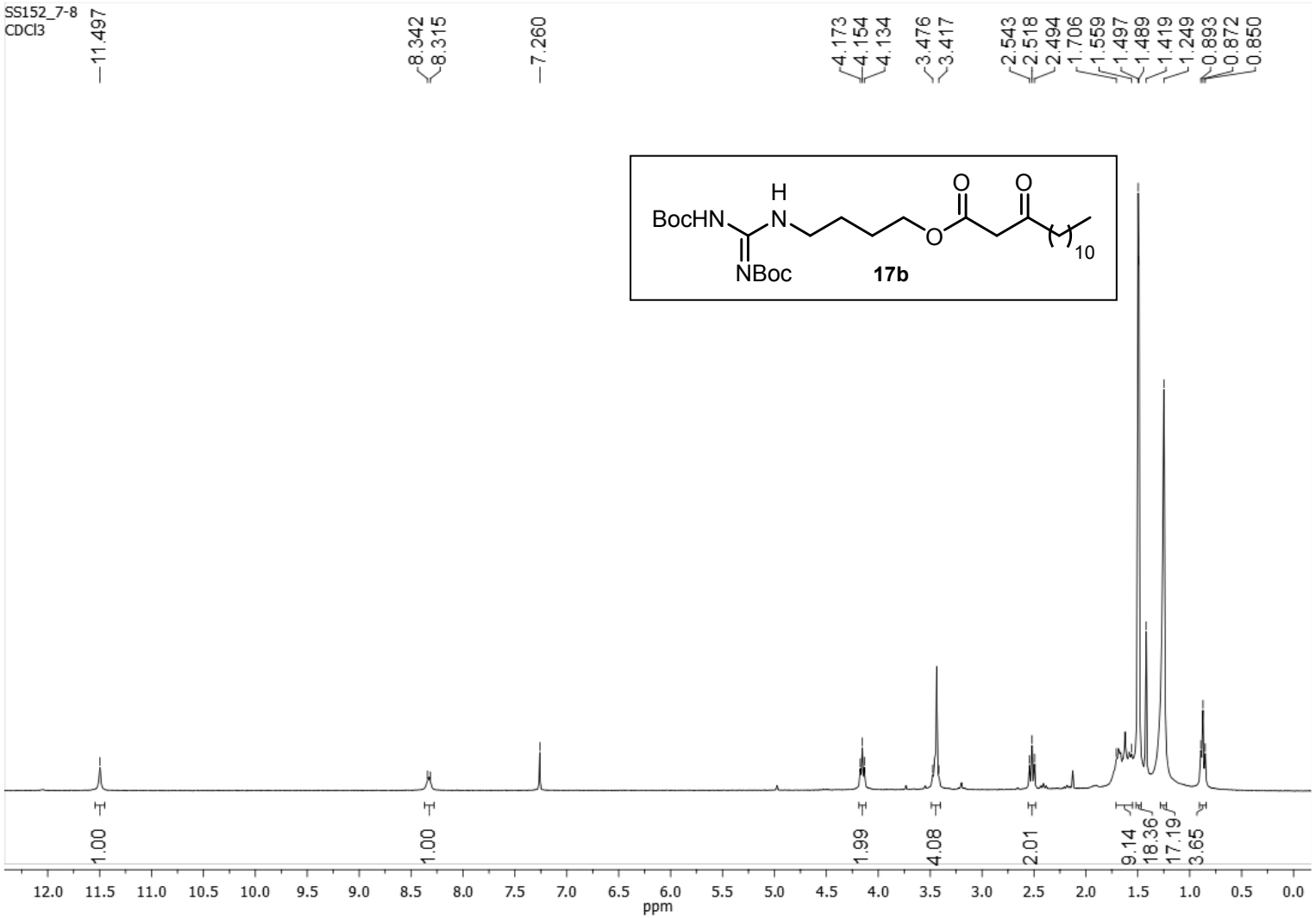

4-(2,3-bis(*tert*-butoxycarbonyl)guanidino)butyl 3-oxotetradecanoate (**17b**) (^{13}C-NMR, 75 MHz, $CDCl_3$)

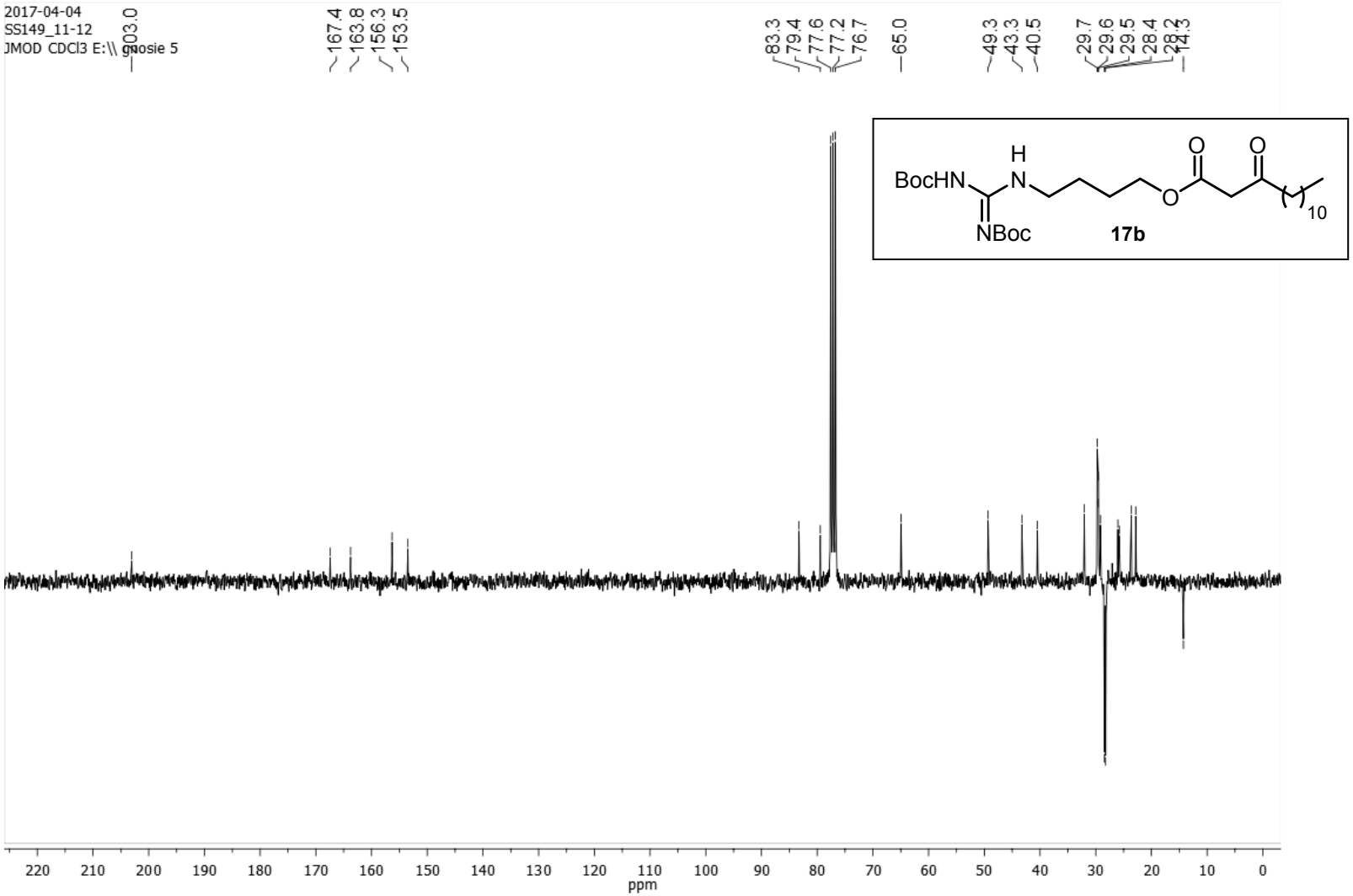

crambescin A2 448 (**5a**) and isocrambescin A2 448 (**5k**) (^{1}H-NMR, 400 MHz, MeOH-d_4)

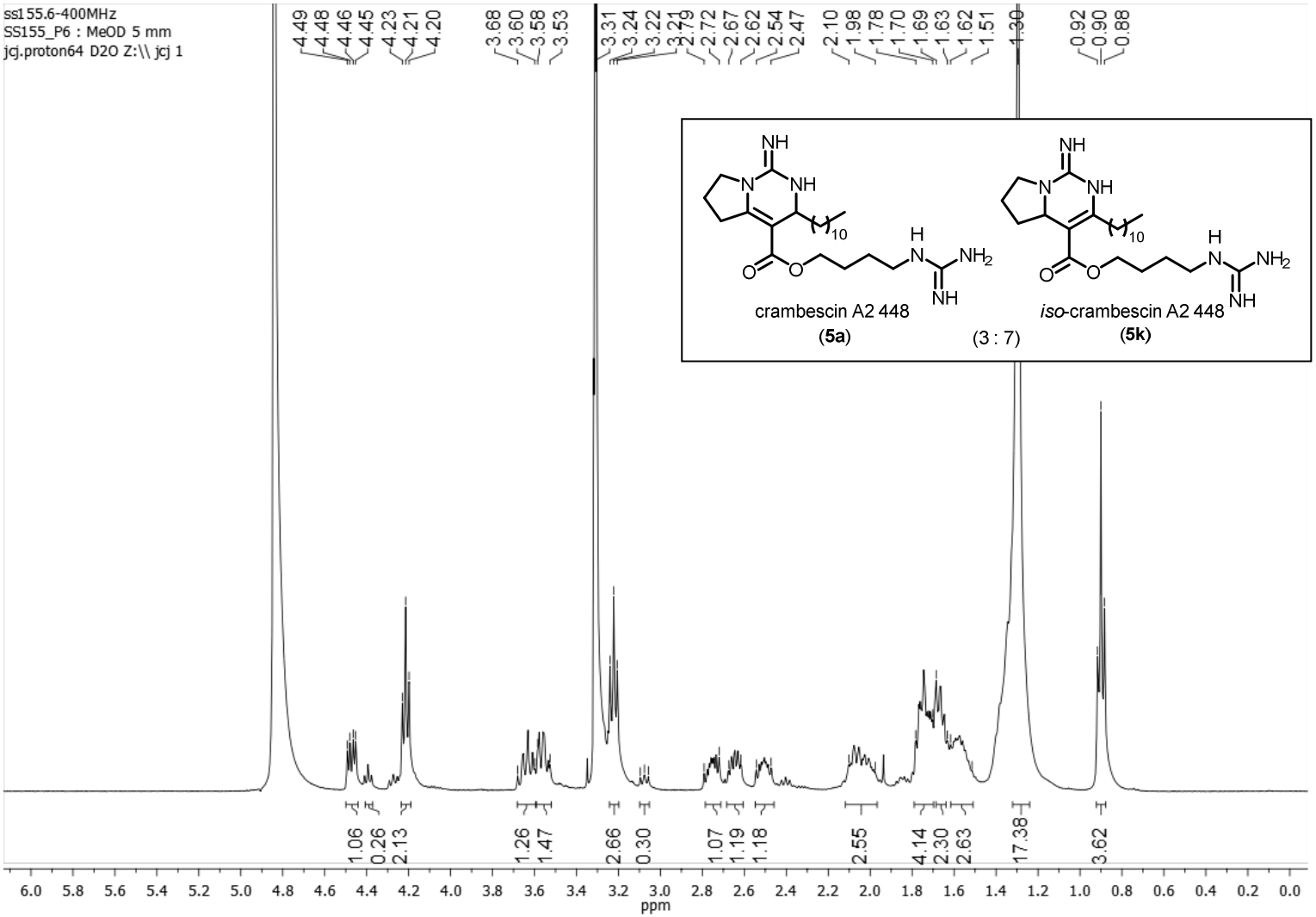

crambescin A2 448 (**5a**) and *iso*-crambescin A2 442 (**5k**) (UDEFT-^{13}C-NMR, 100 MHz, MeOH-d_4)

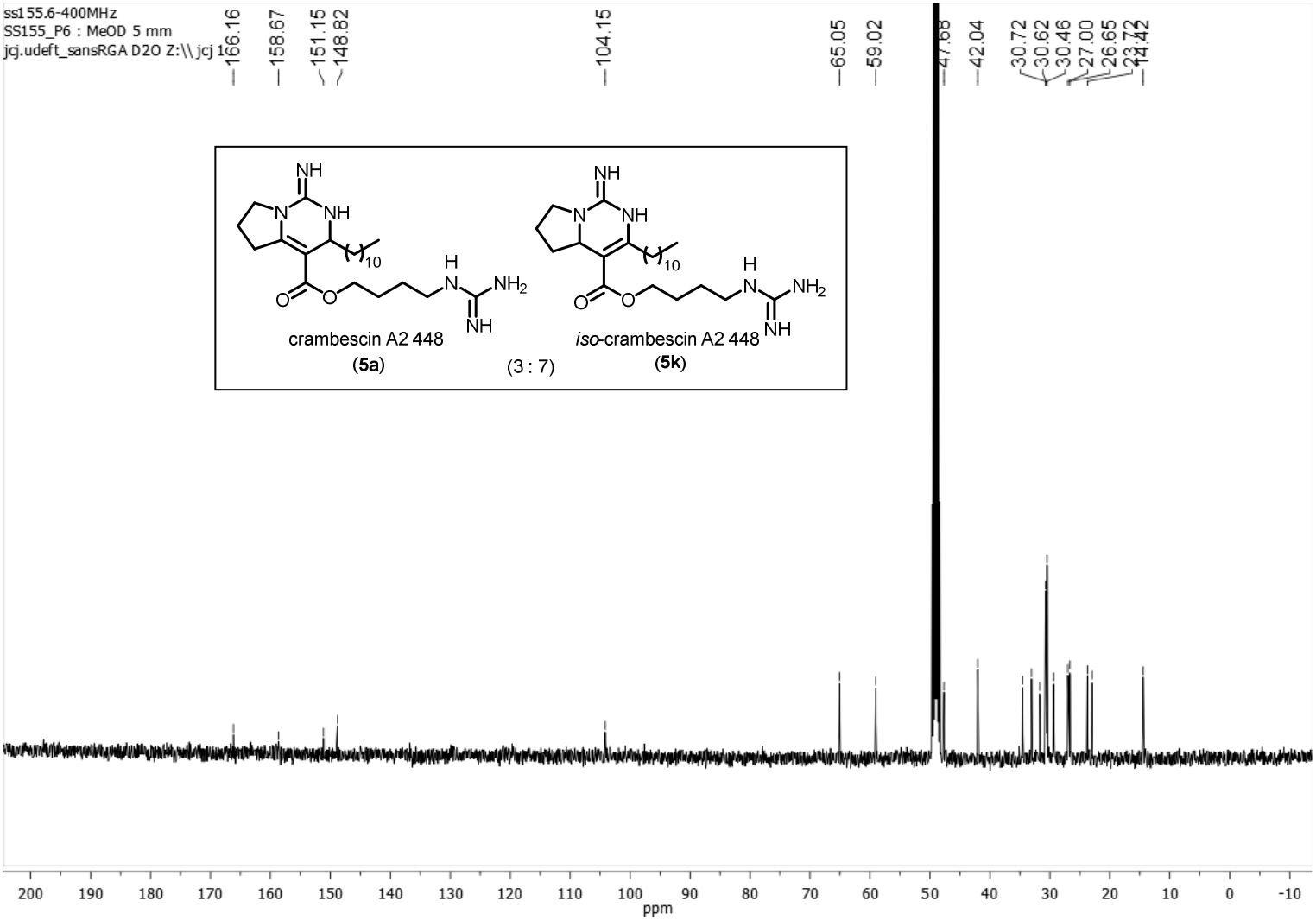

crambescin A2 448 (**5a**) and *iso*-crambescin A2 442 (**5k**) (COSY-^{1}H-NMR, 400 MHz, MeOH-d_4)

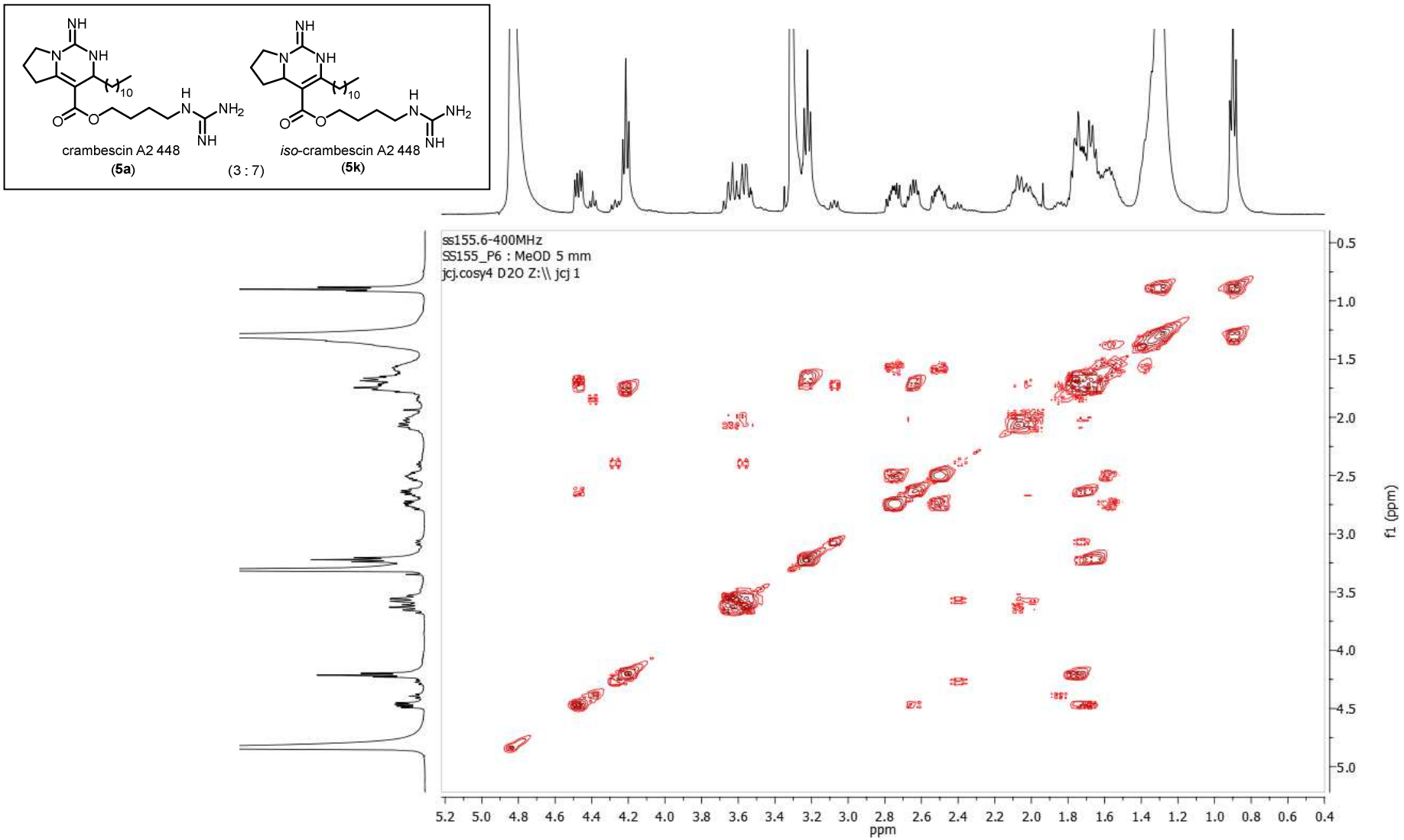

crambescin A2 448 (**5a**) and *iso*-crambescin A2 448 (**5k**) (HSQC-^{1}H and ^{13}C-NMR, 400 MHz and 100 MHz, MeOH-d_4)

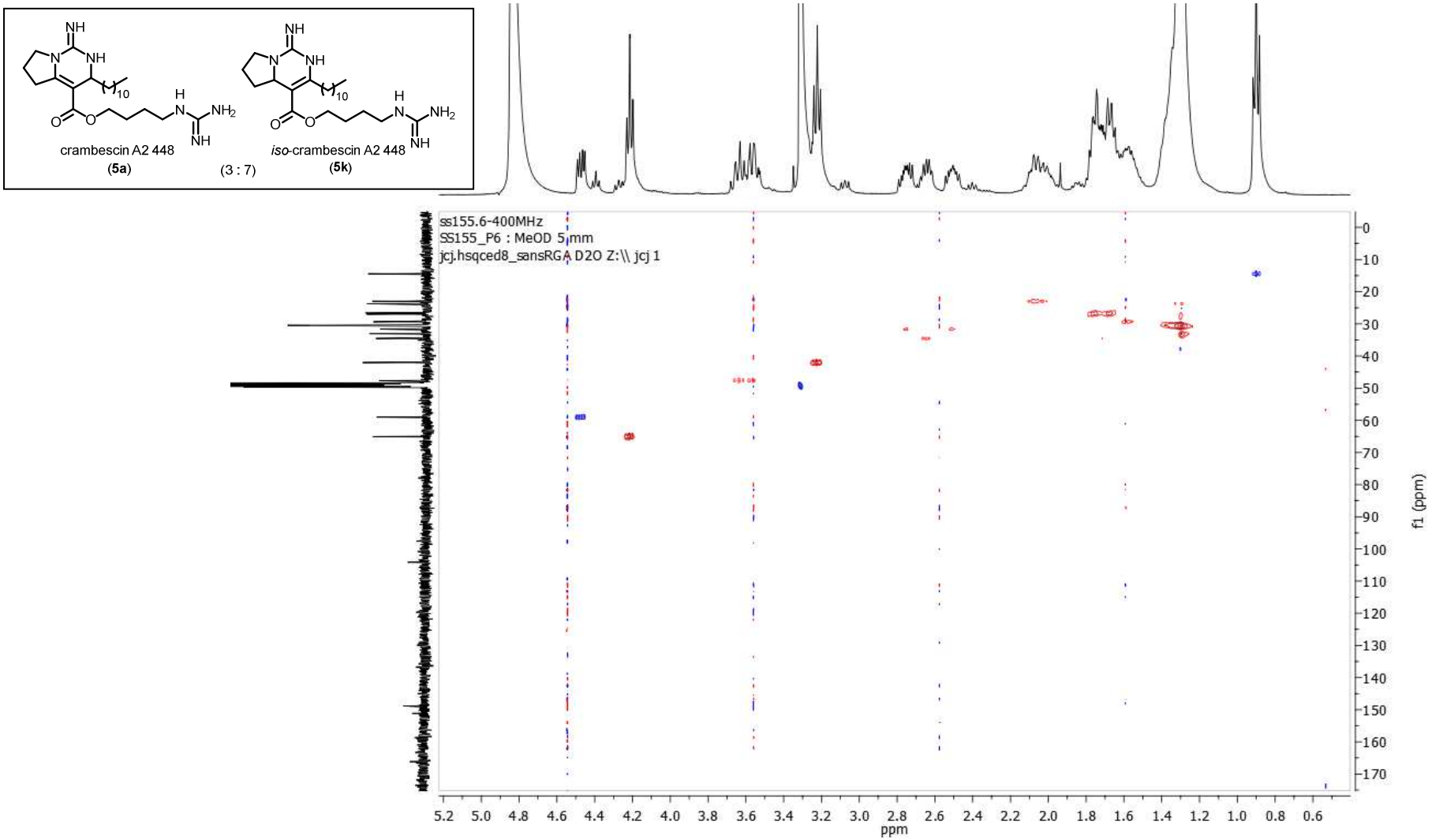

crambescin A2 448 (**5a**) and *iso*-crambescin A2 448 (**5k**) (HMQC-^{1}H and ^{13}C-NMR, 400 MHz and 100 MHz, MeOH-d_4)

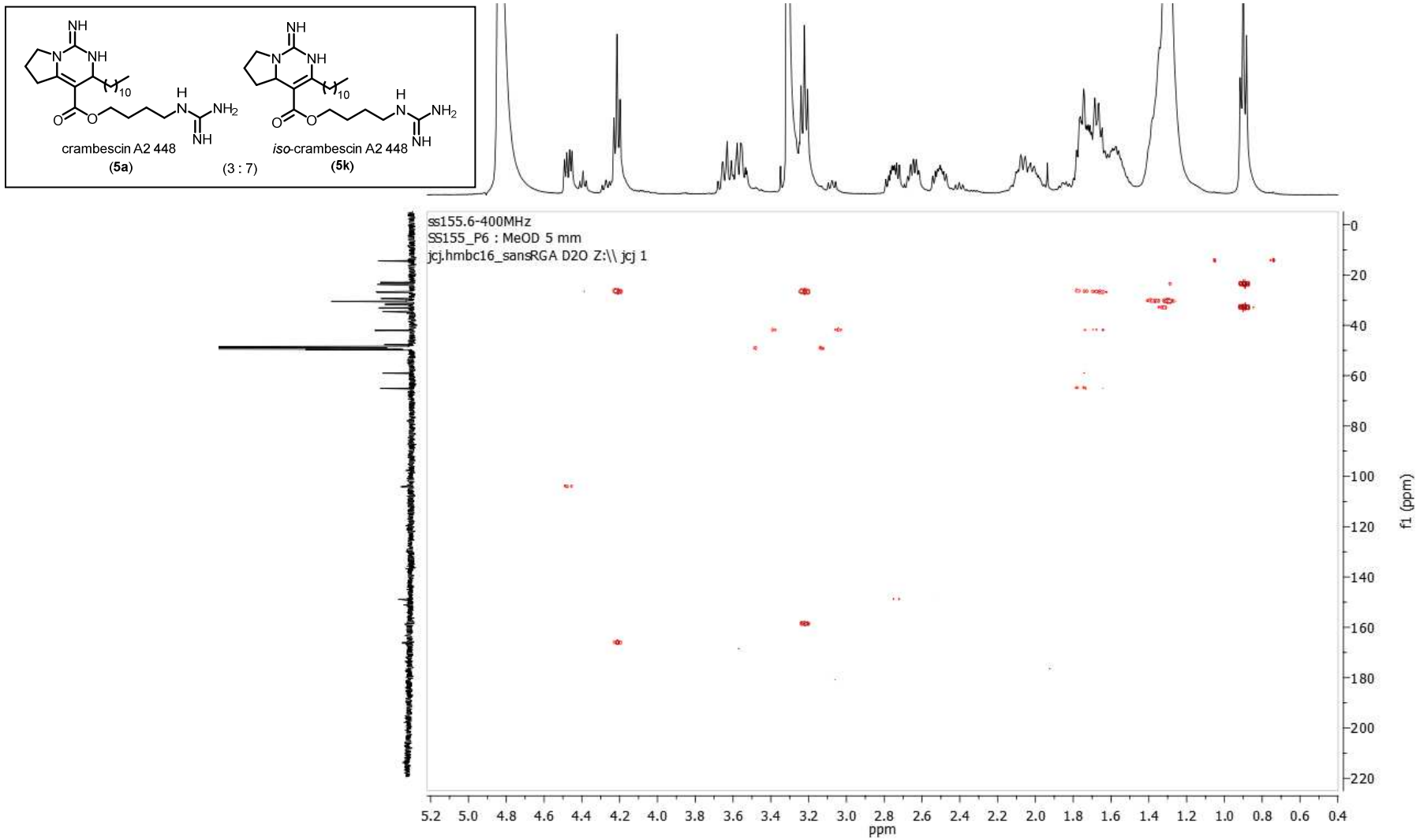

References

References

[1] B. David, J.-L. Wolfender, D. A. Dias, *Phytochem. Rev.* **2015**, *14*, 299-315.
[2] V. Amirkia, M. Heinrich, *Phytochem. Lett.* **2014**, *10*, xlviii-liii.
[3] P. M. Dewick, in *Medicinal Natural Products*, John Wiley & Sons, Ltd, **2009**, pp. 311-420.
[4] J. W. Blunt, B. R. Copp, R. A. Keyzers, M. H. G. Munro, M. R. Prinsep, *Nat. Prod. Rep.* **2015**, *32*, 116-211.
[5] J. Vacelet, N. Boury-Esnault, *Nature* **1995**, *373*, 333-335.
[6] A. M. P. Almeida, R. G. S. Berlinck, E. Hajdu, *Quim. Nova* **1997**, *20*, 170-185.
[7] R. W. M. Van Soest, N. Boury-Esnault, J. N. A. Hooper, K. Rützler, N. J. de Voogd, B. Alvarez de Glasby, E. Hajdu, A. B. Pisera, R. Manconi, C. Schoenberg, M. Klautau, B. Picton, M. Kelly, J. Vacelet, M. Dohrmann, M.-C. Díaz, P. Cárdenas, J. L. Carballo, P. Rios Lopez, in *World Porifera Database*, Acessed at http://www.marinespecies.org/porifera on 2017-09-15, **2017**.
[8] E. Gazave, P. Lapébie, A. Ereskovsky, J. Vacelet, E. Renard, P. Cárdenas, C. Borchiellini, *Hydrobiologia* **2012**, *687*, 3-10.
[9] C. Morrow, P. Cárdenas, *Front. Zool.* **2015**, *12*, 7.
[10] T. K. Huyck, W. Gradishar, F. Manuguid, P. Kirkpatrick, *Nat. Rev. Drug Discov.* **2011**, *10*, 173-174.
[11] A. Casapullo, E. Finamore, L. Minale, F. Zollo, *Tetrahedron Lett.* **1993**, *34*, 6297-6300.
[12] A. Casapullo, L. Minale, F. Zollo, *Tetrahedron Lett* **1994**, *35*, 2421-2422.
[13] A. Casapullo, L. Minale, F. Zollo, J. Lavayre, *J. Nat. Prod.* **1994**, *57*, 1227-1233.
[14] B. B. Snider, F. Song, B. M. Foxman, *J. Org. Chem.* **2000**, *65*, 793-800.
[15] R. W. M. Van Soest, in *Systema Porifera: A Guide to the Classification of Sponges* (Eds.: J. N. A. Hooper, R. W. M. Van Soest, P. Willenz), Springer US, Boston, MA, **2002**, pp. 547-555.
[16] Z. D. Aron, H. Pietraszkiewicz, L. E. Overman, F. Valeriote, C. Cuevas, *Bioorg. Med. Chem. Lett.* **2004**, *14*, 3445-3449.
[17] M. Roel, J. A. Rubiolo, J. Guerra-Varela, S. B. Silva, O. P. Thomas, P. Cabezas-Sainz, L. Sanchez, R. Lopez, L. M. Botana, *Oncotarget* **2016**, *7*, 83071-83087.
[18] S. A. Dyshlovoy, K. M. Tabakmakher, J. Hauschild, R. K. Shchekaleva, K. Otte, A. G. Guzii, T. N. Makarieva, E. K. Kudryashova, S. N. Fedorov, L. K. Shubina, C. Bokemeyer, F. Honecker, V. A. Stonik, G. von Amsberg, *Mar. Drugs* **2016**, *14*.
[19] A. Olszewski, K. Sato, Z. D. Aron, F. Cohen, A. Harris, B. R. McDougall, W. E. Robinson, L. E. Overman, G. A. Weiss, *Proc. Natl. Acad. Sci. USA* **2004**, *101*, 14079-14084.
[20] H. Nagarajaiah, A. Mukhopadhyay, J. N. Moorthy, *Tetrahedron Lett.* **2016**, *57*, 5135-5149.
[21] T. N. Makarieva, E. K. Ogurtsova, V. A. Denisenko, P. S. Dmitrenok, K. M. Tabakmakher, A. G. Guzii, E. A. Pislyagin, A. A. Es' kov, V. B. Kozhemyako, D. L. Aminin, Y.-M. Wang, V. A. Stonik, *Org. Lett.* **2014**, *16*, 4292-4295.
[22] J. A. Rubiolo, E. Ternon, H. López-Alonso, O. P. Thomas, F. V. Vega, M. R. Vieytes, L. M. Botana, *Mar. Drugs* **2013**, *11*, 4419-4434.
[23] J. E. H. Lazaro, J. Nitcheu, N. Mahmoudi, J. A. Ibana, G. C. Mangalindan, G. P. Black, A. G. Howard-Jones, C. G. Moore, D. A. Thomas, D. Mazier, C. M. Ireland, G. P. Concepcion, P. J. Murphy, B. Diquet, *J. Antibiot.* **2006**, *59*, 583-590.
[24] J. A. Rubiolo, H. López-Alonso, M. Roel, M. R. Vieytes, O. Thomas, E. Ternon, F. V. Vega, L. M. Botana, *Br. J. Pharmacol.* **2014**, *171*, 1655-1667.
[25] V. Martin, C. Vale, S. Bondu, O. P. Thomas, M. R. Vieytes, L. M. Botana, *Chem. Res. Toxicol.* **2013**, *26*, 169-178.
[26] J. Vacelet, N. Boury-Esnault, *Trav. Sci. Parc Natl. Port-Cros* **1982**, *8*, 107-113.
[27] R. Laville, O. P. Thomas, F. Berrué, D. Marquez, J. Vacelet, P. Amade, *Journal of Natural Products* **2009**, *72*, 1589-1594.
[28] A. G. Mendez, A. B. Juncal, S. B. L. Silva, O. P. Thomas, V. Martín Vázquez, A. Alfonso, M. R. Vieytes, C. Vale, L. M. Botana, *ACS. Chem. Neurosci.* **2017**, *8*, 1609-1617.
[29] M. J. Garson, *Nat. Prod. Rep.* **1989**, *6*, 143-170.
[30] G. Genta-Jouve, O. P. Thomas, *Phytochem. Rev.* **2013**, *12*, 425-434.
[31] E. Ternon, L. Zarate, S. Chenesseau, J. Croué, R. Dumollard, M. T. Suzuki, O. P. Thomas, *Sci. Rep.* **2016**, *6*, 29474.
[32] P. M. Dewick, in *Medicinal Natural Products*, John Wiley & Sons, Ltd, **2009**, pp. 7-38.
[33] G. Genta-Jouve, O. P. Thomas, in *Advances in Marine Biology, Vol. 62* (Eds.: Mikel A. Becerro, Maria J. Uriz, Manuel Maldonado, Xavier Turon), Academic Press, **2012**, pp. 183-230.
[34] E. Gravel, E. Poupon, *Eur. J. Org. Chem.* **2008**, 27-42.
[35] M. Pozzolini, S. Scarfì, F. Mussino, S. Ferrando, L. Gallus, M. Giovine, *Mar. Biotechnol.* **2015**, *17*, 393-407.
[36] Y. Takeshige, Y. Egami, T. Wakimoto, I. Abe, *Mol. BioSyst.* **2015**, *11*, 1290-1294.
[37] A. L. Lane, B. S. Moore, *Nat. Prod. Rep.* **2011**, *28*, 411-428.
[38] M. J. Garson, *Chem. Rev.* **1993**, *93*, 1699-1733.
[39] K. J. Nicacio, L. P. Ióca, A. M. Fróes, L. Leomil, L. R. Appolinario, C. C. Thompson, F. L. Thompson, A. G. Ferreira, D. E. Williams, R. J. Andersen, A. S. Eustaquio, R. G. S. Berlinck, *J. Nat. Prod.* **2017**, *80*, 235-240.
[40] B. S. Moore, *Nat. Prod. Rep.* **2006**, *23*, 615-629.
[41] G. F. Knoll, *Radiation Detection and Measurement*, John Wiley & Sons, **2010**.
[42] G. Genta-Jouve, N. Cachet, S. Holderith, F. Oberhaensli, J.-L. Teyssie, R. Jeffree, A. Al Mourabit, O. P. Thomas, *Chem. Bio. Chem.* **2011**, *12*, 2298-2301.
[43] N. Barthe, K. Chatti, P. Coulon, S. Maîtrejean, B. Basse-Cathalinat, *Nucl. Instrum. Meth. A* **2004**, *527*, 41-45.
[44] B. B. Snider, Z. Shi, *J. Org. Chem.* **1993**, *58*, 3828-3839.
[45] S. Bondu, G. Genta-Jouve, M. Leiros, C. Vale, J.-M. Guigonis, L. M. Botana, O. P. Thomas, *RSC Adv.* **2012**, *2*, 2828-2835.
[46] G. Genta-Jouve, J. Croué, L. Weinberg, V. Cocandeau, S. Holderith, N. Bontemps, M. Suzuki, O. P. Thomas, *Phytochem. Lett.* **2014**, *10*, 318-323.
[47] R. G. S. Berlinck, J. C. Braekman, D. Daloze, I. Bruno, R. Riccio, D. Rogeau, P. Amade, *J. Nat. Prod.* **1992**, *55*, 528-532.
[48] E. A. Jares-Erijman, A. A. Ingrum, F. Sun, K. L. Rinehart, *J Nat Prod* **1993**, *56*, 2186-2188.
[49] M. Roel, J. A. Rubiolo, L. M. Botana, E. Ternon, O. P. Thomas, O. P. Thomas, M. R. Vieytes, *Mar Drugs* **2015**, *13*, 4633-4653.
[50] R. Osinga, J. Tramper, H. R. Wijffels, *Mar. Biotechnol.* **1999**, *1*, 509-532.
[51] R. Osinga, J. Tramper, R. H. Wijffels, *Trends Biotechnol.* **1998**, *16*, 130-134.
[52] X. Turon, J. Galera, M. J. Uriz, *J. Exp. Zool.* **1997**, *278*, 22-36.
[53] E. H. Belarbi, M. R. Dominguez, G. M. C. Ceron, G. A. Contreras, C. F. Garcia, G. E. Molina, *Biomol. Eng.* **2003**, *20*, 333-337.
[54] H. Hong, T. Fill, P. F. Leadlay, *Angew. Chem. Int. Ed.* **2013**, *52*, 13096-13099.
[55] G. Romagnoli, M. D. Verhoeven, R. Mans, Y. Fleury Rey, R. Bel-Rhlid, M. van den Broek, R. Maleki Seifar, A. Ten Pierick, M. Thompson, V. Müller, S. A. Wahl, J. T. Pronk, J. M. Daran, *Mol. Microbiol.* **2014**, *93*, 369-389.
[56] J. Croué, N. J. West, M.-L. Escande, L. Intertaglia, P. Lebaron, M. T. Suzuki, *Sci. Rep.* **2013**, *3*, 2583.

References

[57] in *Biomimetic Organic Synthesis* (Eds.: E. Poupon, B. Nay), Wiley-VCH Verlag GmbH & Co. KGaA, **2011**, pp. I-XXXV.
[58] T. W. Hanks, G. F. Swiegers, in *Bioinspiration and Biomimicry in Chemistry*, John Wiley & Sons, Inc., **2012**, pp. 1-15.
[59] C. H. Heathcock, *P. Natl. Acad. Sci.* **1996**, *93*, 14323-14327.
[60] B. Nay, N. Riache, in *Biomimetic Organic Synthesis*, Wiley-VCH Verlag GmbH & Co. KGaA, **2011**, pp. 503-535.
[61] S. H. Bertz, *J. Am. Chem. Soc.* **1981**, *103*, 3599-3601.
[62] T. Böttcher, *J. Chem. Inf. Model.* **2016**, *56*, 462-470.
[63] J. B. Hendrickson, P. Huang, A. G. Toczko, *J. Chem. Inf. Comp. Sci.* **1987**, *27*, 63-67.
[64] R. G. S. Berlinck, J. C. Braekman, D. Daloze, K. Hallenga, R. Ottinger, I. Bruno, R. Riccio, *Tetrahedron Lett.* **1990**, *31*, 6531-6534.
[65] C. H. Van Etten, H. C. Nielsen, J. E. Peters, *Phytochemistry* **1965**, *4*, 467-473.
[66] M. T. Jamison, T. F. Molinski, *J. Nat. Prod.* **2015**, *78*, 557-561.
[67] B. B. Snider, Z. Shi, *J. Org. Chem.* **1992**, *57*, 2526-2528.
[68] B. B. Snider, Z. Shi, *Tetrahedron Lett.* **1993**, *34*, 2099-2102.
[69] D. W. Brooks, L. D. L. Lu, S. Masamune, *Angew. Chem. Int. Edit.* **1979**, *18*, 72-74.
[70] V. M. Paradkar, T. B. Latham, D. M. Demko, *Synlett* **1995**, *1995*, 1059-1060.
[71] R. G. Linde, N. C. Birsner, R. Y. Chandrasekaran, J. Clancy, R. J. Howe, J. P. Lyssikatos, C. P. MacLelland, T. V. Magee, J. W. Petitpas, J. P. Rainville, W. G. Su, C. B. Vu, D. A. Whipple, *Bioorg. Med. Chem. Lett.* **1997**, *7*, 1149-1152.
[72] O. I. Shmatova, V. N. Khrustalev, V. G. Nenajdenko, *Org. Lett.* **2016**, *18*, 4494-4497.
[73] S. P. Chavan, Y. T. Subbarao, S. W. Dantale, R. Sivappa, *Synthetic Commun.* **2001**, *31*, 289-294.
[74] S. P. Chavan, K. Shivasankar, R. Sivappa, R. Kale, *Tetrahedron Lett.* **2002**, *43*, 8583-8586.
[75] D. F. Taber, J. C. Amedio, Y. K. Patel, *J. Org. Chem.* **1985**, *50*, 3618-3619.
[76] B. Neises, W. Steglich, *Angew. Chem.Int. Ed. Engl.* **1978**, *17*, 522-524.
[77] G. A. Hiegel, J. C. Lewis, J. W. Bae, *Synthetic Commun.* **2004**, *34*, 3449-3453.
[78] R. P. van Summeren, A. Romaniuk, E. G. Ijpeij, P. L. Alsters, *Catal. Sci. Technol.* **2012**, *2*, 2052-2056.
[79] B. Staskun, T. van Es, *S. Afr. J. Chem.* **2008**, *61*, 144-156.
[80] B. T. Khai, A. Arcelli, *J. Org. Chem.* **1989**, *54*, 949-953.
[81] T. van Es, B. Staskun, *Org. Syn.* **1971**, *51*, 20-23.
[82] T. G. Clarke, N. A. Hampson, J. B. Lee, J. R. Morley, B. Scanlon, *J. Chem. Soc. C* **1970**, 815-817.
[83] T. G. Clarke, N. A. Hampson, J. B. Lee, J. R. Morley, B. Scanlon, *Can. J. Chem.* **1969**, *47*, 1649-1654.
[84] Y. Zelechonok, R. B. Silverman, *J. Org. Chem.* **1992**, *57*, 5787-5790.
[85] Z. D. Aron, L. E. Overman, *Chem. Comm.* **2004**, 253-265.
[86] B. L. Nilsson, L. E. Overman, *J. Org. Chem.* **2006**, *71*, 7706-7714.
[87] S. K. Collins, A. I. McDonald, L. E. Overman, Y. H. Rhee, *Org. Lett.* **2004**, *6*, 1253-1255.
[88] C. O. Kappe, *Acc. Chem. Res.* **2000**, *33*, 879-888.
[89] A. El-Demerdash, C. Moriou, M.-T. Martin, A. d. S. Rodrigues-Stien, S. Petek, M. Demoy-Schneider, K. Hall, J. N. A. Hooper, C. Debitus, A. Al-Mourabit, *J. Nat. Prod.* **2016**, *79*, 1929-1937.
[90] W. L. F. Armarego, C. L. L. Chai, in *Purification of Laboratory Chemicals (Sixth Edition)*, Butterworth-Heinemann, Oxford, **2009**, pp. 1-60.
[91] N. C. Gassner, C. M. Tamble, J. E. Bock, N. Cotton, K. N. White, K. Tenney, O. R. P. St, M. J. Proctor, G. Giaever, R. W. Davis, P. Crews, T. R. Holman, R. S. Lokey, *J. Nat. Prod.* **2007**, *70*, 383-390.
[92] W. J. Christ, L. D. Hawkins, T. Kawata, D. P. Rossignol, S. Kobayashi, O. Asano, Eisai Co., Ltd., USA . **1996**, pp. 92 pp., Cont.-in-part of U.S. Ser. No. 776,100, abandoned.
[93] W. J. Christ, T. Kawata, L. D. Hawkins, S. Kobayashi, O. Asano, D. P. Rossignol, Eisai Co., Ltd., Japan . **1993**, p. 213 pp.
[94] M. A. Mitz, A. E. Axelrod, K. Hofmann, *J. Am. Chem. Soc.* **1950**, *72*, 1231-1232.
[95] V. Rerat, G. Dive, A. A. Cordi, G. C. Tucker, R. Bareille, J. Amédée, L. Bordenave, J. Marchand-Brynaert, *J. Med. Chem.* **2009**, *52*, 7029-7043.

université PARIS-SACLAY | ÉCOLE DOCTORALE Innovation thérapeutique : du fondamental à l'appliqué

Titre: Chimie et biosynthèse de substances naturelles hautement complexes de la biodiversité méditerranéenne

Mots clés: substances naturelles, éponges marines, alkaloïdes, biosynthèse, synthèse biomimétique

Résumé: Le but de ce travail de doctorat est l'étude chimique et biosynthétique de familles d'alcaloïdes guanidiniques d'origine marine provenant d'éponges de Méditerranée.
Le travail est divisé en trois parties successives :
1) l'isolement d'alcaloïdes produits par des éponges marines de l'ordre des Poecilosclerida;
2) l'élucidation de la biosynthèse de la crambescine C1 par des études *in vivo* d'incorporation de précurseurs marqués au ^{14}C;
3) la synthèse biomimétique de la crambescine A2 448 et de dérivés proches.
La famille des alcaloïdes guanidiniques cycliques des crambescines est au coeur de la thèse, ces substances naturelles sont produites par l'éponge incrustante *Crambe crambe*. Ces alcaloïdes ont été découverts dans les années 1990 et ont suscité beaucoup d'intérêt pour leurs propriétés biologiques et écologiques et leurs synthèses totales. Par contre, leur bio-synthèse était encore inconnue à ce jour. La seule synthèse biomimétique disponible était basée sur une hypothèse d'origine polyacétique. Les hypothèses récentes de nos groupes ont permis de mettre en avant une origine mixte: la partie cyclique guanidinique proviendrait d'un pyrrolidinium issu de l'arginine et d'un précurseur "céto-acide" proche des acides gras. Sur la base de cette hypothèse, nous avons mis au point une expérience d'incorporation qui a ensuite inspirée une voie de synthèse biomimétique pour l'accès aux crambescines et dérivés. Les premières conclusions quant à l'origine biosynthétique de ces molécules sont les faits les plus marquants de ce travail. Nous apportons une meilleure compréhension de la biochimie des alcaloïdes guanidiniques marins de structures complexes.

Title: Chemistry and biosynthesis of highly complex marine alkaloids from Mediterranean biodiversity

Keywords: natural products, marine sponges, alkaloids, biosynthesis, biomimetic synthesis

Abstract: This thesis aims at the study of the chemical and biogenetic origin of specialized guanidine-alkaloid metabolites produced by sponges from the Mediterranean Sea.
The work is divided into three main parts:
1) isolation of alkaloids produced by sponges of the Poecilosclerida order;
2) biosynthesis of crambescin C1 by *in vivo* ^{14}C-feeding experiments with *Crambe crambe* sponge;
3) biomimetic synthesis of crambescin A2 448 and derivatives.
The main focus of the thesis will be the family of cyclic-guanidine alkaloids "crambescins", produced by the red incrusting sponge *Crambe crambe*. These alkaloids were discovered in the early 90s and despite the large interest on their biological activities, ecological roles, and synthesis, their biosynthesis is still unknown.
The only available biomimetic synthesis of crambescins was based on a fully polyketide origin hypothesis. Recently our groups suggested an alternative biosynthetic hypothesis in which the guanidine-core would be originated from a condensation between a guanidinated pyrrolidinium derived from arginine and a β-keto fatty acid. Based on this hypothesis, we designed a biosynthesis experiment that inspired a biomimetic synthesis route to access the crambescins and derivatives. The insights from these studies are the first experimental conclusions about the biosynthesis of crambescins. Finally, this work leads to a better comprehension of the biochemistry involved in guanidine marine alkaloids of complex structures.